ANL-6285

MASTER

ANL-6285

322
4-3-61

Argonne National Laboratory

ARGONAUT REACTOR DATABOOK

by

W. J. Sturm and D. A. Daavettila

DISCLAIMER

This report was prepared as an account of work sponsored by an agency of the United States Government. Neither the United States Government nor any agency Thereof, nor any of their employees, makes any warranty, express or implied, or assumes any legal liability or responsibility for the accuracy, completeness, or usefulness of any information, apparatus, product, or process disclosed, or represents that its use would not infringe privately owned rights. Reference herein to any specific commercial product, process, or service by trade name, trademark, manufacturer, or otherwise does not necessarily constitute or imply its endorsement, recommendation, or favoring by the United States Government or any agency thereof. The views and opinions of authors expressed herein do not necessarily state or reflect those of the United States Government or any agency thereof.

DISCLAIMER

Portions of this document may be illegible in electronic image products. Images are produced from the best available original document.

LEGAL NOTICE

This report was prepared as an account of Government sponsored work. Neither the United States, nor the Commission, nor any person acting on behalf of the Commission:

A. Makes any warranty or representation, expressed or implied, with respect to the accuracy, completeness, or usefulness of the information contained in this report, or that the use of any information, apparatus, method, or process disclosed in this report may not infringe privately owned rights; or

B. Assumes any liabilities with respect to the use of, or for damages resulting from the use of any information, apparatus, method, or process disclosed in this report.

As used in the above, "person acting on behalf of the Commission" includes any employee or contractor of the Commission, or employee of such contractor, to the extent that such employee or contractor of the Commission, or employee of such contractor prepares, disseminates, or provides access to, any information pursuant to his employment or contract with the Commission, or his employment with such contractor.

Price $2.75 . *Available from the Office of Technical Services, Department of Commerce, Washington 25, D.C.*

ANL-6285
Reactor Technology
(TID-4500, 16th Ed.)
AEC Research and
Development Report

ARGONNE NATIONAL LABORATORY
9700 South Cass Avenue
Argonne, Illinois

ARGONAUT REACTOR DATABOOK

A compilation of experimental and theoretical results of work done with, or related to, the Argonaut Reactor to July 1960

by

W. J. Sturm and D. A. Daavettila

January 1961

Operated by The University of Chicago
under
Contract W-31-109-eng-38

ARGONAUT REACTOR DATABOOK

by

W. J. Sturm and D. A. Daavettila

ABSTRACT

This compilation has been prepared in order to provide a comprehensive unified summary of the principal elements of the design, operation and nuclear characteristics of the Argonaut Reactor. Its primary content is made up of the theoretical and experimental evaluations of basic reactor parameters, both static and kinetic, which have been made to this date. The Databook includes also some practical information on the reactivity worths of fuel, moderator, and absorbers, as well as some data on radiation in the reactor vicinity.

A world list of Argonaut-type reactors and a bibliography of Argonaut work is included.

INTRODUCTION

This report is a compilation of experimental and theoretical results of work done on, or with, the Argonaut Reactor up to July 1960.

Since the initial operation of the Argonaut in late 1956, numerous investigators have performed experimental and theoretical work with the Argonaut. Designed for university training, the reactor was assigned to the International School of Nuclear Science and Engineering (ISNSE) at Argonne National Laboratory upon its completion. The ISNSE staff, in most cases with the cooperation of the international and American students, set about answering the problems of characterizing the reactor and developing a series of reactor experiments to fulfill its pedagogical needs. The extent to which this was an international cooperative effort can be estimated from a cursory study of the bibliography.

Some form of written record is at hand for much of the pertinent work, and this compilation was made to provide a comprehensive review of the Argonaut literature in a unified and generally accessible form. It is expected to be an aid in the orientation of students and in the planning of staff and student training and research work. It may also be helpful to the growing number of institutions which have their own Argonaut-type reactors.

The scope of the Databook is limited to a reproduction of a representative series of the main results of Argonaut work. For details and discussion of a particular study by Argonne staff, reference must be made to the original published source. All student and some staff work was performed using established techniques and materials, and publication other than in this Databook is not generally available. There is given reference for each curve and table that includes original work and author as given in the bibliography, and includes in addition the reactor core description.

In general, the annular core region of the reactor can be loaded with fuel in any one of several ways to produce a critical system. Much of the work reported has been with the single slab, in which but one quadrant of the annulus contains fuel; other work characterizes the two-slab reactor, involving two loaded quadrants diametrically opposed. In the annular loading, fuel completely surrounds the internal thermal column. All data are identified as pertaining to one of three loading systems.

A modified bibliography arranged according to subject matter is provided as a guide to work areas that have been investigated to date. This bibliography includes both formally published reports and general work projects whose results are considered to be of a preliminary nature. Also this bibliography serves as an author credit list for the data included in this Databook.

TABLE OF CONTENTS

		Page
A.	CHARACTERISTICS OF THE ARGONAUT	11
	1. General	12
	2. Fuel	12
	3. Reactor	12
	4. Primary Coolant	14
	5. Nuclear Data	14
B.	DETAILS OF REACTOR DESIGN	15
	1. Isometric View of Reactor	16
	2. Plan Section of Core Lattice and Reflector	17
	3. Location Coding of the Core and Thermal Column	18
	4. Interlock System	19
	5. Flow Diagram of the Water System	20
	6. BF_3 Proportional Counter Channels	21
	7. B^{10} Ion Chamber Channels	22
	8. Boron Chamber Locations in South Face of Reactor	23
C.	REACTOR OPERATIONS	25
	1. Reactor Checkout	26
	2. General Startup Procedure	28
	3. Shutdown	29
	4. Behavior of Multiplication Meter During Startup of Reactor	30
	5. Multiplication Meter Readings vs k_{ex} for Various Loadings	31
	6. Power Level Trip; Safety Rod Shutdown after Positive Step Reactivity Insertion	32
D.	REACTOR CONSTANTS	33
	1. One-slab - Theoretical Two-group Constants for the Homogenized Argonaut One-slab Loading	34
	a. Core Constants	34
	b. Thermal Group Constants	34
	c. Fast Group Constants	35
	d. Reflector Constants	35
	e. Miscellaneous Constants	36
	2. Two-slab	36
	a. Miscellaneous Thermal	36
	b. Miscellaneous Experimental	36

TABLE OF CONTENTS

Page

3. Annulus - Theoretical Two-group Constants for a Homogenized Annular Loading 36
   a. Core Constants 36
   b. Thermal Group Constants 37
   c. Fast Group Constants 37
   d. Reflector Constants 37
   e. Materials Outside Graphite Reflector 38
   f. Fluxes and Reactivity Effects 38
4. Six Sets of Two Boxes 38

E. KINETICS 39
1. Flux-time Dependence (Theoretical) 40
   a. Positive Reactivity vs Positive Asymptotic Period . . . 41
   b. Flux Ratio vs Positive Reactivity Step for Various Times 42
   c. Flux Ratio vs Time after Positive Step Change in Reactivity 43
   d. Flux Ratio vs Negative Reactivity Step at Time after Step 44
   e. Flux Ratio vs Negative Reactivity Step at Time after Step 45
   f. Positive Reactivity vs Roots of Characteristic (Inhour) Equation 46
   g. Negative Reactivity vs Roots of Characteristic (Inhour) Equation 47
   h. Coefficients of Flux Equation vs Negative Reactivity for Step Change in Reactivity 48
   i. Percent Error in Asymptotic Positive Period Measurement vs Time after Step Change in Reactivity 49
2. Flux-time Dependence as a Function of Delayed Neutron Parameters (Theoretical) 50
   a. Delayed Neutron Parameters 50
   b. Comparison of Hughes and Keepin Delayed Neutron Data in the Calculation of Flux Ratio vs Time after a Negative Step 51
   c. Comparison of Hughes and Keepin Delayed Neutron Data in the Calculation of Flux Ratio vs Time after a Positive Step 52

TABLE OF CONTENTS

Page

3. Flux-time Dependence as a Function of Neutron Lifetime (Theoretical) 53
   a. Flux Ratio vs Time for Short Times after Negative Step Insertions, Comparison of Effect of Neutron Lifetime 54
   b. Flux Ratio vs Time for Short Times after Positive Step Insertions, Comparison of Effect of Neutron Lifetime 55
4. Comparison of Theoretical and Experimental Values of Flux Ratio vs Time after Introduction of Step Change in Reactivity 56
5. Experimental and Theoretical Curves of the Neutron Level Behavior during and after Nitrogen Injection into the Core. 57
6. Theoretical Curves of Neutron Level vs Time for Various Negative Reactivity Steps Inserted while the Reactor was on a Positive Period 58

F. CONTROL ROD CALIBRATION. 59
1. One-slab. 60
   a. Integral Fine Rod Worth 61
   b. Fine Control Rod Calibration for Various Loadings . . 62
   c. Integral Fine Rod Worth as Determined by Four Different Methods of Measurement 63
   d. Composite Control Rod Calibration 64
2. Annulus 65
   a. Coarse Rod Integral Worth. 66
   b. Composite Worths of all Six Rods 67

G. RAMP STARTUP 69
1. Log n vs Time for Various Rates of Removal of Fine Control Rod. 70

H. TRANSFER FUNCTION (ONE-SLAB GEOMETRY) 71
1. Reactivity Worth vs Annular Position of Reactivity Oscillator 72
2. Reactivity Worth vs Angular Position of Regulator 73
3. Argonaut Transfer Function - Gain vs Frequency. 74
4. Argonaut Transfer Function - Phase Shift vs Frequency . . 75

TABLE OF CONTENTS

Page

I. FLUX PLOTS (RELATIVE) 77

1. Core 78

a. One-slab. 78

(1) Radial Total Flux Distribution in Boxes 15 and 16. . 79
(2) Radial Total Flux Distribution, Detailed in Fuel Boxes. 80
(3) Radial Flux Distribution, Total and Epicadmium, Detailed in Fuel Box 16 81
(4) Angular Total Flux Distribution Between Plates 1 and 2 82
(5) Angular Total Flux Distribution Between Plates 8 and 9 83
(6) Angular Total Flux Distribution Between Plates 15 and 16. 84
(7) Angular Epicadmium Flux Distribution Between Plates 8 and 9 85
(8) Angular Total Flux Distribution 86
(9) Vertical Total Flux Distribution 87

b. Two-slab 88

(1) Angular Total Flux Distribution 89
(2) Vertical Flux Distribution, Total, Thermal and Epicadmium 90
(3) Radial Total Flux Distribution 91

c. Annulus 92

(1) Radial Total Flux Distribution Across Internal Thermal Column 93
(2) Vertical Total Flux Distribution 94

2. Thermal Columns. 95

a. Theoretical Radial Fast Neutron Flux Across Core, Internal and External Thermal Columns 96
b. Theoretical Radial Thermal Neutron Flux Across Core, Internal and External Thermal Columns. 97
c. Radial Total Flux Across Core, External and Internal Thermal Columns. 98
d. Axial Total and Epicadmium Flux Distribution in External Graphite Thermal Column 99
e. Axial Cadmium Ratio Variation in External Graphite Thermal Column 100

TABLE OF CONTENTS

Page

3. Water Tank 101
    - a. Foil Activity vs Linear Distance from Fission Plate. . 102
    - b. Neutron Distribution on Axis of Water Tank 103
    - c. Neutron Distribution Normal to Axis of Water Tank . . 104

4. Beam Hole 105
    - a. Measurement of Relative Flux in Beam Hole 106
    - b. Effect of Cadmium Next to Beam Hole 107
    - c. Thermal Neutron Beam External to Reactor Shield from J-10 108
    - d. Epithermal Neutron Beam External to Reactor Shield from J-10 109
    - e. Thermal Neutron Beam from J-10 Traversed with Two Different Resolutions of the Detector. 110

J. ABSOLUTE FLUX MEASUREMENT. 111

1. Absolute Flux at Head of J-10 Stringer with a One-slab Core 112
2. Absolute Flux at Center of One-slab Core. 113
3. Absolute Flux at Center of Each Slab of a Two-slab Core . 113
4. Absolute Thermal Neutron Flux in J-10 Stringer (One-slab Loading). 114
5. Gamma-ray Intensity in the One-slab Core During Operation 115

K. TEMPERATURE COEFFICIENT 117

1. Negative Reactivity vs Temperature (One-slab) 118
2. Negative Reactivity vs Temperature (Two-slab). 119
3. Negative Reactivity vs Temperature (Annular). 120

L. VOID COEFFICIENT. 121

1. Normalized Void Coefficient vs Radial Void Location 122
2. Void Coefficient vs Annular Void Location 123
3. Void Coefficient as a Function of Plate Spacing 124
4. Void Coefficient as a Function of Plate Spacing 125

M. NEUTRON LIFETIME 127

1. Results of Pile Noise Measurement (One-slab) 128
2. Neutron Lifetime for One-slab Loading Determined from Transfer Function Measurements 128

TABLE OF CONTENTS

Page

N. POWER CALIBRATION 129

1. One-slab Power Calibration Data 130
2. Two-slab Power Calibration Data 130
3. Calculated Power and Measured Absolute Thermal Flux Distributions in a Two-slab Core 131

O. REACTIVITY WORTHS 133

1. Fuel and Core Graphite (One- and Two-slab Data) 134
   a. Reactivity Worth of Fuel at Various Locations in the Core 134
   b. k_{ex} vs Mass of U^{235} in Core 135
   c. Reactivity vs Mass of U^{235} in Core 136
   d. Reactivity vs Fuel Location in Two-slab Core 137
   e. Relative Worth of Graphite Volume vs Mass of U^{235} in Core 138
   f. Worth of Large Graphite Wedge vs Position in Core . . 139
   g. Reactivity Worth of U^{235} in Internal Thermal Column . 140
   h. Reactivity Worth of Fuel at Various Locations in the Internal Thermal Column 141
2. Moderator and Reflector 142
   a. Reactivity Worth of Moderator and Reflector (One Slab) 142
   b. Reactivity vs Water Level in Upper Reflector (Two Slab) 143
   c. Worth of Water Moderator and Reflector (One Slab) . . 144
3. Absorber and Voids in J-10 Stringer (One Slab) 145
   a. Some Reactivity Effects in J-10 Stringer 145
   b. Negative Reactivity vs Area of Cadmium Located at End of J-10 146
   c. Negative Reactivity vs Area of Cadmium Located at End of J-10 147
   d. Integral Void Worth vs Void Volume in J-10 148
   e. Differential Void Worth vs Inches of Withdrawal of J-10 Stringer 149
4. Absorbers in Central Thimble (Two Slab) 150
5. Reactivity Worth of Nitrogen Injection (One Slab) 151
6. Summary of Miscellaneous Reactivity Changes for a Two-Slab Core 152
7. Summary of Miscellaneous Reactivity Changes for a 6 x 2 Loading 153

TABLE OF CONTENTS

Page

8. Sensitivity for Various Absorbers at Center of One-slab Core 154

P. CRITICAL MASS AND CORE LOADING 155

1. Critical Mass as a Function of Core Geometry 156
2. Critical Mass as a Function of Plate Spacing (One Slab) . . 156

Q. RADIATION SURVEYS (One Slab) 157

1. Total Gamma-ray Isodose Lines Along Midline N-S Plane of Argonaut 158
2. Total Gamma-ray Isodose Lines in Horizontal Plane About Argonaut 159
3. Gamma Isodose Curves at External Thermal Column 160
4. Fast Neutron Flux on Reactor Top Shielding 161
5. Slow Neutron Flux Along Midline N-S Plane on Reactor Top Shielding 162

R. WORLD LIST OF ARGONAUT-TYPE REACTORS 163

1. List 164
2. Map 167

S. BIBLIOGRAPHY 169

Section A

CHARACTERISTICS OF THE ARGONAUT

The Argonaut Reactor was designed for training in both nuclear engineering and research, and the experience of nearly four years of operation has proved the design to be practical. The reactor, because it is simple to operate and extremely safe, is well suited for training people without previous reactor experience. Safety is a primary design feature. As a research tool, the usefulness of the reactor is enhanced by the fact that the core is readily accessible and that the core geometry is flexible. A graphite thermal column and a large water tank are integral parts of the reactor, and numerous types of experiments can be done in these media.

The 10-kw maximum operating power of the reactor prohibits certain types of experiments, but this disadvantage is far outweighed by the fact that fuel does not become a serious radiation hazard. For all the experiments whose results are presented in this compilation, the operating power was less than 100 watts and for most less than 10 watts.

This section lists some general nuclear and engineering data of the Argonaut Reactor in order to present the basic design. The data cover only the main points of a broad area, but this will be expanded in later sections. The nuclear data given in this section are the result of the first theoretical calculations and preliminary critical studies.

A.1. General (Ref. I-7)

Type:	Training reactor
Design power:	10 kw
Normal operating power:	~100 watts
Normal operating schedule:	8 hours a day, 5 days a week
Principal uses of reactor:	Education and training

A.2. Fuel

Nominal fresh loading:	1 slab: 2.0 kg U^{235} 2 slabs: 3.6 kg U^{235} 3-in. annular: 4.0 kg U^{235}
Total fuel inventory:	6 kg U^{235}
Fuel element shape:	24 x 2.84 x 0.098-in. plates
Fuel mixture:	39 w/o Al, 7.8 w/o $U_3^{235}O_8$, 31.2 w/o $U_3^{238}O_8$; Al matrix.
Fuel dimensions:	24 x 2.84 x 0.094 in.
Cladding thickness:	0.002 in. (avg)
Cladding material:	Aluminum
Type of subassembly:	Stacked parallel plates
No. of elements per subassembly:	17
Subassembly dimensions:	6 x 3 x 24 in.
Normal number of subassemblies in core:	1 slab: 6-9 subassemblies 2 slabs: 12 subassemblies 3-in. annular: 24 subassemblies
Normal arrangements of subassemblies:	1 slab, 2 slabs, or full circle in cylindrical annulus.
Normal lifetime of standard subassemblies:	Indefinite

A.3. Reactor

Overall active core dimensions:	1 slab: Annular sector - 30 in. OD, 24 in. ID, 24 in. high, subtending a 90° angle. 2 slabs: 2 of above, diametrically opposed.

Core-containing vessel:	2 concentric aluminum tanks, one 30 in. in diameter, 48 in. high; the other 24 in. in diameter, 48 in. high. Material: Aluminum Mean operating pressure: atmospheric Mean operating temperature: Room temperature
Moderator:	H_2O between plates; graphite between subassemblies.
Reflector:	Vertical: 1 ft of water Radial: 1 ft of graphite
Biological shield:	Ordinary concrete block on sides; heavy concrete top plug, masonite and steel in some experimental facilities. Present shield is sufficient for normal operating power of approximately 100 watts.
Reactor control:	I. Control and safety mechanisms: a. Three 7 x 7-in. cadmium vertical safety blades with steel cladding; motor driven. b. Three 7 x 7-in. (or less) cadmium vertical control blades with steel cladding; motor driven. c. Water moderator and reflector dumping. d. Inert gas injection in core. II. Scram-initiating features: a. High-level, low-level, and period trips. b. High-background monitors, and personnel alarm. c. Experimental facilities and top shield interlocks. d. Manual III. Startup: Manual; automatic operation at power available.

A.4. Primary Coolant

Fluid:	Water
Circulation:	
a. Direction of flow:	Upward
b. Flow induced by forced circulation.	
Heat dissipation method:	Water to water heat exchanger.
Avg core heat flux:	360 Btu/ft^2/hr at 10 kw.
Ratio of maximum to average heat flux:	3
Means of purification:	Mechanical filter and ion-exchange column.

A.5. Nuclear Data

Fuel Loading:	
a. Minimum critical mass:	1980 gm U^{235} for 1-slab loading.
b. Normal fresh fuel loading:	2010 gm U^{235} for 1-slab loading.
c. Excess k, fresh loading:	0.5%
Fluxes:	
a. Avg thermal flux:	2×10^{11} n/cm^2/sec at 10 kw
b. Peak thermal flux:	5×10^{11} n/cm^2/sec at 10 kw
c. Avg fast flux:	4×10^{11} n/cm^2/sec at 10 kw
d. Peak fast flux:	5×10^{11} n/cm^2/sec at 10 kw
Reactivity Coefficients:	
a. Temperature:	-1×10^{-4} $\Delta k/k/°C$
b. Void:	-2×10^{-3} $\Delta k/k/\%$ void

Section B

DETAILS OF REACTOR DESIGN

An expanded view of the system design and layout is presented in this section. The physical relationship between the various components is shown, together with dimensions in some cases. This information will aid in visualizing the location and understanding the data of the experiments discussed in the following sections.

Some of the safety philosophy in the reactor design can be realized from a study of the drawing of the interlock system. The interlock system requires that startup operations follow a definite order and prohibits possibly unsafe steps in the subsequent operation, because the electrical power required to perform a step is available only if all the required previous steps are completed. During reactor operation, an attempt to undo a necessary completed step partially will automatically cause the reactor to shut down. The interlock system partially assures safe startup procedure and operation. Period meters and power level instrumentation complete the assurance, practically regardless of the capabilities of the reactor operator.

The period meter limits the maximum rate of change of reactor power to be less than a factor of 2.7 in 10 seconds. The power level instrumentation requires an instrument range change for every change of a decade in power or the reactor will automatically shut down. This instrumentation requires that the reactor operator be aware of the power level at all times, and it finally limits the maximum power.

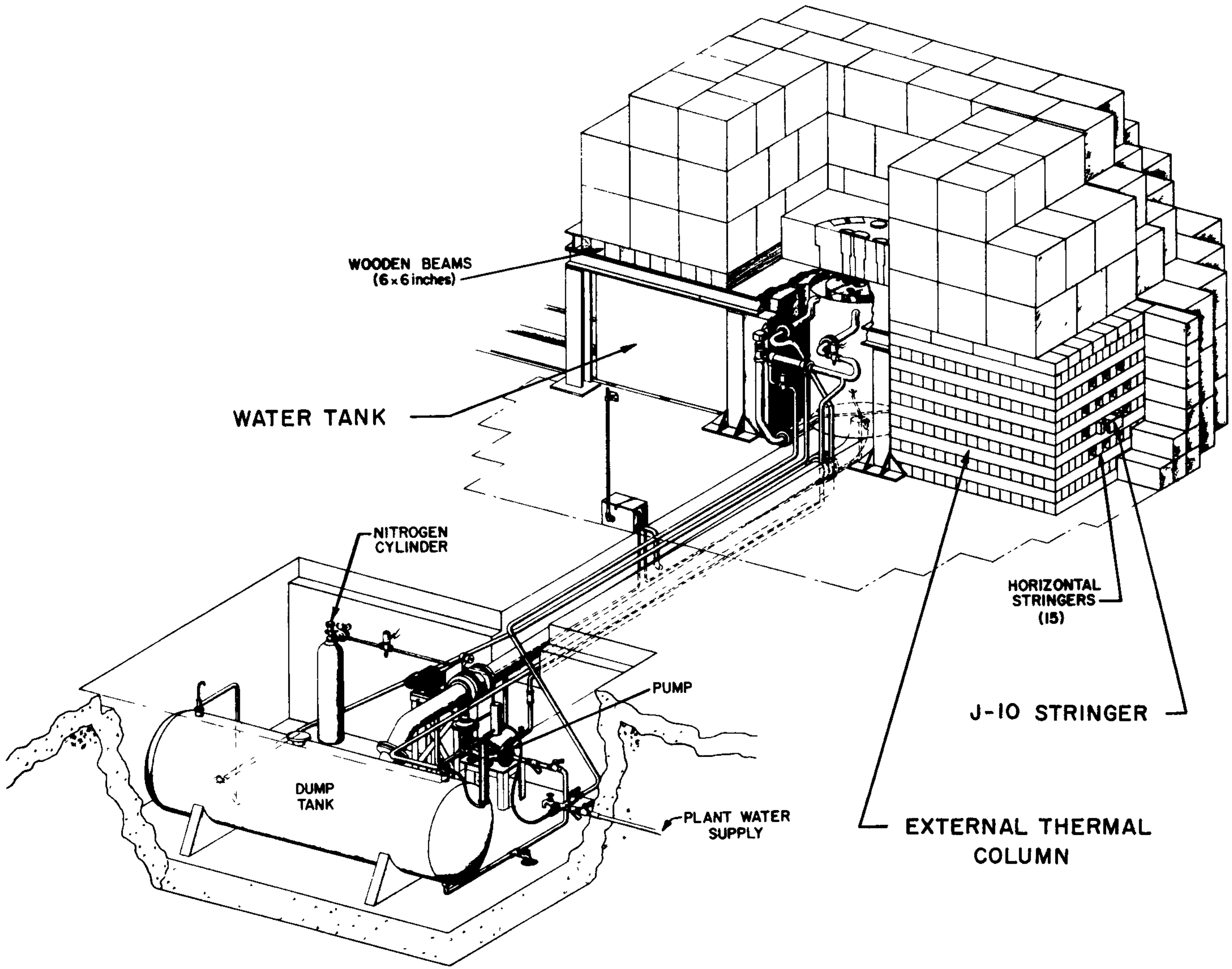

B.1. ISOMETRIC VIEW OF REACTOR (Ref. I-1)

B.2. PLAN SECTION OF CORE LATTICE AND REFLECTOR (Ref. I-7)

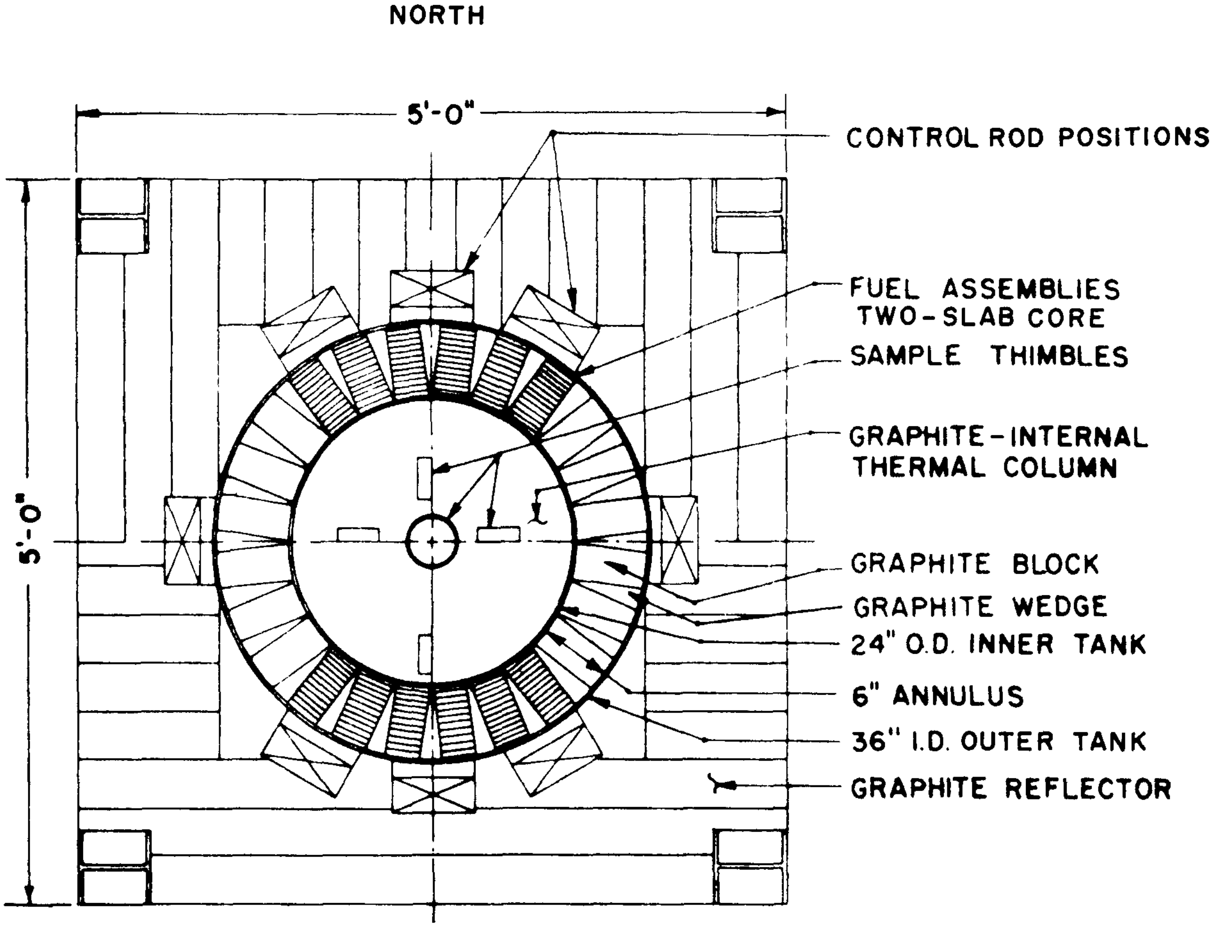

B.3. LOCATION CODING OF THE CORE AND THERMAL COLUMNS

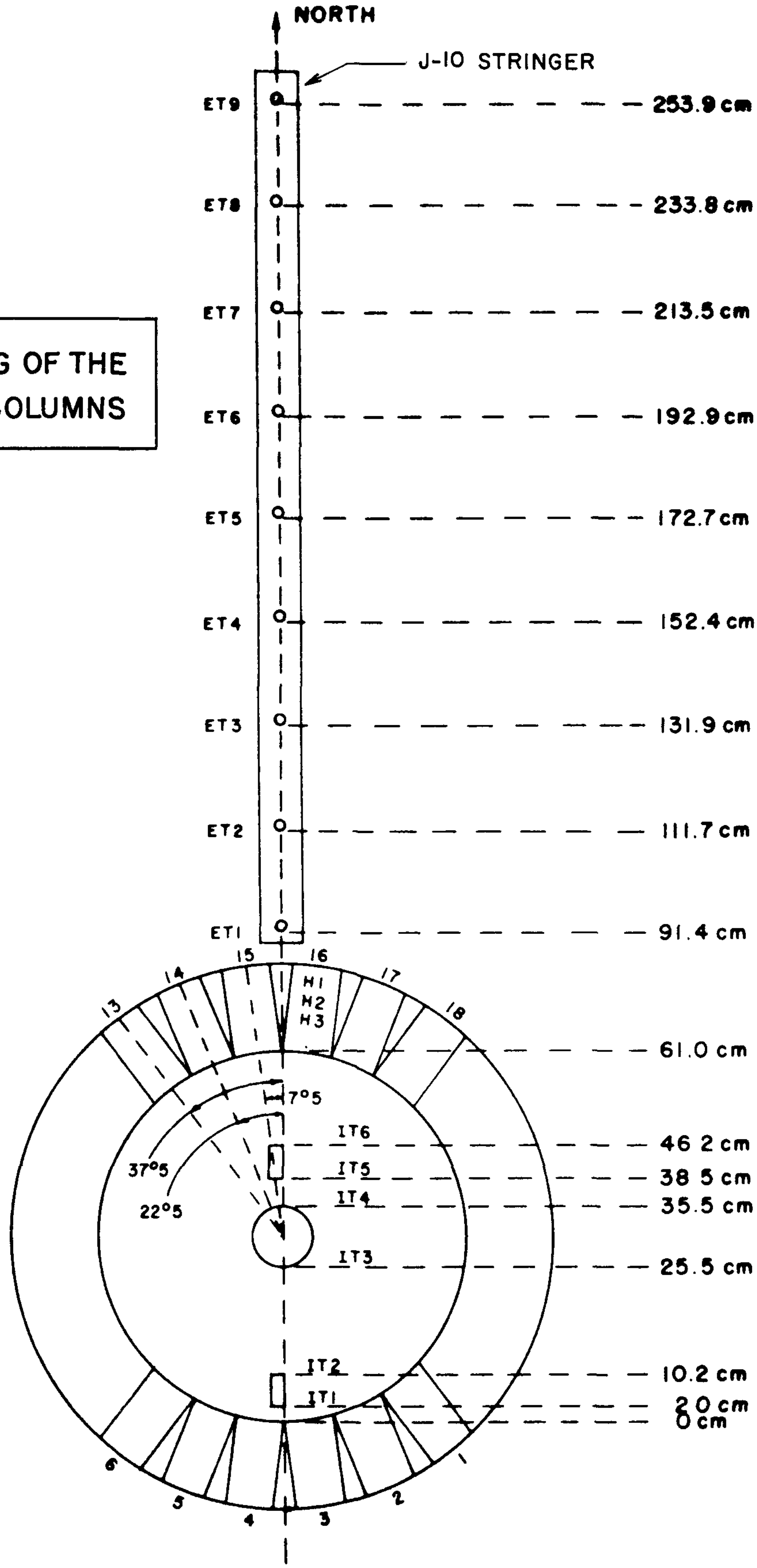

B.4. INTERLOCK SYSTEM
(Ref. I-7)

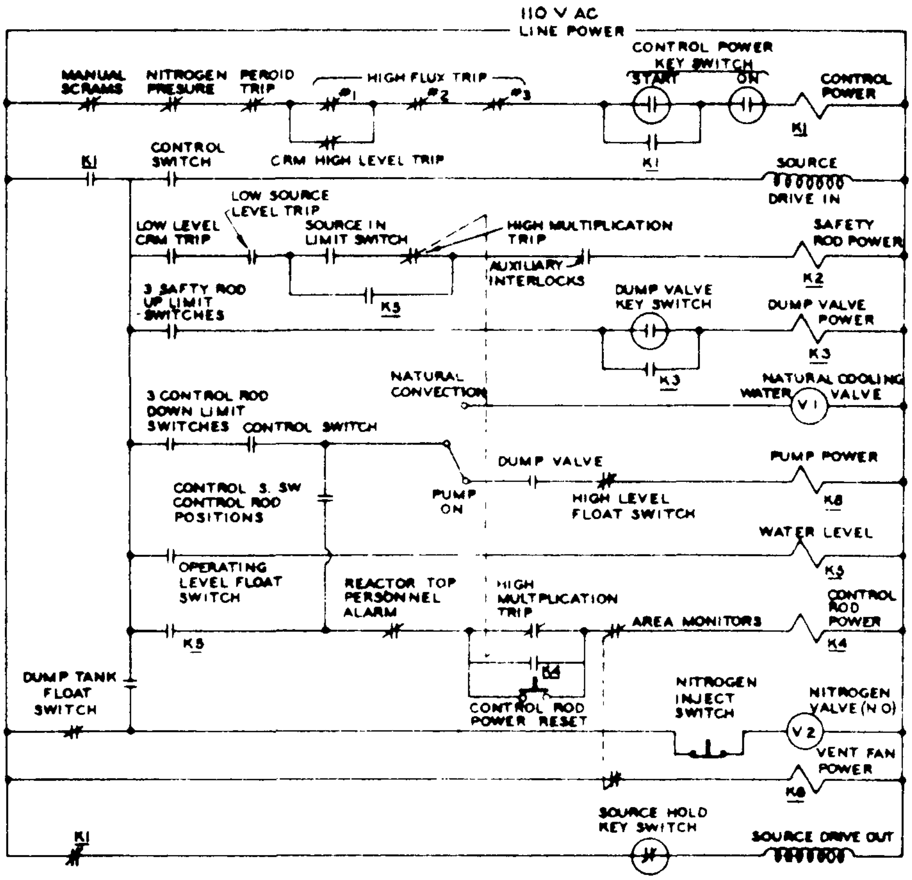

NOTE:

THE SEQUENCE OF STEPS DURING STARTUP IS FROM TOP TO BOTTOM.

B.5. FLOW DIAGRAM OF THE WATER SYSTEM (Ref. I-7)

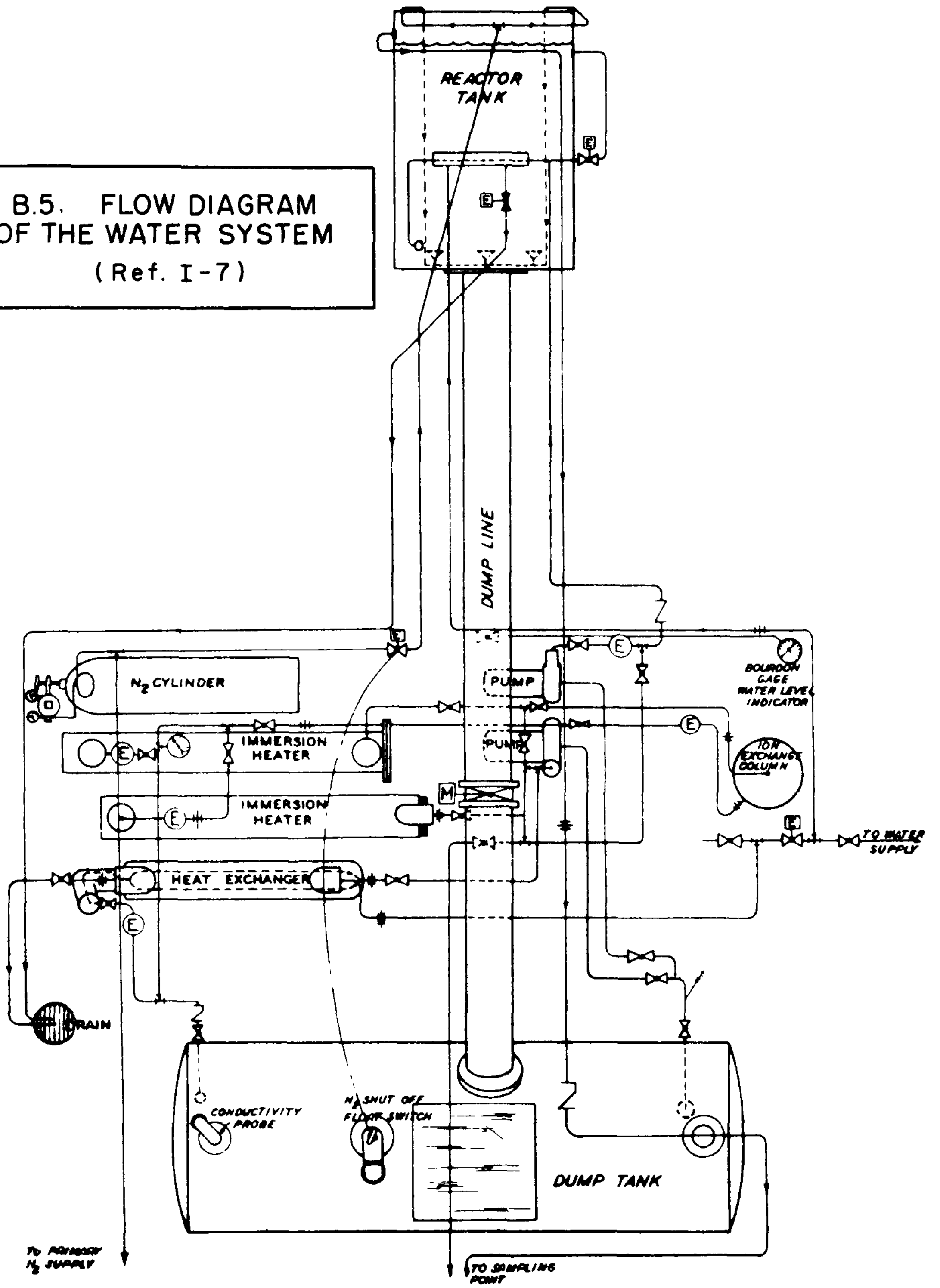

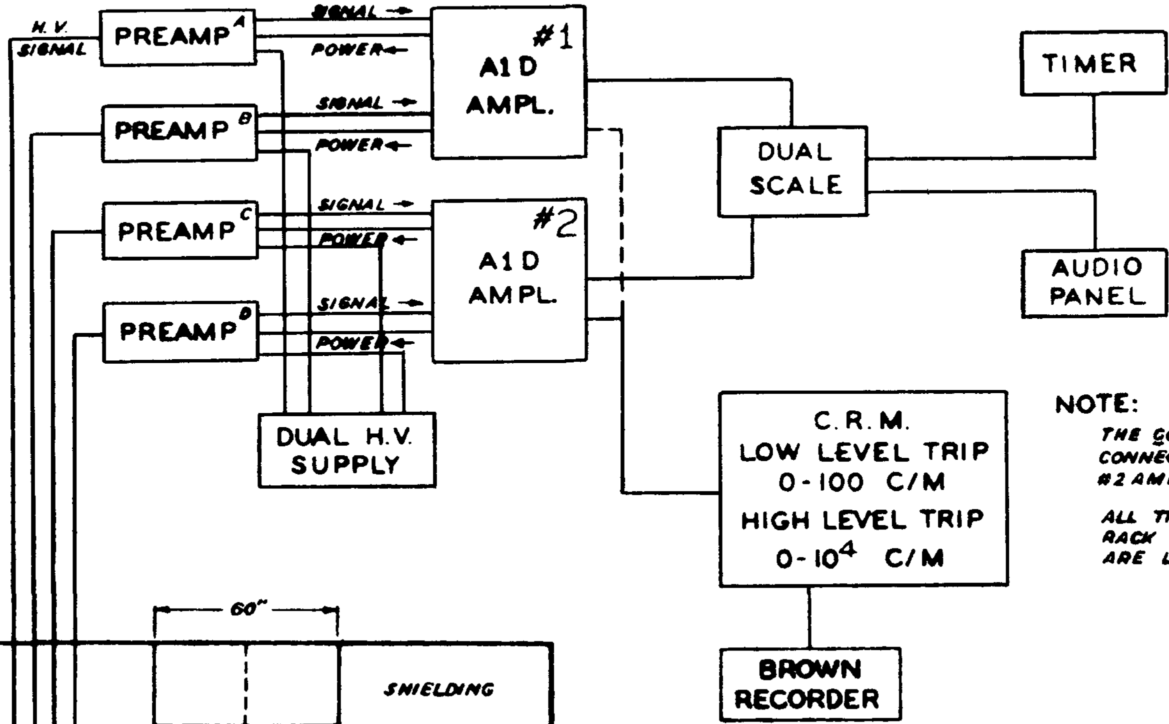

NOTE:
THE COUNTER RATE METER CAN BE CONNECTED TO #1 AMP (A-B) OR #2 AMP (C-D)

ALL THE CHASSIS ARE IN THE NORTH RACK EXCEPT THE PREAMPS WHICH ARE LOCATED IN THE REACTOR SHIELDING

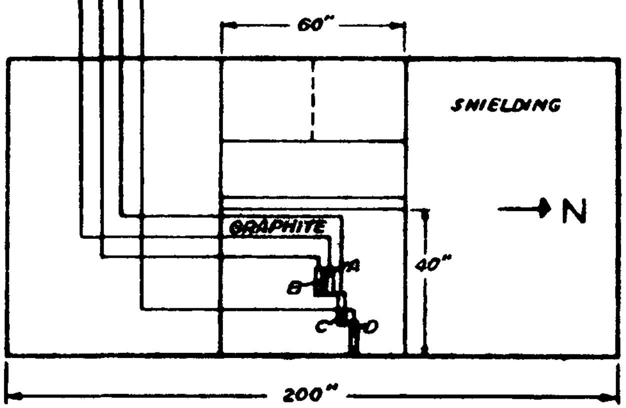

COUNTERS B AND D ARE COVERED WITH Cd

CROSS SECTION OF EAST FACE TAKEN OUTSIDE THE REFLECTOR WHERE THE DETECTORS ARE LOCATED

B.6. BF_3 PROPORTIONAL COUNTER CHANNELS
(Ref. I-7)

B.7. B^{10} ION CHAMBER CHANNELS (Ref. I-7)

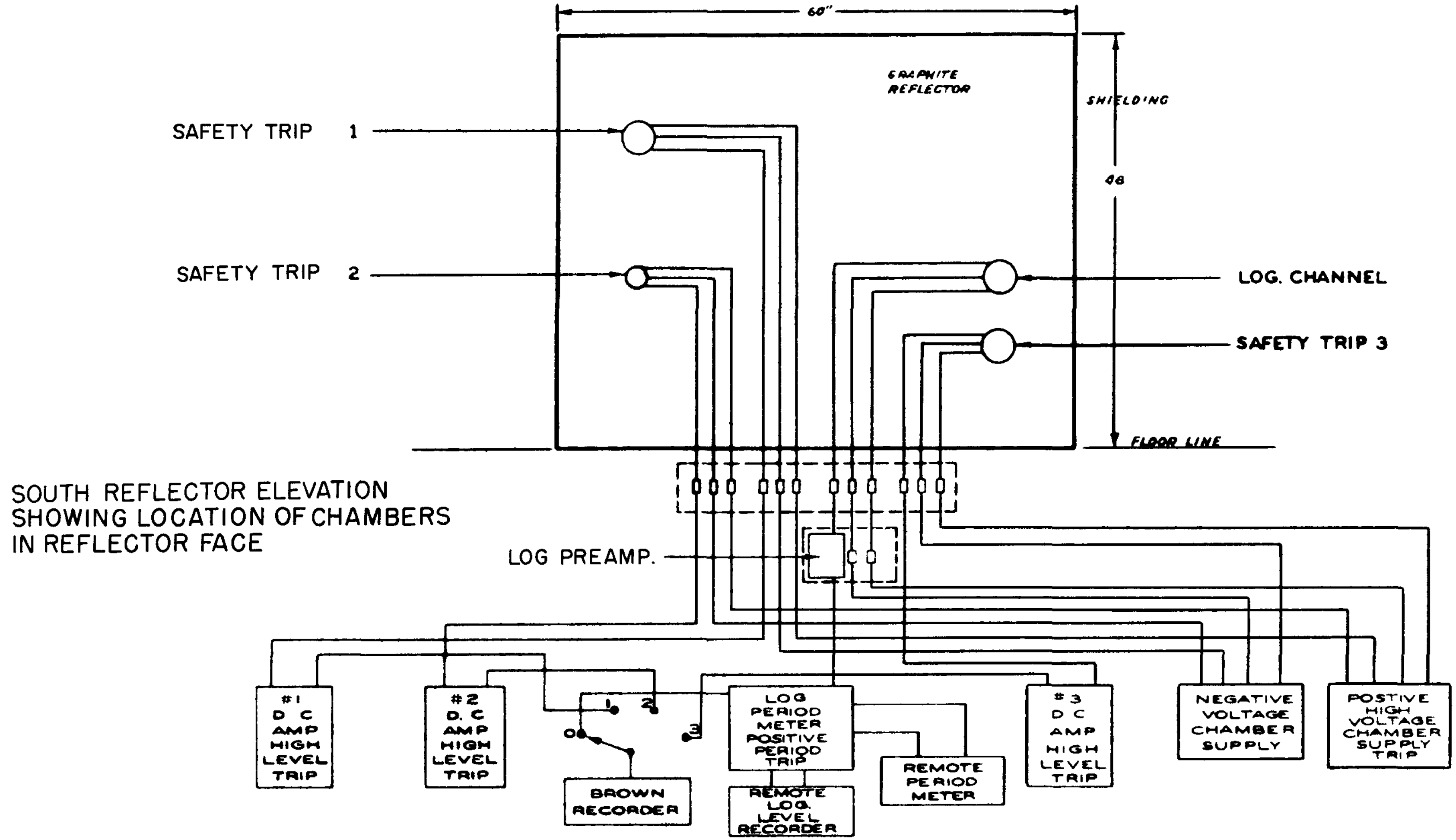

ALL CHASSIS IN THE SOUTH RACK EXCEPT LOG PREAMP., REMOTE PERIOD METER & THE LOG LEVEL RECORDER

B.8. BORON CHAMBER LOCATIONS IN SOUTH FACE OF REACTOR (Ref. V-12)

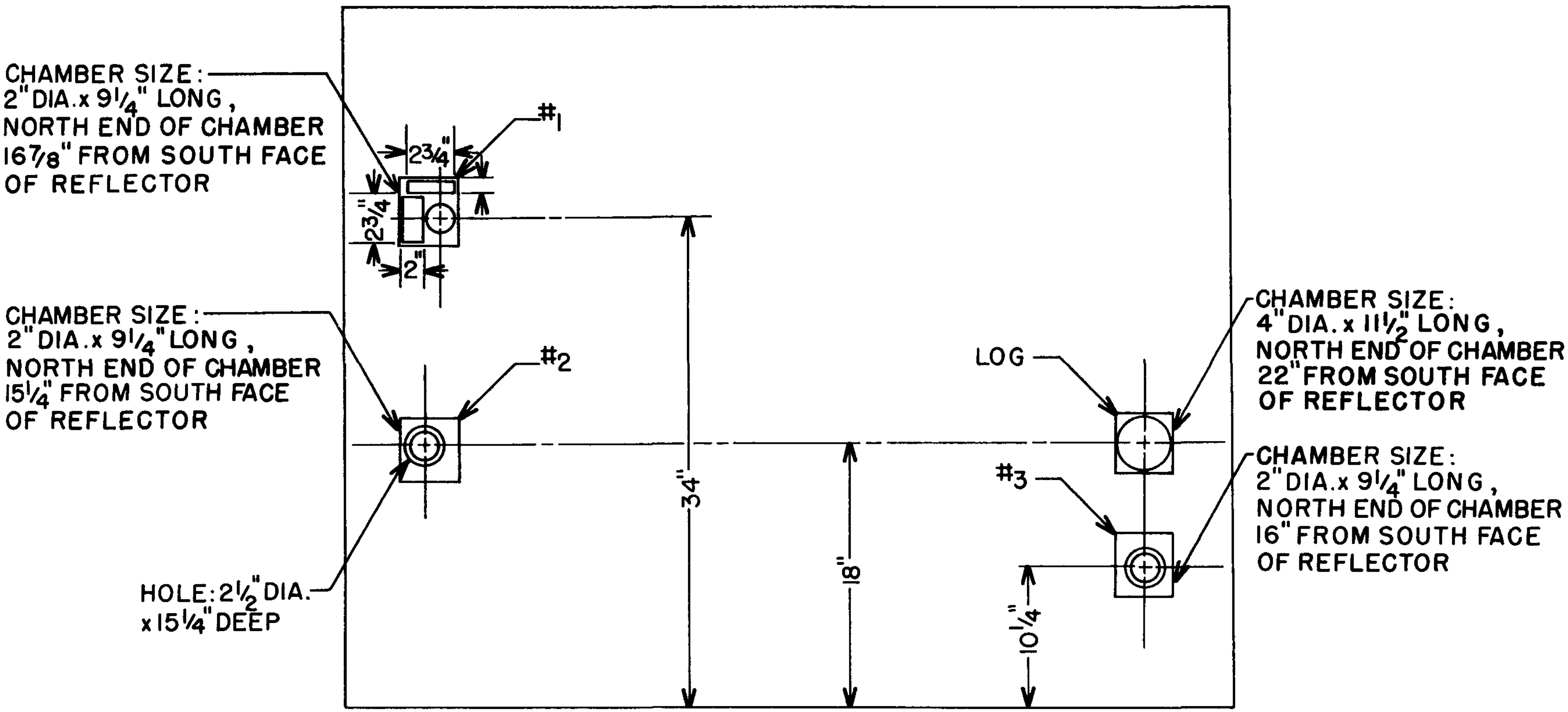

Section C

REACTOR OPERATIONS

This section outlines in some detail the procedures to be followed during checkout, startup, operation, and shutdown of the reactor. Many principles of safe operation are implied. The typical behavior of the multiplication meter during startup is shown. Also, the use of the meter as a safety device is presented by showing how its reading is related to k_{ex} during startup. A calculated curve showing the expected neutron flux behavior after step reactivity insertion and consequent power level trip is included to point out the essential safety of the system.

C.1. Reactor Checkout (Ref. I-7)

1. Renew, standardize and date log level chart.
2. Renew Brown recorder charts if necessary.
3. Turn on high voltage to BF_3 counters.
4. Turn pulse height, band width and gain controls in pulse amplifiers to operating positions.
5. Set all linear channels and CRM to most sensitive ranges.
6. Clear high-level, period and multiplication trips.
7. Obtain keys for reactor control power, dump valve clutch, and source-hold.
8. Obtain control power by turning key switch to start position.
9. Determine trip condition in low-level trips. Attempt to reset trips. If resetting is not possible, proceed to next step.
10. Insert source-hold key and energize circuit.
11. Turn master selector switch to source position, push control switch forward to drive source in until period meter reads about ten seconds. If period trip occurs at that time and control power is lost, proceed to next step.
12. Reset period trip, regain control power and drive source all the way in.
13. If, with source in, safety rod clutches are not energized (orange light off) before resetting low-level trips, proceed to next step.
14. Clear low-level trips; set high-level trips at normal operating conditions (90% of full scale).
15. Turn master selector switch to #1 safety rod position and drive rod out for about 15 sec, until orange light goes off.
16. Induce trip condition in CRM and linear channel #1 by changing trip setting. If control power is lost as indicated by orange light, proceed to next step.
17. Move trip settings back to normal, reset trips, regain control power.
18. If orange light indicates that safety rod #1 has dropped, proceed to next step.
19. Turn master selector switch to #2 safety rod position and drive rod out for about 15 sec, until orange light goes off.

20. Change trip setting in linear channel #2 to induce trip condition. If control power is lost and safety rod falls all the way in, proceed to next step.
21. Take trip settings back to normal, reset trips, regain control power.
22. Turn master selector switch to #3 safety rod position and drive rod out for about 15 sec, until orange light goes off.
23. Change trip setting in linear channel #3 to induce trip condition. If control power is lost and safety rod falls all the way, proceed to next step.
24. Move trip settings back to normal, reset trips, regain control power.
25. Drive each safety rod out. Insert dump valve clutch key and turn to start position. Close dump valve by turning master selector switch to dump valve position and by pushing forward on the control switch until green light turns on.
26. Close main nitrogen supply valve; bypass dump tank float switch by depressing button in pit.
27. Depress scram button. If dump valve opens freely and if nitrogen pressure reading in pressure gage falls to zero, proceed to next step.
28. Watch green light at console for indication of nitrogen pressure. If light is off and control power cannot be obtained with key switch, proceed to next step.
29. Open main valve for nitrogen supply; regain control power with key switch.
30. Drive out all three safety rods, close dump valve and pump water until normal operating level is achieved, as indicated by green light. Plug in photo cell. Pumping time: about 12 min.
31. Withdraw shim control rod for about 15 sec, until orange light goes off.
32. With hand gamma source induce trip condition in North area monitor. If power to control rod clutches and the heating and ventilating fans is lost, and if shim rod falls all the way in, proceed to next step.
33. Reset area monitor trip.
34. Withdraw coarse control rod for about 15 sec, until orange light goes off.

35. With hand gamma source induce trip condition in West area monitor, if power to control rod clutches and the heating and ventilating fans is lost, and if coarse rod falls all the way in, proceed to next step.

36. Reset area monitor trip.

37. Withdraw fine control rod for about 15 sec, until orange light goes off.

38. With hand gamma source induce trip condition in South area monitor. If power to control rod clutches and the heating and ventilating fans is lost, and if fine rod falls all the way in, proceed to next step.

39. Reset area monitor trip.

40. Withdraw any control rod for about 15 sec, until orange light goes off.

41. Interrupt light beam to photocell. Power to control rod clutches should be lost if alarm system is working properly.

C.2. General Startup Procedure (Ref. I-7)

The following is a condensed version of the process as described in ANL-6036, Operating Manual for the Argonaut Reactor.

1. Secure the keys for reactor control power, and dump valve clutch.
2. Turn on both the high-voltage supplies to the four BF_3 counters.
3. Turn the pulse-height selector and the gain controls in the A1D amplifiers to their normal operating positions.
4. Set range-selector switches of all three linear trip channels to their most sensitive scales (10^{-10} amp full scale).
5. Reset the four high-level, the positive period and the high-multiplication trips.
6. Turn on the nitrogen pressure.
7. Insert both keys and turn the control power on.
8. Turn the master selector switch to the "Source" position. Insert the source by pushing forward on the control switch.
9. Make log book entries in the appropriate columns.
10. Reset the low-level trips in the source interlock and the count rate channels.
11. Raise each safety rod.

12. Turn the selector switch to the "Dump Valve" position; energize the "Dump Valve Clutch" key switch and push forward on the control switch to close the valve.
13. Turn selector switch to "Water Level" position. Turn pump switch to "Pump on." Hold control switch in the forward position, admitting water to the core.
14. Make the appropriate log book entries.
15. Raise the control rods as required for criticality.
16. To increase the power to a desired operating level, a control rod (coarse or fine) should be withdrawn further to produce a conveniently short positive period. When the reactor power nears the desired level, minor readjustments needed to maintain criticality can be made.
17. Make the appropriate log book entries.
18. Additional log book entries should be made when reactor power level is changed; any other significant event occurs; or run is terminated.

C.3. Shutdown (Ref. I-7)

The following is a condensed version of the process as described in ANL-6036, Operating Manual for the Argonaut Reactor.

1. Depress the scram button (manual scram).
2. Turn off the high voltage to BF_3 counters.
3. Make appropriate entries in the log book.
4. Determine that the experimental facilities are plugged and locked, that power to the crane is shut off and locked, and that the keys are put away in the key safe.
5. Withdraw the reactor keys and store them in the key safe.

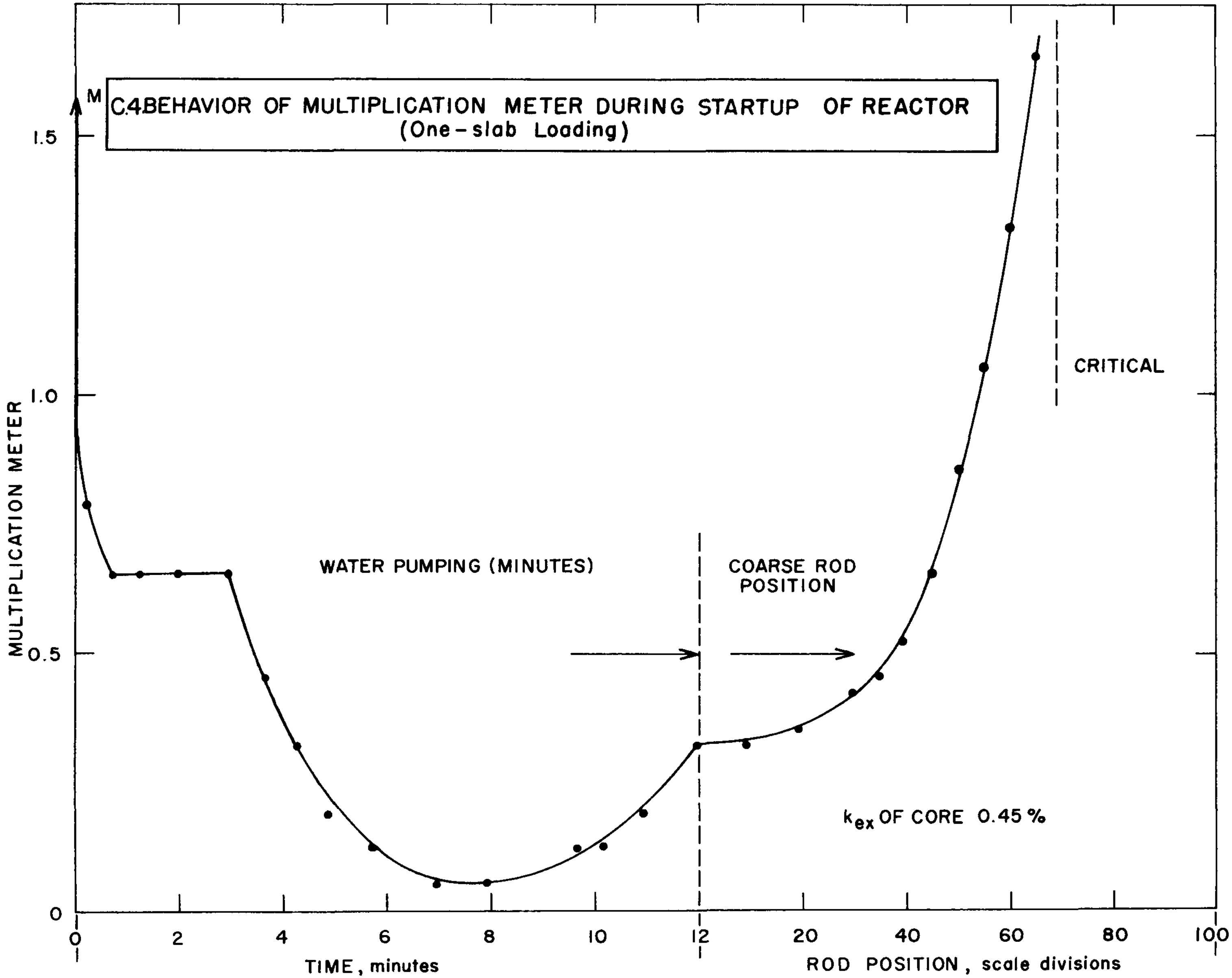

C.4 BEHAVIOR OF MULTIPLICATION METER DURING STARTUP OF REACTOR
(One-slab Loading)

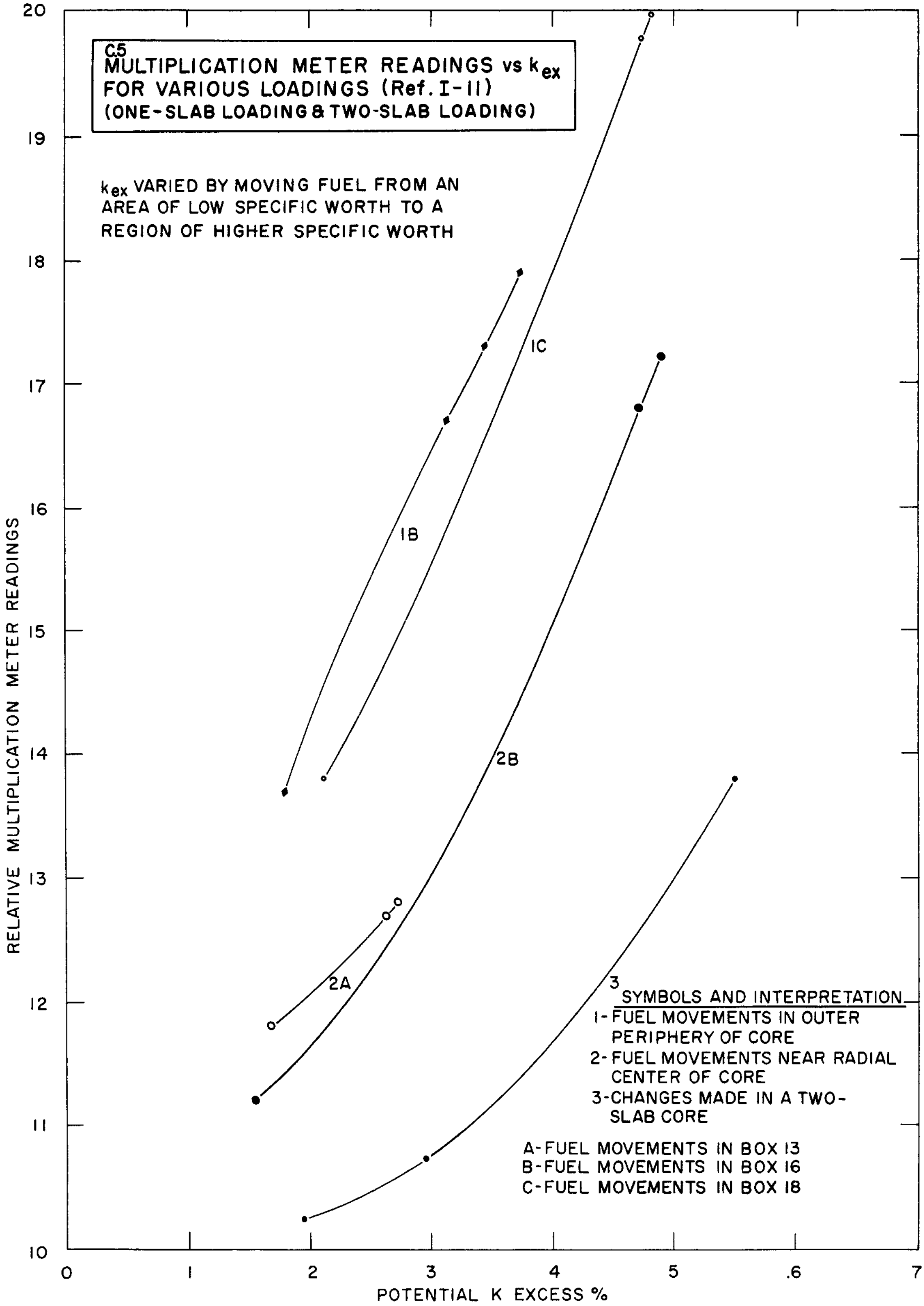
C5
MULTIPLICATION METER READINGS vs k_{ex}
FOR VARIOUS LOADINGS (Ref. I-11)
(ONE-SLAB LOADING & TWO-SLAB LOADING)
k_{ex} VARIED BY MOVING FUEL FROM AN AREA OF LOW SPECIFIC WORTH TO A REGION OF HIGHER SPECIFIC WORTH
1B
1C
2A
2B
3
SYMBOLS AND INTERPRETATION
1- FUEL MOVEMENTS IN OUTER PERIPHERY OF CORE
2- FUEL MOVEMENTS NEAR RADIAL CENTER OF CORE
3-CHANGES MADE IN A TWO-SLAB CORE
A- FUEL MOVEMENTS IN BOX 13
B- FUEL MOVEMENTS IN BOX 16
C- FUEL MOVEMENTS IN BOX 18
RELATIVE MULTIPLICATION METER READINGS
POTENTIAL K EXCESS %
10
11
12
13
14
15
16
17
18
19
20
0
1
2
3
4
5
.6
7

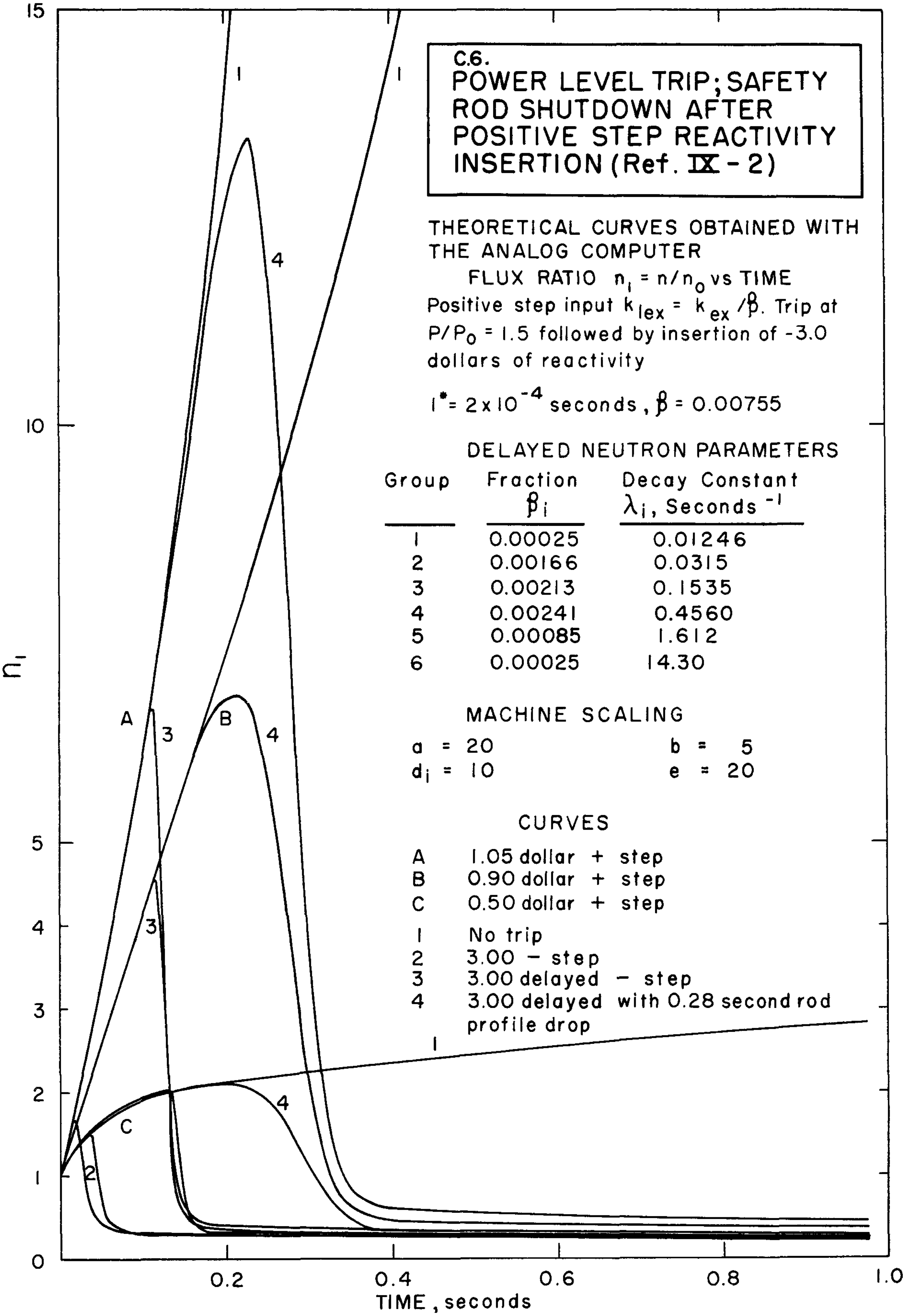
C.6.
POWER LEVEL TRIP; SAFETY ROD SHUTDOWN AFTER POSITIVE STEP REACTIVITY INSERTION (Ref. IX - 2)
THEORETICAL CURVES OBTAINED WITH THE ANALOG COMPUTER
FLUX RATIO $n_1 = n/n_0$ vs TIME
Positive step input $k_{1ex} = k_{ex}/\beta$. Trip at $P/P_0 = 1.5$ followed by insertion of -3.0 dollars of reactivity
$l^* = 2 \times 10^{-4}$ seconds, $\beta = 0.00755$
DELAYED NEUTRON PARAMETERS
Group
Fraction β_i
Decay Constant λ_i, Seconds $^{-1}$
1 0.00025 0.01246
2 0.00166 0.0315
3 0.00213 0.1535
4 0.00241 0.4560
5 0.00085 1.612
6 0.00025 14.30
MACHINE SCALING
a = 20
b = 5
d_i = 10
e = 20
CURVES
A 1.05 dollar + step
B 0.90 dollar + step
C 0.50 dollar + step
1 No trip
2 3.00 − step
3 3.00 delayed − step
4 3.00 delayed with 0.28 second rod profile drop
n_1
TIME, seconds
0
1
2
3
4
5
10
15
0.2
0.4
0.6
0.8
1.0
A
B
C

Section D

REACTOR CONSTANTS

The nuclear and engineering constants of a reactor are basic to the initial design work. After the reactor construction, they are of fundamental importance in the design of experiments and in the understanding of the results.

Various constants for the core and reflector of one-slab, two-slab, and annular core loadings are given. Most of the data is the result of theoretical calculations using two-group theory and assuming a homogenized core, with the remainder being experimental values.

D.1. <u>One Slab - Theoretical Two-group Constants for the Homogenized Argonaut One-slab Loading.</u> (Ref. II-4)

The constants given below were used to calculate the critical mass (kg U^{235}) of the Argonaut one-slab loading when located on the North side of the annulus. A PDQ code on the IBM-704 was used to make the calculation. The annular one-slab loading was approximated by a straight slab of volume equal to six fuel boxes plus five graphite wedges. The critical mass of U^{235} obtained from this calculation was 1.90 kg; the experimental value was 1.93 kg for a loading with even distribution of U^{235}.

W_{25} = kilograms of U^{235} in Argonaut

D.1.a. <u>Core Constants</u>

<u>Volume Fractions</u>

$f(\text{graphite}) = 0.211170$ $\quad f(\text{Al}) = 0.205380 - 0.0133114\,W_{25}$

$f(H_2O) = 0.583450$ $\quad f(U_3O_8) = 0.0133114\,W_{25}$

<u>Temperatures</u>

$T_{\text{moderator}} = 20°C$

D.1.b. <u>Thermal Group Constants</u> (including disadvantage factors and temperature effects)

<u>Disadvantage Factors</u>

$$\frac{\bar{\phi}_{H_2O}}{\bar{\phi}_{\text{fuel plate}}} = 1.0577 \text{ (P-3 calculation assuming 20 g } U^{235} \text{ per plate)}$$

$$\frac{\bar{\phi}_{\text{graphite}}}{\bar{\phi}_{\text{fuel plate}}} = 1.097 \quad \text{(diffusion theory)}$$

$$\bar{\Sigma}_a = 0.013545 + 0.025273\,W_{25}\ \text{cm}^{-1}$$

$$\nu\bar{\Sigma}_{\text{fiss}} = 0.0518305\,W_{25}\ \text{cm}^{-1}$$

$$L^2 = \frac{1}{0.064073 + 0.11955\,W_{25}}\ \text{cm}^2$$

$$\left.\begin{array}{l} D_{th} = 0.21503\ \text{cm} \\ \bar{\Sigma} = 1.5502\ \text{cm}^{-1} \end{array}\right\}\ \text{approx. independent of } W_{25}$$

$$K_\infty = \frac{\nu\bar{\Sigma}_f}{\Sigma_a} = 1.5996 \text{ for } W_{25} = 1.90\ \text{kg}$$

$$\Sigma_{\text{fiss}} = 0.020984\,W_{25}\ \text{cm}^{-1}$$

D.1.c. Fast Group Constants

$\tau = 61.3\ cm^2$

$D_f = 1.300\ cm$

$E_c = 0.181\ ev$

$\Sigma_f = 0.02120\ cm^{-1}$

D.1.d. Reflector Constants

Graphite

$L_{th}^2 = 1700\ cm^2$ (experimental)

$\tau = 385\ cm^2$

$D_{th} = 0.916\ cm$

$D_f = 1.14\ cm$

$\Sigma_a = 0.000539\ cm^{-1}$

$\Sigma_f = 0.002961\ cm^{-1}$

Water

$B_z^2 = 0.00176\ cm^{-2}$

$\tau = 31.8\ cm^2$

$D_{th} = 0.142\ cm$

$D_f = 1.19\ cm$

$\Sigma_a = 0.0195\ cm^{-1}$

$\Sigma_f = 0.0374\ cm^{-1}$

Total Reflector Savings (theoretical)

$R_z = 14.0\ cm$

$R_x = 22.9\ cm$

$R_y = 28.5\ cm$

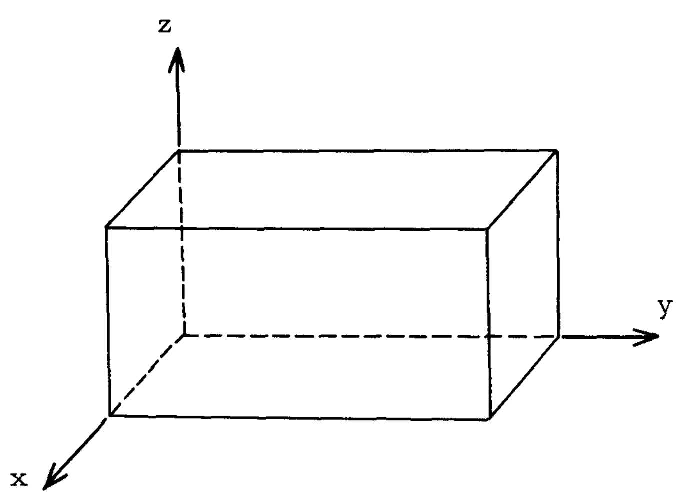

D.1.e. Miscellaneous Constants (Ref. II-1)

Volume fraction per kg U^{235} = 9.86060×10^{-4}/kg

	at 2 kg	at 2.2 kg
Σ_{au}	$0.05641912 \text{ cm}^{-1}$	$0.06206097 \text{ cm}^{-1}$
Σ_{am}	$0.01303442 \text{ cm}^{-1}$	$0.01303186 \text{ cm}^{-1}$
L^2	3.92866935 cm^2	3.63363576 cm^2
B^2	$0.01038971 \text{ cm}^{-2}$	$0.01089301 \text{ cm}^{-2}$
k_∞	1.6896420	1.71903181

D.2. Two Slab

D.2.a. Miscellaneous Thermal (Ref. II-1)

	at 2 kg	at 2.2 kg
Σ_{au}	$0.05641912 \text{ cm}^{-1}$	$0.06206097 \text{ cm}^{-1}$
Σ_{am}	$0.01303442 \text{ cm}^{-1}$	$0.01303186 \text{ cm}^{-1}$
L^2	3.92866935 cm^2	3.63363576 cm^2
B_c^2	0.00983 cm^{-2}	$0.01089301 \text{ cm}^{-2}$
k_∞	1.6896420	1.71903181

D.2.b. Miscellaneous Experimental (Ref. IV-6)

1957 ASEE-AEC Summer Institute Report

Two-slab loading of 12 fuel boxes

Reflector saving	9.9 cm
Vertical buckling	0.01 cm^{-2}
Peak flux at 10 kw in thermal column center	1.16×10^{11} n/cm²/sec

Average flux = 0.618 peak flux

D.3. Annulus - Theoretical Two-group Constants for a Homogenized Annular Loading

D.3.a. Core Constants (Ref. II-1 and II-6)

$\tau = 65 \text{ cm}^2$ $\qquad$ $\Sigma_a = 0.07715 \text{ cm}^{-1}$

$D_{th} = 0.27286$ cm $\qquad$ $\Sigma_{au} = 0.06412 \text{ cm}^{-1}$

$D_f = 1.27$ cm $\qquad \Sigma_{am} = 0.01303$ cm^{-1}

$k_\infty = 1.72868$ $\qquad \Sigma_{af} = 0.01953$ cm^{-1}

$$B_z^2 = 0.00175 \text{ cm}^{-2}$$

Core volume fraction per kg U = 5.603×10^{-4} (M in kg)

Inner reflector: $D_f = 1.1$

$D_{th} = 0.903$

$W_{25} = 4.0$ kg

$T_M = 20°C$

$V_c = 87.003$ liters

D.3.b. Thermal Group Constants

$\Sigma_a = 0.014701 + 0.016226\ W_{25}$ cm^{-1}

$\Sigma_{fiss} = 0.033223\ W_{25}$ cm^{-1}

$L^2 = 2.657$ cm^2

D.3.c. Fast Group Constants

$\tau = 58.8$ cm^2

$D_f = 1.315$ cm^2

$\Sigma_f = 0.022364$ cm^{-1}

D.3.d. Reflector Constants

Graphite	H_2O	Concrete
$\tau = 385$ cm^2	$\tau = 31.8$ cm^2	$\tau = 205$ cm^2
$D_f = 1.14$ cm	$D_f = 1.19$ cm	$D_f = 1.51$ cm
$D_{th} = 0.916$ cm	$\Sigma_f = 0.0374$ cm^{-1}	$\Sigma_f = 0.00737$ cm^{-1}
$\Sigma_f = 0.002961$ cm^{-1}	$D_{th} = 0.142$ cm	$D_{th} = 0.707$ cm
$\Sigma_a = 0.000539$ cm^{-1}	$\Sigma_a = 0.0195$ cm	$\Sigma_a = 0.00736$ cm^{-1}

D.3.e. Materials outside Graphite Reflector

2/3 concrete, 1/6 graphite, 1/6 H_2O

$\tau = 140 \text{ cm}^2$

$D_f = 1.37$ cm

$\Sigma_f = 0.00979 \text{ cm}^{-1}$

$D_{th} = 0.439$ cm

$\Sigma_a = 0.00822 \text{ cm}^{-1}$

D.3.f. Fluxes and Reactivity Effects

$\bar{\phi}(th)_{core} = 6.5 \times 10^{10}$ n/cm²/sec

for 10-kw operation

$$\frac{\phi(th)_{max}}{\bar{\phi}(th)_{core}} = 2.22$$

where the maximum is in the internal thermal column

Worth of Al tanks and thin H_2O shell $\sim -1.3\%$ $\Delta k/k$

Worth of control plate voids $\sim -0.3\%$ $\Delta k/k$

D.4. Six Sets of Two Boxes

$k_\infty = 1.76062$	$B^2 = 0.01161 \text{ cm}^{-2}$
$\Sigma_a = 0.8484 \text{ cm}^{-1}$	$B_z^2 = 0.00175 \text{ cm}^{-2}$
$1/L^2 = 0.31092 \text{ cm}^2$	$\Sigma_{au} = 0.07182 \text{ cm}^{-1}$
$1/L^2 + 1/\tau = 0.32758 \text{ cm}^{-2}$	$\tau = 60 \text{ cm}^2$

Section E

KINETICS

A series of theoretical curves interrelating neutron density, time, and the magnitude of step changes in reactivity is presented. One important use of this series is for control rod calibration; a calibrated control rod is a basic reactivity standard for other reactor experiments. The following section (Section F) deals with rod calibration.

The sensitivity of the above curves to the basic assumptions of neutron lifetime and choice of delayed neutron parameters is shown. One curve is included that compares the theoretical and experimental determinations of flux ratio with time after a negative step change in reactivity. Theoretical and experimental curves of the effect of nitrogen injection on reactor power are given. The effect of introducing a negative reactivity step when the reactor is on a positive period has been studied experimentally and with the analog computer; the results are included.

E.1. Flux-time Dependence (Theoretical)

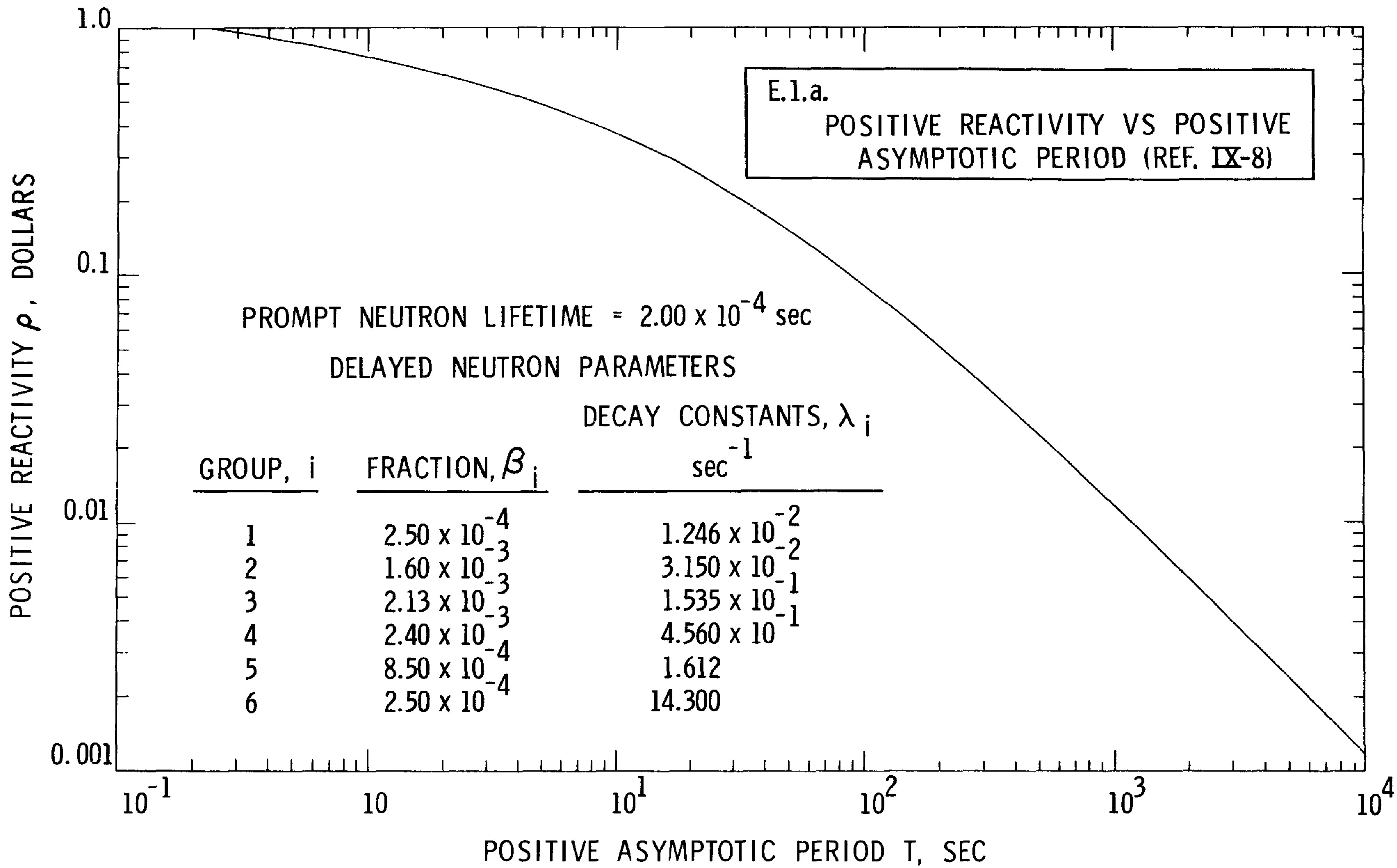
E.1.a.
POSITIVE REACTIVITY VS POSITIVE ASYMPTOTIC PERIOD (REF. IX-8)
PROMPT NEUTRON LIFETIME = 2.00 x 10^-4 sec
DELAYED NEUTRON PARAMETERS
GROUP, i
FRACTION, β_i
DECAY CONSTANTS, λ_i sec^-1
1 2.50 x 10^-4 1.246 x 10^-2
2 1.60 x 10^-3 3.150 x 10^-2
3 2.13 x 10^-3 1.535 x 10^-1
4 2.40 x 10^-3 4.560 x 10^-1
5 8.50 x 10^-4 1.612
6 2.50 x 10^-4 14.300
1.0
0.1
0.01
0.001
POSITIVE REACTIVITY ρ, DOLLARS
10^-1
10
10^1
10^2
10^3
10^4
POSITIVE ASYMPTOTIC PERIOD T, SEC

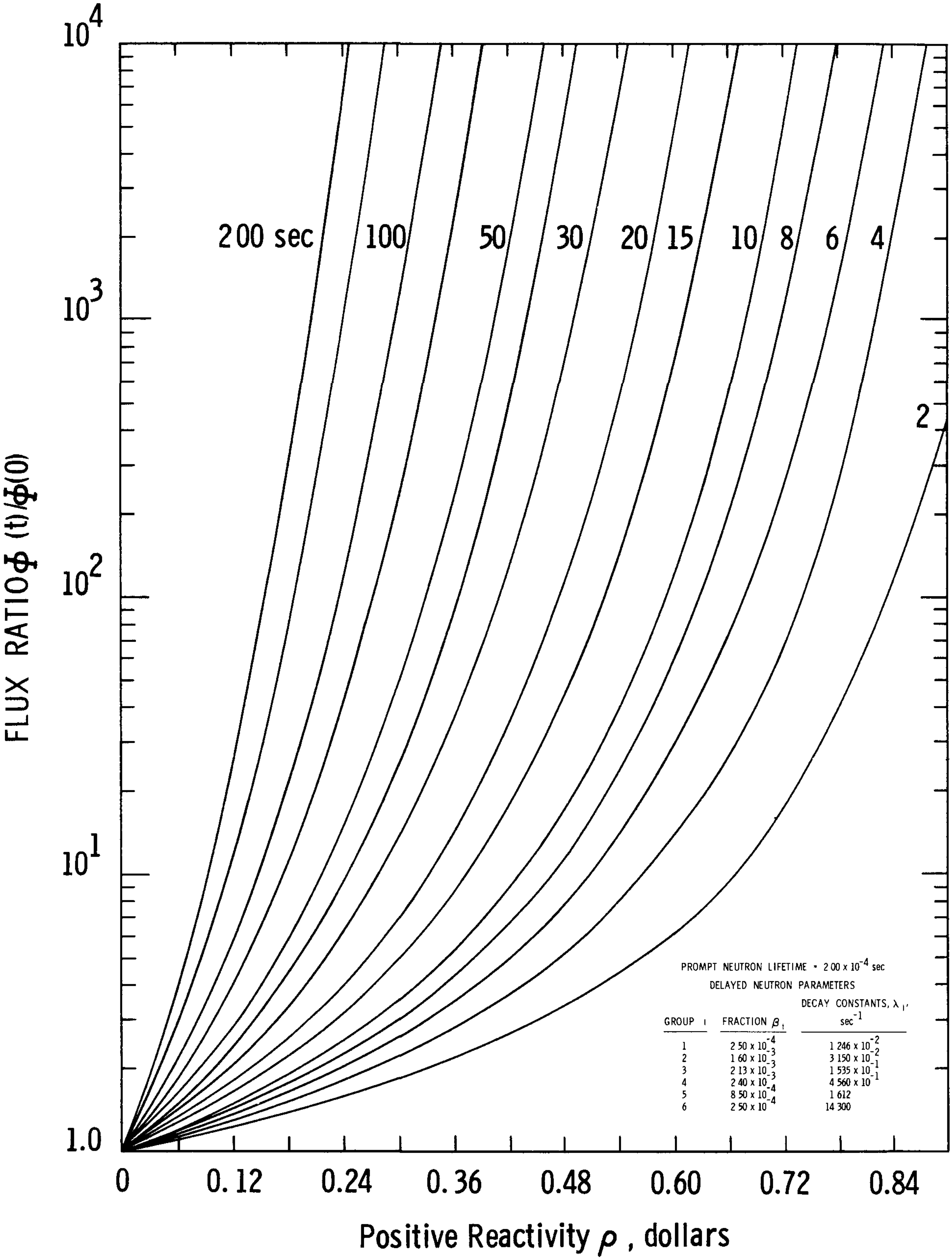

E.1.b.
FLUX RATIO VS POSITIVE REACTIVITY STEP FOR VARIOUS TIMES (REF. PRIVATE COMMUNICATION - AUTHORS OF IX-8)

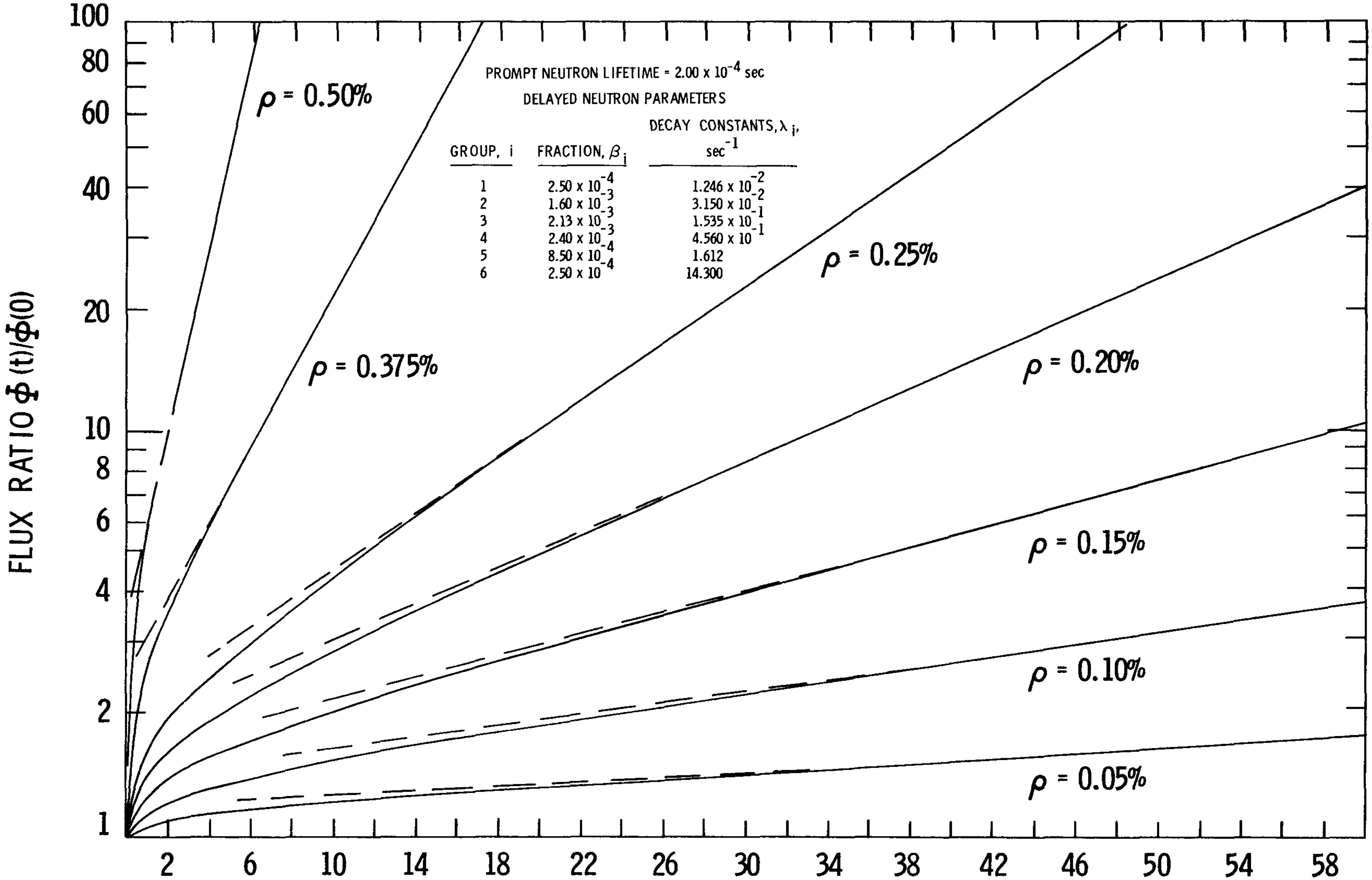

E.1.c.
FLUX RATIO VS TIME AFTER POSITIVE STEP CHANGE IN REACTIVITY (REF. PRIVATE COMMUNICATION - AUTHORS OF IX-8)

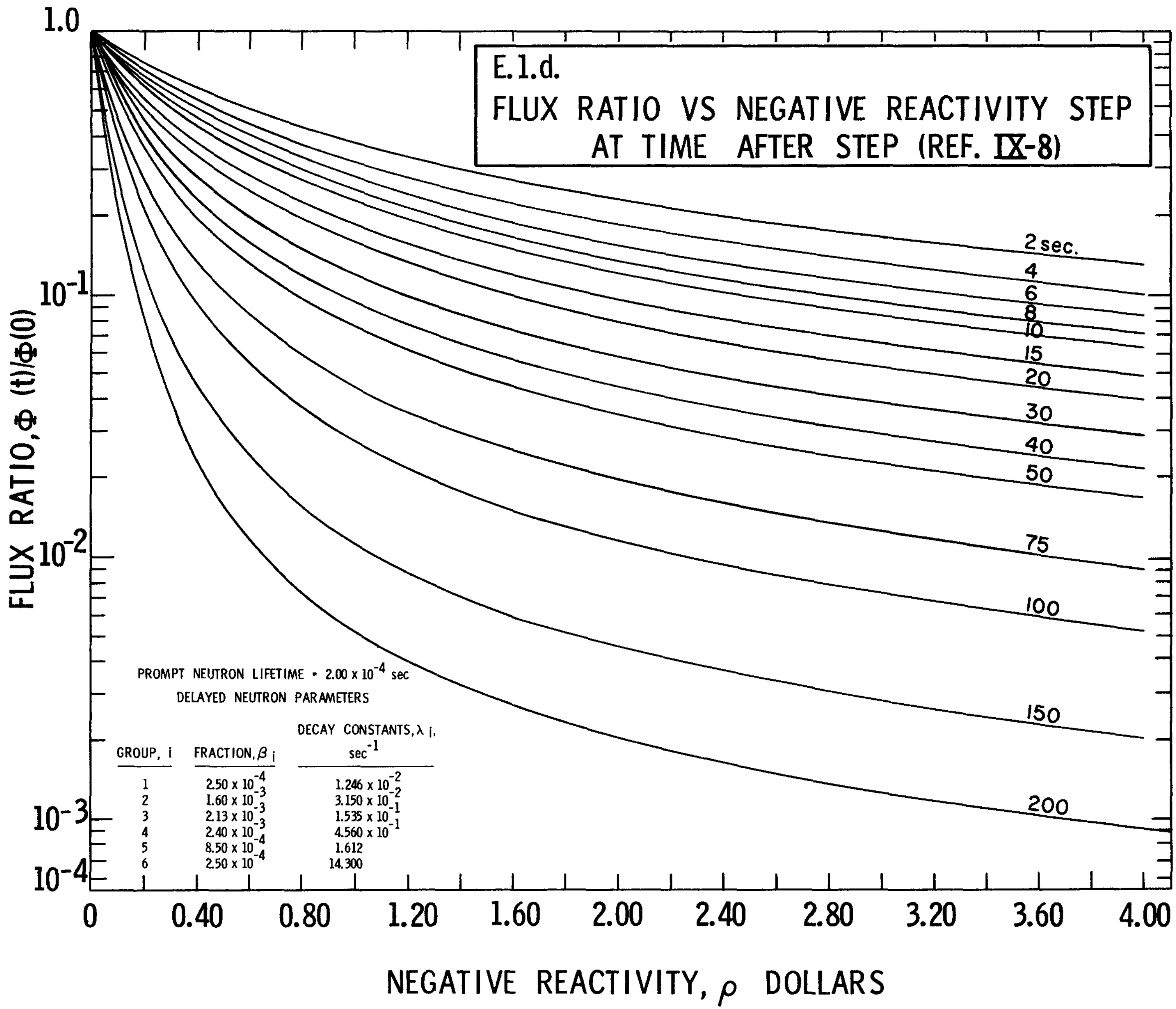

GROUP, i	FRACTION, β_i	DECAY CONSTANTS, λ_i, sec^{-1}
1	2.50×10^{-4}	1.246×10^{-2}
2	1.60×10^{-3}	3.150×10^{-2}
3	2.13×10^{-3}	1.535×10^{-1}
4	2.40×10^{-3}	4.560×10^{-1}
5	8.50×10^{-4}	1.612
6	2.50×10^{-4}	14.300

E.1.d.
FLUX RATIO VS NEGATIVE REACTIVITY STEP AT TIME AFTER STEP (REF. IX-8)

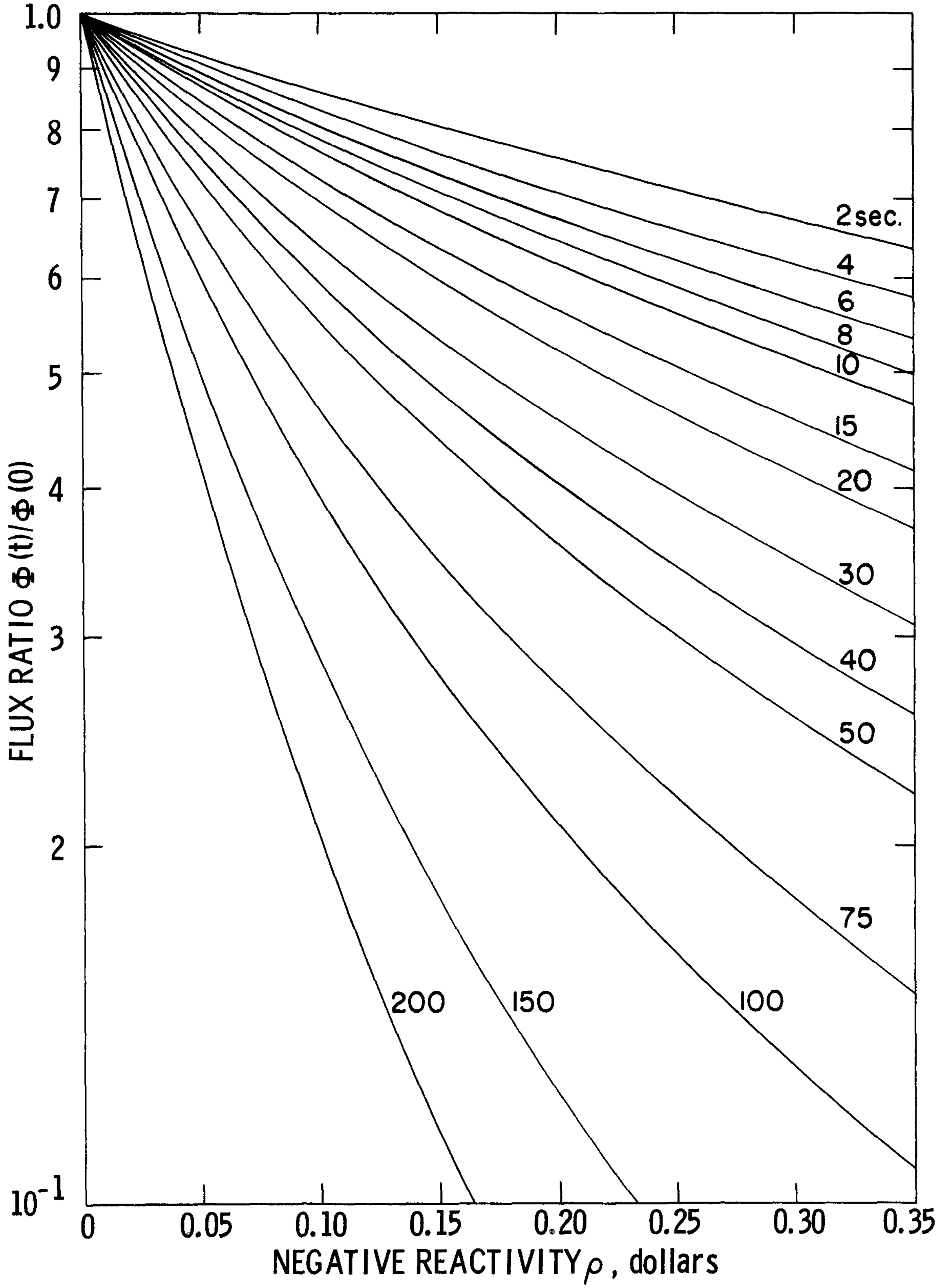

E.1.e.
FLUX RATIO VS NEGATIVE REACTIVITY STEP AT TIME AFTER STEP (REF. PRIVATE COMMUNICATION - AUTHORS OF IX-8)

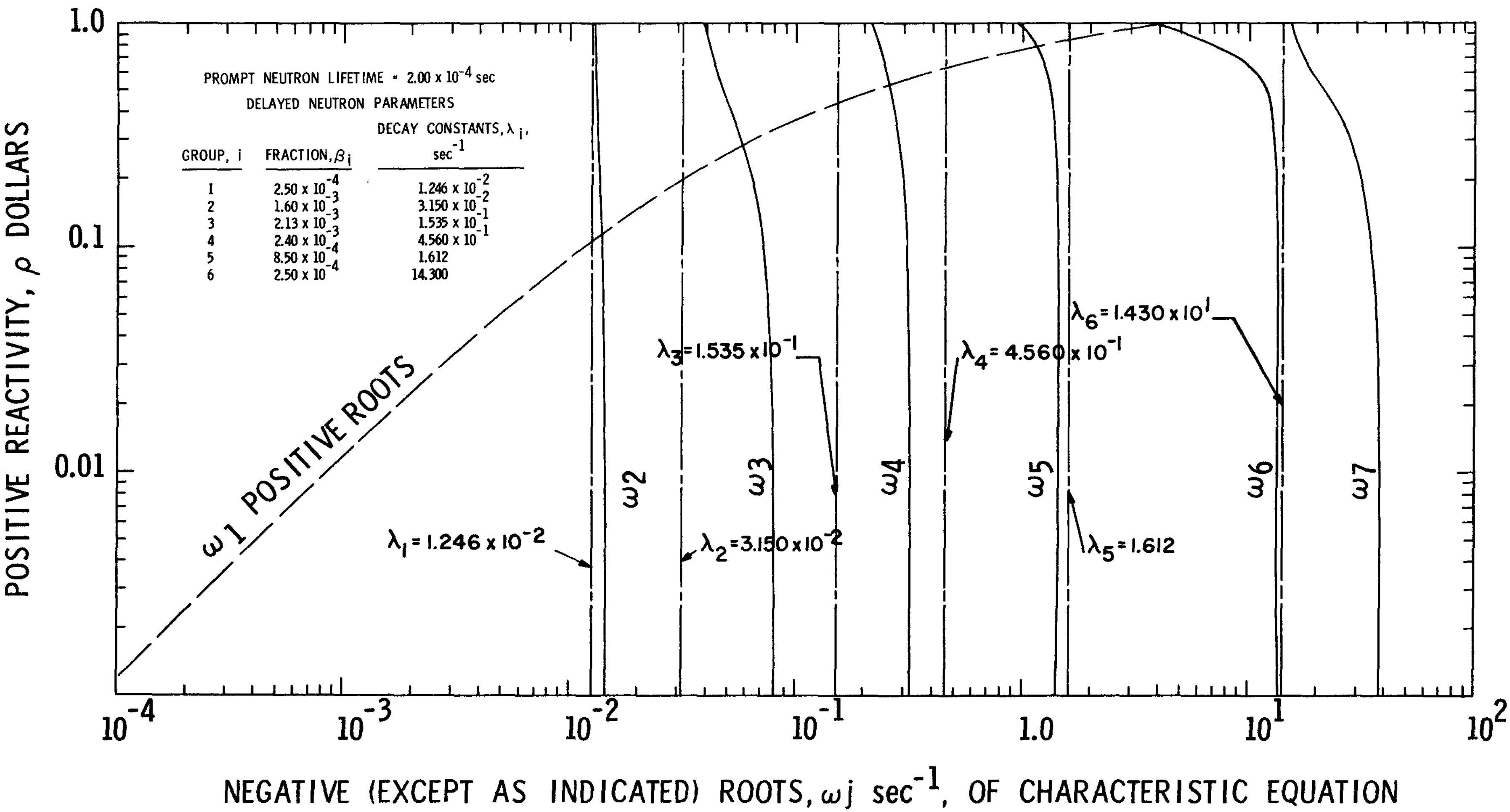

E.1.f.

POSITIVE REACTIVITY VS ROOTS OF CHARACTERISTIC (INHOUR) EQUATION
(REF. PRIVATE COMMUNICATION - AUTHORS OF IX-8)

E.1.g.
NEGATIVE REACTIVITY VS ROOTS OF CHARACTERISTIC (INHOUR) EQUATION (REF. IX-8)

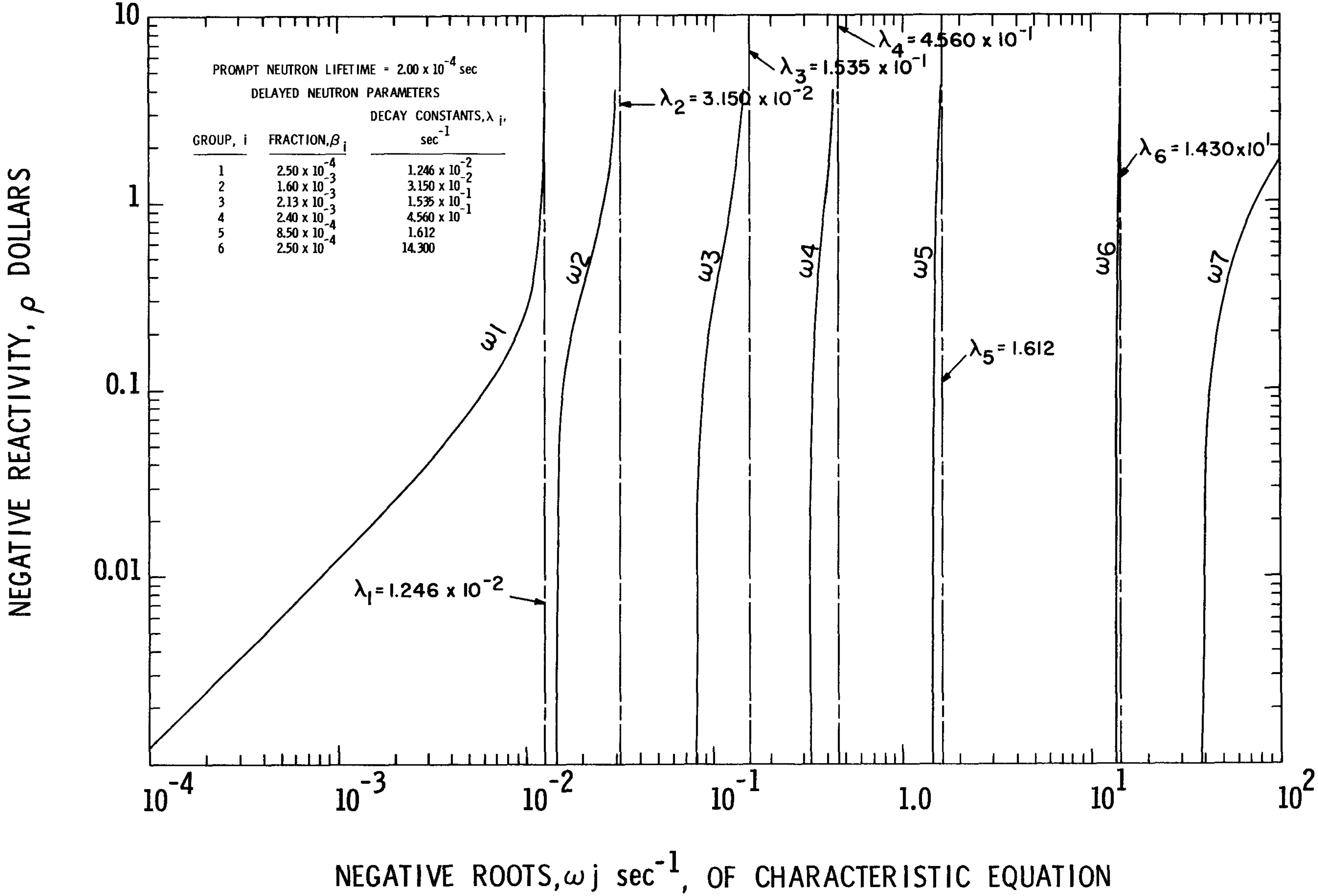

E.1.h.

COEFFICIENTS OF FLUX EQUATION VS NEGATIVE REACTIVITY FOR STEP CHANGE IN REACTIVITY (REF. IX-8)

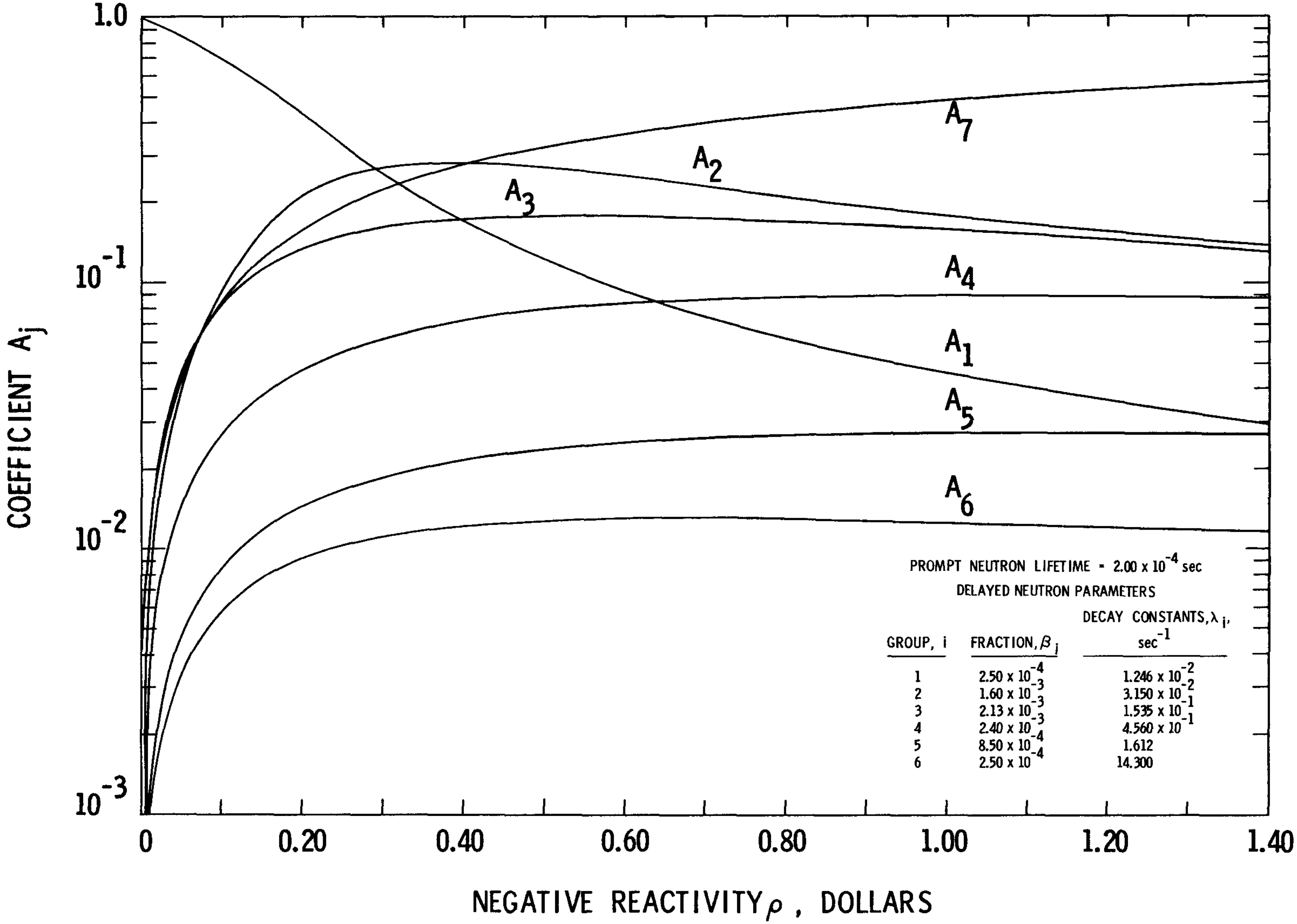

E.1.i
PER CENT ERROR IN ASYMPTOTIC POSITIVE PERIOD MEASUREMENT
VS TIME AFTER STEP CHANGE IN REACTIVITY
(REF. PRIVATE COMMUNICATION - AUTHORS OF IX-8)

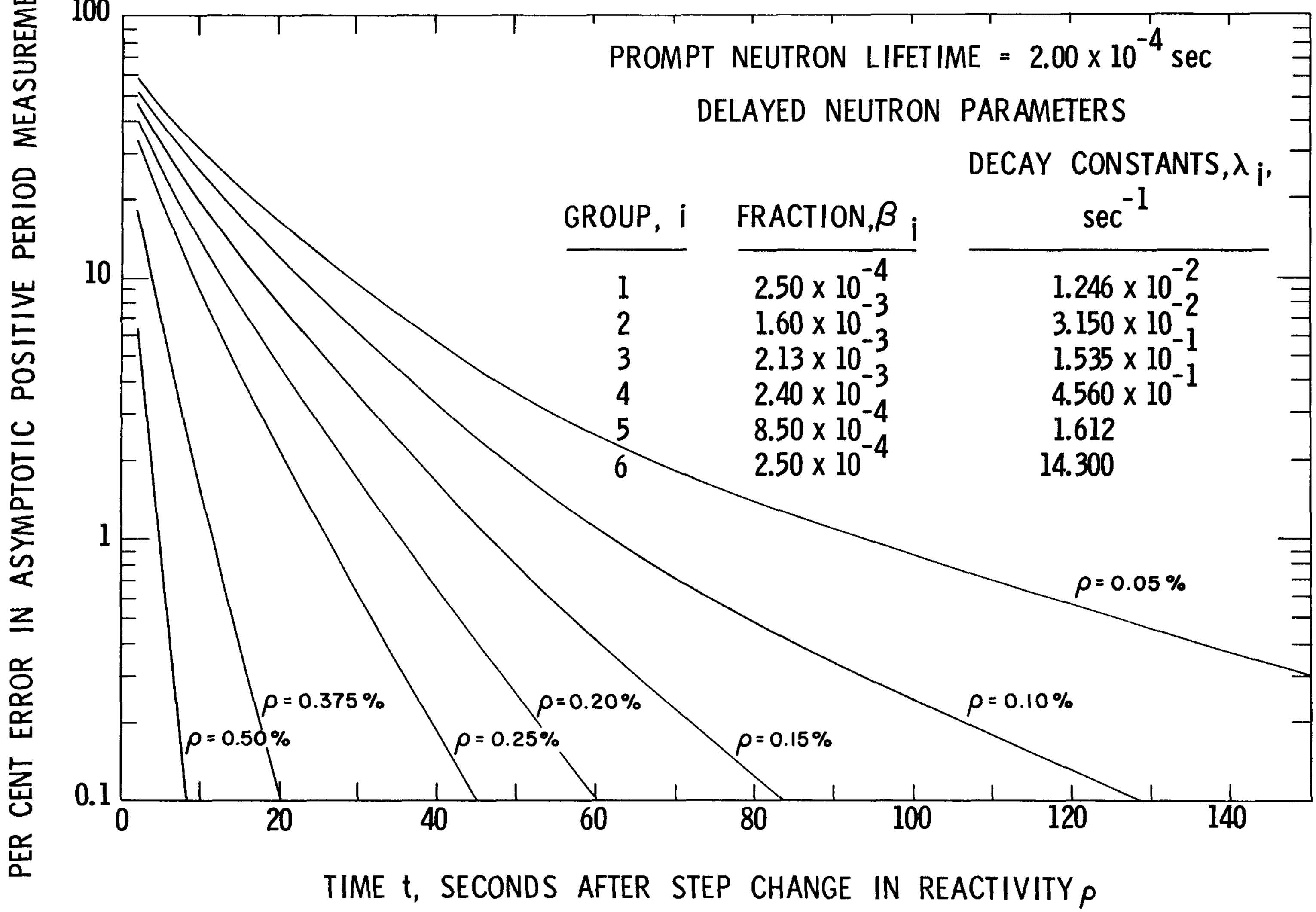

E.2. Flux-time Dependence as a Function of Delayed Neutron Parameters (Theoretical)

E.2.a. Delayed Neutron Parameters (Ref. IX-2)

Hughes Delayed Neutron Data

Group	Fraction	Decay Constants
1	2.50×10^{-4}	1.246×10^{-2} sec^{-1}
2	1.66×10^{-3}	3.150×10^{-2} sec^{-1}
3	2.13×10^{-3}	1.535×10^{-1} sec^{-1}
4	2.41×10^{-3}	4.560×10^{-1} sec^{-1}
5	8.50×10^{-4}	1.612
6	2.50×10^{-4}	14.300

Keepin Delayed Neutron Data [Phys. Rev., 107, (4)]

Slow fission: Group Index i	Half-life, T_i	Relative abundance, a_i/a	Absolute group yield (%)
	U^{235} (99.9% 235; $n/F = 0.0158 \pm 0.0005$)		
1	55.72 ± 1.28	0.033 ± 0.003	0.052 ± 0.005
2	22.72 ± 0.71	0.219 ± 0.009	0.346 ± 0.018
3	6.22 ± 0.23	0.196 ± 0.022	0.310 ± 0.036
4	2.30 ± 0.09	0.395 ± 0.011	0.624 ± 0.026
5	0.610 ± 0.083	0.115 ± 0.009	0.182 ± 0.015
6	0.230 ± 0.025	0.042 ± 0.008	0.066 ± 0.008

Fast fission: Group Index i	Half-life, T_i	Relative abundance, a_i/a	Absolute group yield (%) (for pure isotope)
	U^{235} (99.9% 235; $n/F = 0.0165 \pm 0.0005$)		
1	54.51 ± 0.94	0.038 ± 0.003	0.063 ± 0.005
2	21.84 ± 0.54	0.213 ± 0.005	0.351 ± 0.011
3	6.00 ± 0.17	0.188 ± 0.016	0.310 ± 0.03
4	2.23 ± 0.06	0.407 ± 0.007	0.672 ± 0.00
5	0.496 ± 0.029	0.128 ± 0.008	0.211 ± 0.00
6	0.179 ± 0.017	0.026 ± 0.003	0.043 ± 0.00
	U^{238} (99.98% 238; $n/F = 0.0412 \pm 0.0017$)		
1	52.38 ± 1.29	0.013 ± 0.001	0.054 ± 0.005
2	21.58 ± 0.39	0.137 ± 0.002	0.564 ± 0.025
3	5.00 ± 0.19	0.162 ± 0.020	0.667 ± 0.087
4	1.93 ± 0.07	0.388 ± 0.012	1.599 ± 0.081
5	0.490 ± 0.023	0.225 ± 0.013	0.927 ± 0.060
6	0.172 ± 0.009	0.075 ± 0.005	0.309 ± 0.024

E.2.b.

COMPARISON OF HUGHES AND KEEPIN DELAYED NEUTRON DATA IN THE CALCULATION OF FLUX RATIO VS TIME AFTER A NEGATIVE STEP. (REF. IX-2)

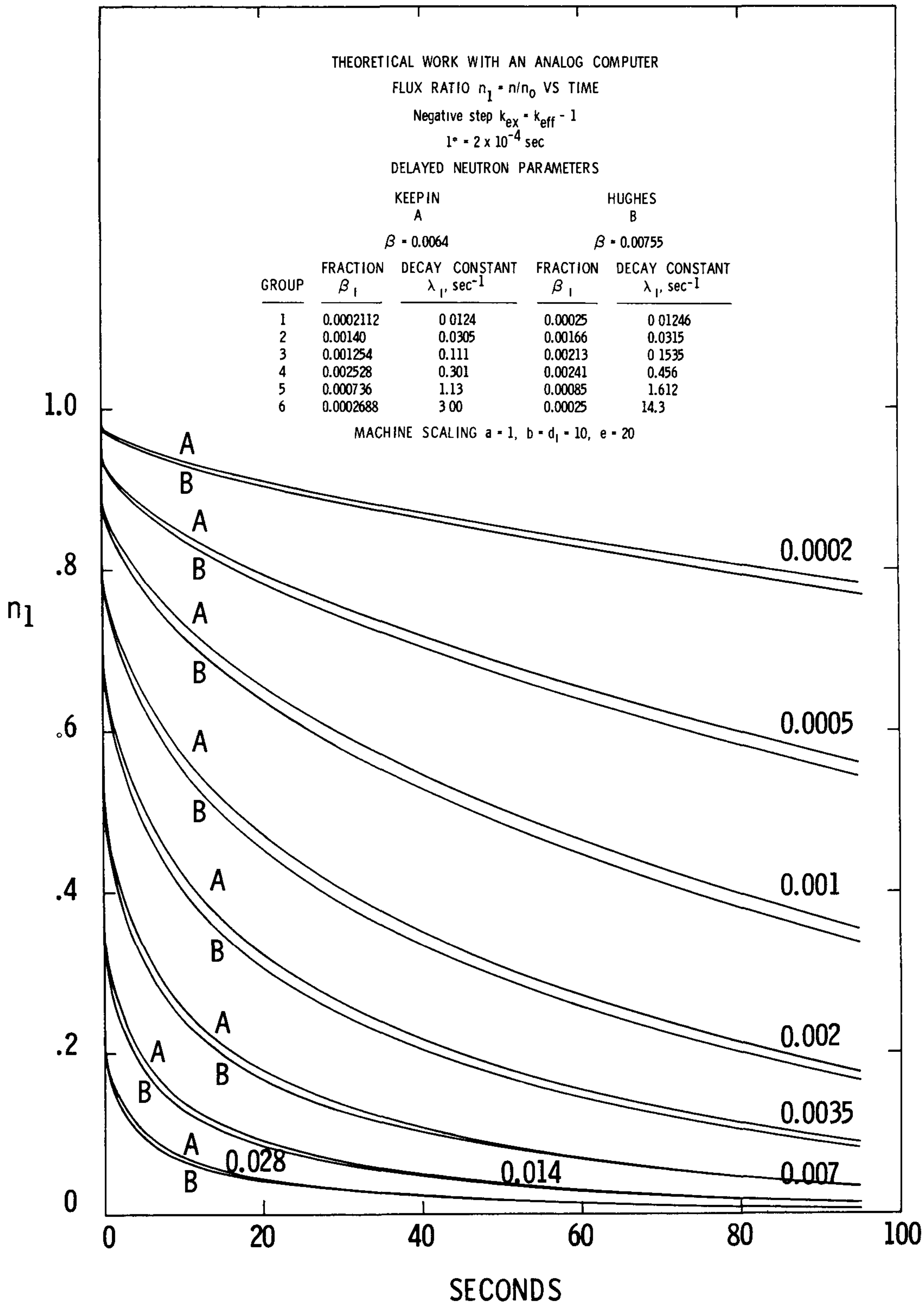

E.2.c.
COMPARISON OF HUGHES AND KEEPIN DELAYED NEUTRON DATA IN THE CALCULATION OF FLUX RATIO VS TIME AFTER A POSITIVE STEP (REF. IX-2)

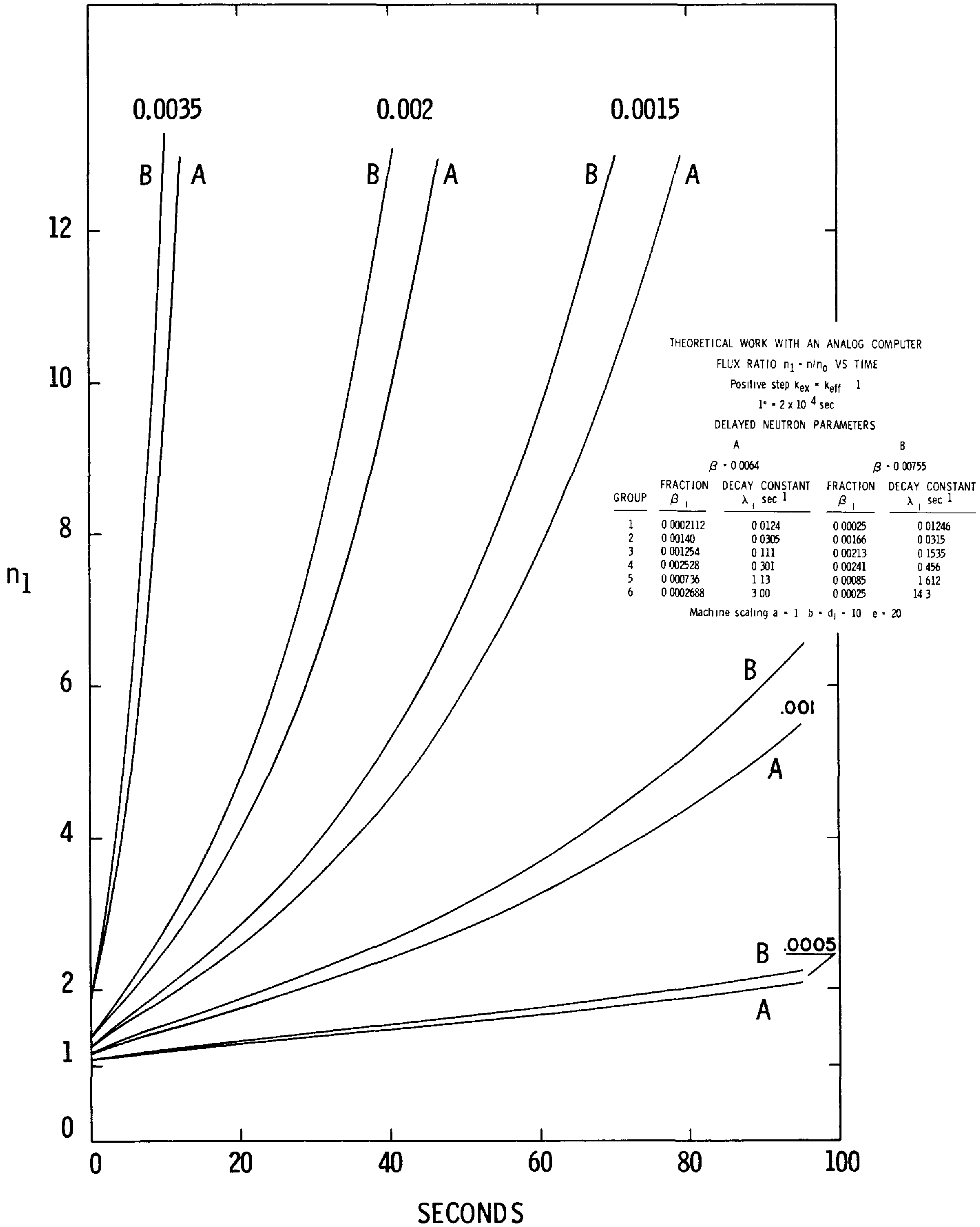

	A		B	
	β = 0 0064		β = 0 00755	
GROUP	FRACTION β_i	DECAY CONSTANT λ_i sec 1	FRACTION β_i	DECAY CONSTANT λ_i sec 1
1	0 0002112	0 0124	0 00025	0 01246
2	0 00140	0 0305	0 00166	0 0315
3	0 001254	0 111	0 00213	0 1535
4	0 002528	0 301	0 00241	0 456
5	0 000736	1 13	0 00085	1 612
6	0 0002688	3 00	0 00025	14 3

E.3. Flux-time Dependence as a Function of Neutron Lifetime (Theoretical)

E.3.a.

FLUX RATIO VS TIME FOR SHORT TIMES AFTER NEGATIVE STEP INSERTIONS, COMPARISON OF EFFECT OF NEUTRON LIFETIME (REF. IX-2)

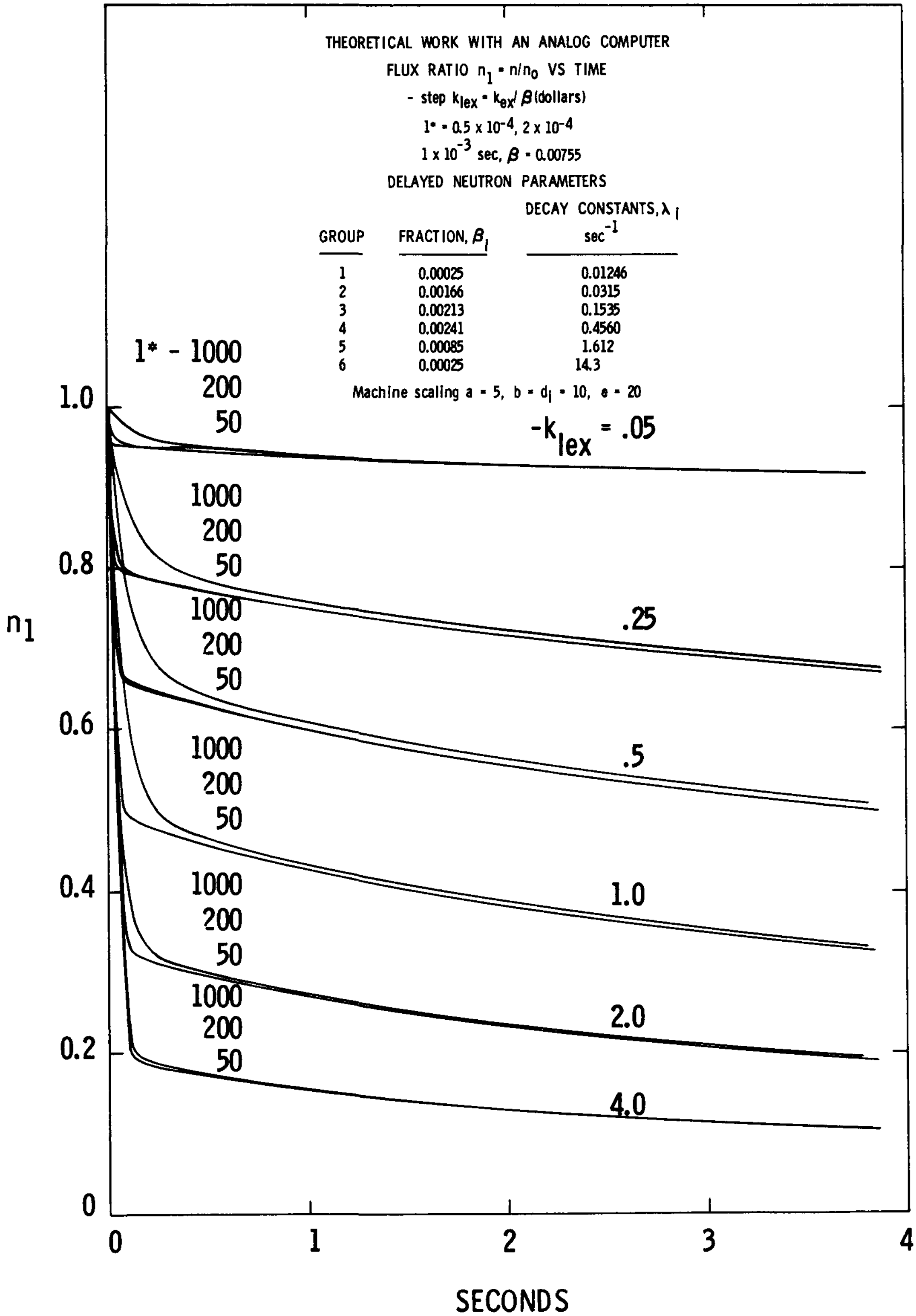

E.3.b.
FLUX RATIO VS TIME FOR SHORT TIMES AFTER POSITIVE STEP INSERTIONS, COMPARISON OF EFFECT OF NEUTRON LIFETIME (REF. IX-2)

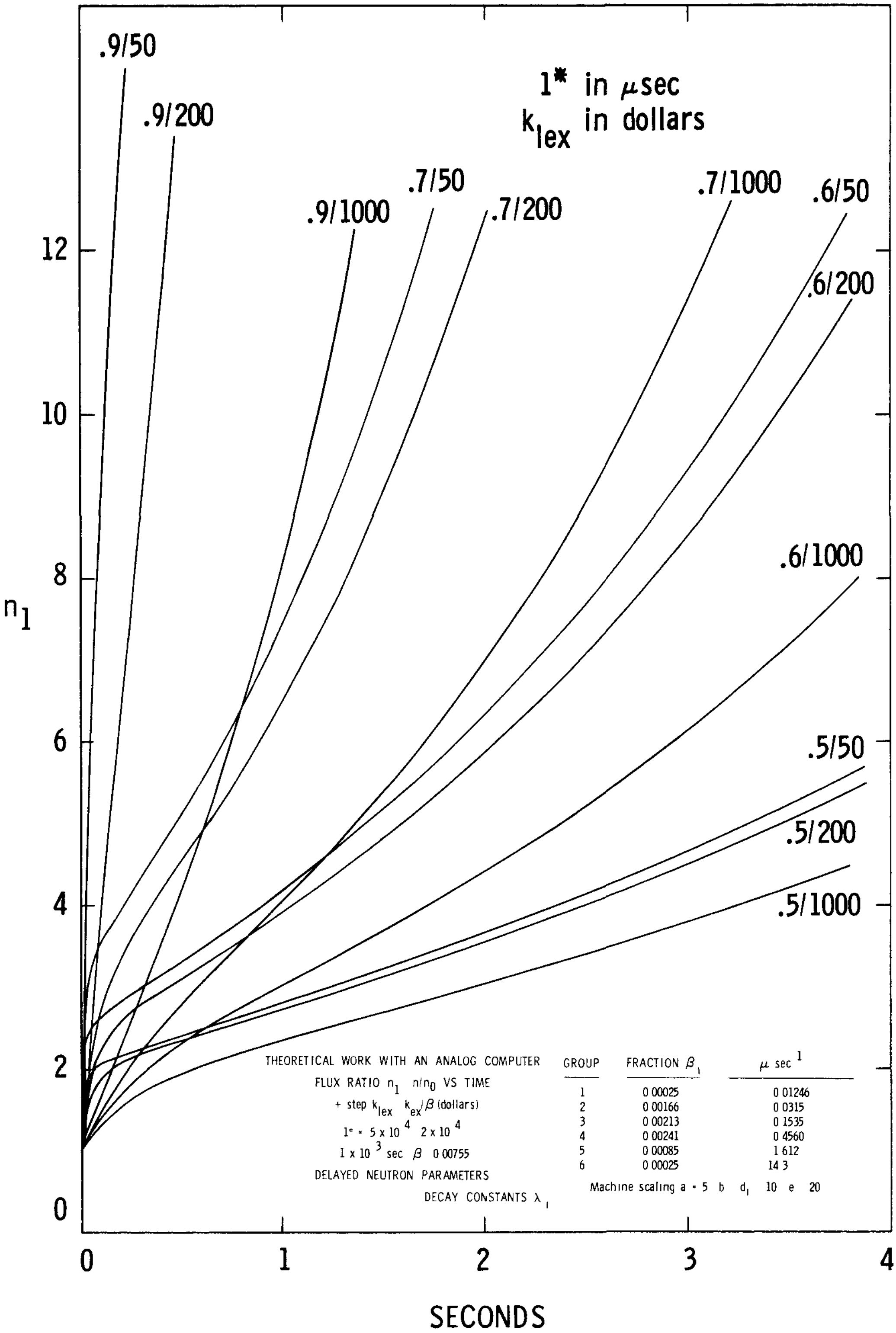

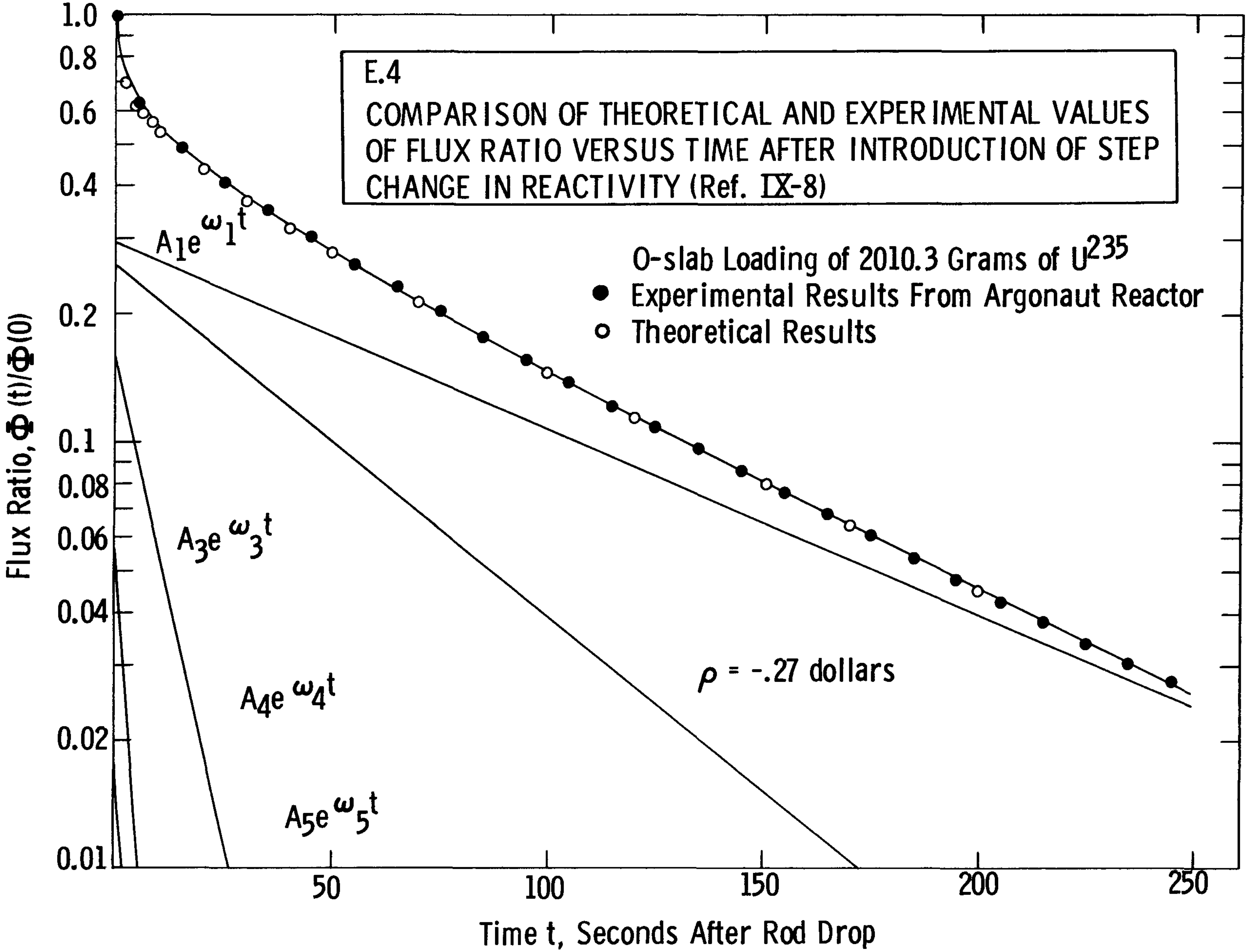

E.4
COMPARISON OF THEORETICAL AND EXPERIMENTAL VALUES OF FLUX RATIO VERSUS TIME AFTER INTRODUCTION OF STEP CHANGE IN REACTIVITY (Ref. IX-8)

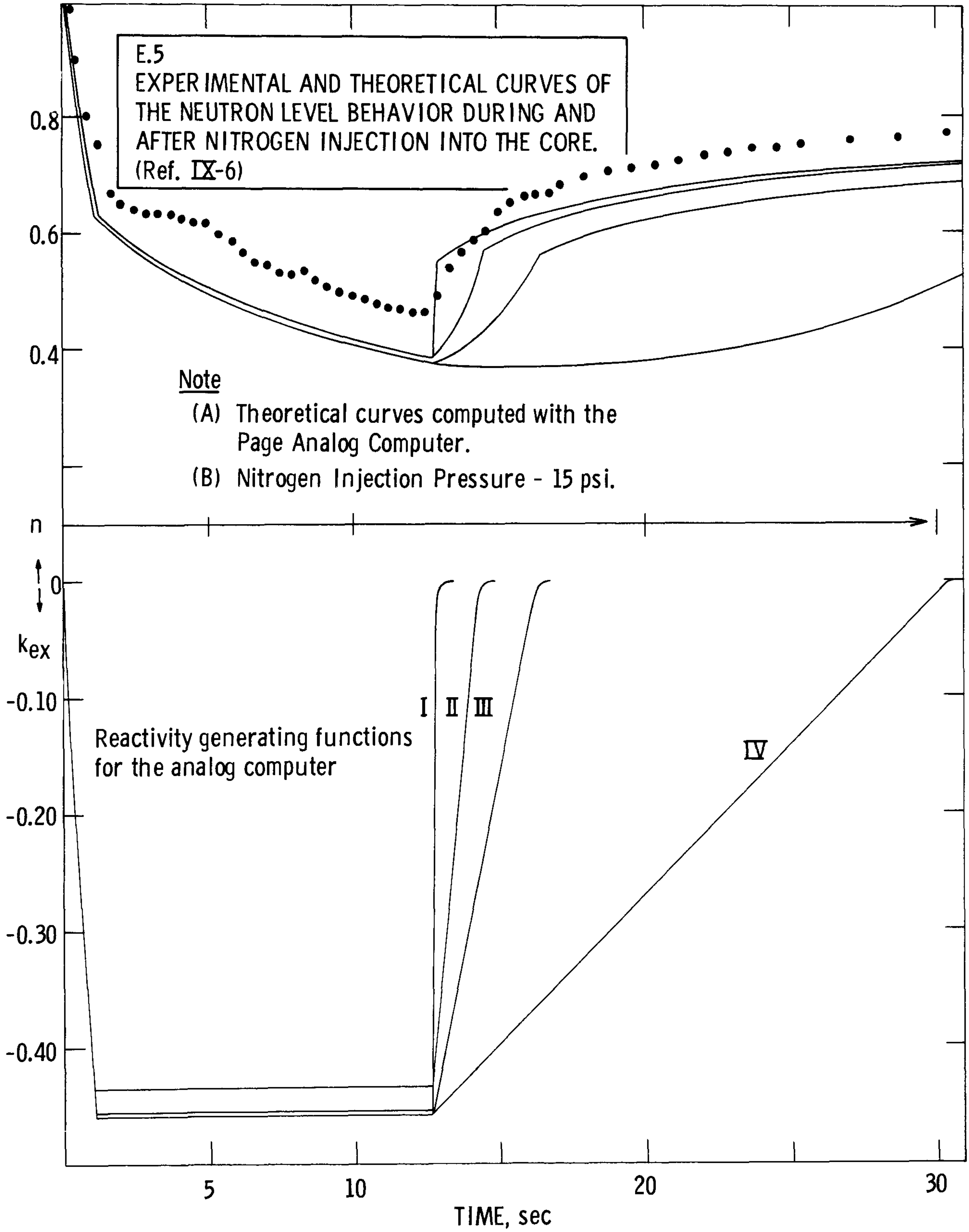
E.5
EXPERIMENTAL AND THEORETICAL CURVES OF THE NEUTRON LEVEL BEHAVIOR DURING AND AFTER NITROGEN INJECTION INTO THE CORE.
(Ref. IX-6)
0.8
0.6
0.4
Note
(A) Theoretical curves computed with the Page Analog Computer.
(B) Nitrogen Injection Pressure - 15 psi.
n
0
k_{ex}
-0.10
-0.20
-0.30
-0.40
I
II
III
IV
Reactivity generating functions for the analog computer
5
10
20
30
TIME, sec

E.6
THEORETICAL CURVES AT NEUTRON LEVEL VS TIME FOR VARIOUS NEGATIVE REACTIVITY STEPS INSERTED WHILE THE REACTOR WAS ON A POSITIVE PERIOD (Ref. IX-7)

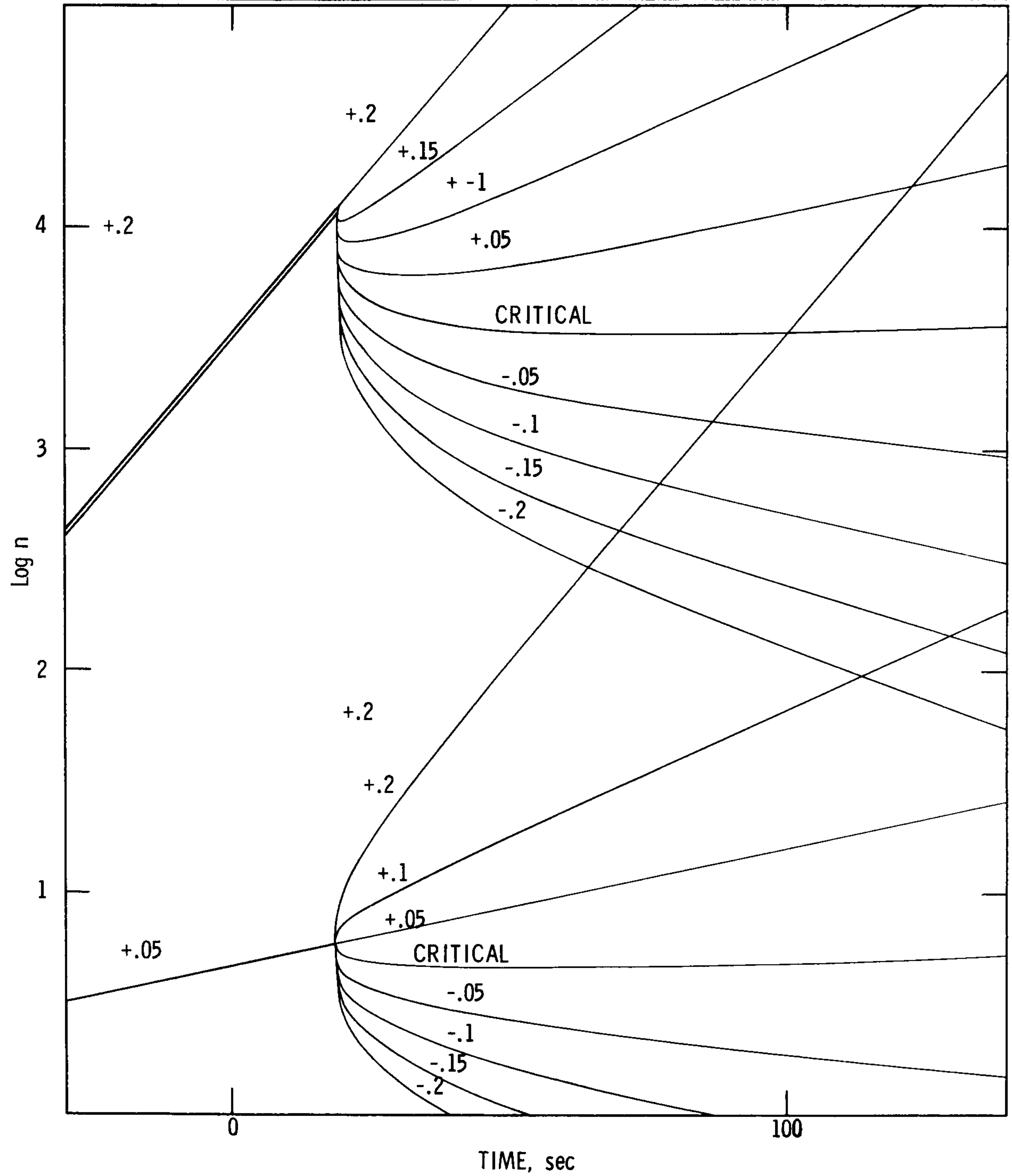

Section F

CONTROL ROD CALIBRATION

A calibrated control rod is one for which there exists a curve of reactivity versus the rods vertical position. The particular curve is dependent on the core geometry and conditions that existed during calibration. A representative series of control rod calibration curves for a number of loadings is given. Some effects on the calibration curve of small changes in core makeup and type of measurement employed have been investigated and the results are presented. Composite curves showing the relative worths of the various rods are included.

Control rod calibration is a standard student experiment. The common procedure is to start with a critical reactor at a relatively high power, then the rod to be calibrated is dropped, and the neutron level change with time observed. From the observed results and the kinetics curves, the magnitude of the negative reactivity step can be determined. An alternate method is to withdraw the rod from its critical position and to measure the period of the reactor. The period is converted to reactivity with the aid of the kinetics curves.

F.1. One-slab Control Rod Calibrations

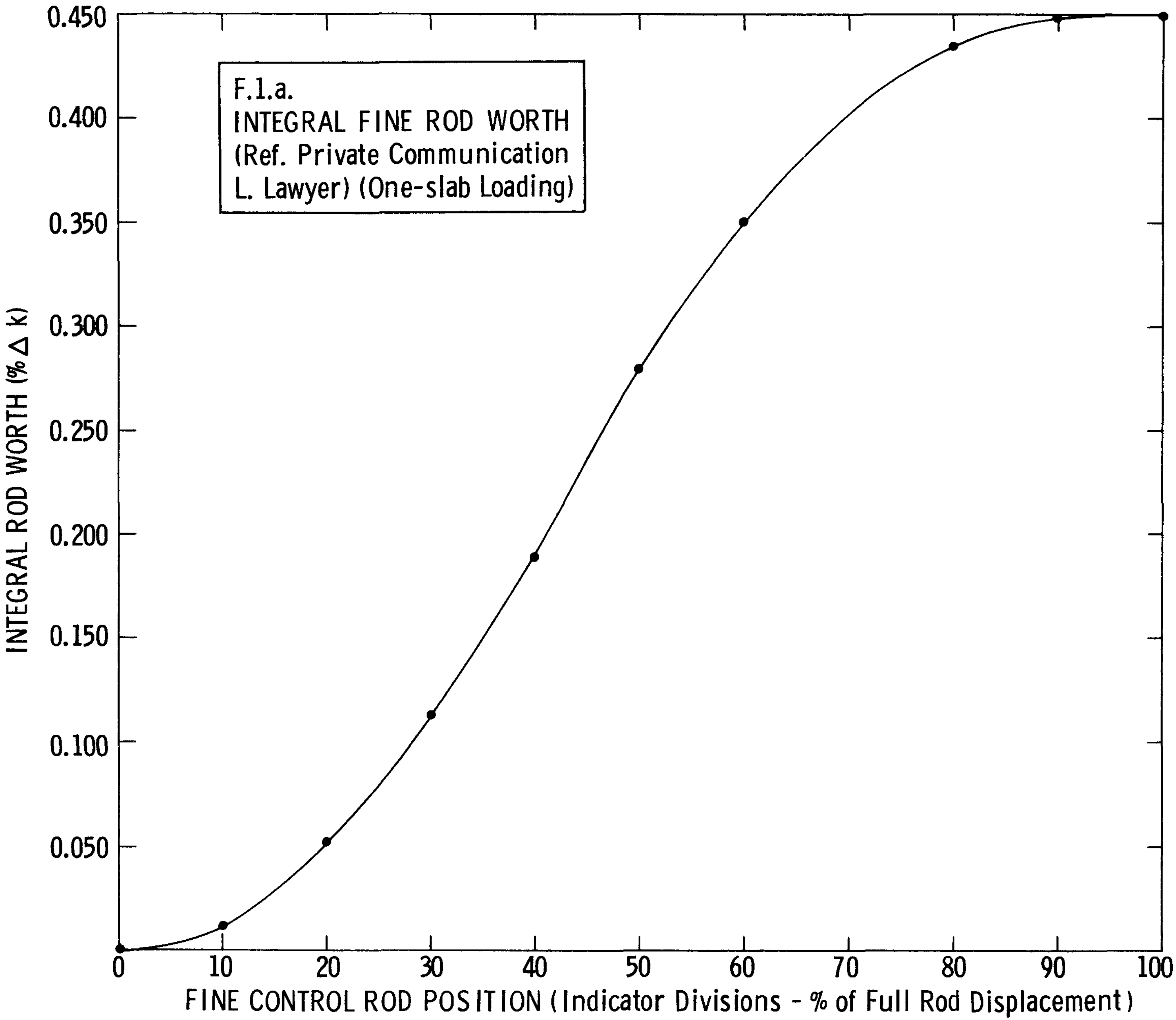

F.1.a.
INTEGRAL FINE ROD WORTH
(Ref. Private Communication
L. Lawyer) (One-slab Loading)
INTEGRAL ROD WORTH (% Δ k)
0.450
0.400
0.350
0.300
0.250
0.200
0.150
0.100
0.050
0
10
20
30
40
50
60
70
80
90
100
FINE CONTROL ROD POSITION (Indicator Divisions - % of Full Rod Displacement)

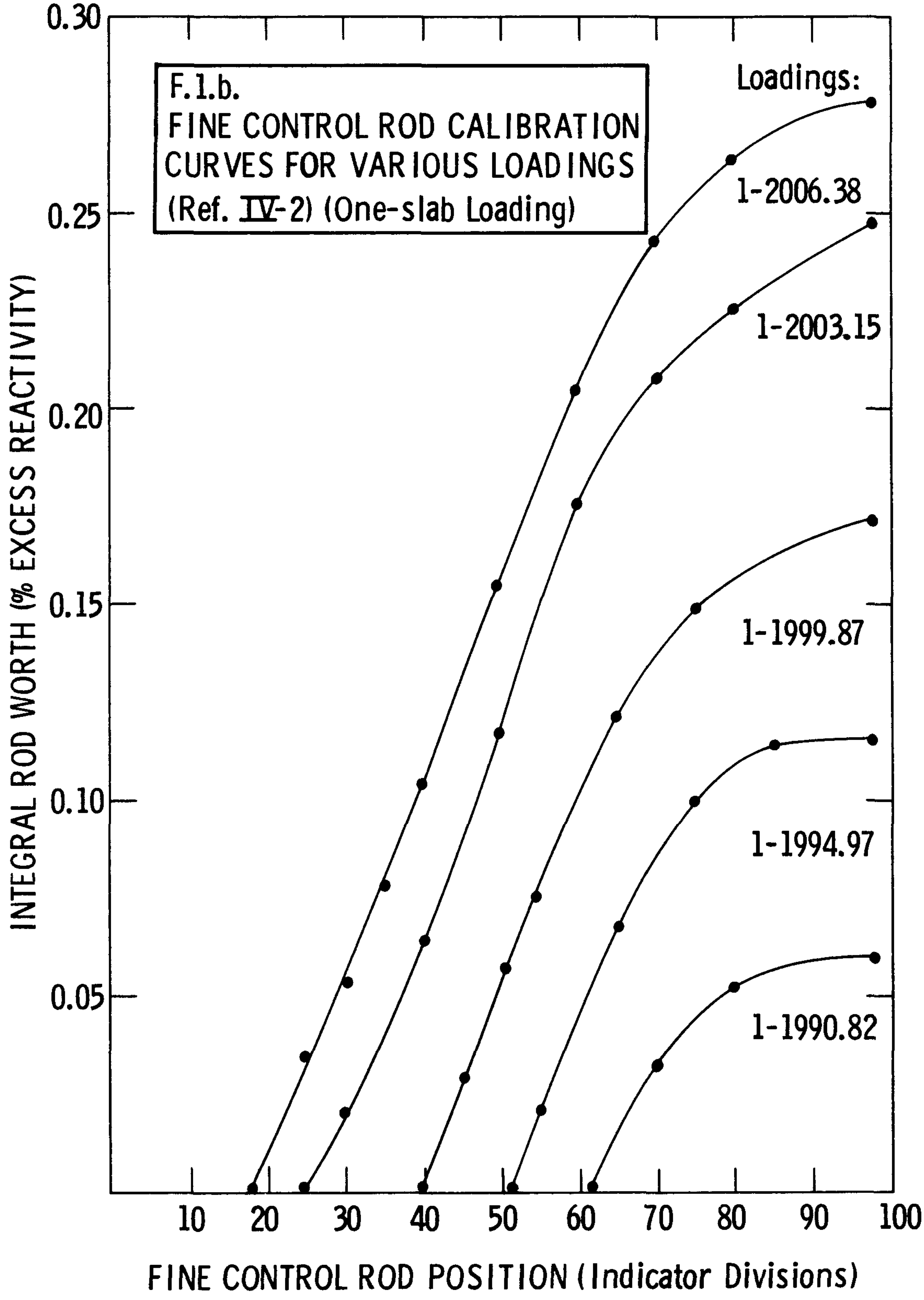
F.1.b.
FINE CONTROL ROD CALIBRATION CURVES FOR VARIOUS LOADINGS (Ref. IV-2) (One-slab Loading)
Loadings:
1-2006.38
1-2003.15
1-1999.87
1-1994.97
1-1990.82
0.30
0.25
0.20
0.15
0.10
0.05
INTEGRAL ROD WORTH (% EXCESS REACTIVITY)
10
20
30
40
50
60
70
80
90
100
FINE CONTROL ROD POSITION (Indicator Divisions)

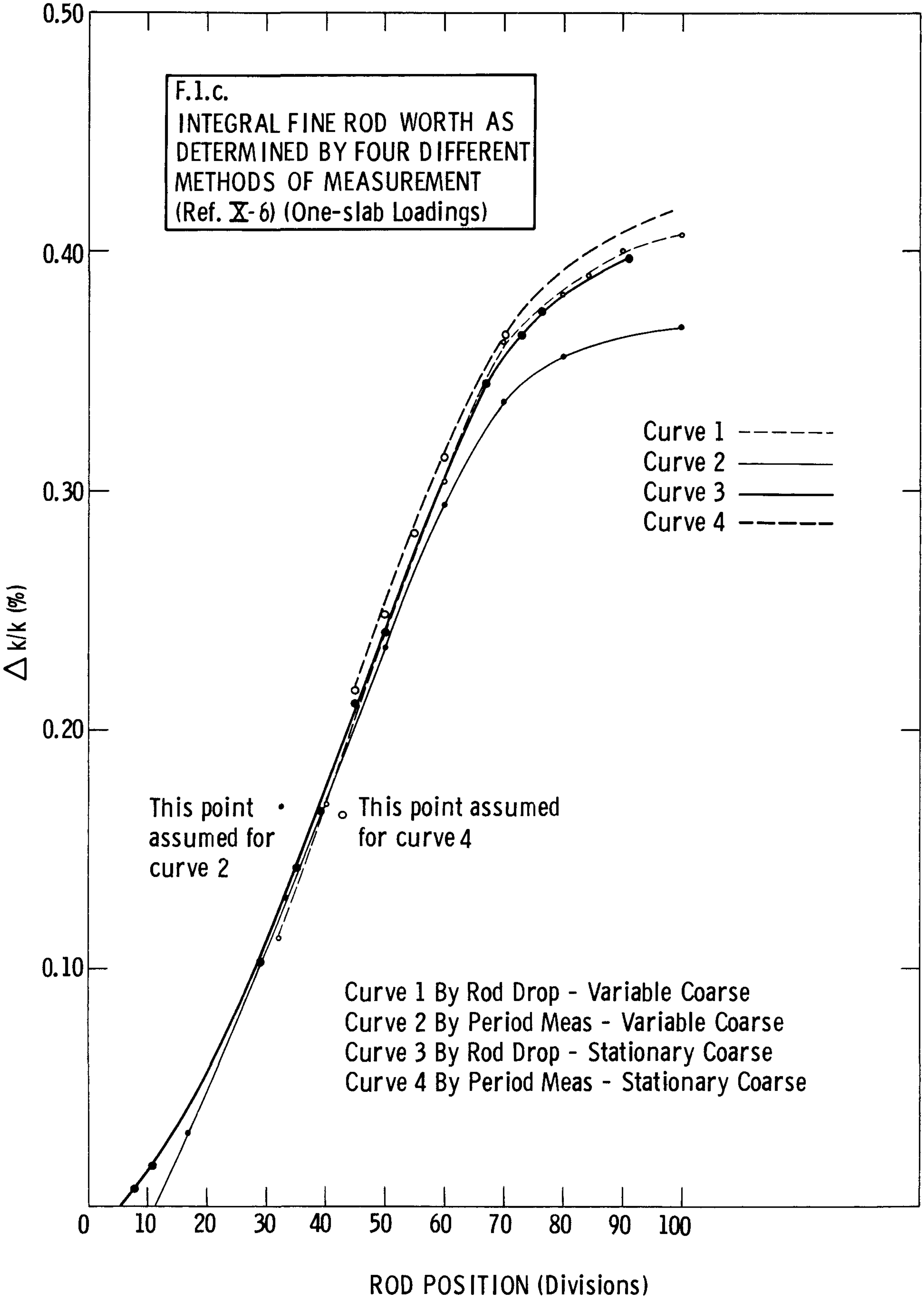

F.1.c.
INTEGRAL FINE ROD WORTH AS DETERMINED BY FOUR DIFFERENT METHODS OF MEASUREMENT (Ref. X-6) (One-slab Loadings)
0.50
0.40
0.30
0.20
0.10
Δ k/k (%)
0
10
20
30
40
50
60
70
80
90
100
ROD POSITION (Divisions)
Curve 1
Curve 2
Curve 3
Curve 4
This point assumed for curve 2
This point assumed for curve 4
Curve 1 By Rod Drop - Variable Coarse
Curve 2 By Period Meas - Variable Coarse
Curve 3 By Rod Drop - Stationary Coarse
Curve 4 By Period Meas - Stationary Coarse

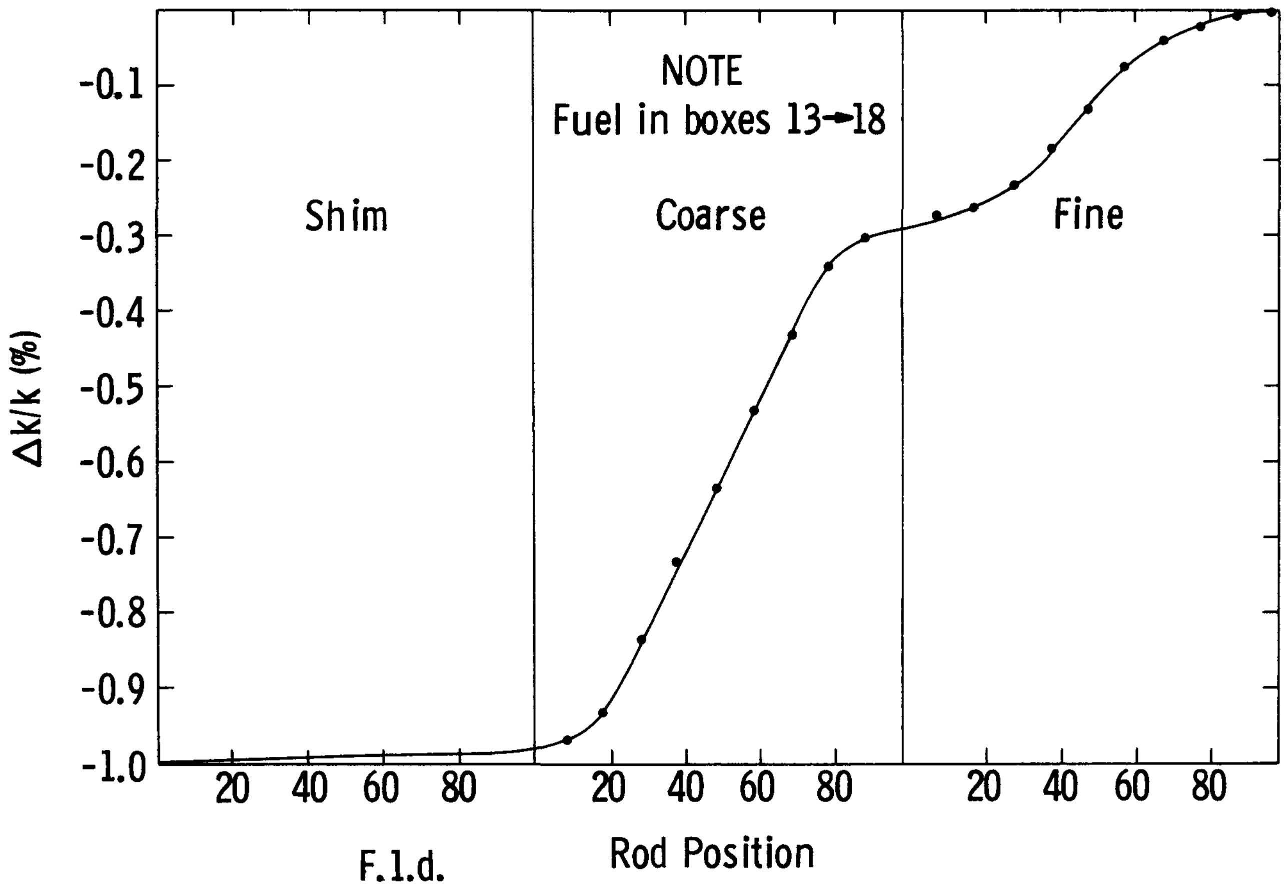

F.1.d.

COMPOSITE CONTROL ROD CALIBRATION
(Ref. X-9) (One-slab Loading)

F.2. Control Rod Calibrations, Annular Loading

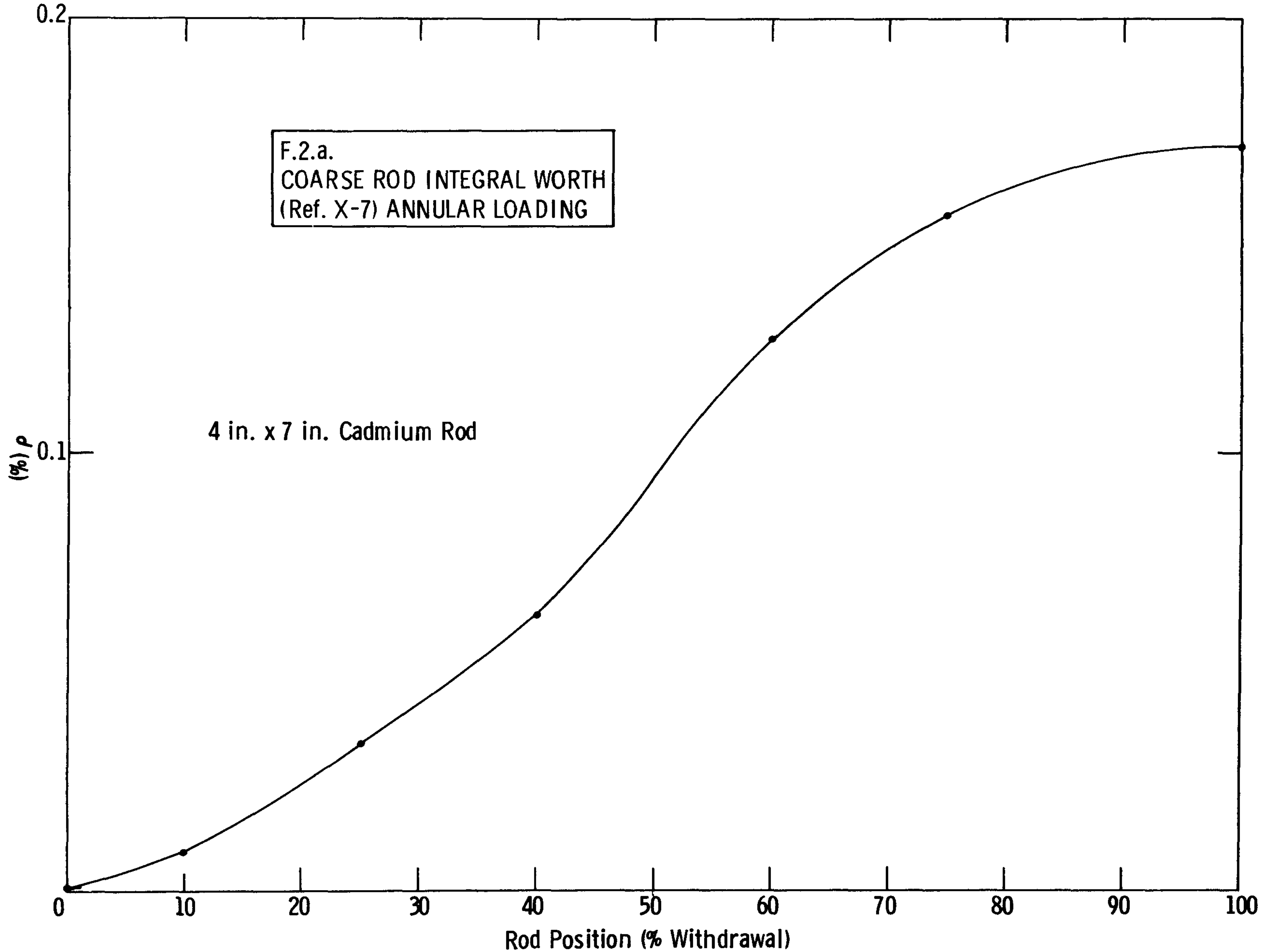

F.2.a.
COARSE ROD INTEGRAL WORTH
(Ref. X-7) ANNULAR LOADING
4 in. x 7 in. Cadmium Rod
ρ (%)
0.2
0.1
0
10
20
30
40
50
60
70
80
90
100
Rod Position (% Withdrawal)

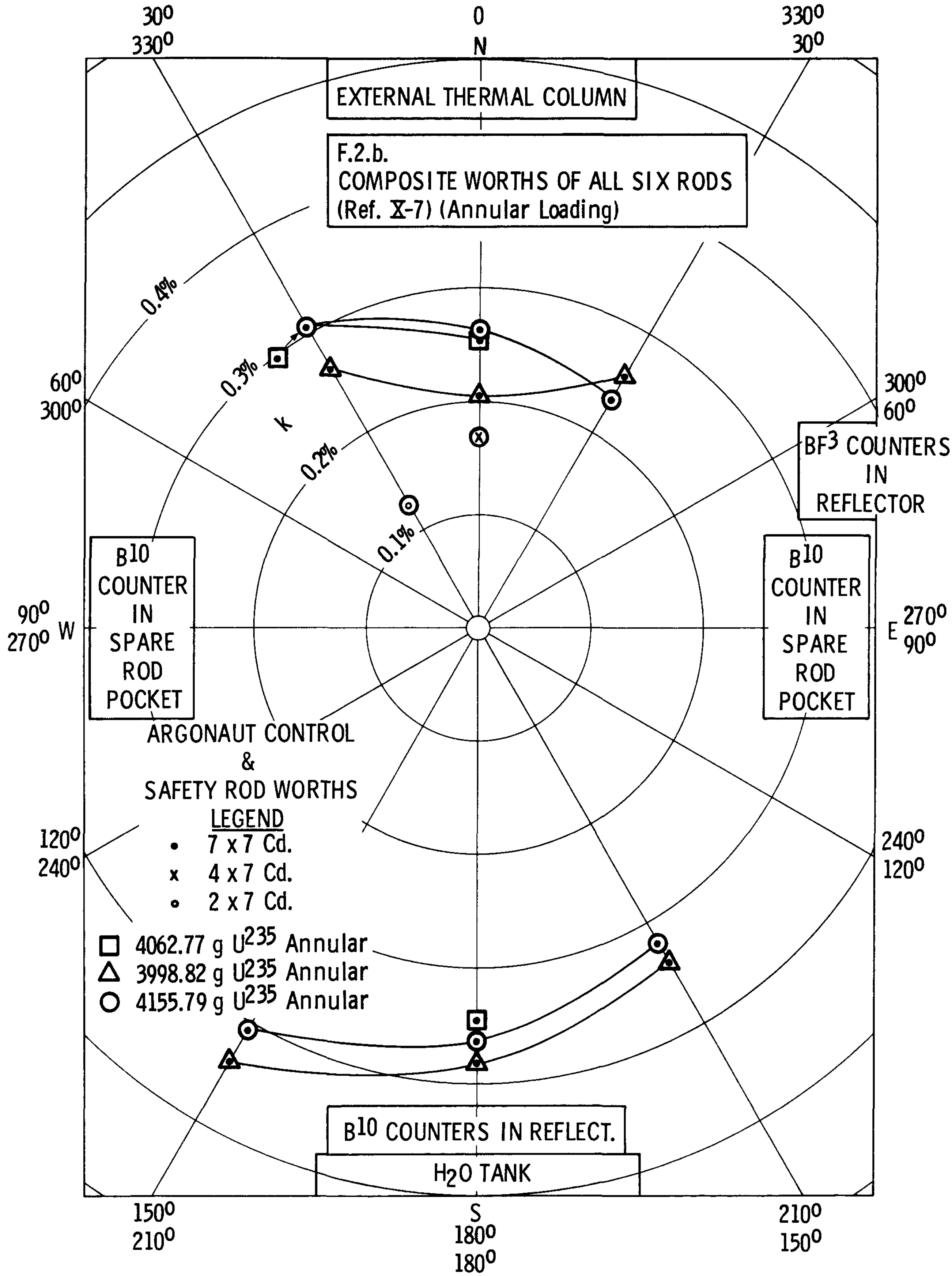
30°
330°
0
N
330°
30°
EXTERNAL THERMAL COLUMN
F.2.b.
COMPOSITE WORTHS OF ALL SIX RODS
(Ref. X-7) (Annular Loading)
0.4%
0.3%
0.2%
0.1%
K
60°
300°
300°
60°
BF3 COUNTERS IN REFLECTOR
B10 COUNTER IN SPARE ROD POCKET
90°
270° W
E 270°
90°
B10 COUNTER IN SPARE ROD POCKET
ARGONAUT CONTROL & SAFETY ROD WORTHS
LEGEND
• 7 x 7 Cd.
x 4 x 7 Cd.
∘ 2 x 7 Cd.
□ 4062.77 g U235 Annular
△ 3998.82 g U235 Annular
○ 4155.79 g U235 Annular
120°
240°
240°
120°
B10 COUNTERS IN REFLECT.
H2O TANK
150°
210°
S
180°
180°
210°
150°

Section G

RAMP STARTUP

Usually, reactivity changes introduced into the Argonaut are step changes because they are easier to understand and perform. A step reactivity change is assumed to take zero time, while during a ramp input the reactivity is changing with time, usually linearly. Very little work has been done with the experimental study of ramp inputs to date at the Argonaut.

Curves of power level versus time for various rates of removal of the fine control rod (ramp input of reactivity) are presented, but because of the shape of the rod calibration curve, this is not a linear ramp input. The time to reach criticality depends on the removal rate of the control rods, which in turn depends on the Variac setting of the rod speed control.

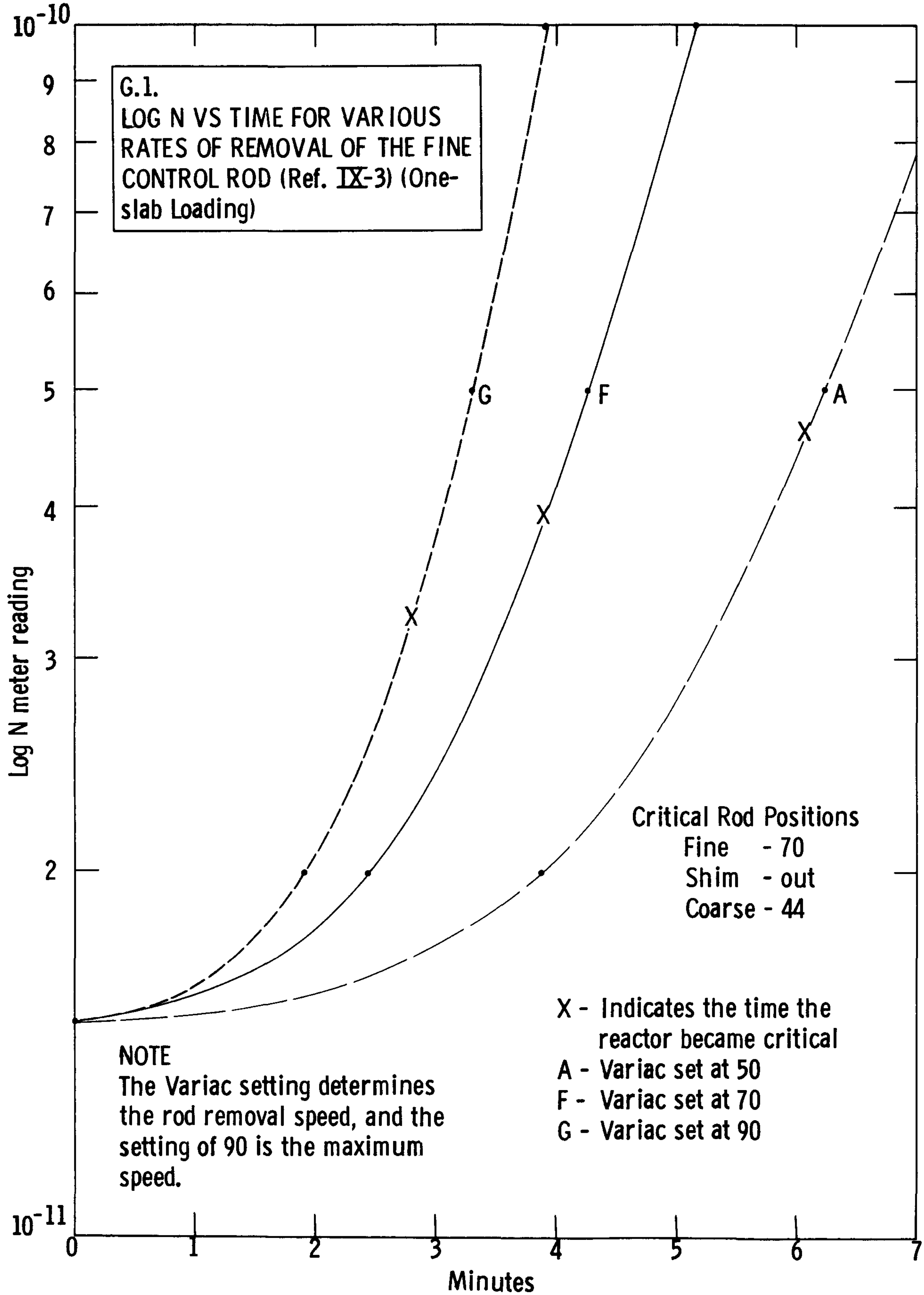
G.1.
LOG N VS TIME FOR VARIOUS RATES OF REMOVAL OF THE FINE CONTROL ROD (Ref. IX-3) (One-slab Loading)
10^{-10}
9
8
7
6
5
4
3
2
10^{-11}
Log N meter reading
0
1
2
3
4
5
6
7
Minutes
G
F
A
X
Critical Rod Positions
Fine - 70
Shim - out
Coarse - 44
X - Indicates the time the reactor became critical
A - Variac set at 50
F - Variac set at 70
G - Variac set at 90
NOTE
The Variac setting determines the rod removal speed, and the setting of 90 is the maximum speed.

Section H

TRANSFER FUNCTION (ONE-SLAB GEOMETRY)

A typical series of curves obtained performing the student automatic reactor control experiment are presented together with measurements of the reactor transfer function. This transfer function describes the relation between a sinusoidal input reactivity disturbance, $\delta k(s)$, and the resulting neutron level behavior, $\delta n(s)$:

$$G(s) = \delta n(s)/\delta k(s) \quad .$$

The phase shift and magnitude of $G(s)$ depend on the frequency of the reactivity disturbance. The curves of the phase shift and magnitude of $G(s)$ versus frequency constitute the transfer function.

Work to date has only been with the one-slab core.

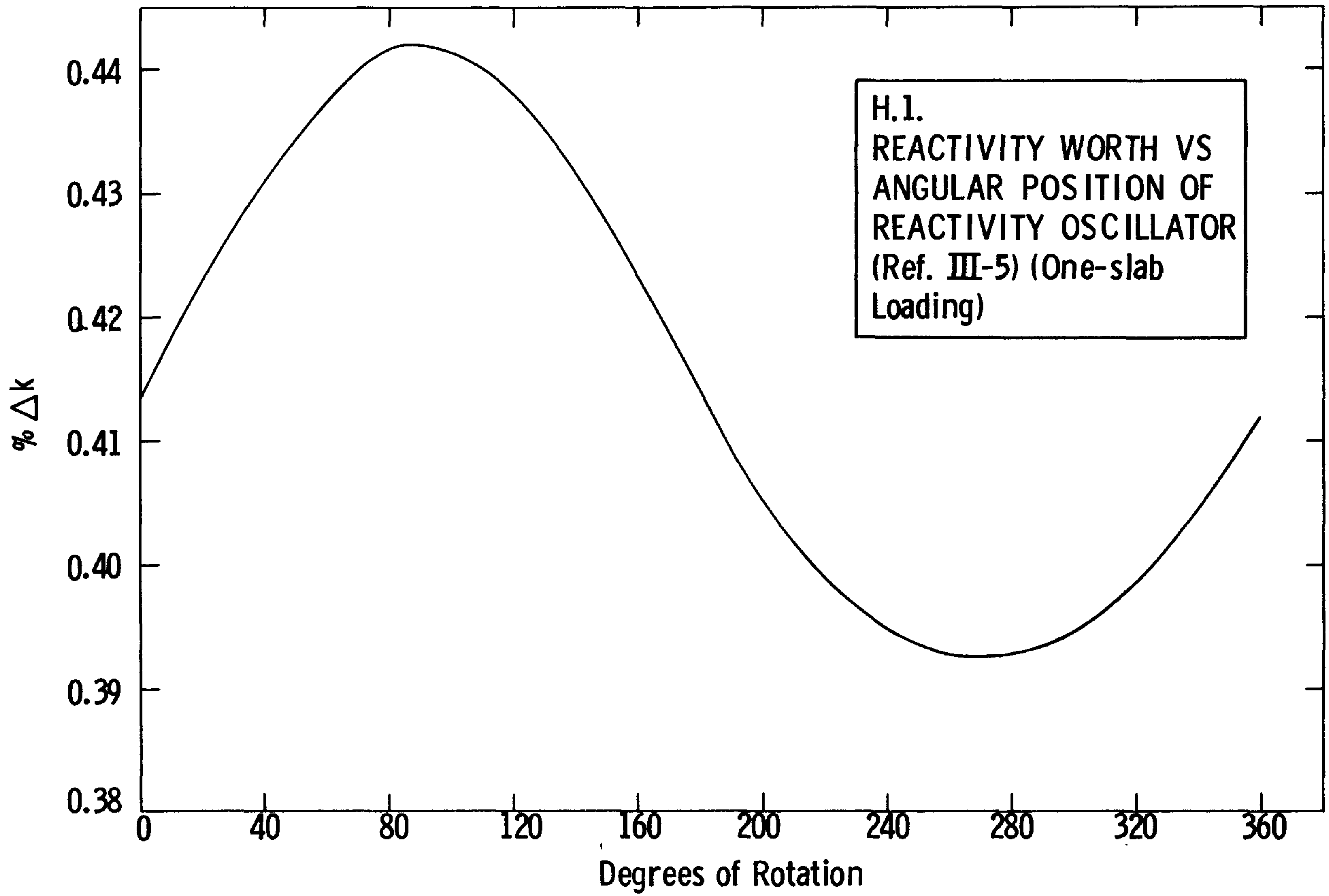

H.1.
REACTIVITY WORTH VS ANGULAR POSITION OF REACTIVITY OSCILLATOR (Ref. III-5) (One-slab Loading)

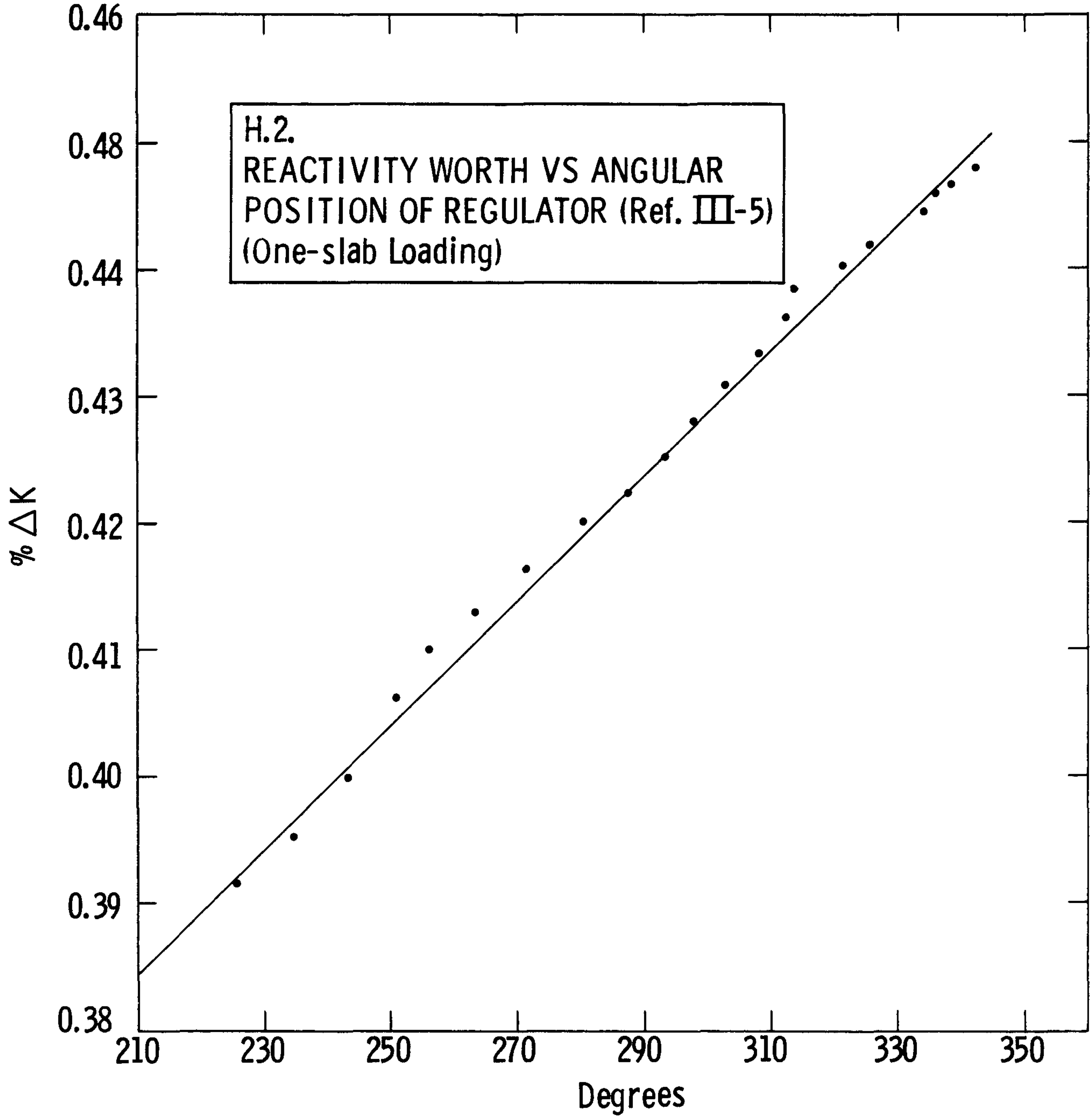

H.2.
REACTIVITY WORTH VS ANGULAR POSITION OF REGULATOR (Ref. III-5)
(One-slab Loading)

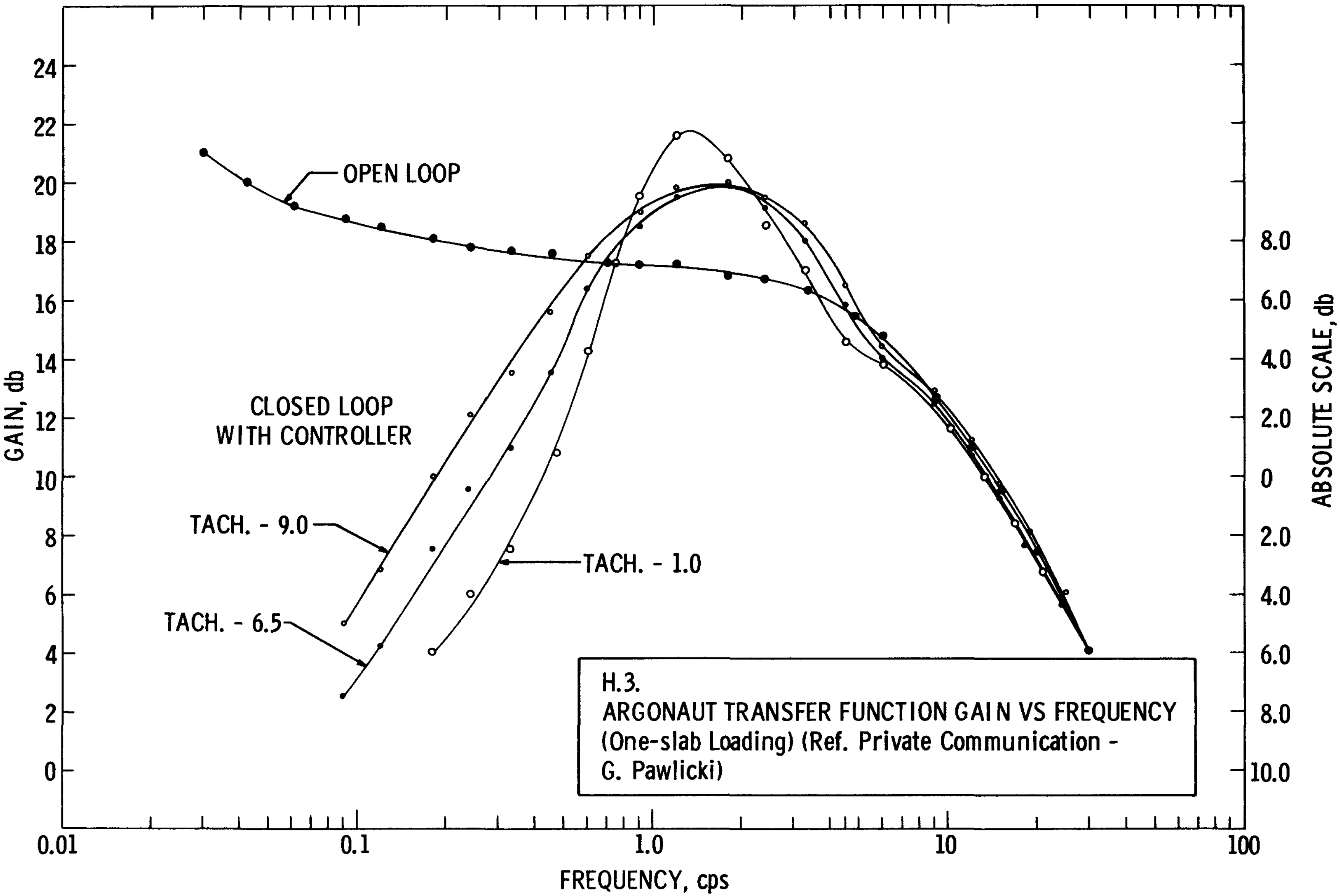

H.3.
ARGONAUT TRANSFER FUNCTION GAIN VS FREQUENCY (One-slab Loading) (Ref. Private Communication - G. Pawlicki)

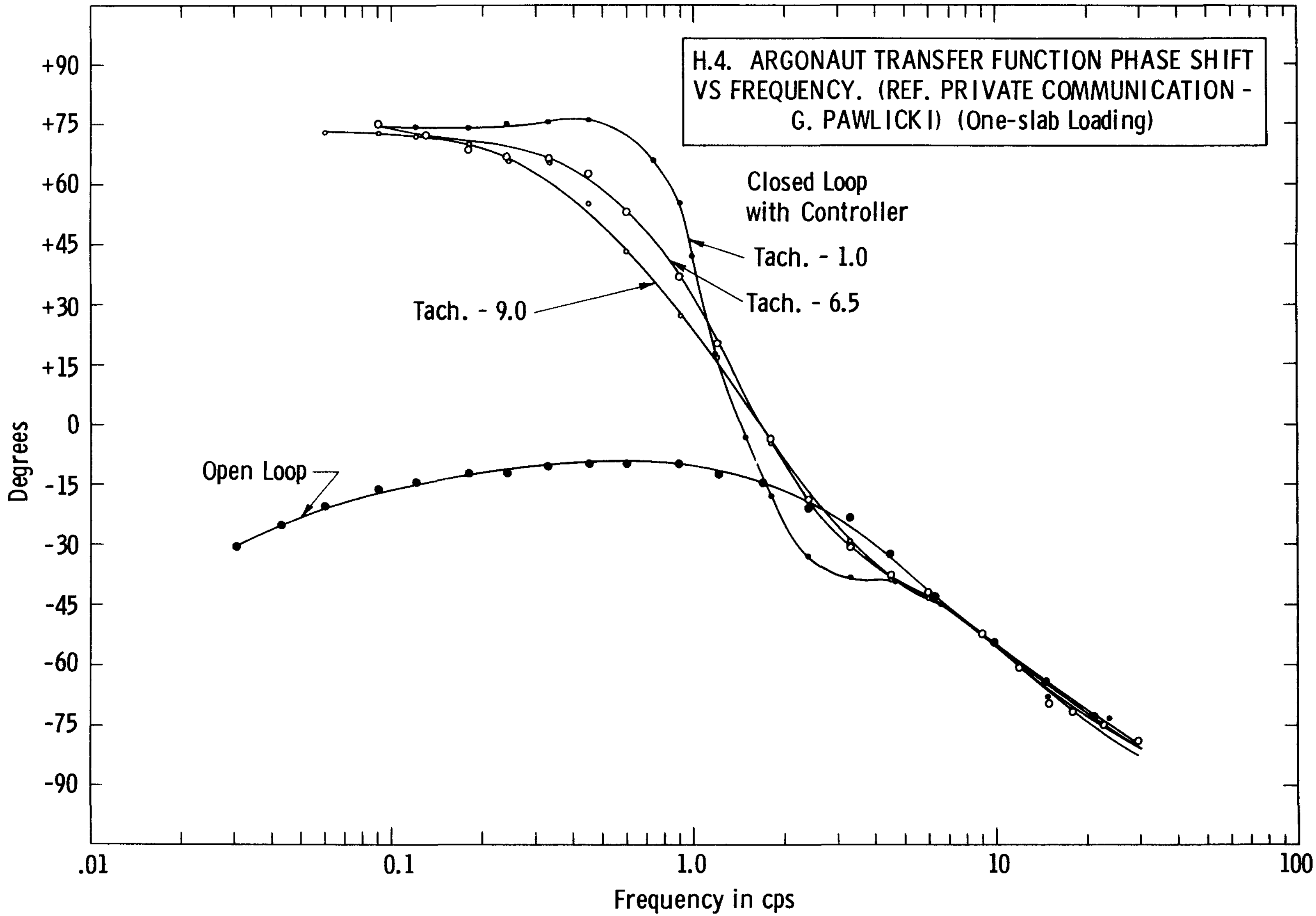
H.4. ARGONAUT TRANSFER FUNCTION PHASE SHIFT VS FREQUENCY. (REF. PRIVATE COMMUNICATION - G. PAWLICKI) (One-slab Loading)
Closed Loop with Controller
Tach. - 1.0
Tach. - 6.5
Tach. - 9.0
Open Loop
+90
+75
+60
+45
+30
+15
0
-15
-30
-45
-60
-75
-90
Degrees
.01
0.1
1.0
10
100
Frequency in cps

Section I

FLUX PLOTS (RELATIVE)

Relative flux means that the experimental points have not been determined in absolute units of neutrons per cm^2 per second, but rather in other units, such as counts per minute per gram of foil weight. Relative flux then is the neutron distribution in arbitrary units. The determination of the total, fast, and slow neutron flux distributions in the core, reflector and thermal columns is a standard student experiment. Because knowledge of the various distributions is basic to the design of experiments and in the study of experimental results, much early student effort has been directed to this measurement. Although it is clear that there is room for better work to be done, the following curves at least indicate the results of the theoretical and experimental effort made to date.

The results were obtained with bare and cadmium-covered gold and indium foils, but other techniques are possible.

I.1. Core

I.1.a. Flux Distribution in the One-slab Core

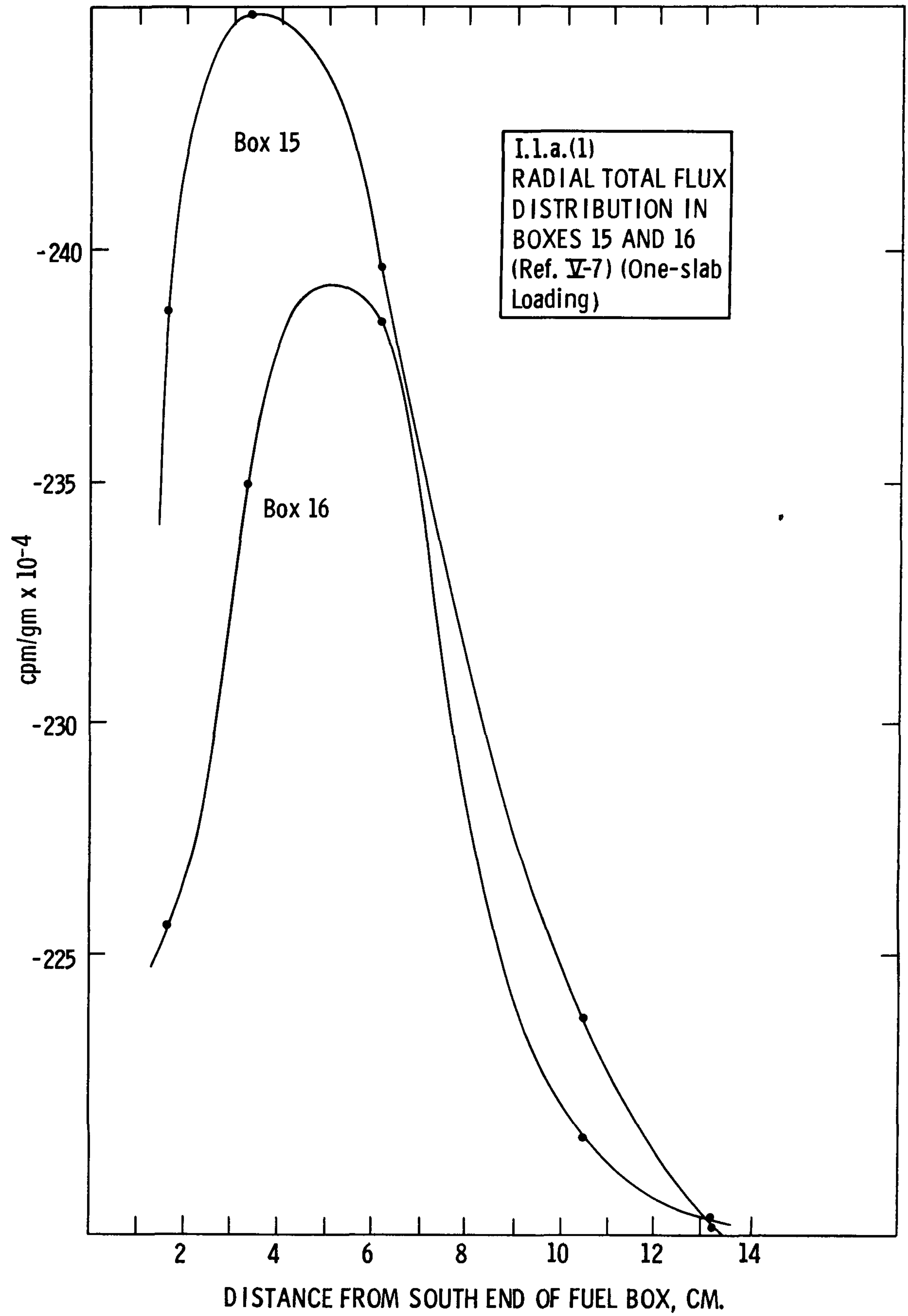
I.1.a.(1)
RADIAL TOTAL FLUX DISTRIBUTION IN BOXES 15 AND 16 (Ref. V-7) (One-slab Loading)
Box 15
Box 16
-240
-235
-230
-225
cpm/gm x 10-4
2
4
6
8
10
12
14
DISTANCE FROM SOUTH END OF FUEL BOX, CM.

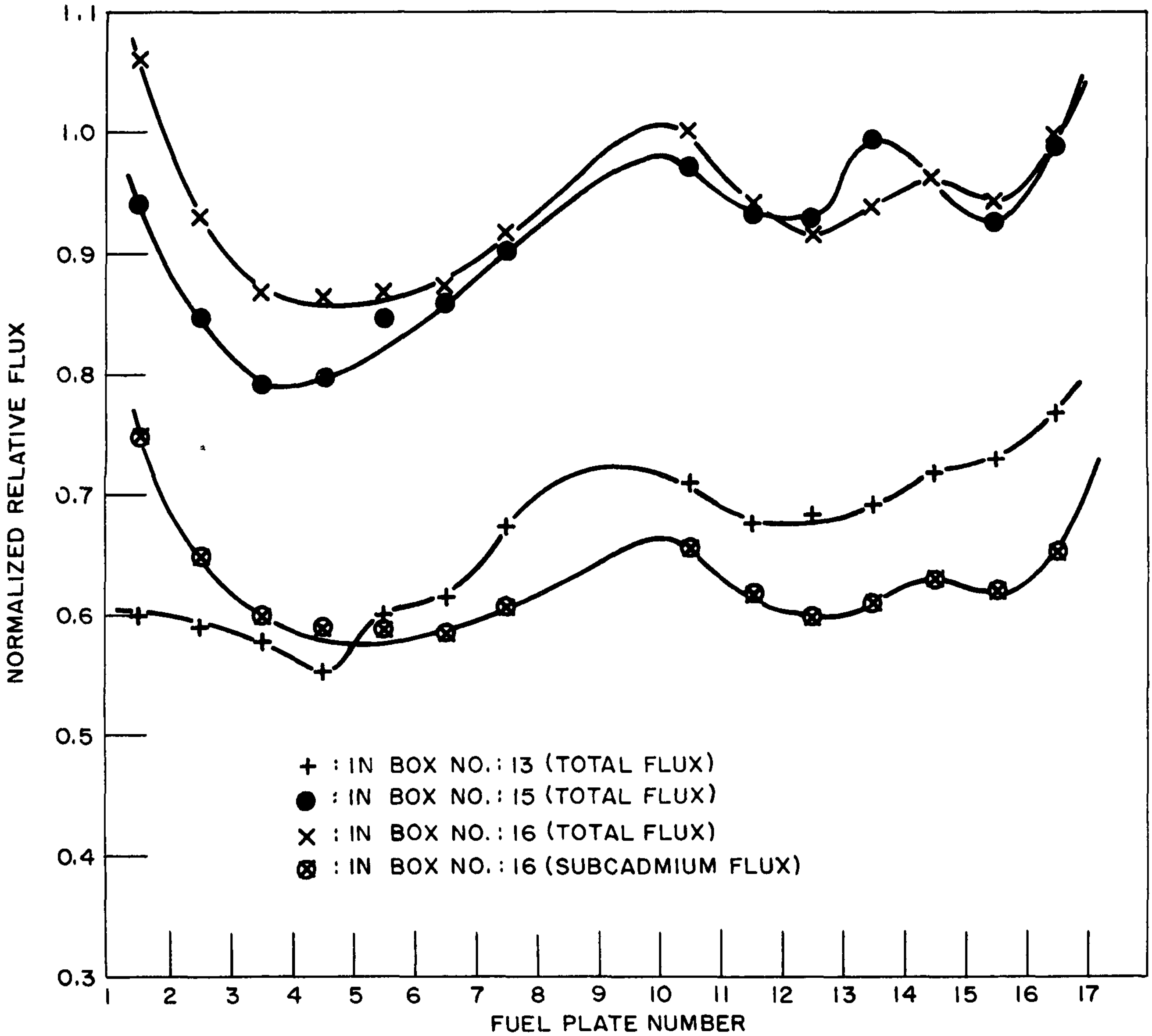

I.1.a.(2)
RADIAL TOTAL FLUX DISTRIBUTIONS DETAILED IN FUEL BOXES (Ref. Private Communication - A. Cilesiz and G. S. Klaiber)

I.1.a.(3)
RADIAL FLUX DISTRIBUTION, TOTAL AND EPICADMIUM, DETAILED IN FUEL BOX 16 (Ref. V-8) (One-slab Loading)

Measured with 3/4 in. Indium Foils Located 11-1/8 in. Down from Top of Fuel.

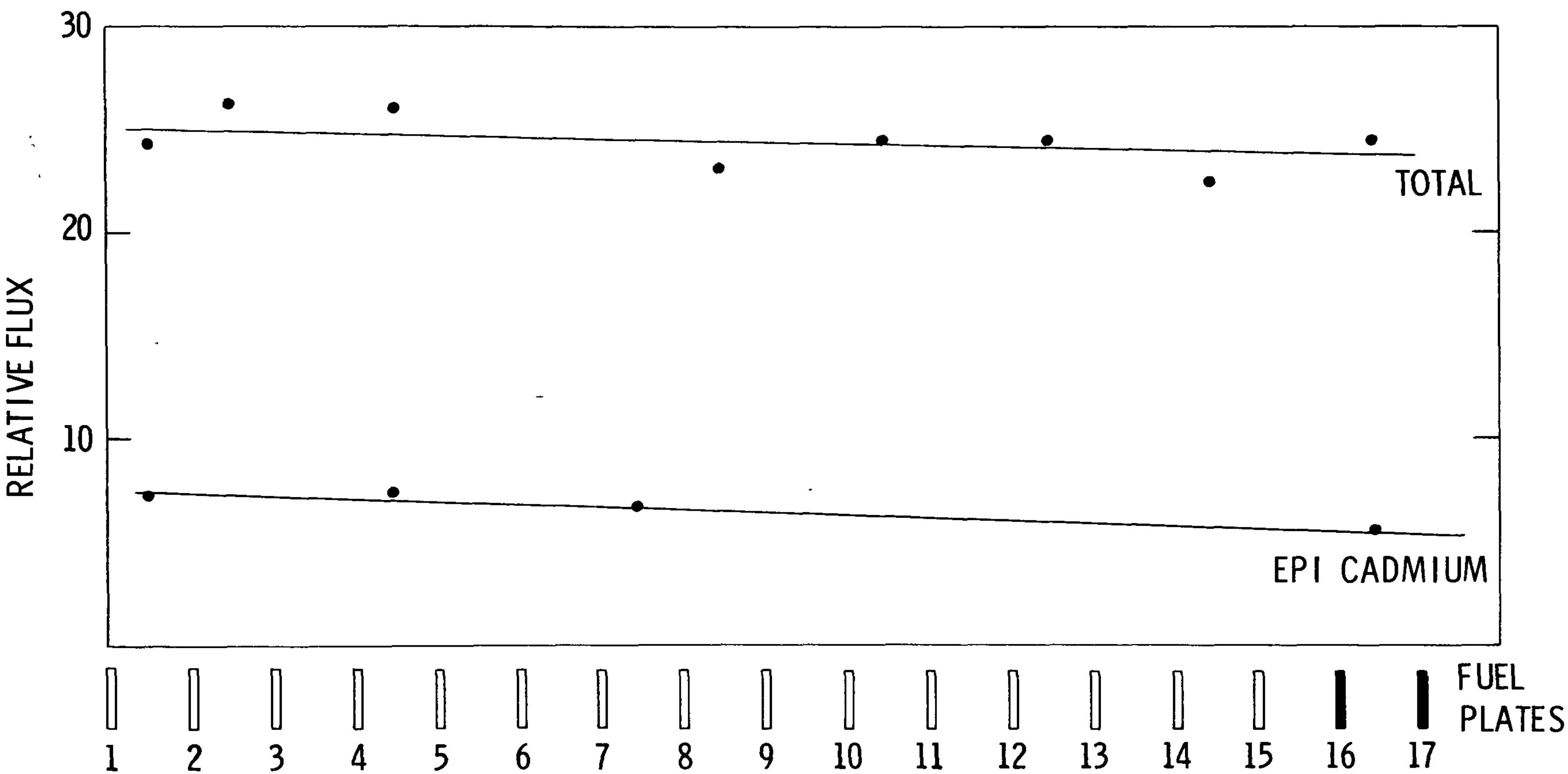

I.1.a.(4)
ANGULAR TOTAL FLUX DISTRIBUTION BETWEEN PLATES 1 AND 2 (Ref. V-8) (One-slab Loading)

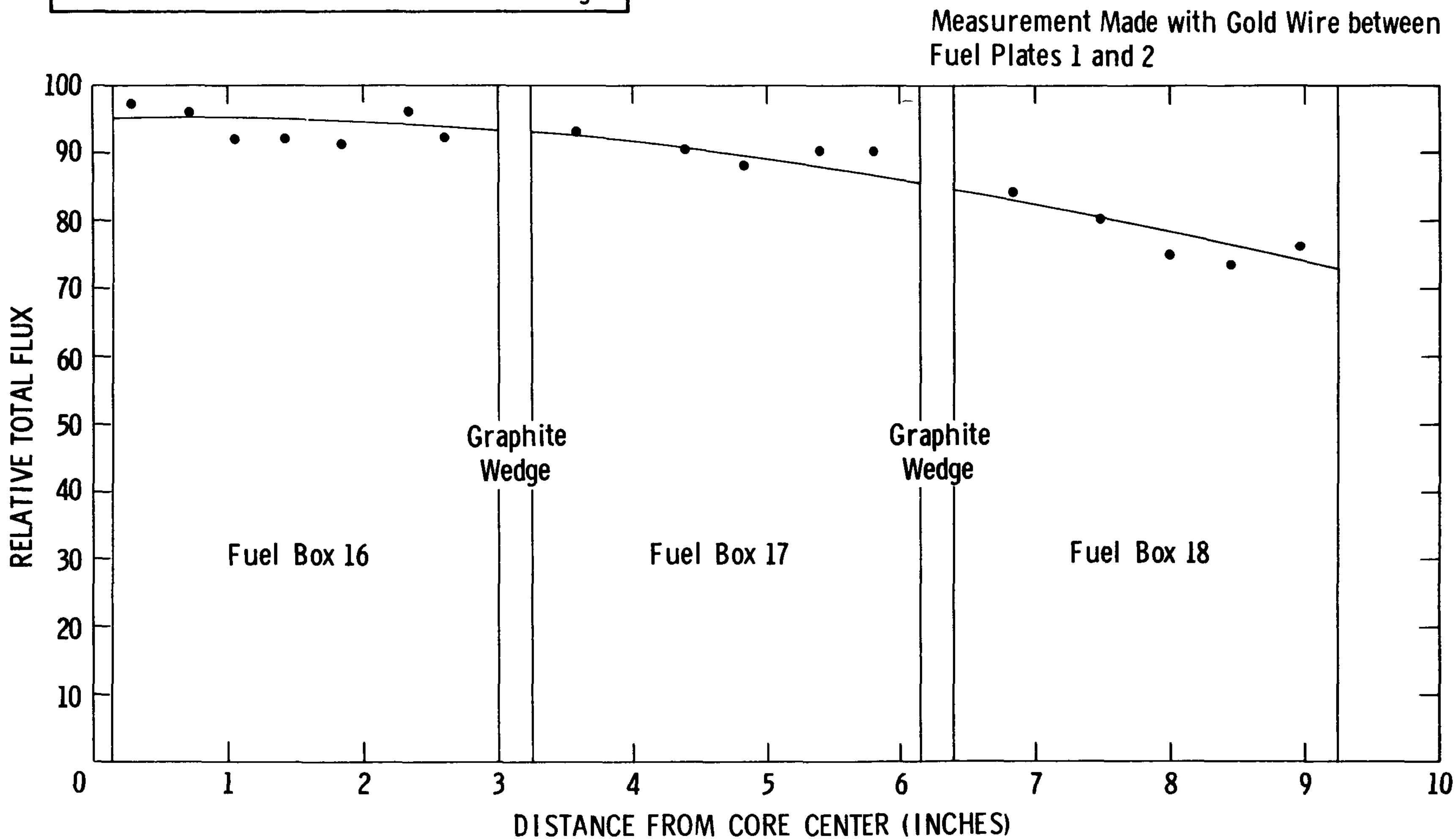

I.1.a.(5)
ANGULAR TOTAL FLUX DISTRIBUTION BETWEEN PLATES 8 AND 9 (Ref. V-8) (One-slab Loading)

Measurement Made with Gold Wire between Fuel Plates 8 and 9

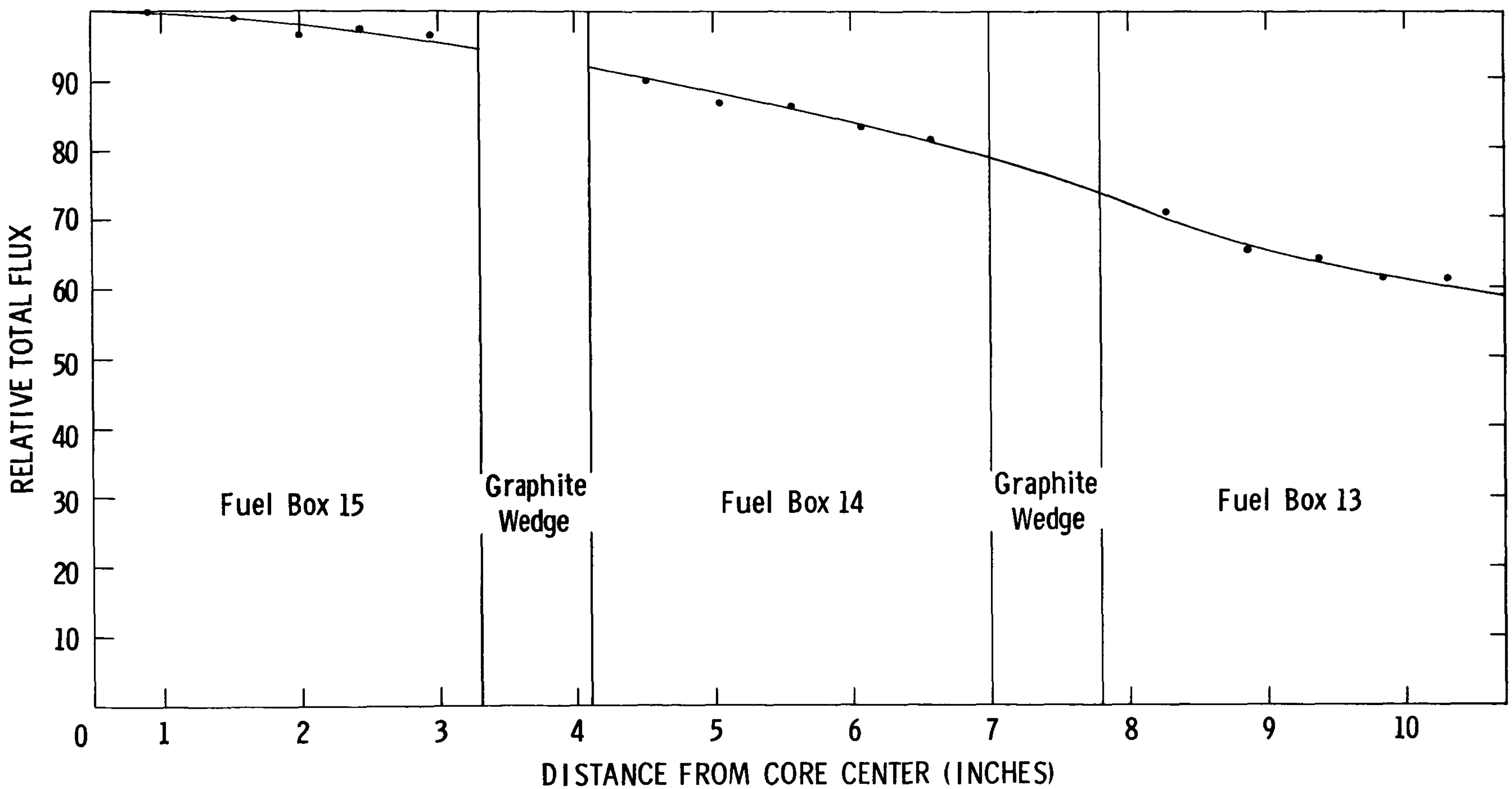

I.1.a.(6)
ANGULAR TOTAL FLUX DISTRIBUTION BETWEEN PLATES 15 AND 16 (Ref. V-8) (One-slab Loading)

Measurement Made with Gold Wire between Fuel Plates 15 and 16

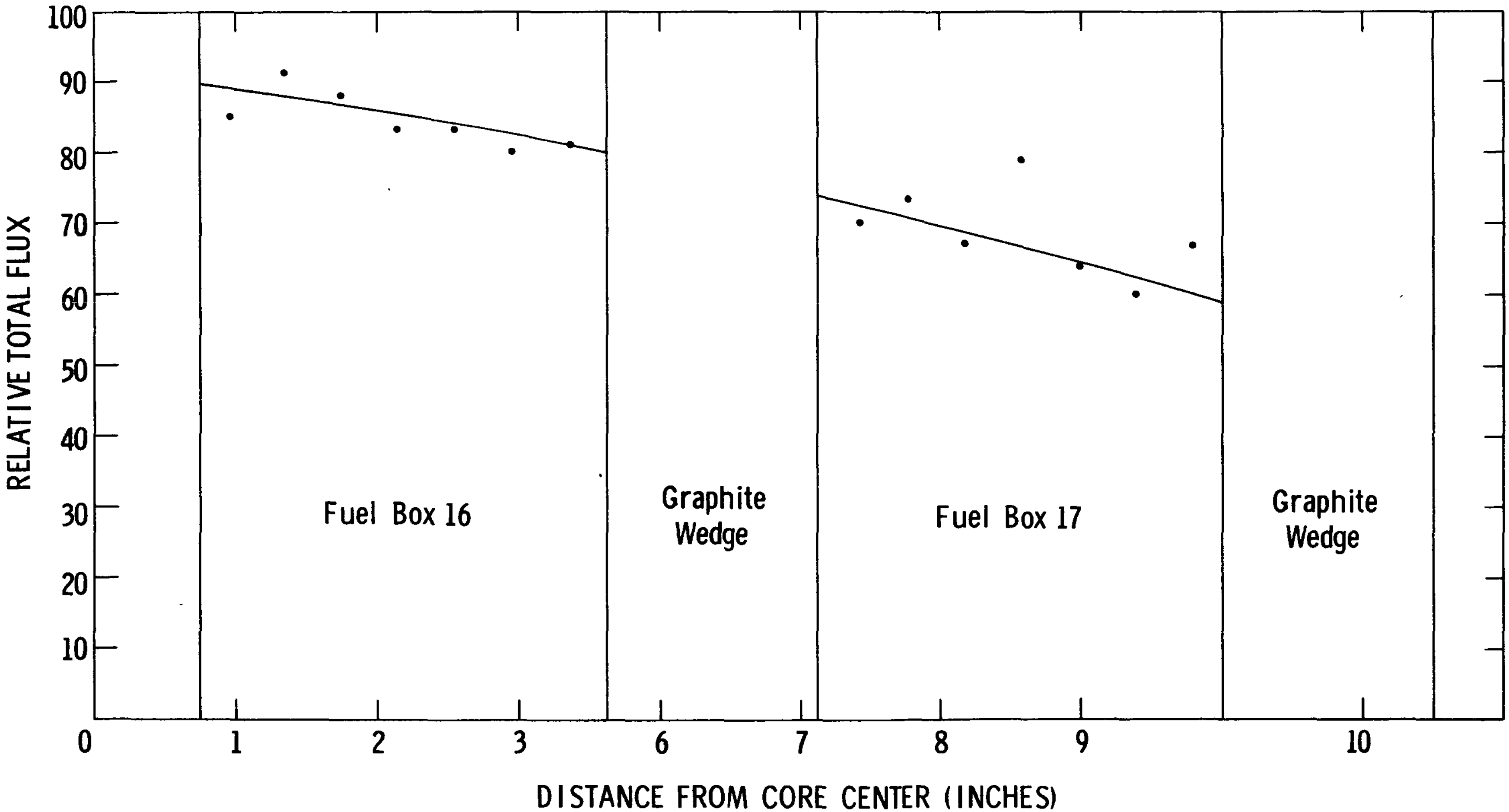

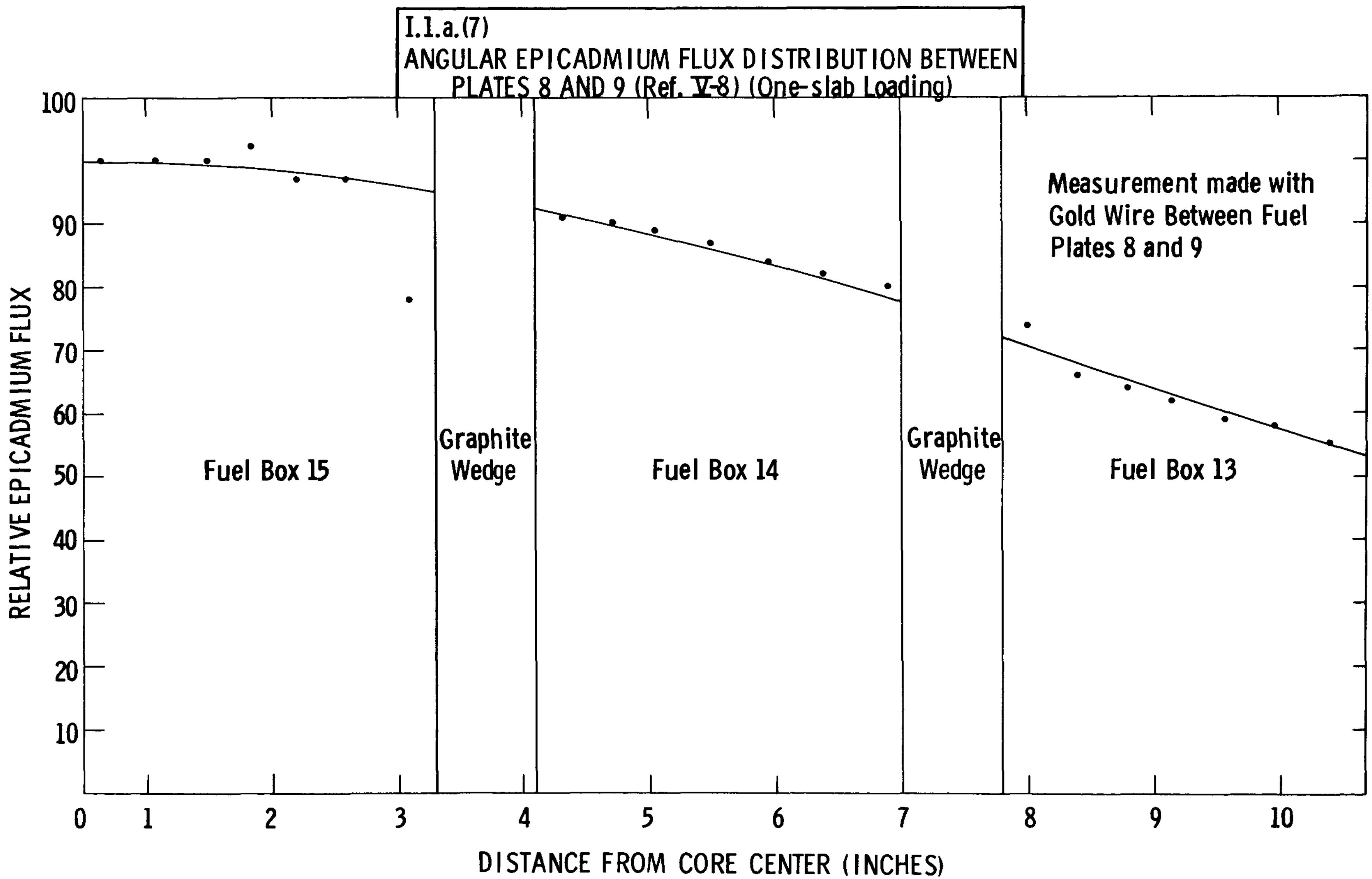
I.1.a.(7)
ANGULAR EPICADMIUM FLUX DISTRIBUTION BETWEEN PLATES 8 AND 9 (Ref. V-8) (One-slab Loading)
Measurement made with Gold Wire Between Fuel Plates 8 and 9
Fuel Box 15
Graphite Wedge
Fuel Box 14
Graphite Wedge
Fuel Box 13
RELATIVE EPICADMIUM FLUX
DISTANCE FROM CORE CENTER (INCHES)
100
90
80
70
60
50
40
30
20
10
0
1
2
3
4
5
6
7
8
9
10

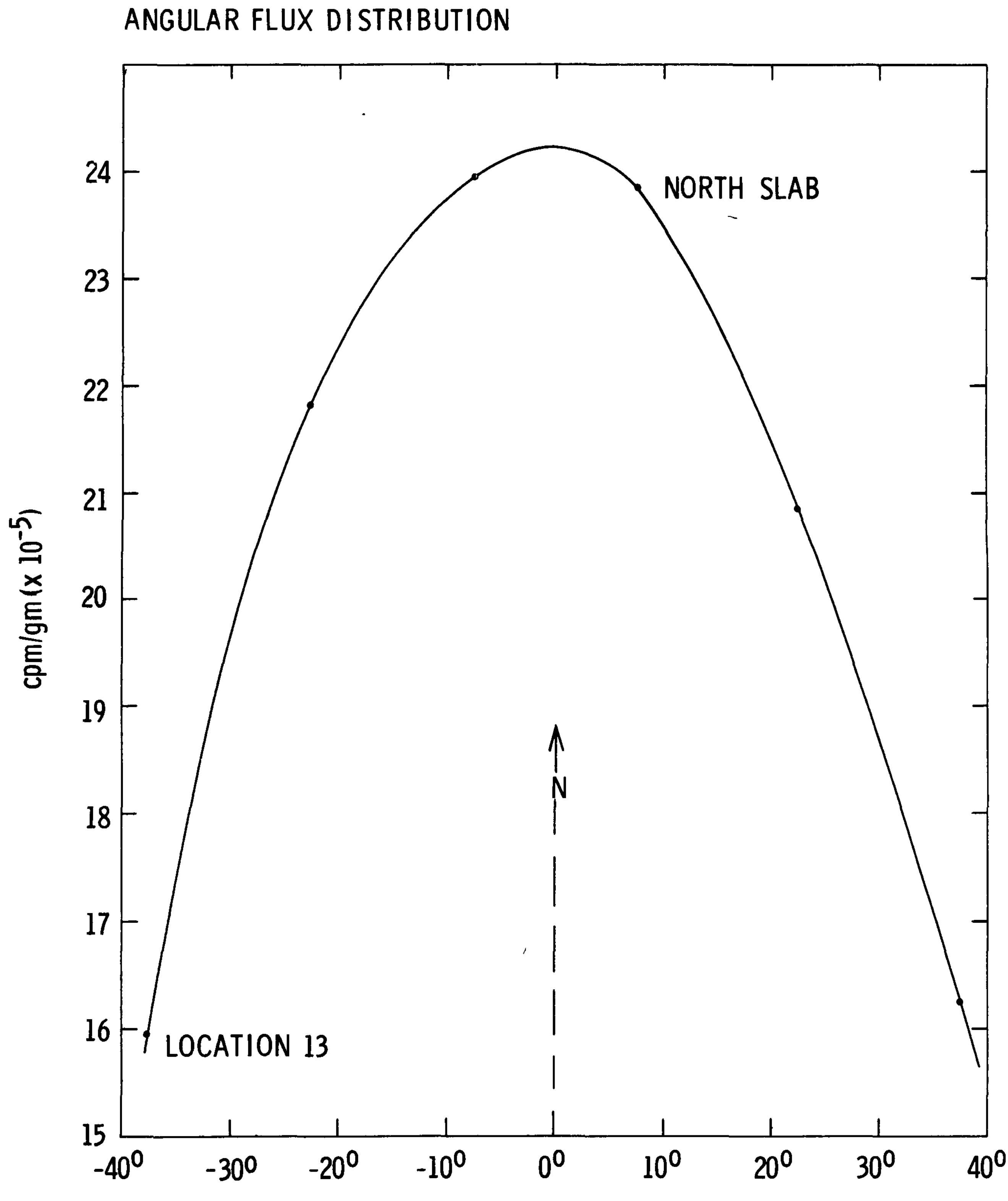

I.1.a.(8)
ANGULAR TOTAL FLUX DISTRIBUTION
(Ref. V-7) (One-slab Loading)

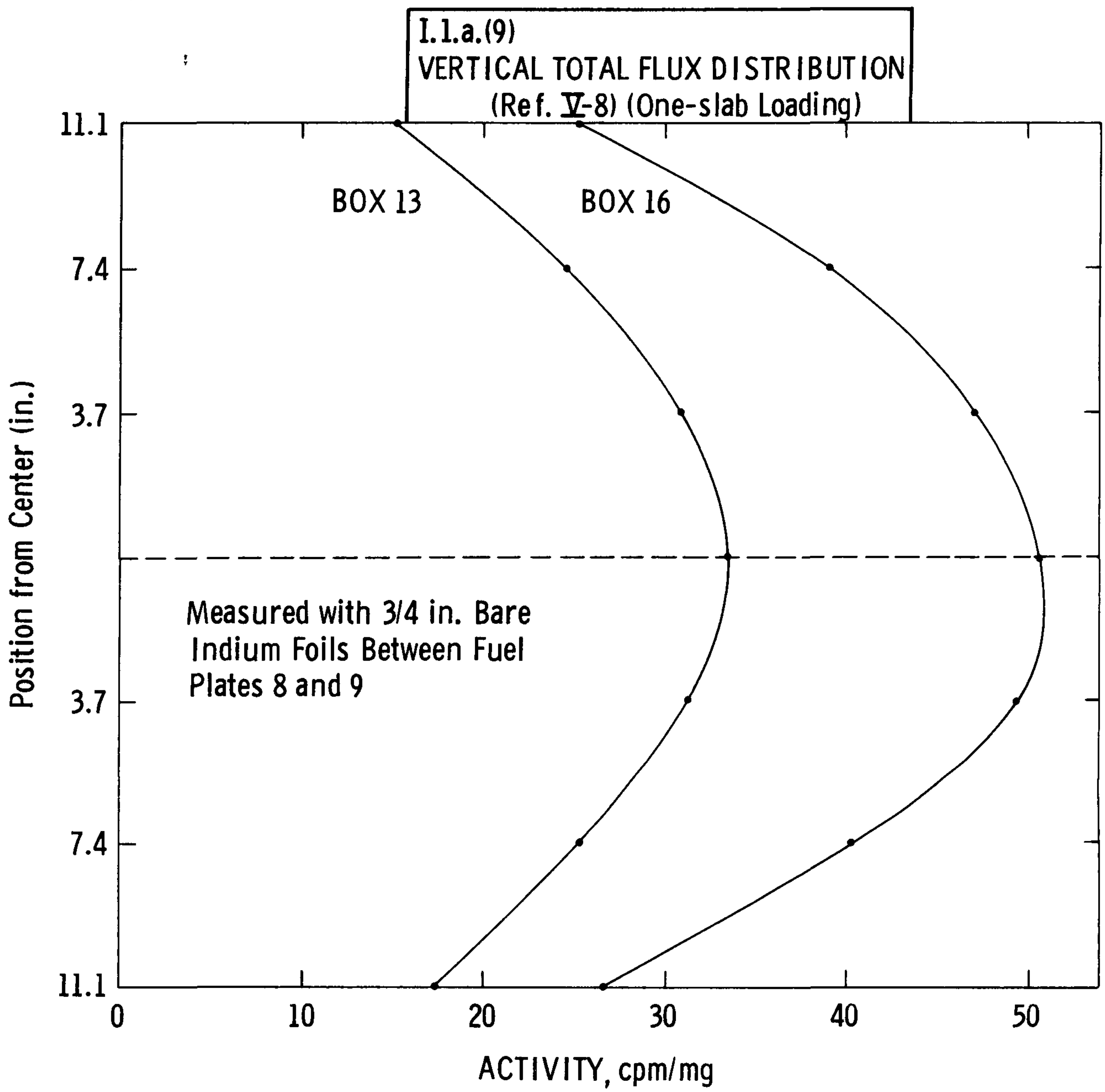
I.1.a.(9)
VERTICAL TOTAL FLUX DISTRIBUTION
(Ref. V-8) (One-slab Loading)
BOX 13
BOX 16
Measured with 3/4 in. Bare Indium Foils Between Fuel Plates 8 and 9
Position from Center (in.)
11.1
7.4
3.7
3.7
7.4
11.1
0
10
20
30
40
50
ACTIVITY, cpm/mg

I.1.b. Flux Distributions in the Two-slab Core

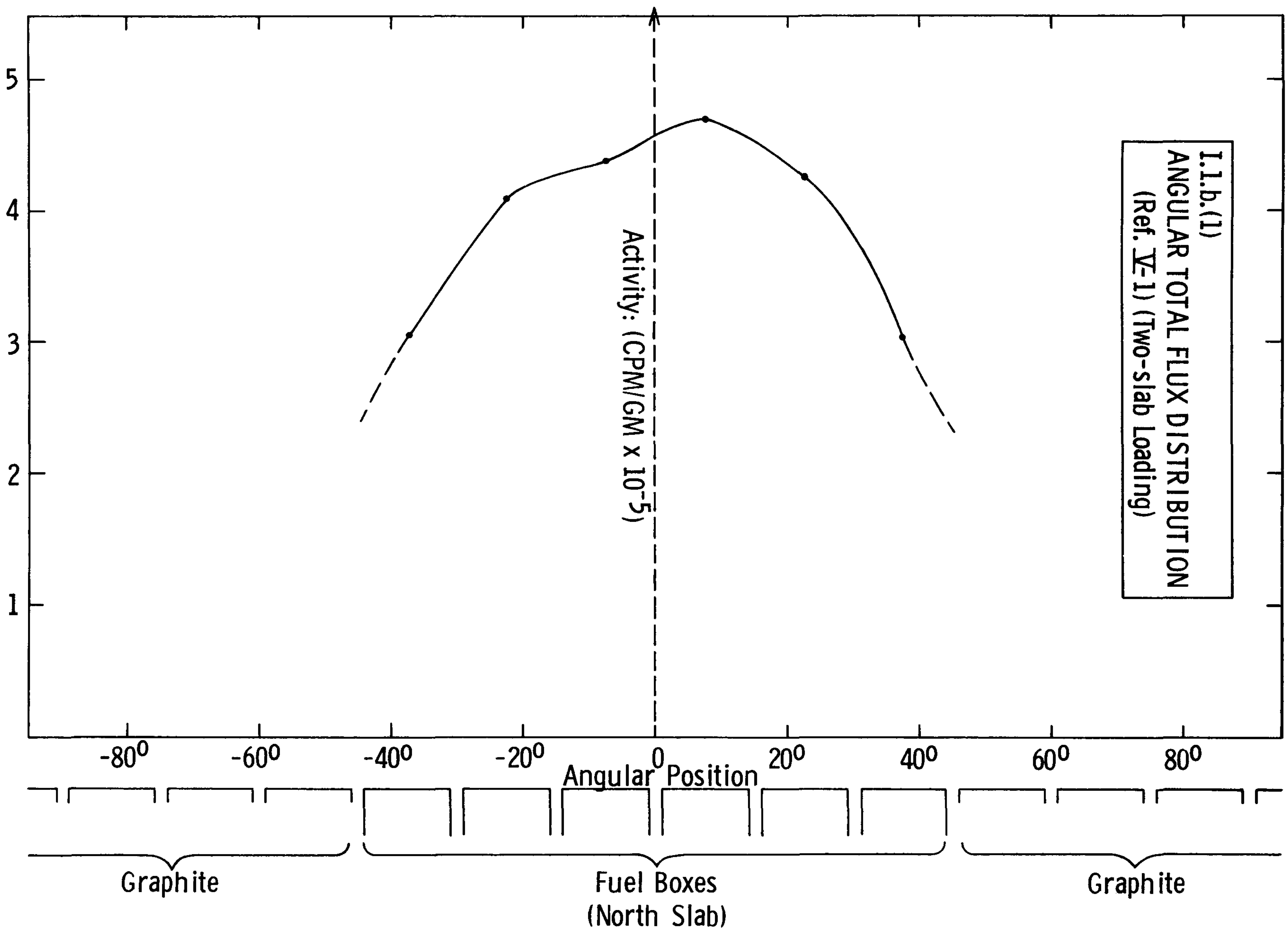

I.1.b.(1)
ANGULAR TOTAL FLUX DISTRIBUTION
(Ref. V-1) (Two-slab Loading)
Activity: (CPM/GM x 10^{-5})
5
4
3
2
1
-80^0
-60^0
-40^0
-20^0
0
20^0
40^0
60^0
80^0
Angular Position
Graphite
Fuel Boxes
(North Slab)
Graphite

I.1.b.(2)
VERTICAL FLUX DISTRIBUTION, TOTAL, THERMAL AND EPICADMIUM (Ref. V-1)
(Two-slab Loading)

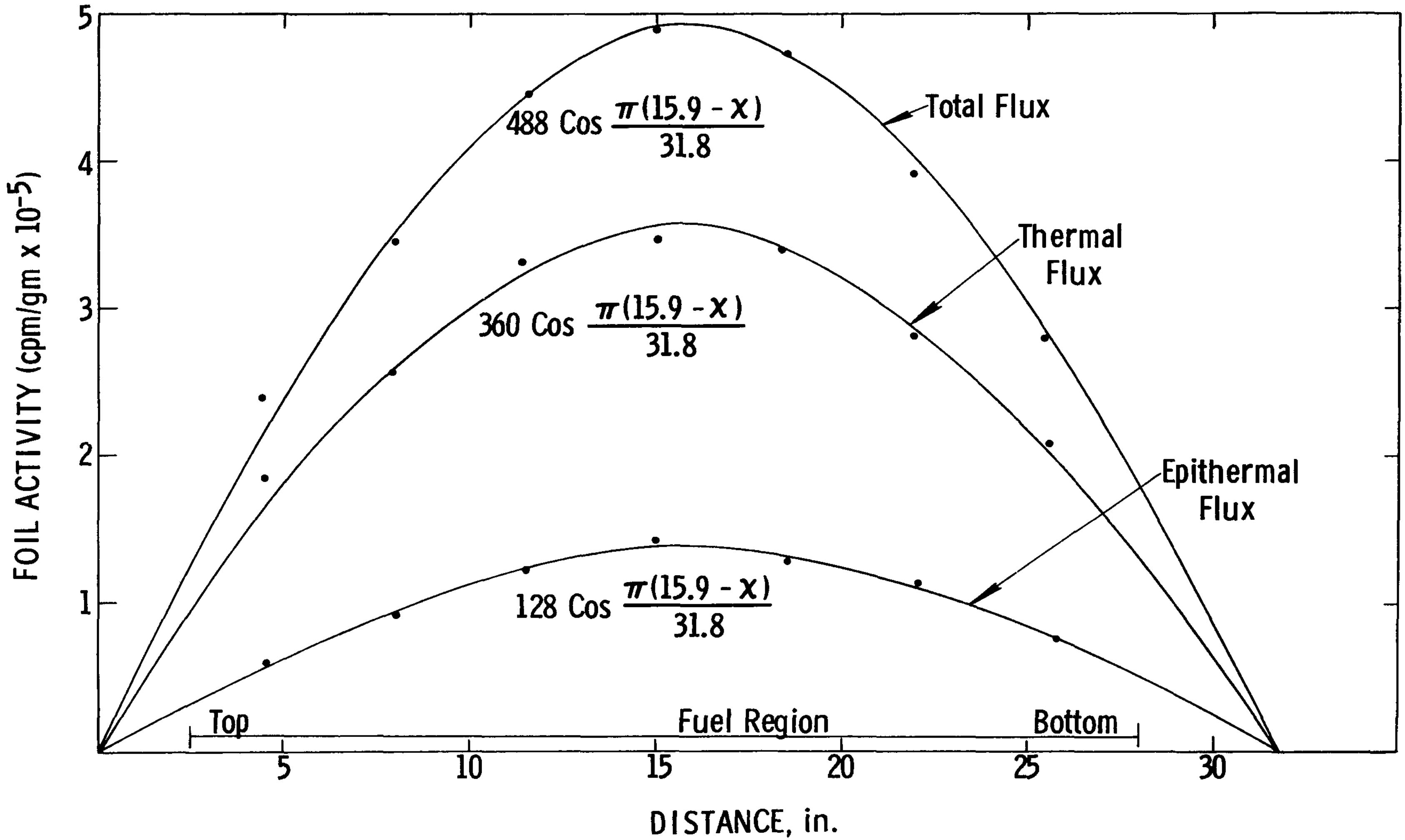

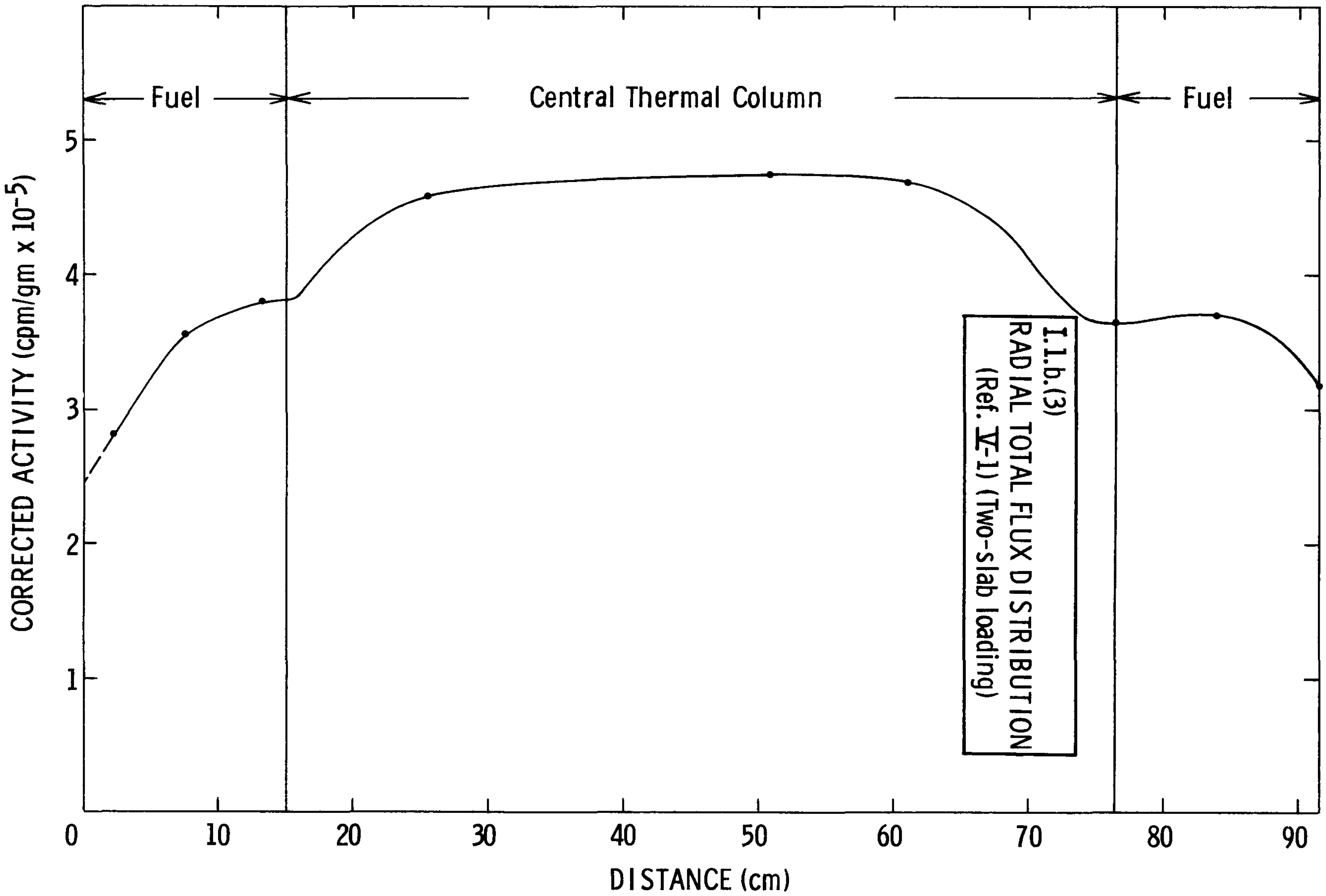

I.1.b.(3)
RADIAL TOTAL FLUX DISTRIBUTION
(Ref. V-1) (Two-slab loading)

I.1.c. Flux Distributions in the Annular Core

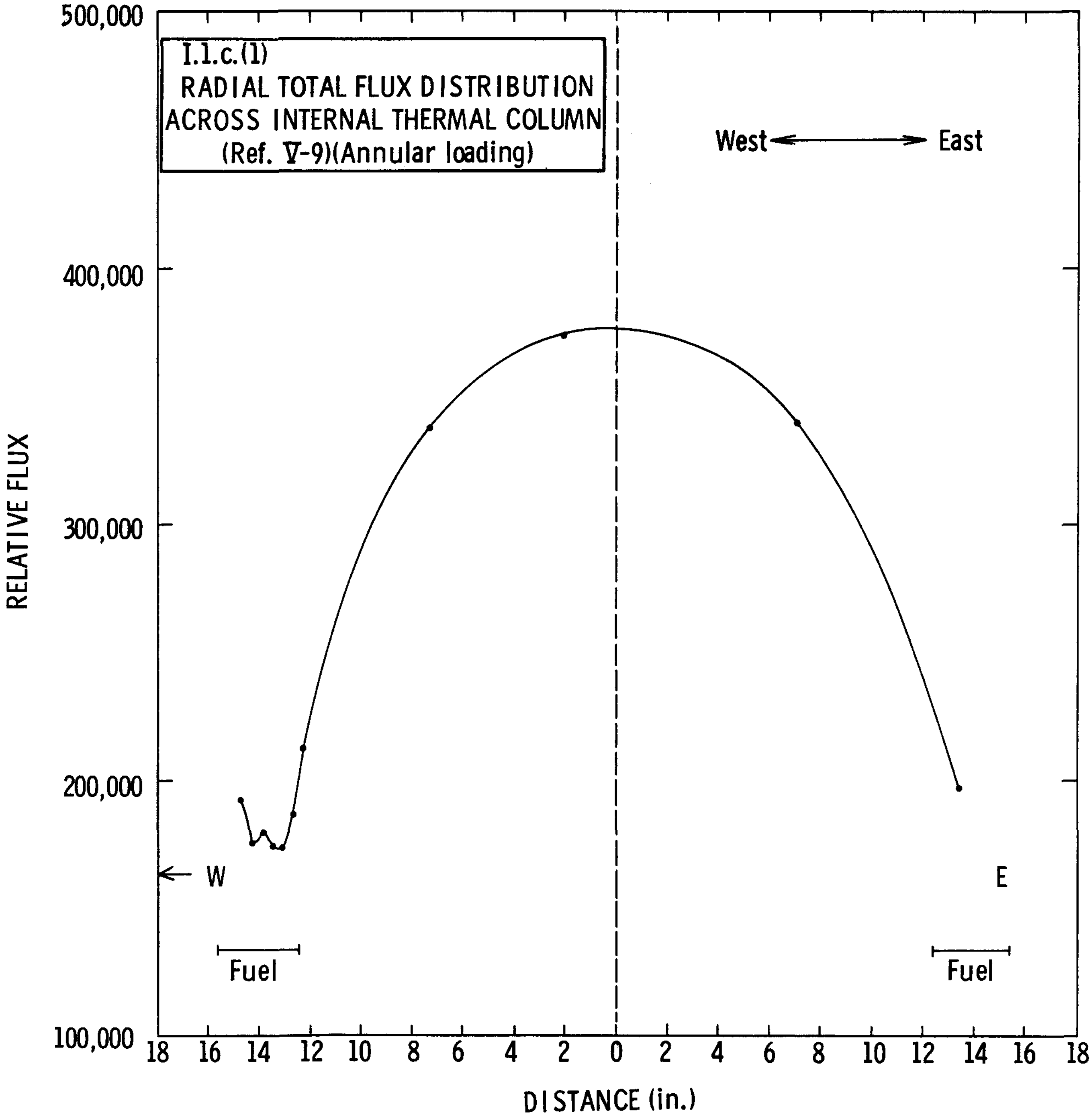
I.1.c.(1)
RADIAL TOTAL FLUX DISTRIBUTION
ACROSS INTERNAL THERMAL COLUMN
(Ref. V-9)(Annular loading)
West ←→ East
500,000
400,000
300,000
200,000
100,000
RELATIVE FLUX
W
E
Fuel
Fuel
18 16 14 12 10 8 6 4 2 0 2 4 6 8 10 12 14 16 18
DISTANCE (in.)

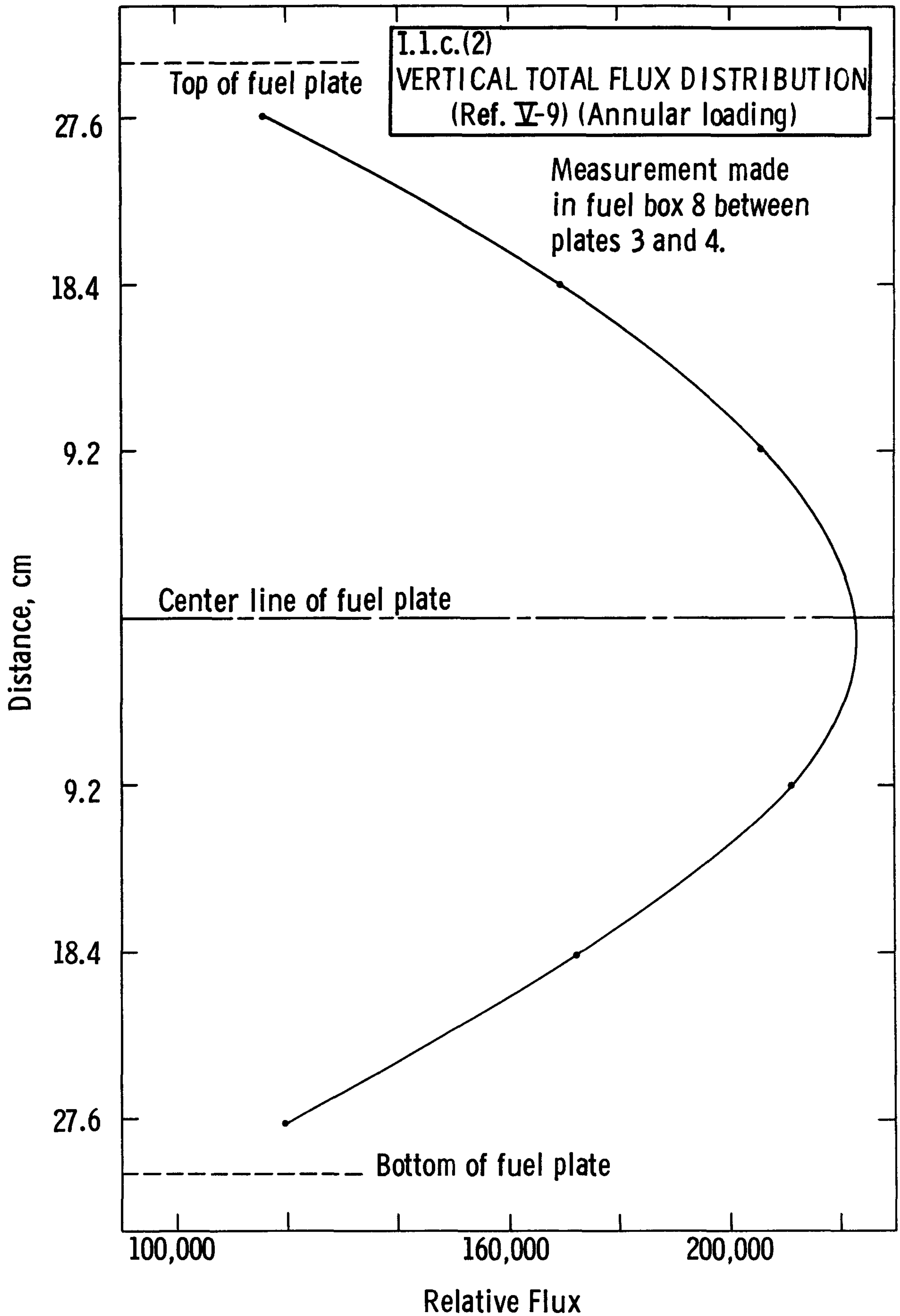
I.1.c.(2)
VERTICAL TOTAL FLUX DISTRIBUTION
(Ref. V-9) (Annular loading)
Measurement made
in fuel box 8 between
plates 3 and 4.
Top of fuel plate
Center line of fuel plate
Bottom of fuel plate
27.6
18.4
9.2
9.2
18.4
27.6
Distance, cm
100,000
160,000
200,000
Relative Flux

I.2. Flux Distributions in the Thermal Columns

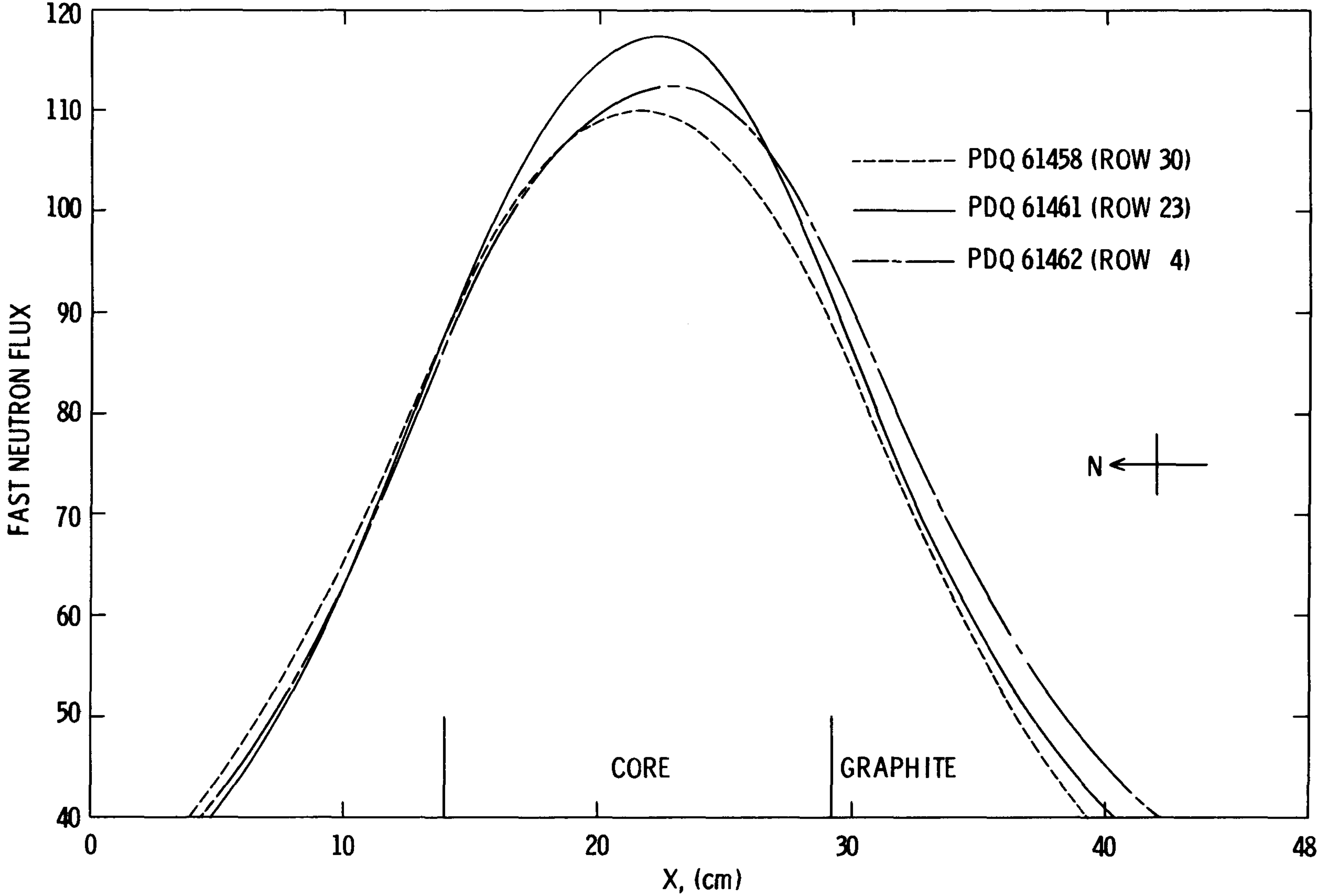

I.2.a.
THEORETICAL RADIAL FAST NEUTRON FLUX ACROSS CORE, INTERNAL AND EXTERNAL THERMAL COLUMNS (Ref. II-5) (one-slab loading)

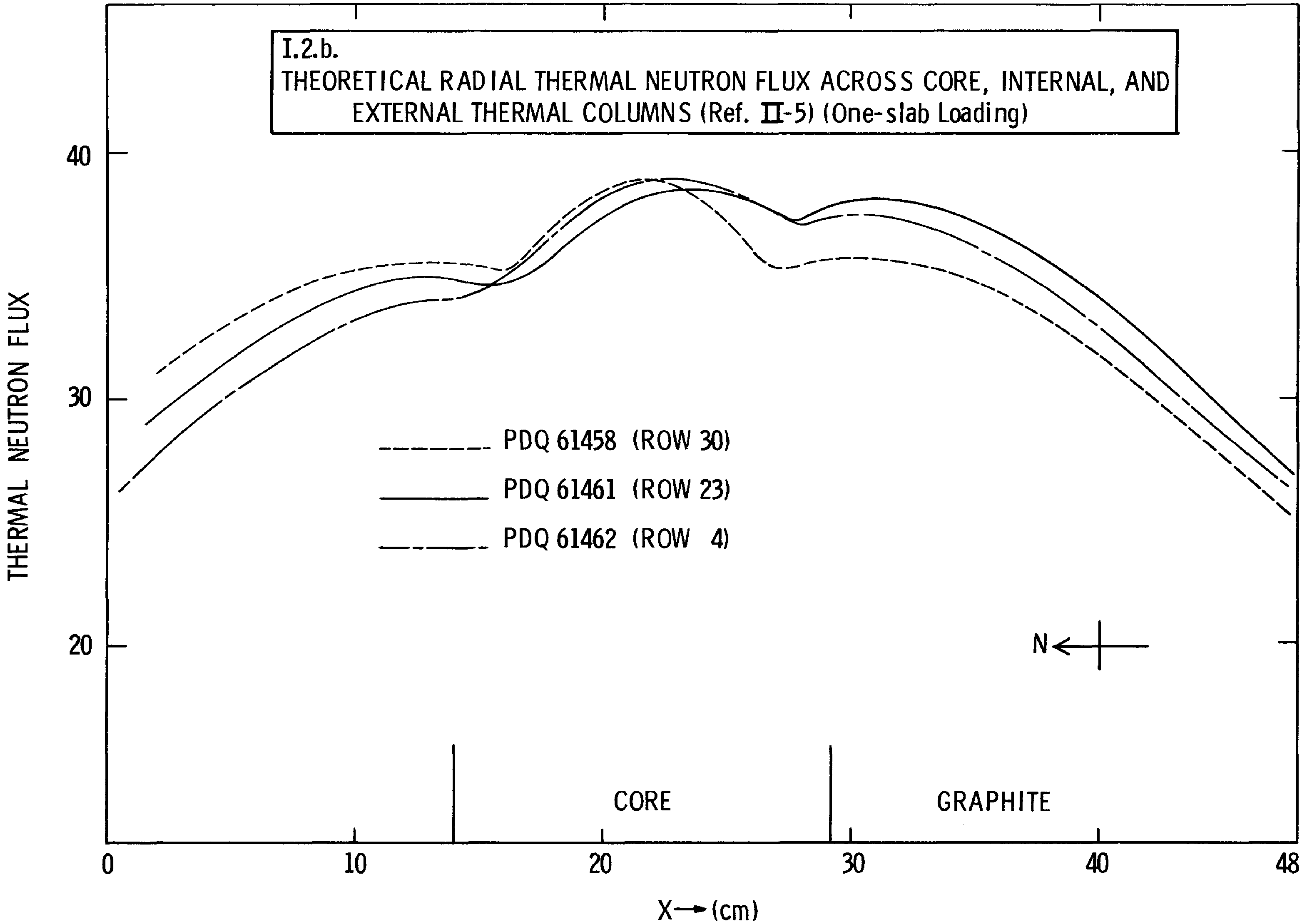

I.2.b.
THEORETICAL RADIAL THERMAL NEUTRON FLUX ACROSS CORE, INTERNAL, AND EXTERNAL THERMAL COLUMNS (Ref. II-5) (One-slab Loading)
THERMAL NEUTRON FLUX
40
30
20
PDQ 61458 (ROW 30)
PDQ 61461 (ROW 23)
PDQ 61462 (ROW 4)
N
CORE
GRAPHITE
0
10
20
30
40
48
X→ (cm)

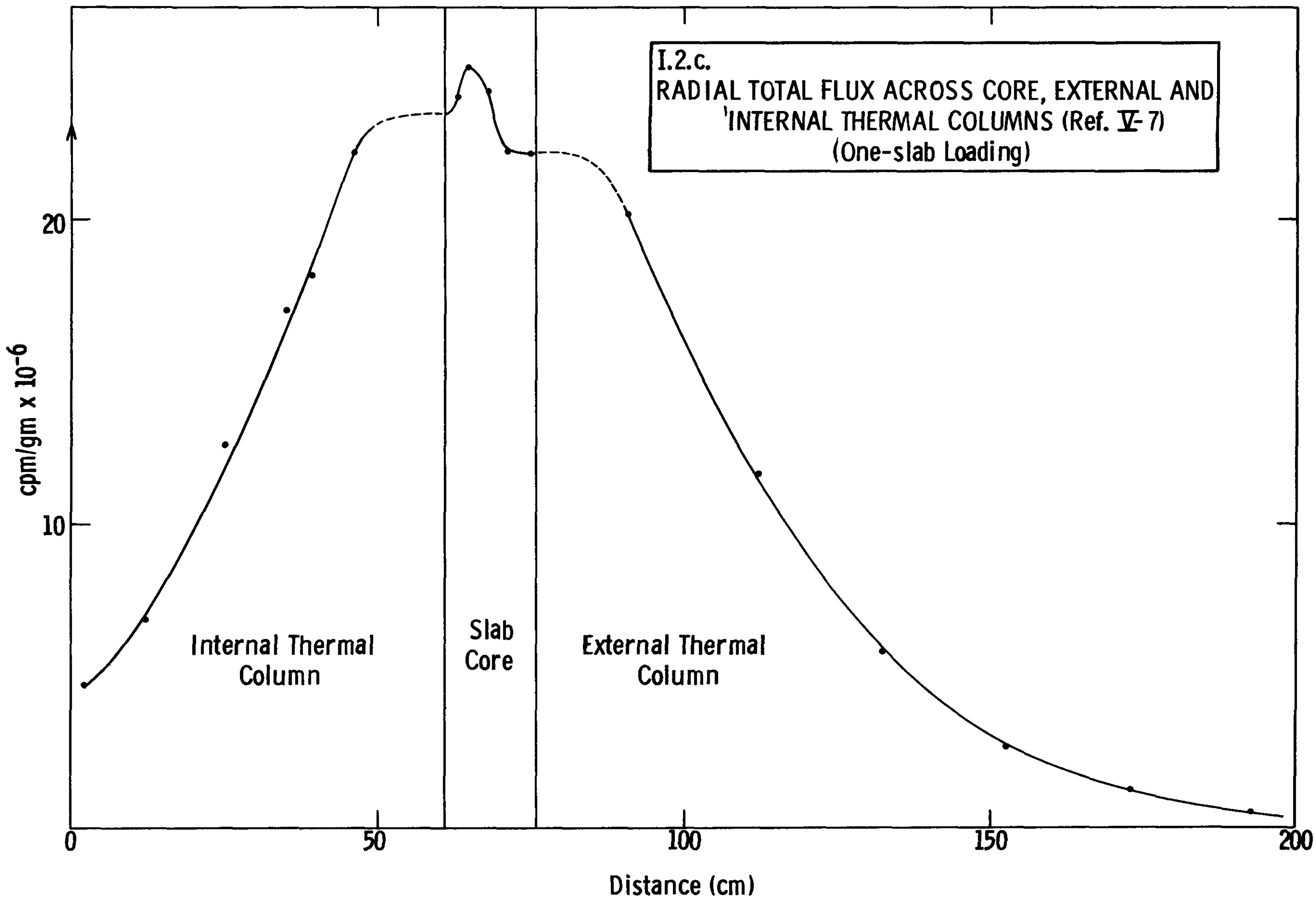
I.2.c.
RADIAL TOTAL FLUX ACROSS CORE, EXTERNAL AND INTERNAL THERMAL COLUMNS (Ref. V-7)
(One-slab Loading)
cpm/gm x 10^{-6}
20
10
0
50
100
150
200
Distance (cm)
Internal Thermal Column
Slab Core
External Thermal Column

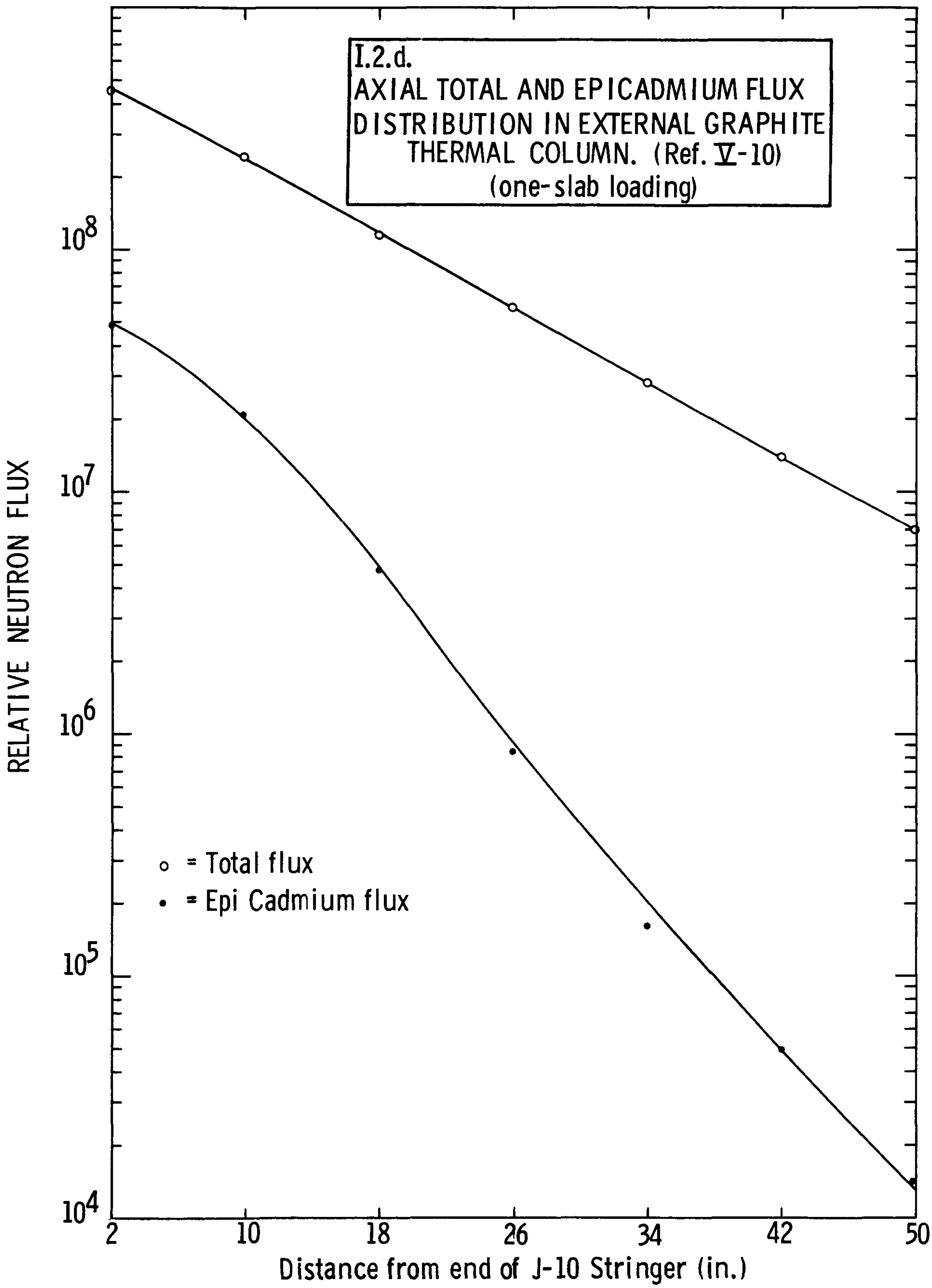
I.2.d.
AXIAL TOTAL AND EPICADMIUM FLUX DISTRIBUTION IN EXTERNAL GRAPHITE THERMAL COLUMN. (Ref. V-10)
(one-slab loading)
RELATIVE NEUTRON FLUX
10^8
10^7
10^6
10^5
10^4
○ = Total flux
• = Epi Cadmium flux
2
10
18
26
34
42
50
Distance from end of J-10 Stringer (in.)

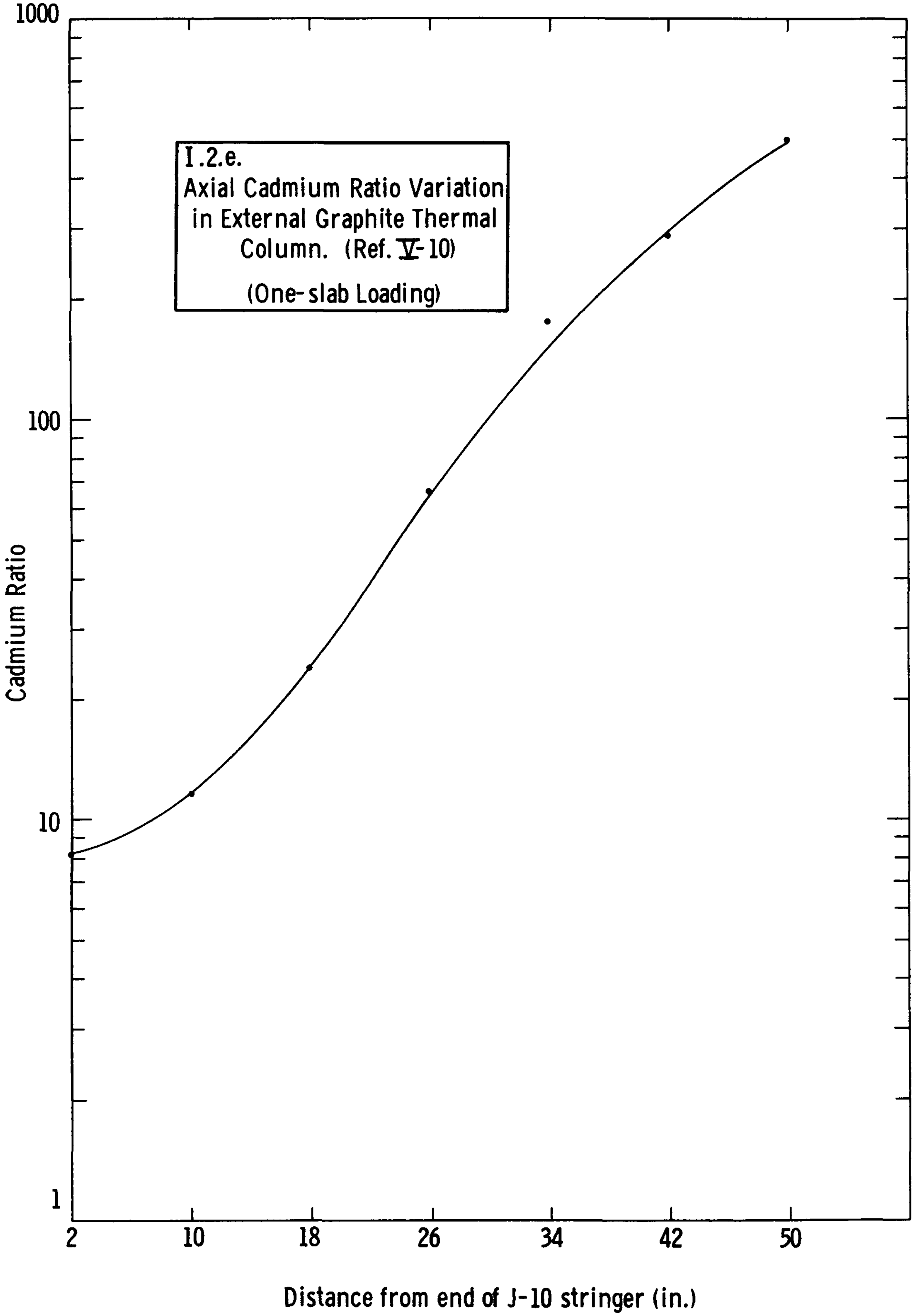

I.2.e.
Axial Cadmium Ratio Variation in External Graphite Thermal Column. (Ref. V-10)
(One-slab Loading)
1000
100
10
1
Cadmium Ratio
2
10
18
26
34
42
50
Distance from end of J-10 stringer (in.)

I.3. Flux Distributions in the Water Shielding Tank

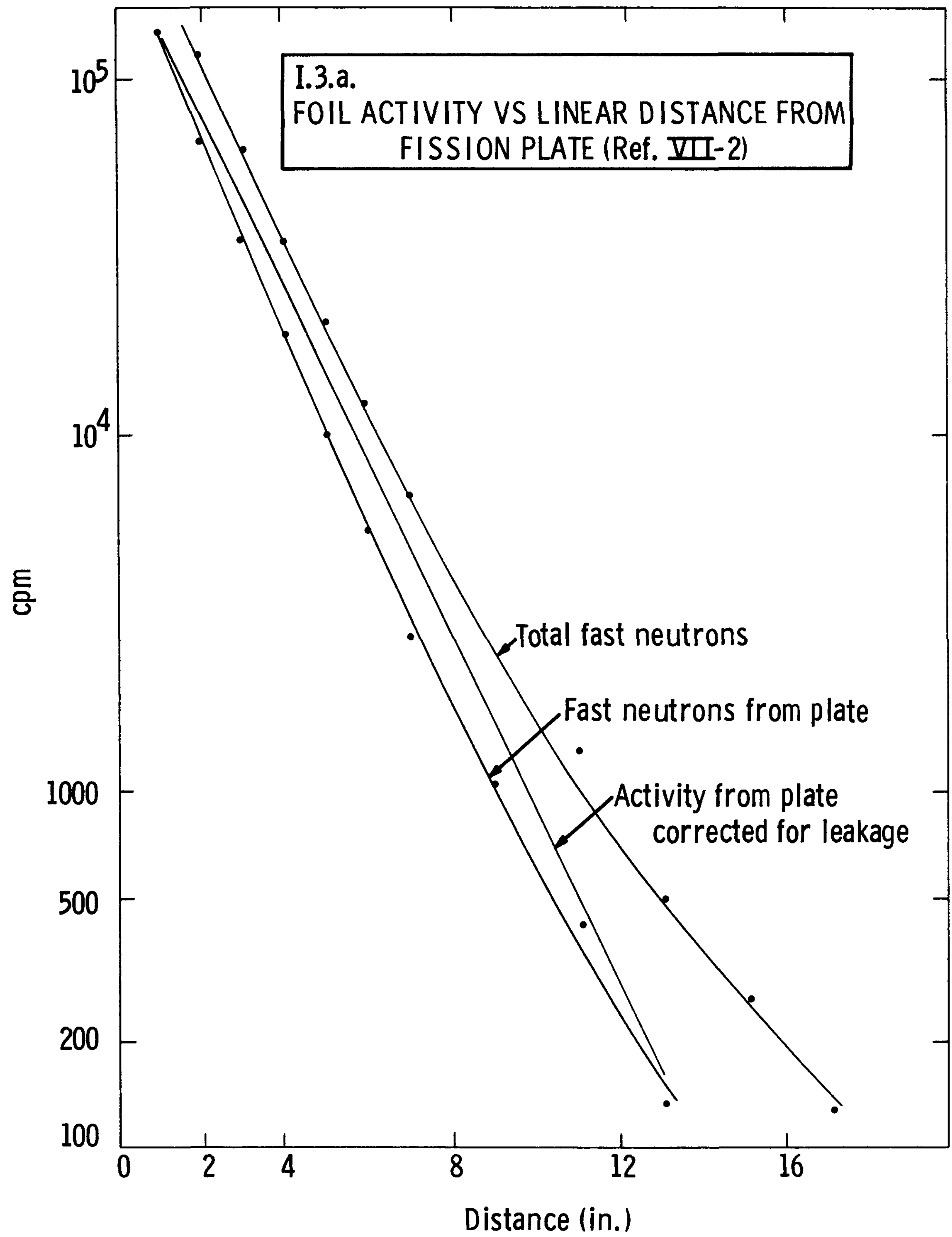
I.3.a.
FOIL ACTIVITY VS LINEAR DISTANCE FROM FISSION PLATE (Ref. VII-2)
Total fast neutrons
Fast neutrons from plate
Activity from plate corrected for leakage
cpm
10^5
10^4
1000
500
200
100
0
2
4
8
12
16
Distance (in.)

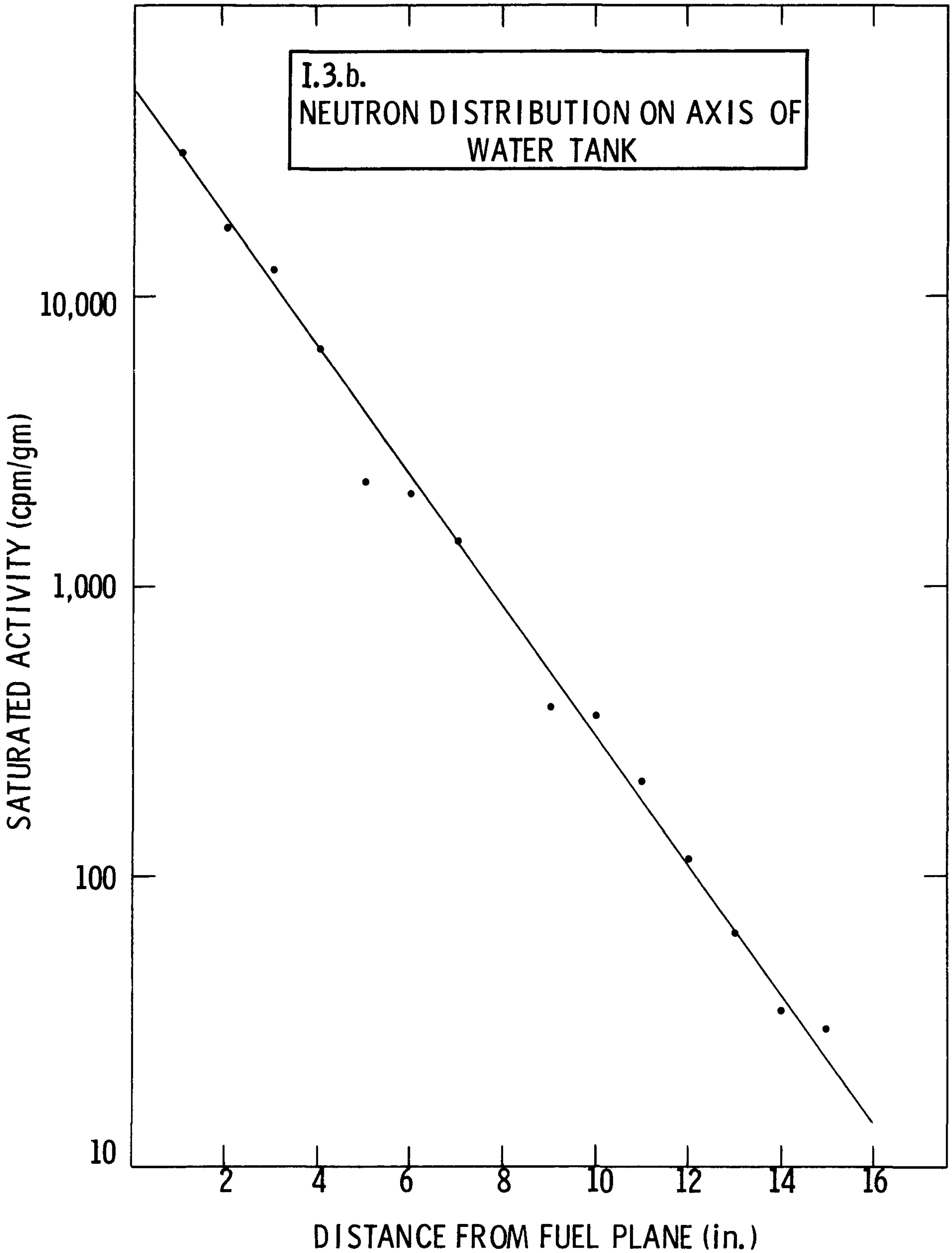
I.3.b.
NEUTRON DISTRIBUTION ON AXIS OF WATER TANK
10,000
1,000
100
10
SATURATED ACTIVITY (cpm/gm)
2
4
6
8
10
12
14
16
DISTANCE FROM FUEL PLANE (in.)

I.3.c.
NEUTRON DISTRIBUTION NORMAL TO AXIS OF WATER TANK

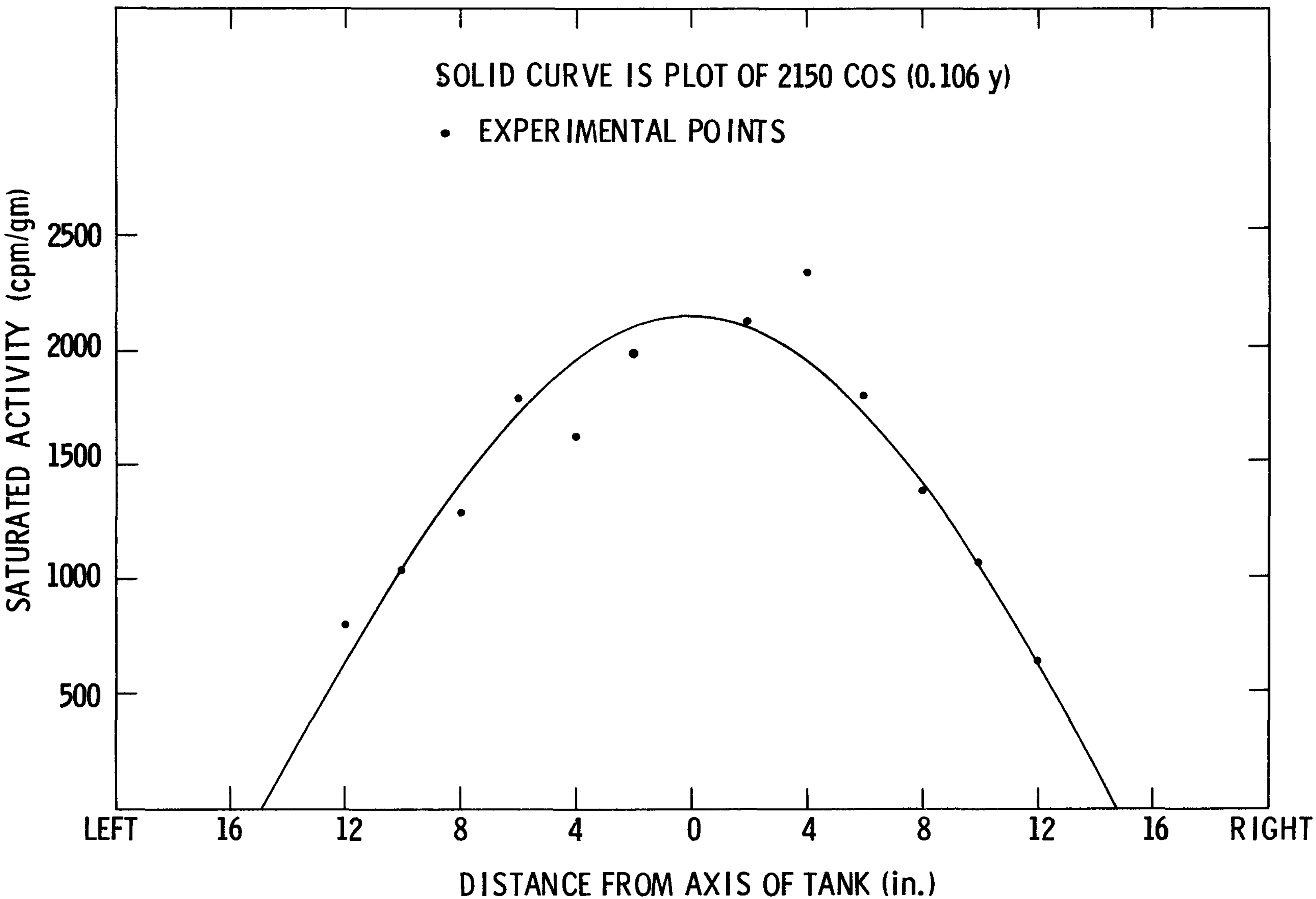

I.4. Flux Measurements in Beams and Beam Channels

I.4.a.
MEASUREMENT OF RELATIVE FLUX IN BEAM HOLES
(Ref. V-5)(Two-slab Loading)

Foil activity in cpm as a function of position.
Reactor operated at 1 watt for 54 minutes.

x = Cd covered In
o = Al covered In

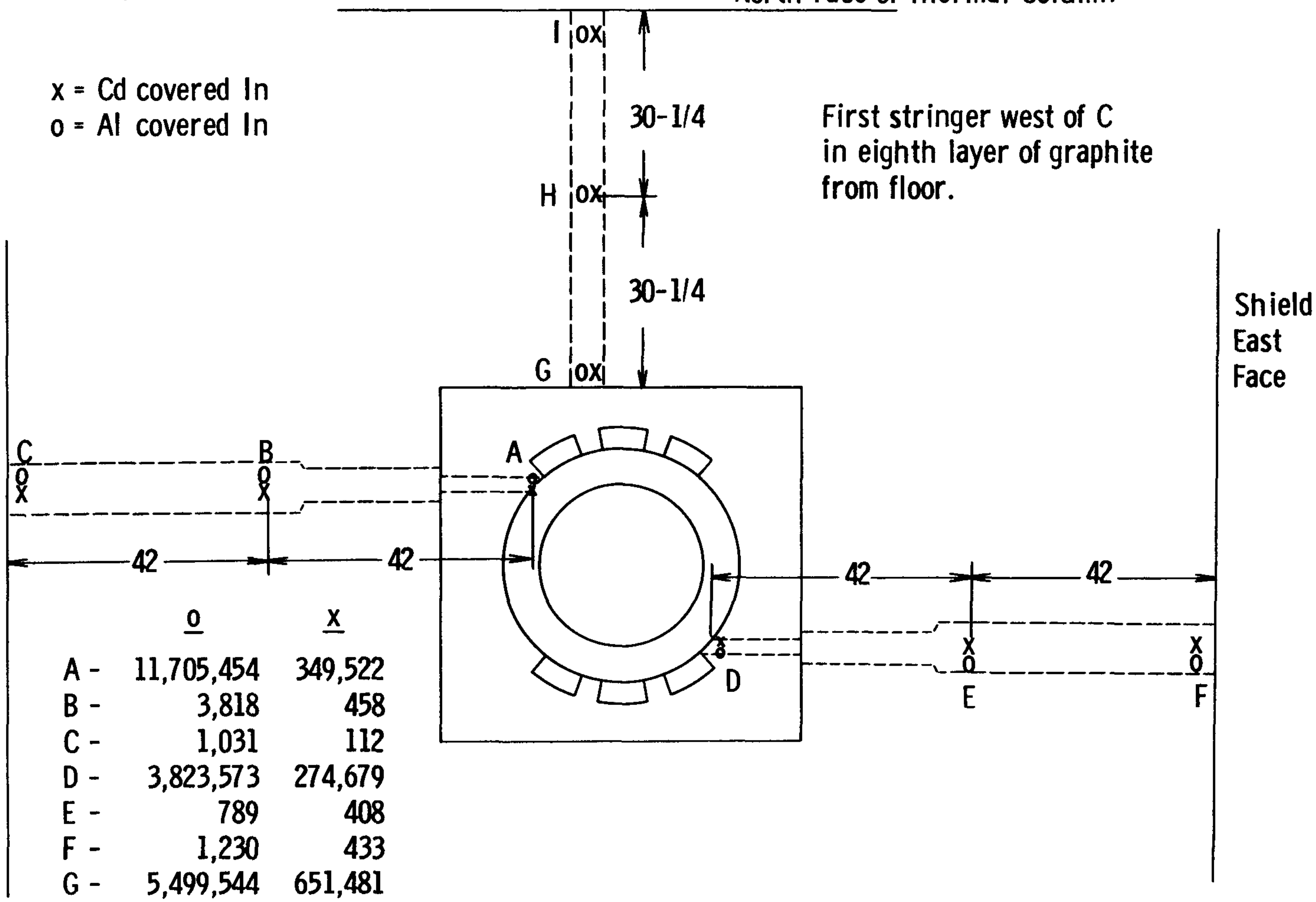

	o	x
A -	11,705,454	349,522
B -	3,818	458
C -	1,031	112
D -	3,823,573	274,679
E -	789	408
F -	1,230	433
G -	5,499,544	651,481
H -	1,101,969	6,979
I -	30,284	488

I.4.b. Effect of Cadmium Next to Beam Hole. (Ref: II-6)

The neutron beam from a 1-inch square beam hole in the J-10 stringer was monitored using a BF_3 long counter outside the biological shield. The effect measured was the reduction in neutron flux when 8 square inches of Cd was replaced by 15 square inches placed next to the beam hole at the reactor face.

Reduction in thermal neutron current 4.6 ± 1.1%.

Reduction in epicadmium neutron current 11.2 ± 2.5%.

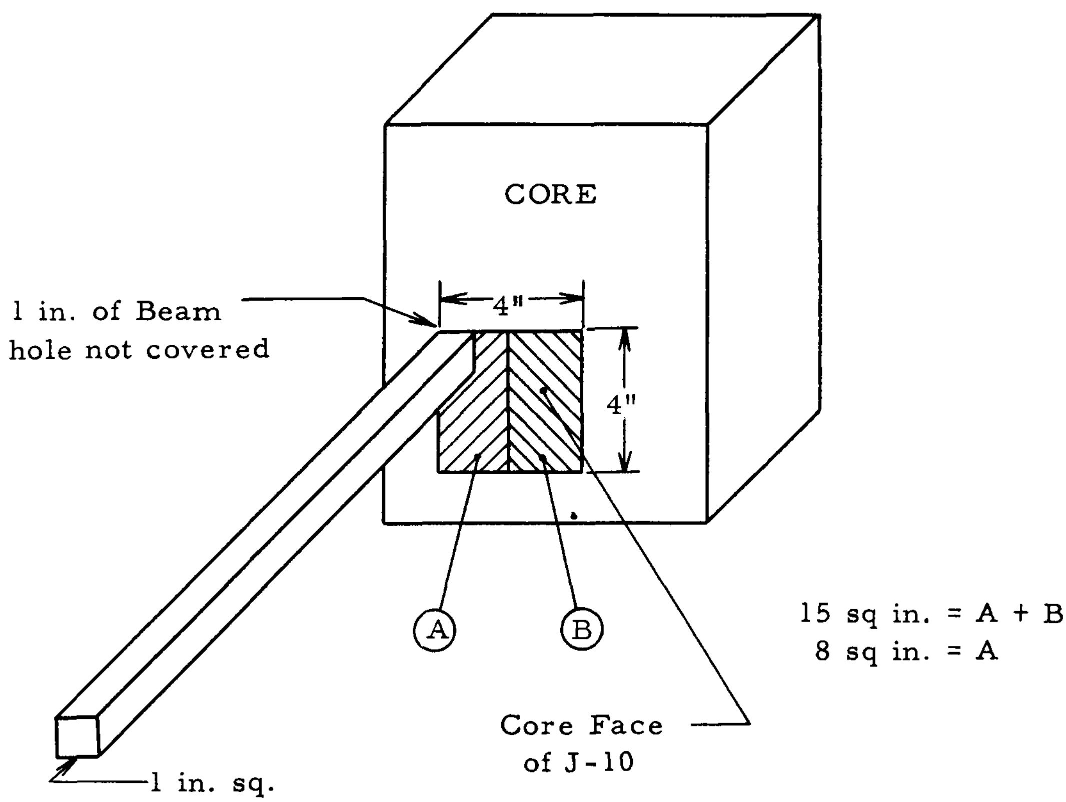

I.4.c.
THERMAL NEUTRON BEAM EXTERNAL TO REACTOR SHIELD FROM J-10 (Ref. XIII-5)(Two-slab Loading)

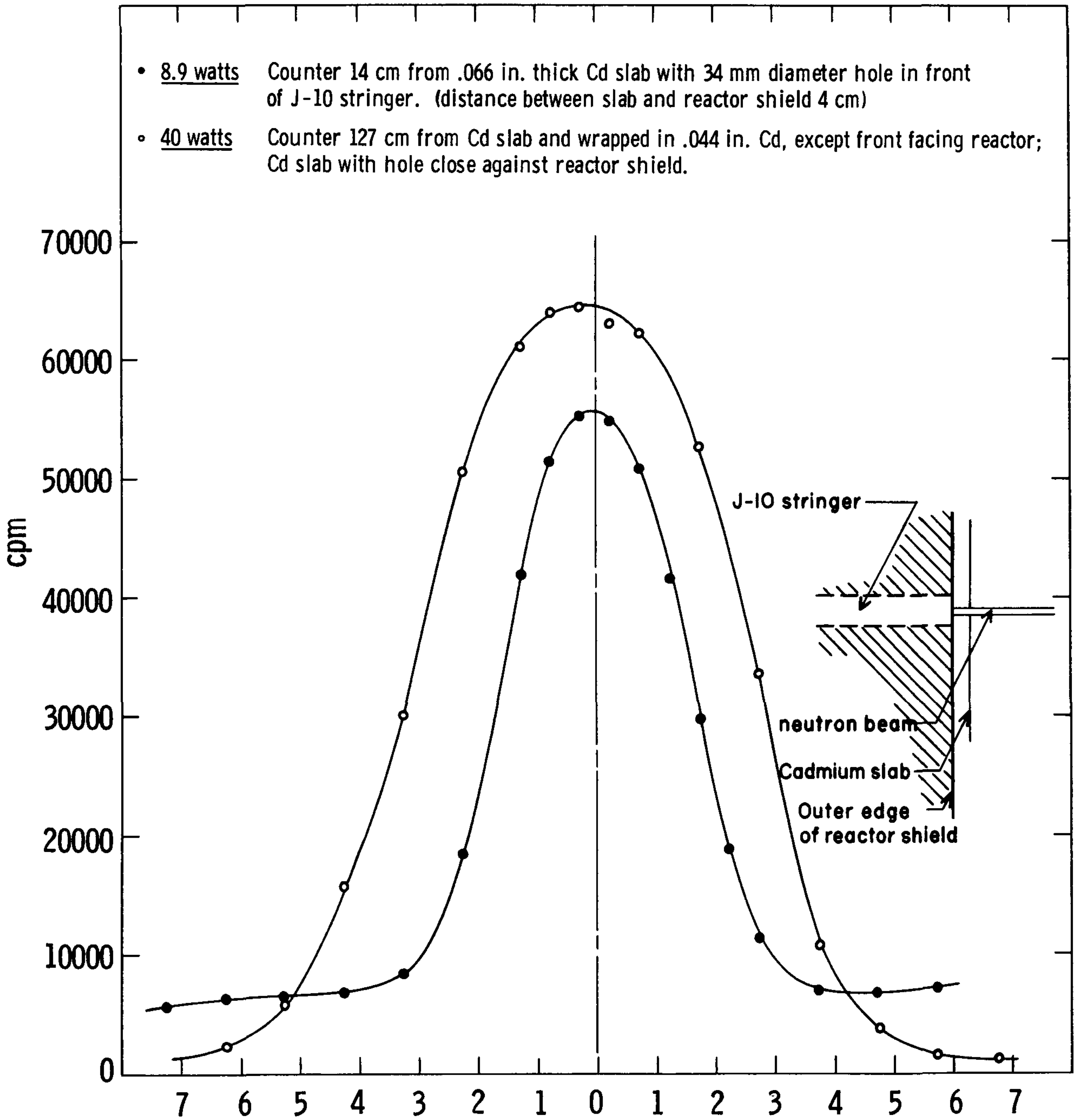

$B^{10}F_3$ counter (12 cm pressure, 14 in. long, 1 in. diameter) parallel to beam.

Beam through 1 in.^{2} hole in J-10 stringer.

I.4.d.
EPITHERMAL NEUTRON BEAM EXTERNAL TO REACTOR SHIELD FROM J-10 (Ref. XIII-5)(Two-slab Loading)

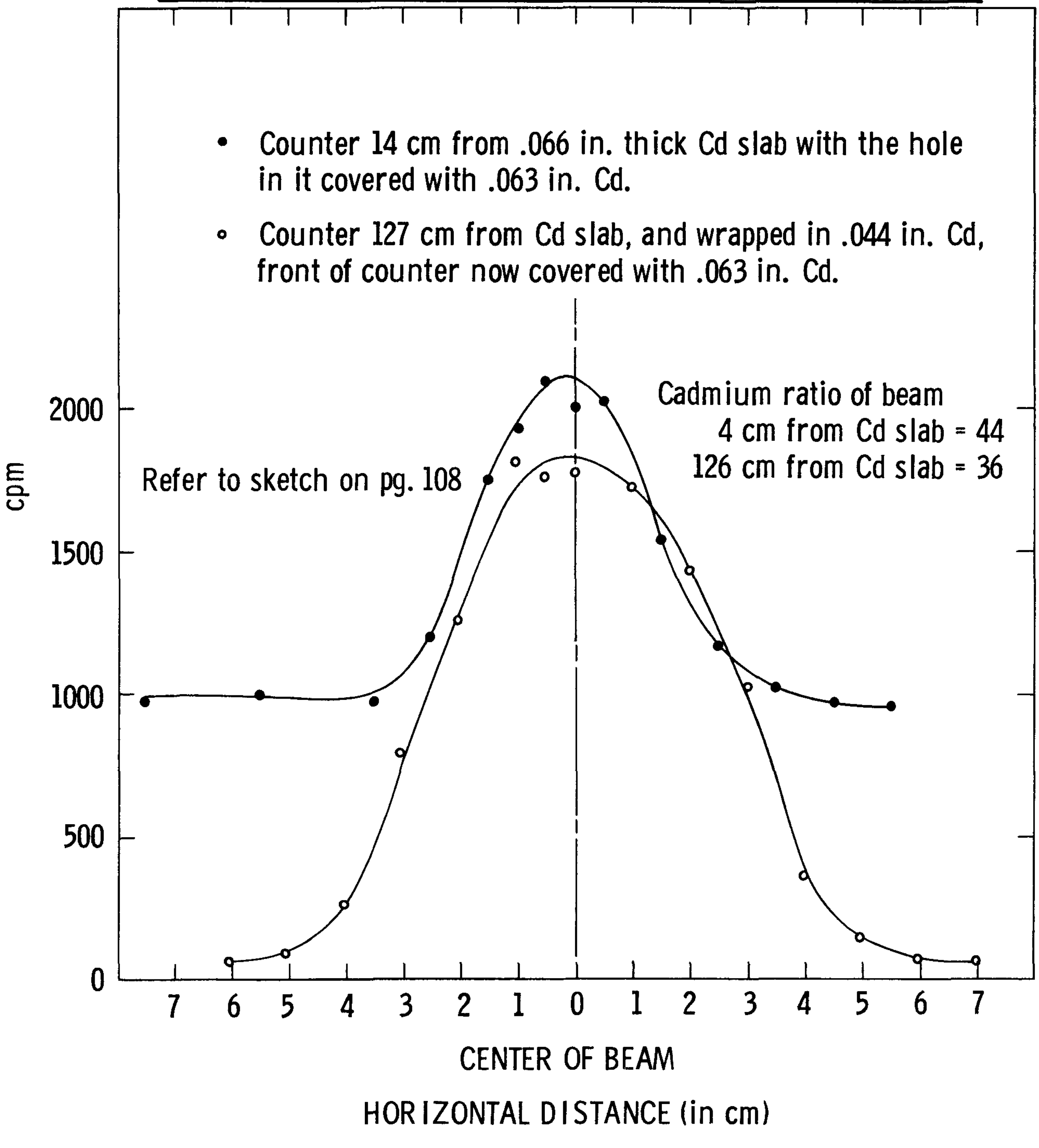

$B^{10}F_3$ counter (12 cm pressure, 14 in. long, 1 in. diameter

Beam through 1 in.^{2} hole in J-10 stringer

I.4.e.
THERMAL NEUTRON BEAM FROM J-10 TRAVERSED WITH TWO DIFFERENT RESOLUTIONS OF THE DETECTOR (Ref. XIII-5)(Two-slab Loading)

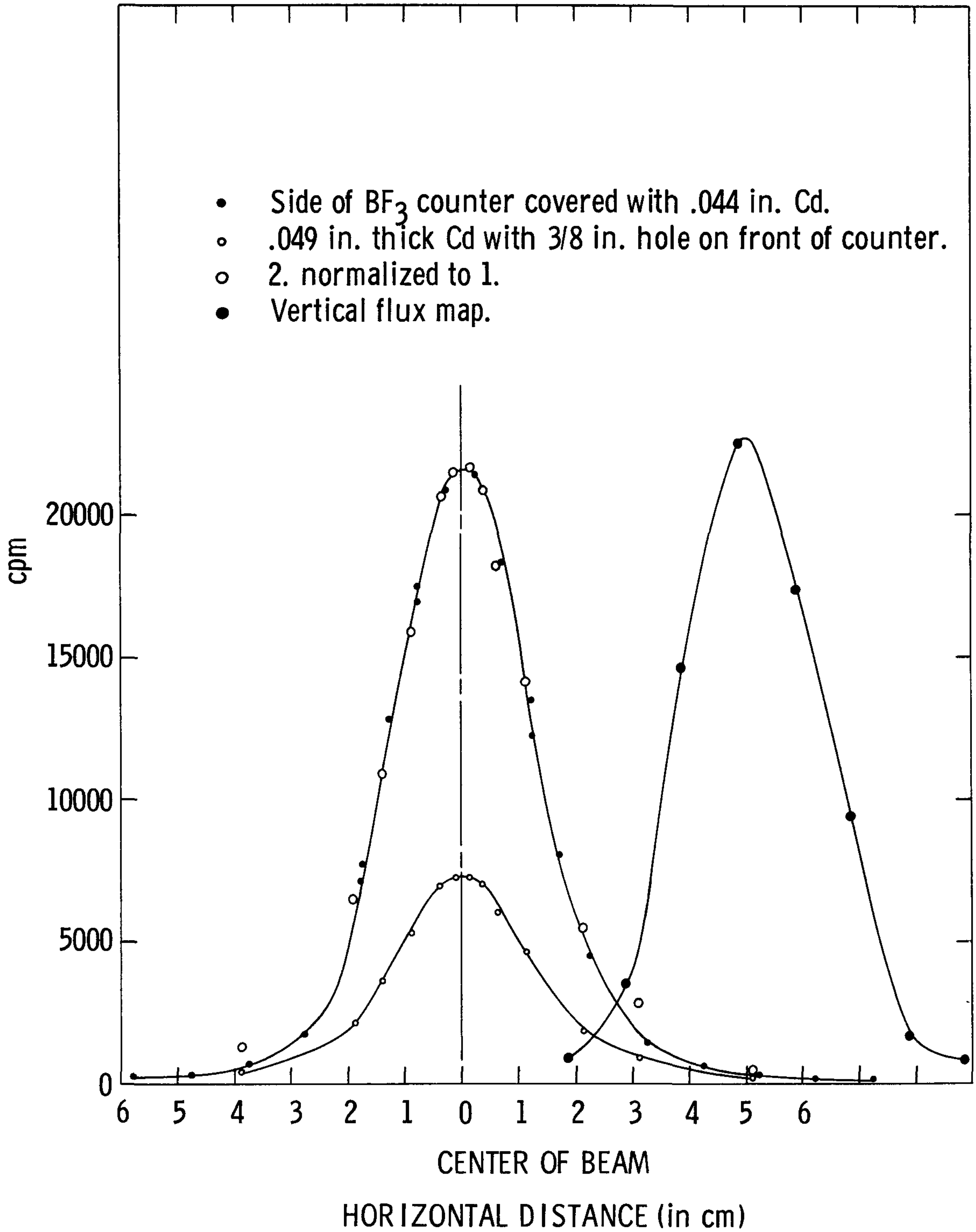

Power: 40 watts. Beam through 1 in.^{2} hole in J-10 stringer in line with 3/8 in. hole in .066 in. thick Cd plate against reactor shield.
BF_3 counter 127 cm from reactor.

Section J

ABSOLUTE FLUX MEASUREMENTS

The experimental results of absolute thermal-neutron-flux measurements in the core and external thermal column are given. Also, one measurement of the gamma flux in the operating reactor has been made and the results presented in terms of r/hr/watt. The absolute flux is a basic bit of knowledge in the design of and in work with the reactor.

An absolute flux measurement is one which determines the flux at a certain point in units of neutrons/cm^2/sec. The absolute flux is proportional to the reactor power level as indicated by ion chamber current readings; hence, the ion chamber readings are given with the flux. Also, this measurement will strongly depend on the core geometry and conditions that exist during measurement.

The technique involves the irradiation of a gold foil at a steady power for a known time. A comparison of the activity of this gold foil to one irradiated in the Argonne standard pile yields the absolute flux.

J.1. Absolute Flux at Head of J-10 Stringer with a One-slab Core (Ref. V-11)

Core Loading:	One slab, north side of reactor, containing six fuel boxes with 1896.08 grams.
Foil Location:	In first hole of J-10 measured from core end of J-10.
Instrument Reading (amp):	Log 1×10^{-5} #1 - 0.69×10^{-6} #2 - 0.12×10^{-5} #3 - 0.23×10^{-6} Power level - 230 watts
Thermal Flux:	2.05×10^{9} cm^{-2} sec^{-1}
Cadmium Ratio:	4.5

Core Loading:	One-slab loading of six fuel boxes on north side of reactor. (Ref. V-6)
Foil Location:	On core end of J-10.
Instrument Reading (amp):	Log 1×10^{-5} #1 - 0.89×10^{-6} #2 - 0.16×10^{-5} #3 - 0.36×10^{-6} Power level - 360 watts
Thermal Flux:	3.61×10^{9} cm^{-2} sec^{-1}

Core Loading:	One-slab, north side of reactor, containing six fuel boxes with 1898.59 grams. (Ref. V-12)
Foil Location:	In pocket 2 in. from core end of J-10 stringer.
Instrument Reading (amp):	Log 8×10^{-8} #1 - 0.16×10^{-7} #2 - 0.22×10^{-7} #3 - 0.06×10^{-7} Power level - 5.7 watts
Absolute Thermal Flux:	5.90×10^{7} cm^{-2} sec^{-1}

J.2. Absolute Flux at Center of One-slab Core (Ref. V-13)

Core Loading:	One slab, north side of reactor, containing six fuel boxes with 1898.59 grams.
Foil Location:	Central, vertically, radially, and azimuthally.
Instrument Reading (amp):	Log 5.0×10^{-8} #1 - 0.28×10^{-8} #2 - 0.8×10^{-8} #3 - 0.11×10^{-8} Power level - 1.05 watts
Absolute Thermal Flux:	1.47×10^{7} cm^{-2} sec^{-1}

J.3. Absolute Flux at Center of Each Slab of a Two-slab Core (Ref. V-16)

Core Loading:	Two-slab loading of six fuel boxes. 1918.67 grams U^{235} in north slab and 1935.79 in south slab.
Instrument Reading (amp):	Log 8.0×10^{-7} #1 - 0.18×10^{-7} #2 - 0.075×10^{-6} #3 - 0.12×10^{-7}
Results:	Power Level - total = 2.64 watts north slab = 1.330 watts south slab = 1.313 watts
Thermal Neutron Flux:	North slab - 2.080×10^{7} $n/cm^{2}/sec$ South slab - 2.275×10^{7} $n/cm^{2}/sec$
Cadmium Ratios:	North slab gold foil - 1.79 South slab gold foil - 1.98 North slab in fuel plate - 15.95 South slab in fuel plate - 16.72

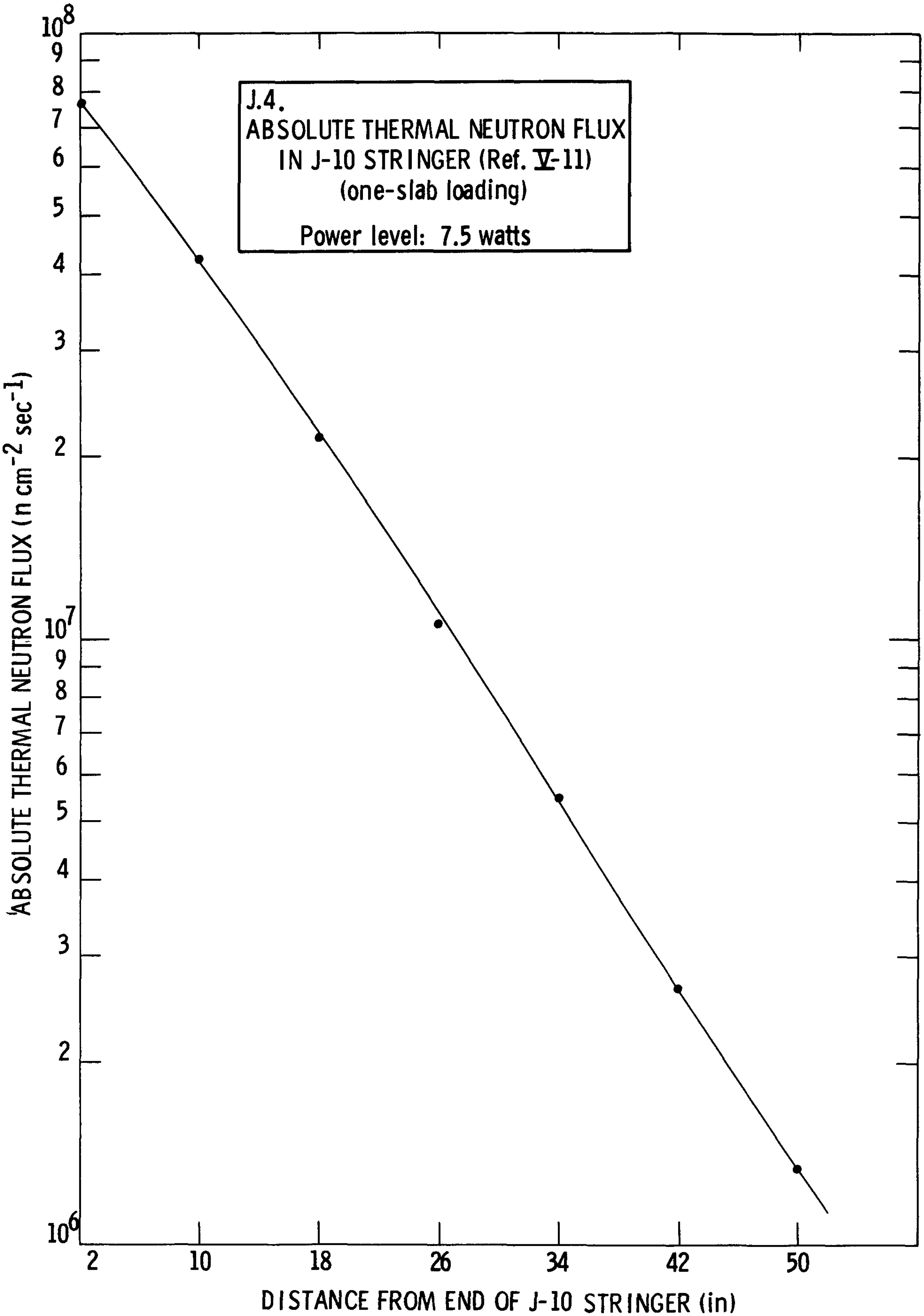
J.4.
ABSOLUTE THERMAL NEUTRON FLUX
IN J-10 STRINGER (Ref. V-11)
(one-slab loading)
Power level: 7.5 watts
ABSOLUTE THERMAL NEUTRON FLUX (n cm^{-2} sec^{-1})
10^8
9
8
7
6
5
4
3
2
10^7
9
8
7
6
5
4
3
2
10^6
2
10
18
26
34
42
50
DISTANCE FROM END OF J-10 STRINGER (in)

J.5. Gamma-ray Intensity in the One-slab Core during Operation (Ref. V-13)

At the power level of 0.1 watt the following reactor instrument readings (amp) were observed.

Log - 4×10^{-9}	Linear #2 - 0.06×10^{-8}
Linear #1 - 0.19×10^{-9}	Linear #3 - 0.05×10^{-9}

Results:

(1) At the approximate center of reactor core the intensity is 270 r/hour/watt.

(2) At the head of the J-10 stringer the intensity is 50 r/hour/watt.

These values can probably be taken as reliable within ±50%. They were obtained with film packets loaded with duPont type 535 film, and the packets were procurred from and purchased by R. S. Landauer and Company.

Section K

TEMPERATURE COEFFICIENT

If the temperature of core changes, the critical reactor will become supercritical or subcritical, depending on the sign of the temperature coefficient of reactivity. Low-power research reactors like the Argonaut are usually designed to have a negative coefficient as a safety measure. In such a case an accidental reactor power increase would tend to be self-limiting.

The temperature coefficient is an important concept in reactor theory and in practice, especially with power reactors. A measurement of this type is a common student experiment and the results presented are mainly their work. The coefficient has been measured in the one-slab, two-slab, and annular core loadings.

The technique employed to determine the coefficient is to observe the critical rod positions and the core (water) temperature. The core temperature is changed (increased or decreased) and the new critical rod positions observed. From previously determined rod calibration curves the corresponding reactivity change can be calculated. Because of thermal time-lag effects in the graphite moderator and reflector, the nonequilibrium temperature coefficient will depend on whether the water was being heated or cooled; in sufficient time (approximately 1 hour) equilibrium will be reached and a terminal net coefficient can be measured.

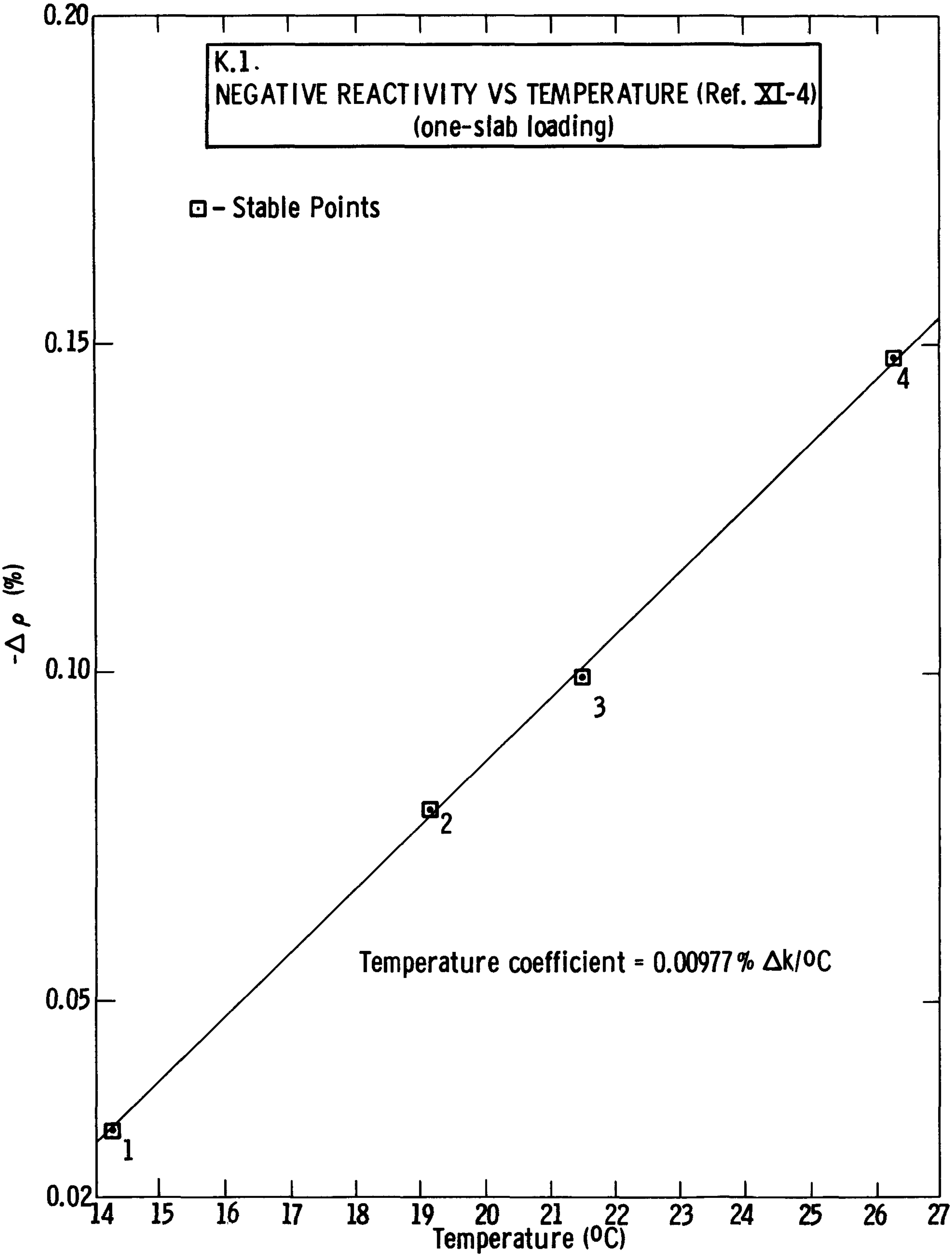

K.1.
NEGATIVE REACTIVITY VS TEMPERATURE (Ref. XI-4)
(one-slab loading)
□ - Stable Points
Temperature coefficient = 0.00977 % Δk/°C
-Δρ (%)
0.20
0.15
0.10
0.05
0.02
1
2
3
4
14
15
16
17
18
19
20
21
22
23
24
25
26
27
Temperature (°C)

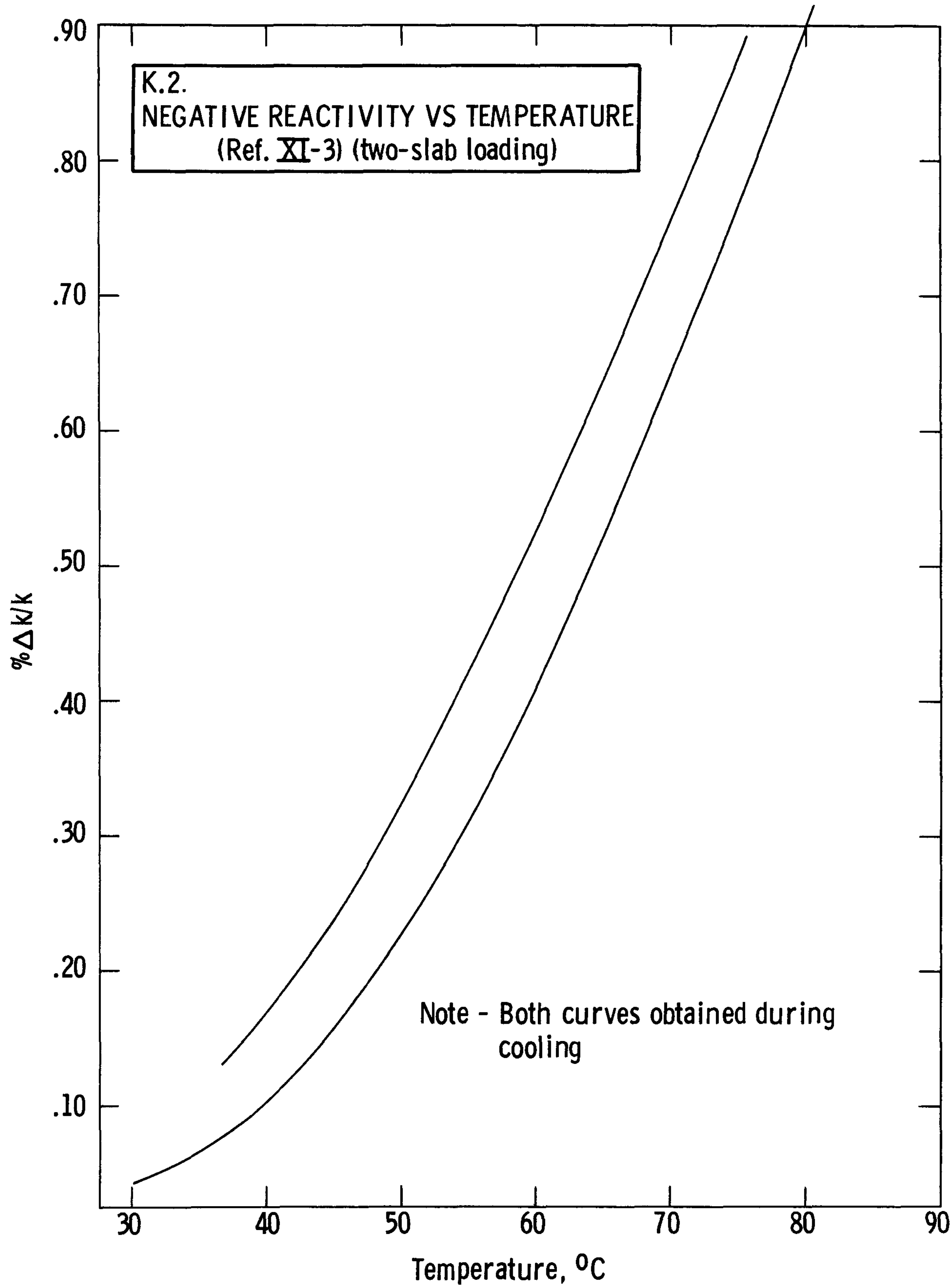
K.2.
NEGATIVE REACTIVITY VS TEMPERATURE
(Ref. XI-3) (two-slab loading)
.90
.80
.70
.60
.50
.40
.30
.20
.10
%Δk/k
Note - Both curves obtained during cooling
30
40
50
60
70
80
90
Temperature, °C

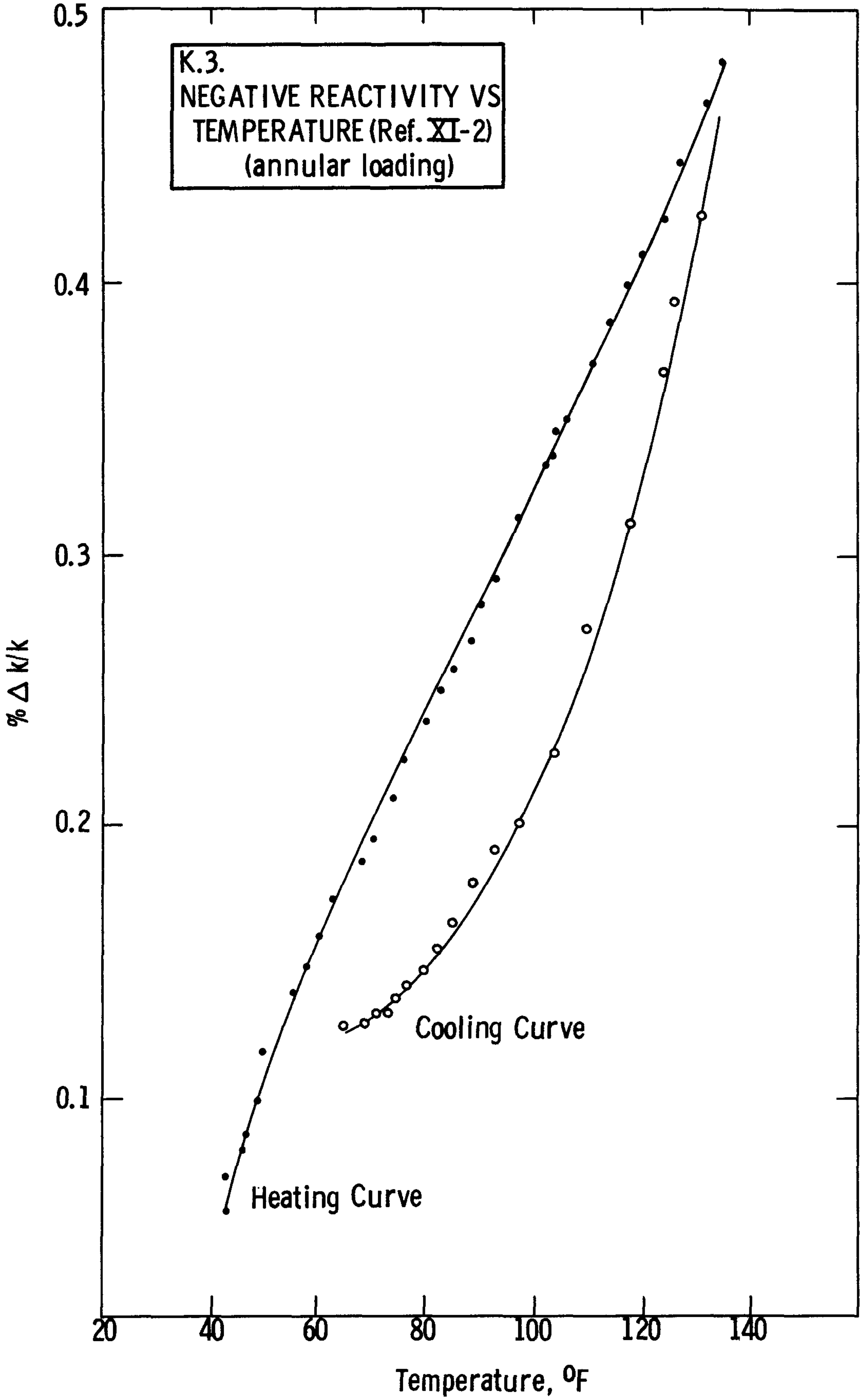
K.3.
NEGATIVE REACTIVITY VS
TEMPERATURE (Ref. XI-2)
(annular loading)
0.5
0.4
0.3
0.2
0.1
% Δ k/k
Cooling Curve
Heating Curve
20
40
60
80
100
120
140
Temperature, °F

Section L

VOID COEFFICIENT (ONE-SLAB GEOMETRY)

Because safety is an important aspect of the Argonaut reactor, it is designed to have a negative void coefficient. Then should the reactor power increase sufficiently to raise the core temperature to 100°C, the water moderator will boil (form voids) and negative reactivity will be effectively inserted. The power rise will thus tend to be self-limiting. It follows that the void coefficient is an important consideration of water or liquid-moderated reactors.

Because the flux distribution in the core is not flat, the void coefficient will be dependent upon position. The coefficient as a function of position in the reactor is determined as a standard student experiment. Lately, the investigation has been broadened to seek a more basic understanding of the nature of the void coefficient, and some studies of the effect of fuel plate spacing on the magnitude and sign of the coefficient have been made. The results of these experiments are shown with some typical results of the spatial void worth experiments.

The experimental technique is to determine the critical rod positions of the bare core, or with the void holders filled with water. Then the control rod critical positions are redetermined after the voids are in position. The change in critical rod positions is converted to a reactivity change with the aid of the rod calibration curves.

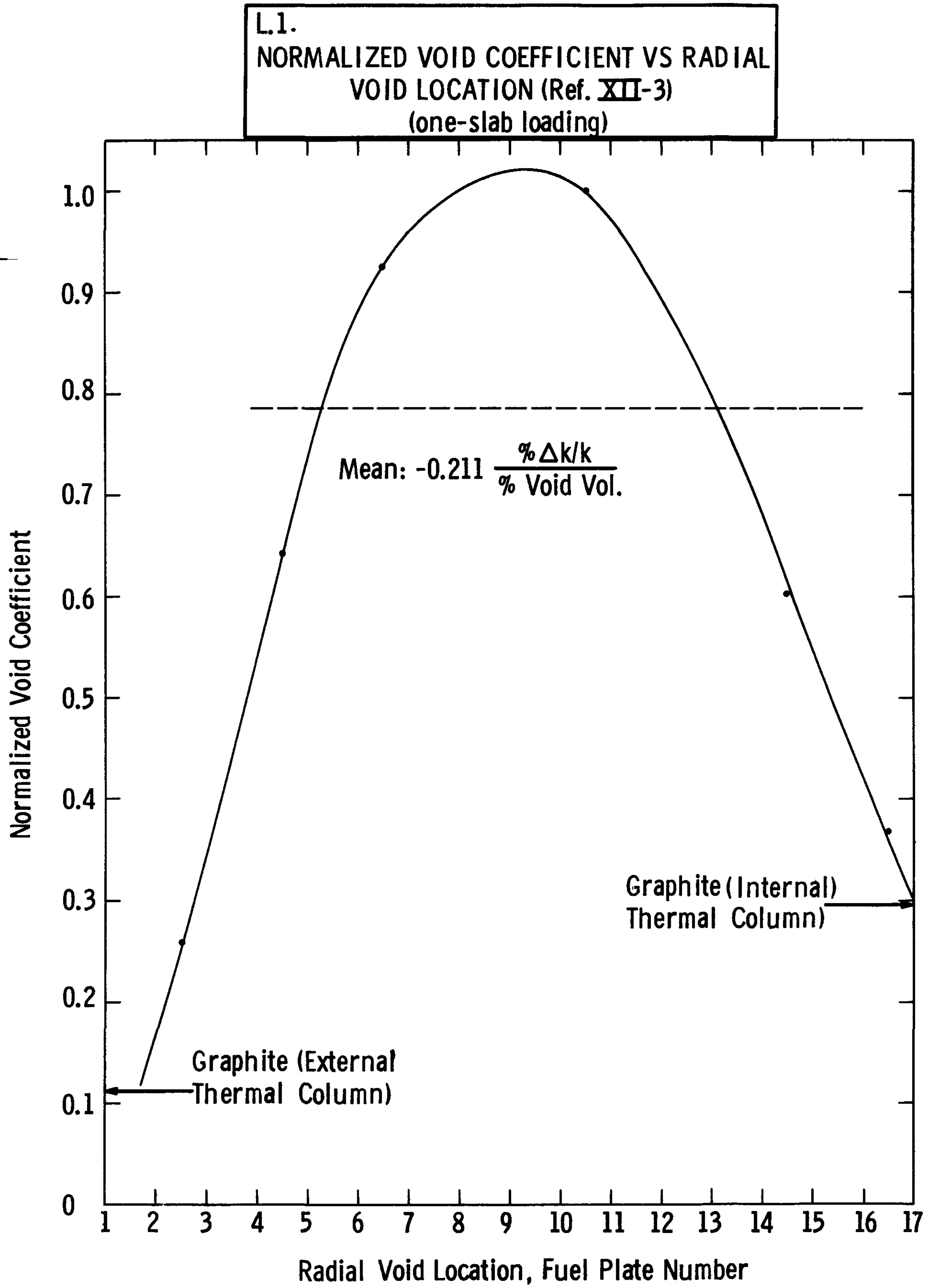
L.1.
NORMALIZED VOID COEFFICIENT VS RADIAL VOID LOCATION (Ref. XII-3)
(one-slab loading)
Mean: -0.211 %Δk/k / % Void Vol.
Graphite (Internal) Thermal Column)
Graphite (External Thermal Column)
Normalized Void Coefficient
0
0.1
0.2
0.3
0.4
0.5
0.6
0.7
0.8
0.9
1.0
1 2 3 4 5 6 7 8 9 10 11 12 13 14 15 16 17
Radial Void Location, Fuel Plate Number

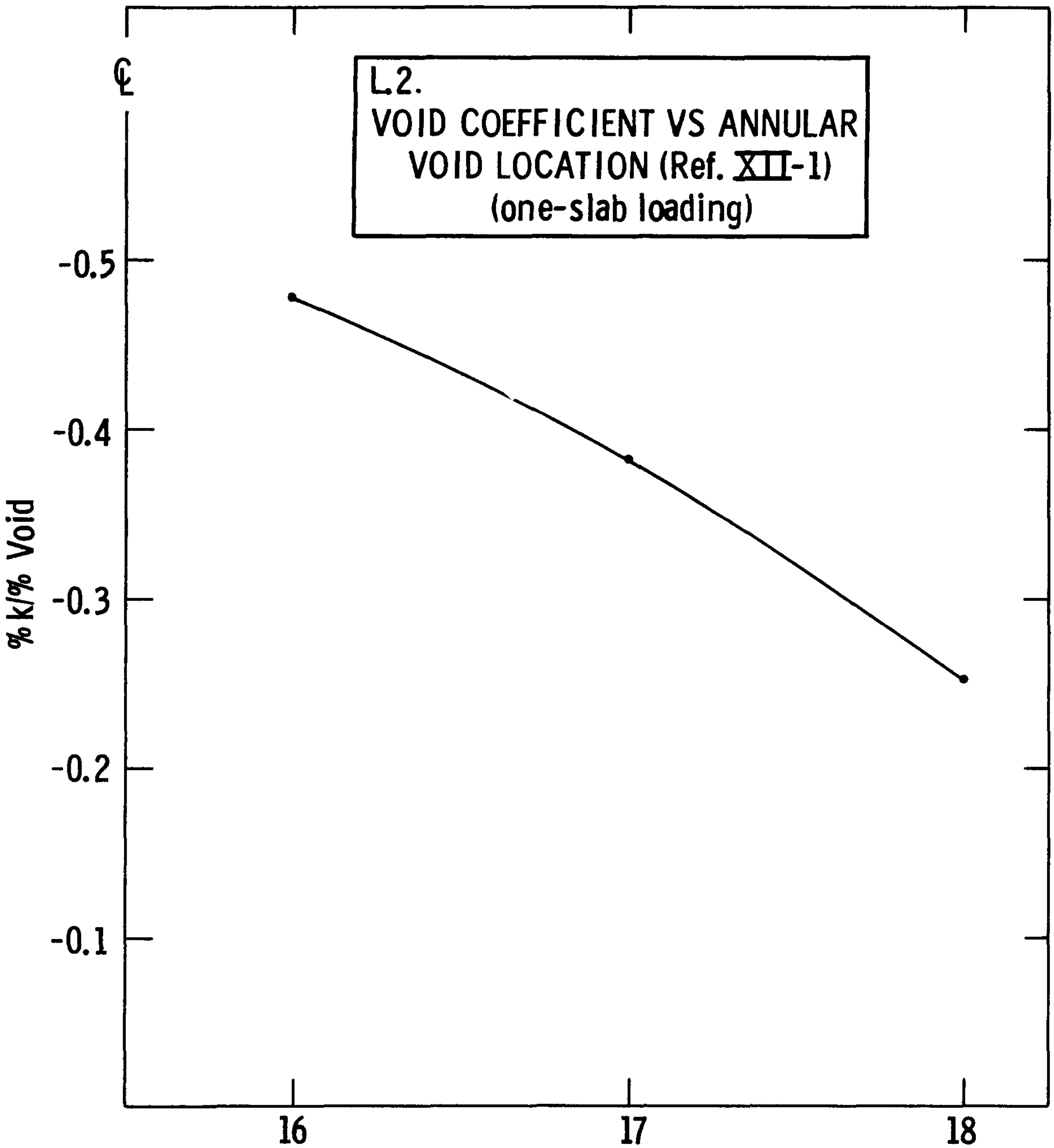

Annular Void Location, Fuel Box No.
3-1/4-in. voids placed between
plates 6-7, 7-8, and 8-9 for each box

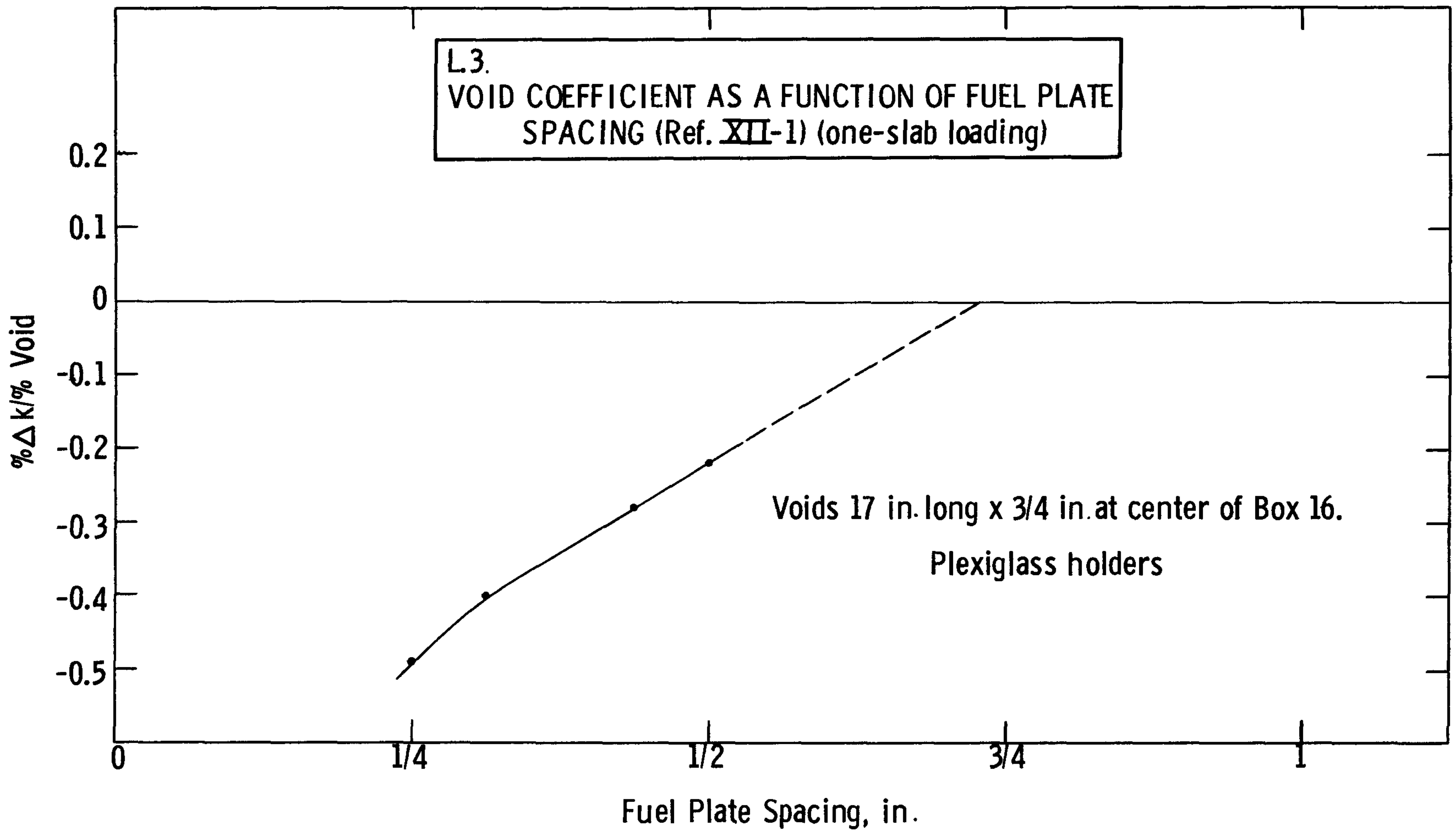

L.3.
VOID COEFFICIENT AS A FUNCTION OF FUEL PLATE SPACING (Ref. XII-1) (one-slab loading)

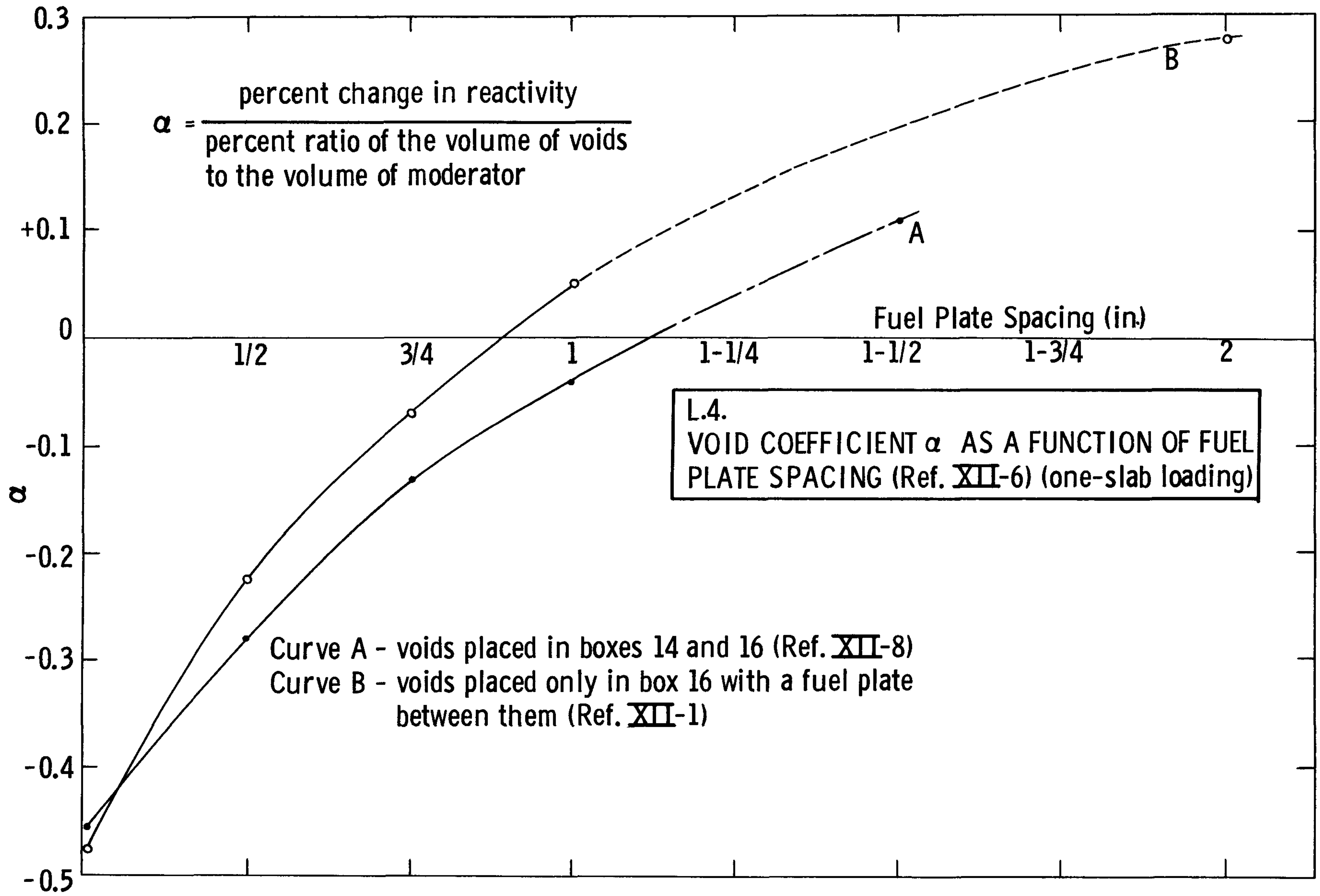

L.4.
VOID COEFFICIENT α AS A FUNCTION OF FUEL PLATE SPACING (Ref. XII-6) (one-slab loading)

Section M

NEUTRON LIFETIME

The neutron lifetime is the average time that elapses from the fission capture of a neutron in one nucleus until one of the neutrons released in the subsequent fission suffers a fission capture by another nucleus. It is a fundamental reactor parameter, but, unfortunately, it is difficult to measure. Relatively little effort has been made in this category to date.

One of the two quoted values is the result of a pile noise measurement. The other is from transfer function measurements. It is hoped that more results will be obtained from work with the pulse neutron source experiments that are now being considered.

M.1. Results of Pile Noise Measurement (One-slab) (Ref. XIII-2)

Assuming $B_{eff} = 0.0070$, the lifetime was $142 \begin{smallmatrix} +295 \\ -58 \end{smallmatrix}$ microseconds.

M.2. Neutron Lifetime for the One-slab Loading Determined from Transfer Function Measurements (Ref. Private Communication - G. Pawlicki)

The neutron lifetime was determined to be $1.80 \pm 0.05 \times 10^{-4}$ sec.

The value of the lifetime was determined by comparing the shape of the experimental transfer function magnitude with digital computations of the linearized kinetic equations, using the Hughes data for delayed neutron parameters. The comparison of experiment and computation was made in the frequency range from 1 to 30 cps. The digital computation was done on IBM 650 using the BUM code.

It has been shown experimentally that the measured phase shift of the Argonaut transfer function does not agree with the phase shift of the lowest mode bare reactor kinetic equation. The discrepancy in the phase shift becomes extremely large at higher frequencies when the ion chamber is located in the external thermal column at large distances from the fuel region. Even if the ion chamber is cadmium covered in measuring the transfer function, there is some measurable difference in the phase-shift curve when compared to the 180-microsecond lifetime phase-shift computation. Regardless of the chamber location or cadmium covering, the shape of the transfer function magnitude agrees with the digital computation within 0.5 db at all frequencies.

Section N

POWER CALIBRATION

The Argonaut reactor power level is indicated by B^{10}-coated ion chambers. The current output in amperes is not a convenient unit for analyzing or understanding all experimental results; in addition, the reading itself is dependent upon the chamber location, voltage, and the associated electronic circuits. A more useful unit is the watt, because the reactor power in watts is directly related to the fission rate and neutron flux. Some effort to relate the ion chamber readings to power in watts has been made, and the results are reported in this section.

The experimental techniques require determining the core flux distribution and the irradiation of a gold foil at a steady power (indicated by the ion chambers) for a known time. The counting of this gold foil and one irradiated in the Argonne standard pile, enables the absolute thermal flux to be determined. With knowledge of the absolute flux and the fuel mass, the power in watts is calculated, assuming a homogeneous core.

N.1. One-slab Power Calibration Data (Ref. V-12)

Core Loading: One-slab, north side of reactor, six fuel boxes with 1898.59 grams

Foil Location: Central vertically, radially and azimuthally.

Instrument Reading:

Chamber No.	Current Reading (amp x 10^8)	Chassis Serial No.
1	0.28	56267
2	0.8	Special test unit
3	0.11	56269
Log	5.0	56266

The detectors were located as shown in diagram on page 23, Section B.

Reactor Power Level: 1.05 watts ± 8.7%

N.2. Two-slab Power Calibration Data (Ref. V-14)

Core Loading: Two slabs of six boxes in each slab. Fuel weight in north slab is 1918.67 grams, and in the south is 1935.79 grams.

Instrument Reading:

Chamber No.	Current Reading (amp)	Chassis Serial No.
1	0.18×10^{-7}	56267
2	0.075×10^{-6}	56268
3	0.12×10^{-7}	56269
Log	8.0×10^{-7}	56266

Reactor Power Level: north slab = 1.33 watts
south slab = 1.31 watts

total = 2.64 watts

The error is believed to be ± 13.9%.

N.3.
CALCULATED POWER AND MEASURED ABSOLUTE THERMAL FLUX DISTRIBUTIONS IN A TWO-SLAB CORE (Ref. V-14)

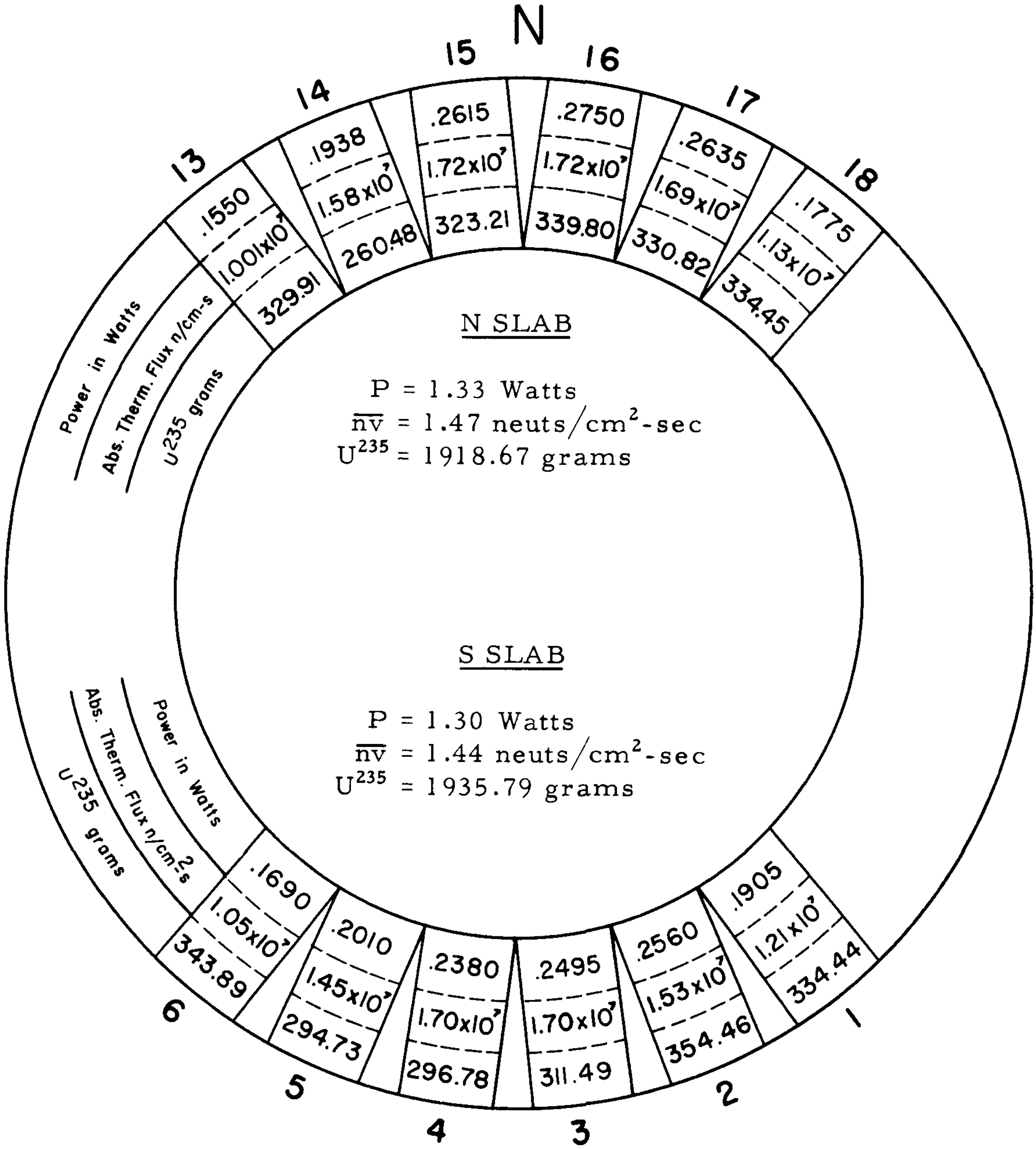

Section O

REACTIVITY WORTHS

Any change in the core or reflector composition or geometry will introduce a reactivity disturbance that will affect the reactor. This fact is a basic consideration of reactor safety, and of research into reactor physics and reactor engineering, i.e., kinetics, control rod design, fuel worth, and compensation for burnout and poison buildup. Also, numerous other types of experiments such as cross-section and danger coefficient measurements make use of the sensitivity of the reactor to perturbations. It is obvious that there is a large number of these cause and effect relationships to study.

Some reactivity worths of fuel, moderator, and reflector have been measured in various core geometries. The fuel worth has been measured as a function of core position, fuel mass, and worth relative to graphite. The worth of the graphite moderator has also been determined as a function of position. Integral and differential worths of the water and graphite reflector and moderator have been measured. The reactivity effects of gold foils and other absorbers placed in the core or thermal columns have been determined, and the results are presented.

O.1. Fuel and Core Graphite (One and Two-slab Data)

O.1.a. Reactivity Worth of Fuel at Various Locations in the Core (Private Communication - W. E. Carey)

Date	Location of Fuel Change	Fuel Change M, gm	Reactivity Change, $	Reactivity Worth of Fuel, $/gm
4/19/58	Box 16, Position 2 near outer edge	4.52	0.093	0.0206
4/10/58	Box 16, Position 9 in middle	4.52	0.040	0.0088
4/11/58	Box 16, Position 16 near inner edge	4.52	0.080	0.0177

(one-slab loading.)

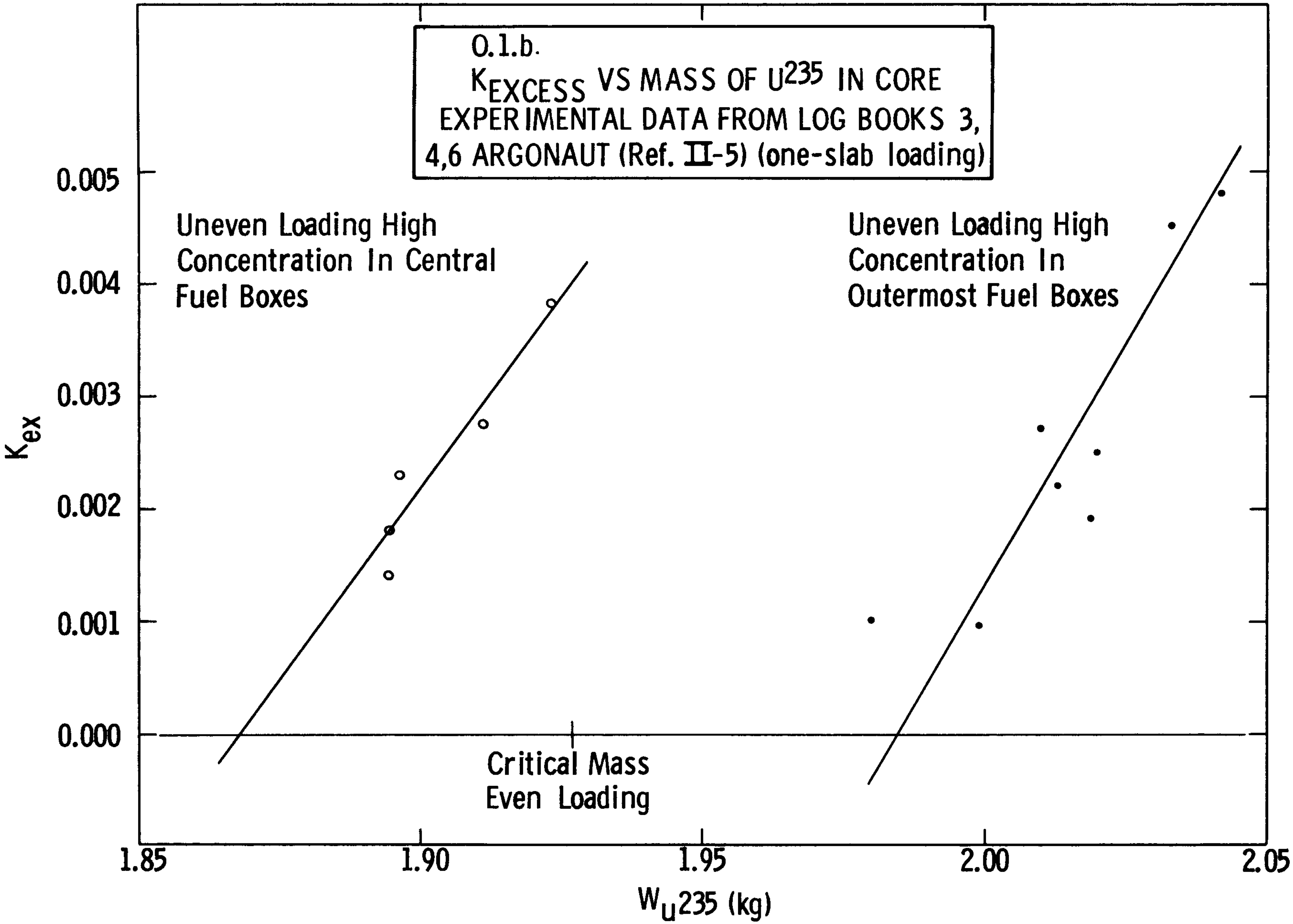
0.1.b.
K EXCESS VS MASS OF U235 IN CORE
EXPERIMENTAL DATA FROM LOG BOOKS 3, 4,6 ARGONAUT (Ref. II-5) (one-slab loading)
Uneven Loading High Concentration In Central Fuel Boxes
Uneven Loading High Concentration In Outermost Fuel Boxes
Critical Mass Even Loading
Kex
0.005
0.004
0.003
0.002
0.001
0.000
1.85
1.90
1.95
2.00
2.05
WU235 (kg)

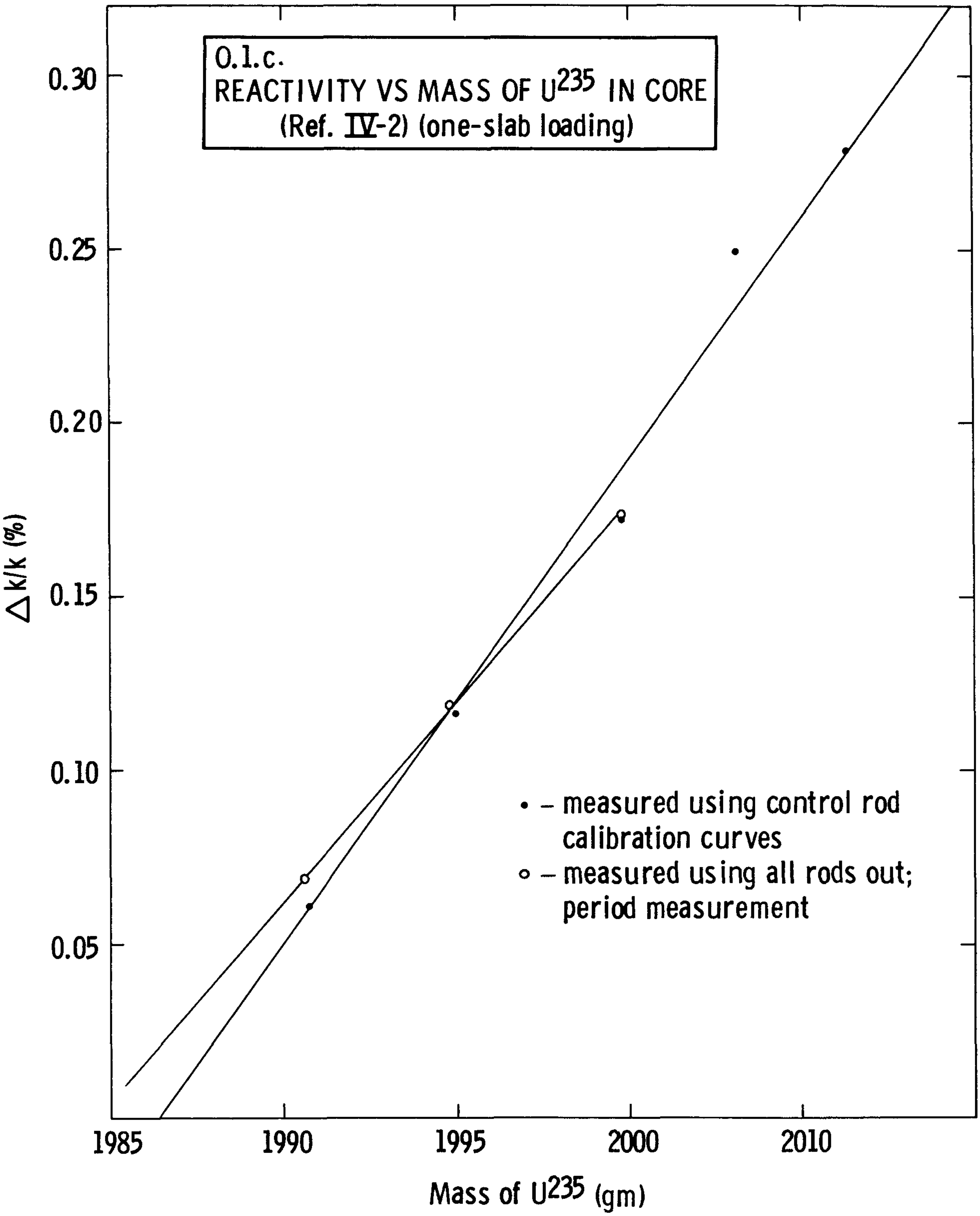
O.1.c.
REACTIVITY VS MASS OF U^{235} IN CORE
(Ref. IV-2) (one-slab loading)
0.30
0.25
0.20
0.15
0.10
0.05
$\Delta k/k$ (%)
• – measured using control rod calibration curves
o – measured using all rods out; period measurement
1985
1990
1995
2000
2010
Mass of U^{235} (gm)

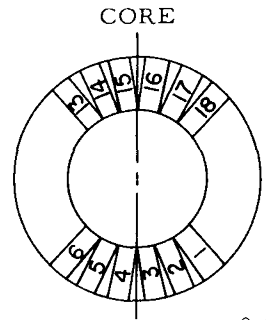

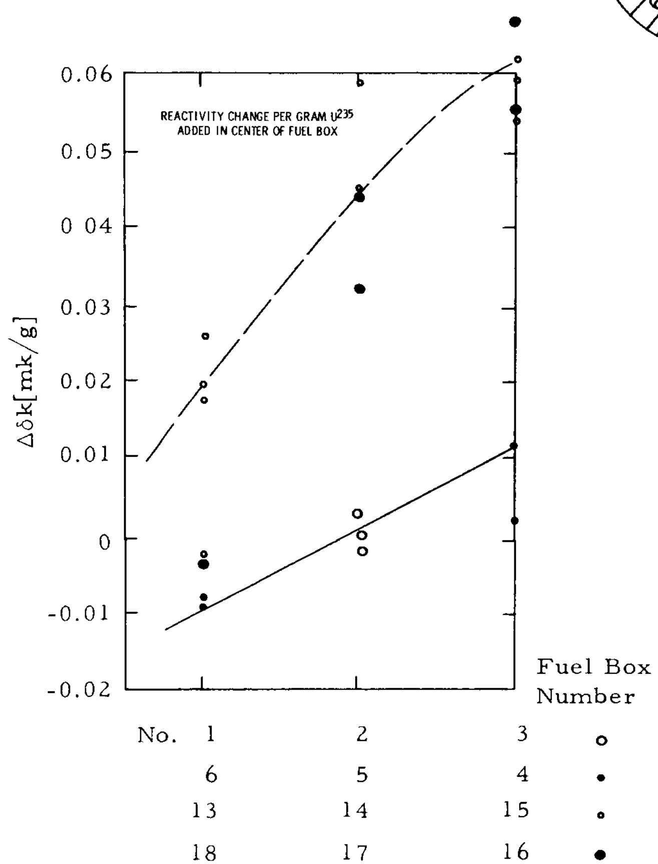

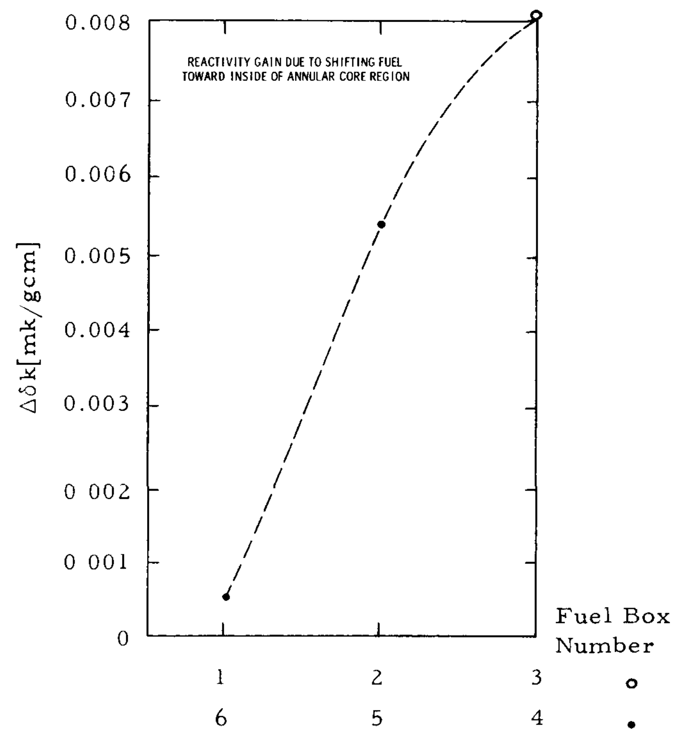

0.1.d.
REACTIVITY VS FUEL LOCATION IN TWO-SLAB CORE
(Ref. I-8)

O.1.e.
RELATIVE WORTH OF GRAPHITE VOLUME VS MASS OF U^{235} IN CORE (Ref. IV-3) (one-slab loading)

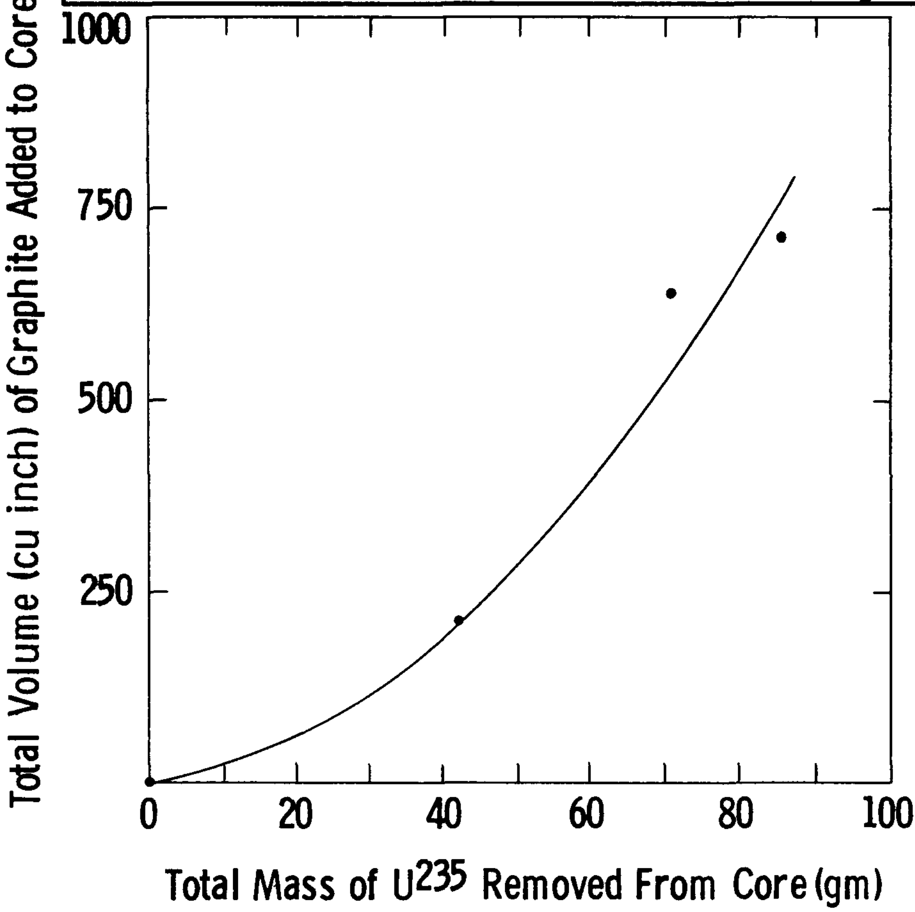

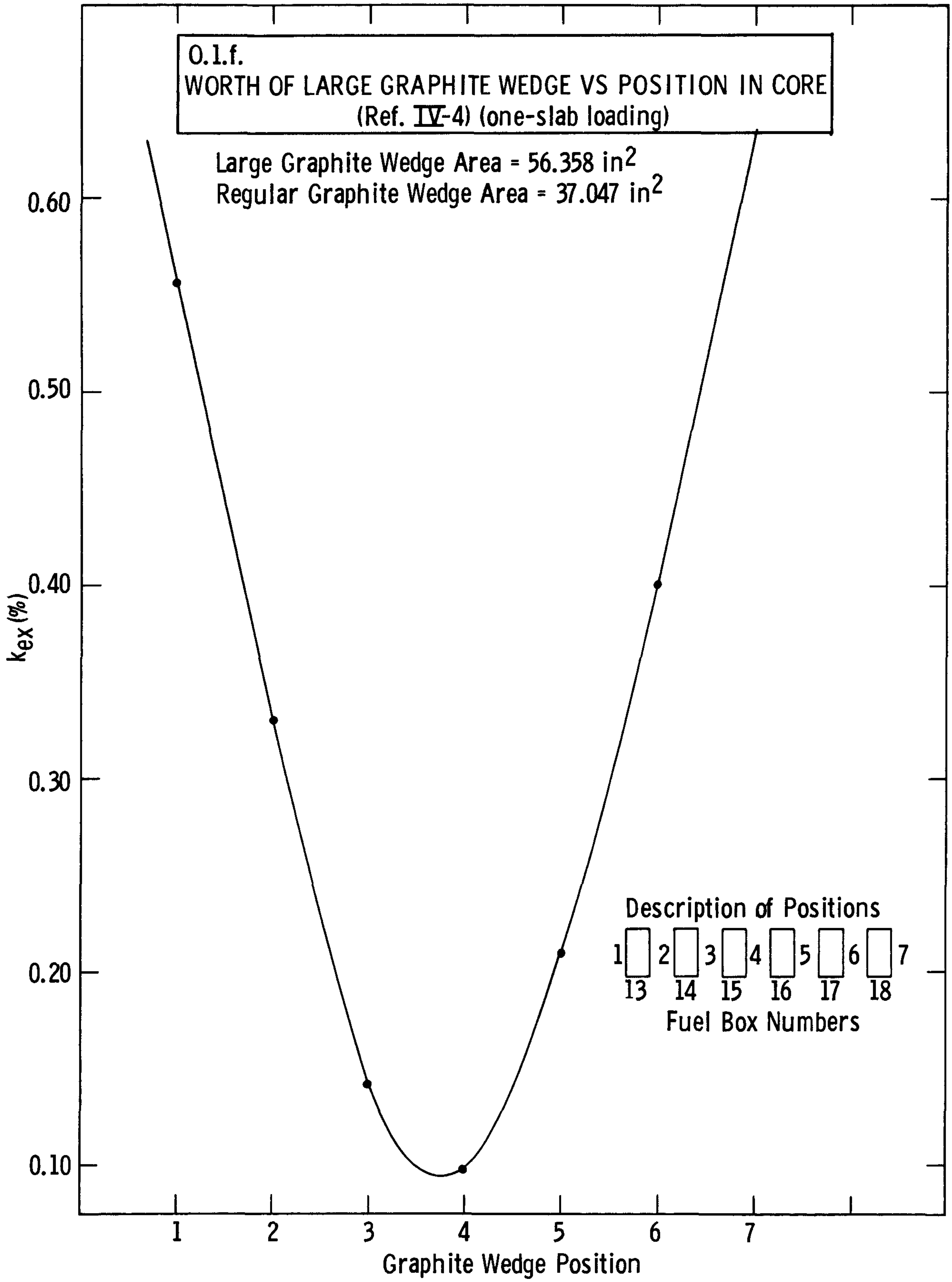

0.1.f.
WORTH OF LARGE GRAPHITE WEDGE VS POSITION IN CORE
(Ref. IV-4) (one-slab loading)
Large Graphite Wedge Area = 56.358 in²
Regular Graphite Wedge Area = 37.047 in²
0.60
0.50
0.40
0.30
0.20
0.10
kex (%)
Description of Positions
1 2 3 4 5 6 7
13 14 15 16 17 18
Fuel Box Numbers
1 2 3 4 5 6 7
Graphite Wedge Position

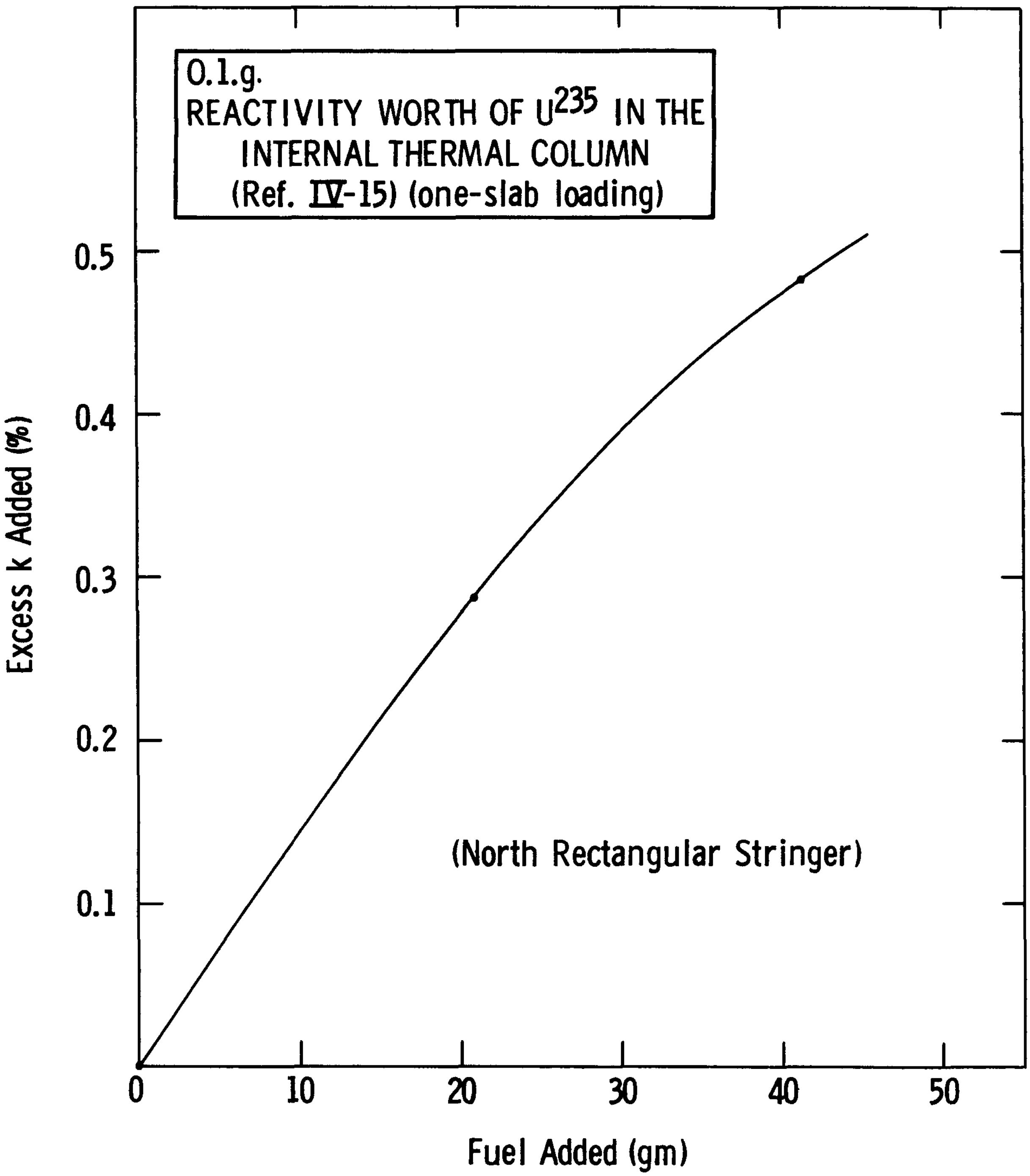

0.1.g.
REACTIVITY WORTH OF U^{235} IN THE INTERNAL THERMAL COLUMN
(Ref. IV-15) (one-slab loading)

O.1.h. Reactivity Worth of Fuel at Various Locations in the Internal Thermal Column (Ref. IV-19)

Core geometry: One-slab on north side of reactor.

A fuel plate containing 21.01 grams U^{235} was placed at the locations shown on the sketch, and the reactivity effect was determined from control rod worth curves.

Notation of Fuel Plate	Reactivity Worth, % Δk/k	Average Specific Worth, %/gm	Total Excess Reactivity of Lattice in which Measurement Was Made, %
North stringer	0.29	0.014	0.29
North side of East stringer	0.121	0.00576	0.298
South side of East stringer	0.097	0.00462	0.319
East side of South stringer	0.006	0.000285	0.319

INTERNAL THERMAL COLUMN

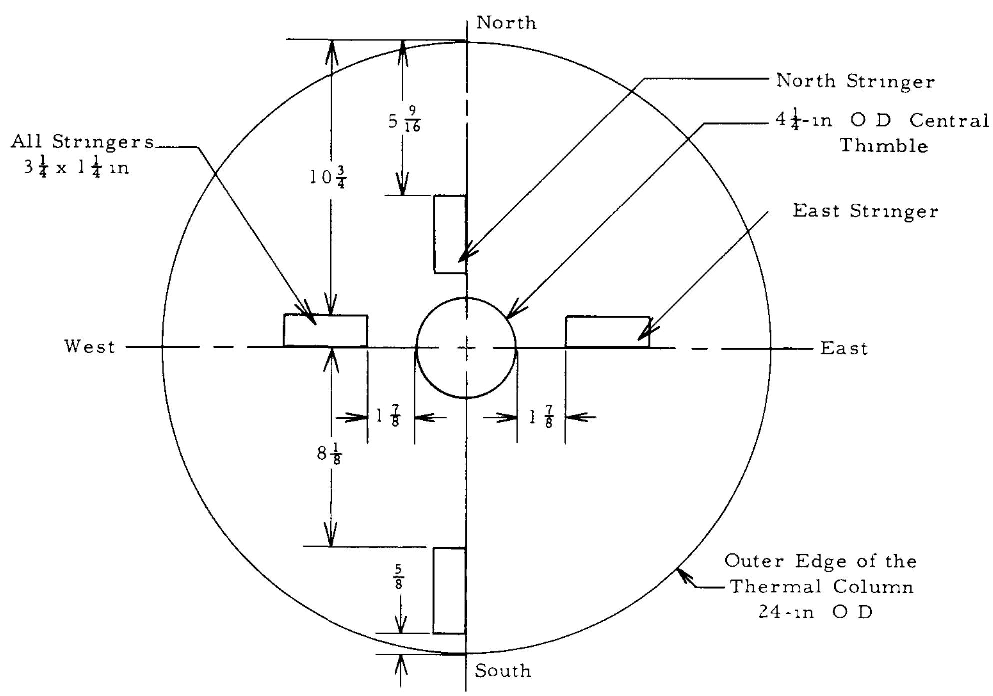

(dimensions in inches)

O.2. Moderator and Reflector

O.2.a. Reactivity Worth of Moderator and Reflector (One Slab) (Ref. IV-6)

The following data apply only to a specific experimental test section in the graphite reflector, but perhaps they are of interest as relative numbers.

(A) D_2O compared to graphite = +260 Arbitrary Units
(B) D_2O compared to void = +260 Arbitrary Units
(C) Graphite compared to void = +100 Arbitrary Units

The loading was a 7-box, one-slab loading of 2273.90 gms.

(Ref. IV-7)

(1) The worth of reflector was found to be $11.6 \times 10^{-3}\ \delta k$ for 22.3-cm reflector. The effectiveness of the reflector about 15 cm above top of fuel was almost negligible.

(2) The worth of moderator was found to be $0.86 \times 10^{-3}\ \delta k$ for 31.2-cm moderator. This value corresponds to 31.2 cm below top of fuel. The total height of fuel was 61 cm.

(3) In the Argonaut reactor the effective reflector is about 15 cm or 5 diffusion lengths, the diffusion length in water being 2.88 cm.

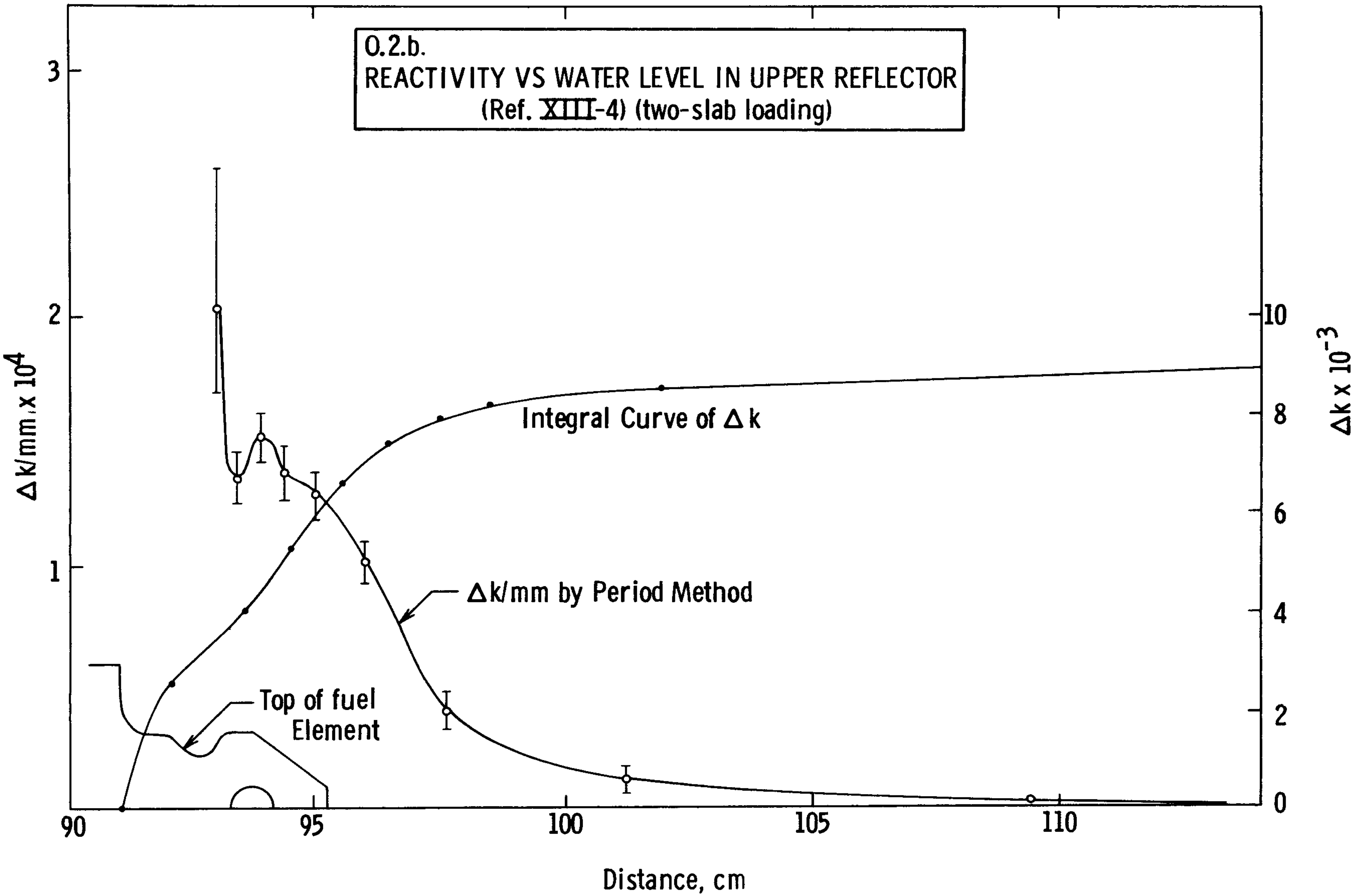
O.2.b.
REACTIVITY VS WATER LEVEL IN UPPER REFLECTOR
(Ref. XIII-4) (two-slab loading)
Integral Curve of Δ k
Δ k/mm by Period Method
Top of fuel
Element
Δ k/mm x 10^4
Δ k x 10^-3
Distance, cm
3
2
1
10
8
6
4
2
0
90
95
100
105
110

O.2.c. WORTH OF WATER MODERATOR AND REFLECTOR (Ref. IV-7) (one-slab loading)

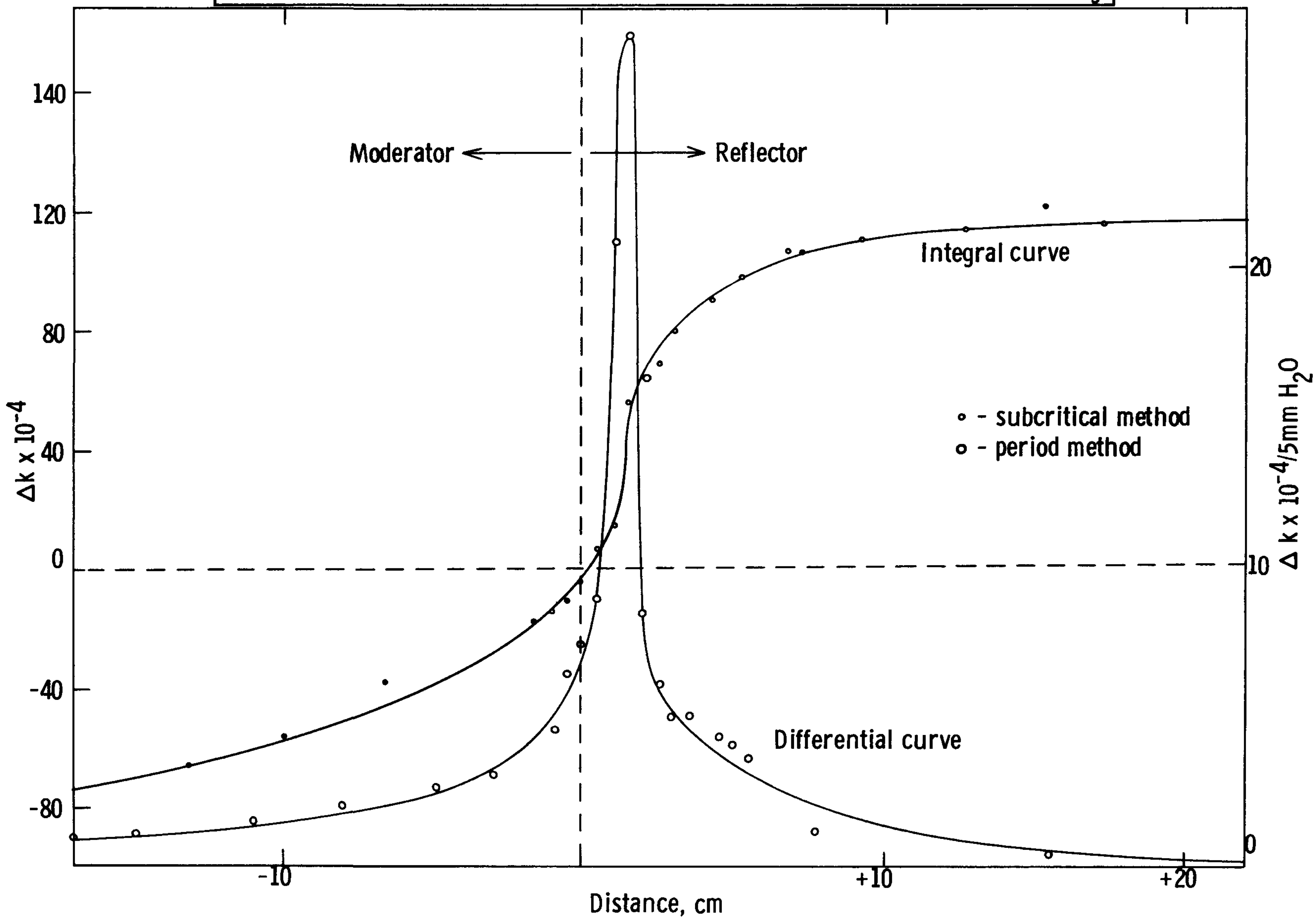

O.3. Absorber and Voids in J-10 Stringer (One Slab)

O.3.a. Some Reactivity Effects in J-10 Stringer (Ref. IV-14)

A series of measurements of reactivity effects on the Argonaut reactor due to changes in the J-10 stringer and water tank were performed and the reactivity effects observed are tabulated below.

One-slab Geometry (North)	$\Delta\rho$,%
1. Reactor in integral condition: J-10 stringer in; water tank in; no absorber or voids involved.	0
2. Same reactor system; J-10 stringer completely removed.	-0.175
3. J-10 stringer reinserted with 4 x 4-in. cadmium on front face.	-0.370
4. Stringer completely removed; 4 x 4-in. cadmium plate left at head of channel (south); plane of cadmium normal to axis of channel. The change was negative and in extent, greater than the maximum measurable under the conditions of the experiment.	$>$-0.399
5. J-10 stringer removed, 4 x 4-in. cadmium plate drawn back 20 cm from the south end of the channel.	-0.300
6. J-10 stringer removed, 4 x 4-in. cadmium plate drawn back 40 cm from the south end of the channel.	-0.212
7. The water tank was completely withdrawn, its front face covered with cadmium ($\sim$16 ft^2), and reactivity effects measured as a function of tank position relative to the reactor core. In range of 4 ft withdrawn to fully inserted no reactivity effect, either positive or negative, was observable.	0

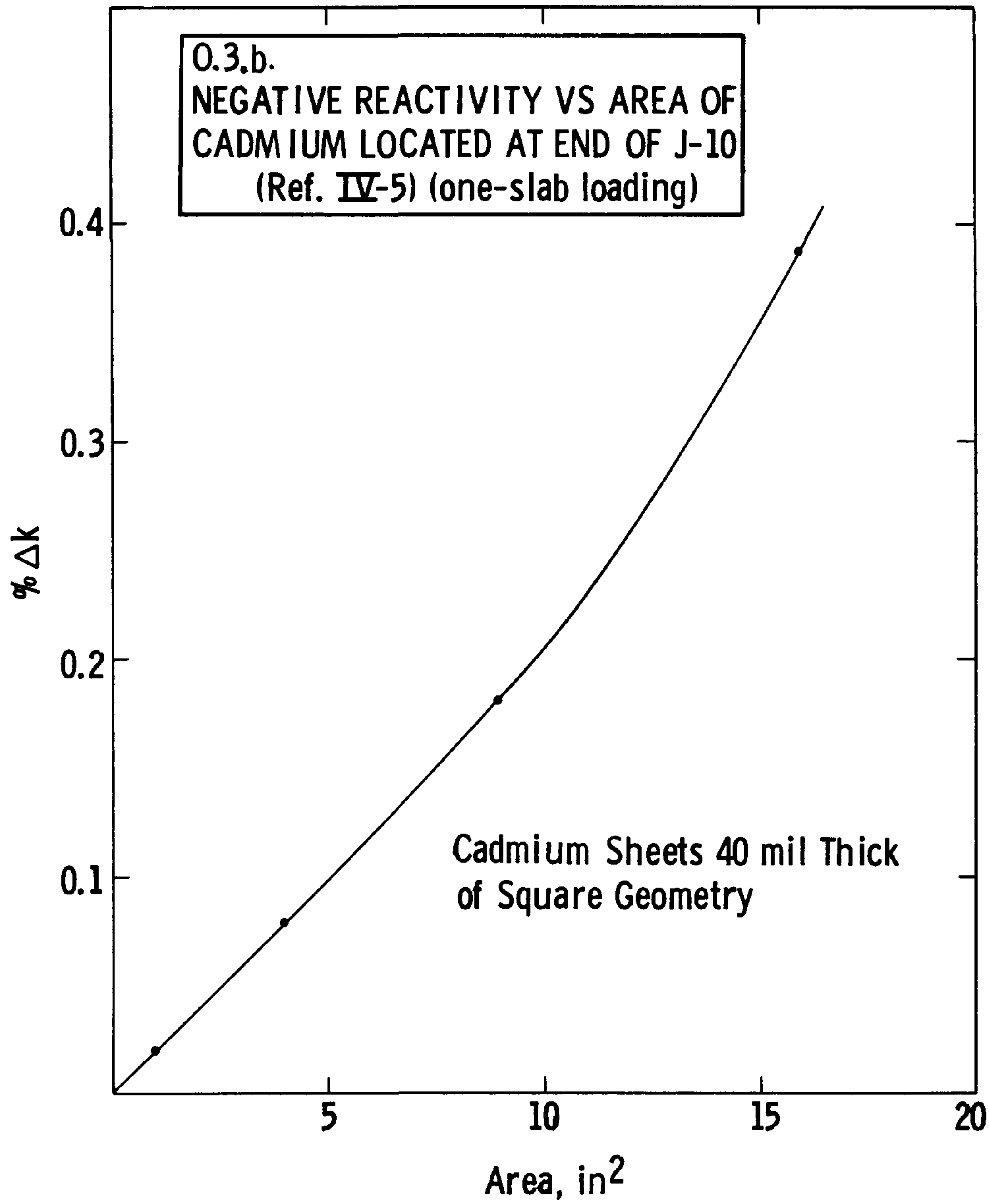
0.3.b.
NEGATIVE REACTIVITY VS AREA OF CADMIUM LOCATED AT END OF J-10 (Ref. IV-5) (one-slab loading)
0.4
0.3
0.2
0.1
% Δk
Cadmium Sheets 40 mil Thick of Square Geometry
5
10
15
20
Area, in2

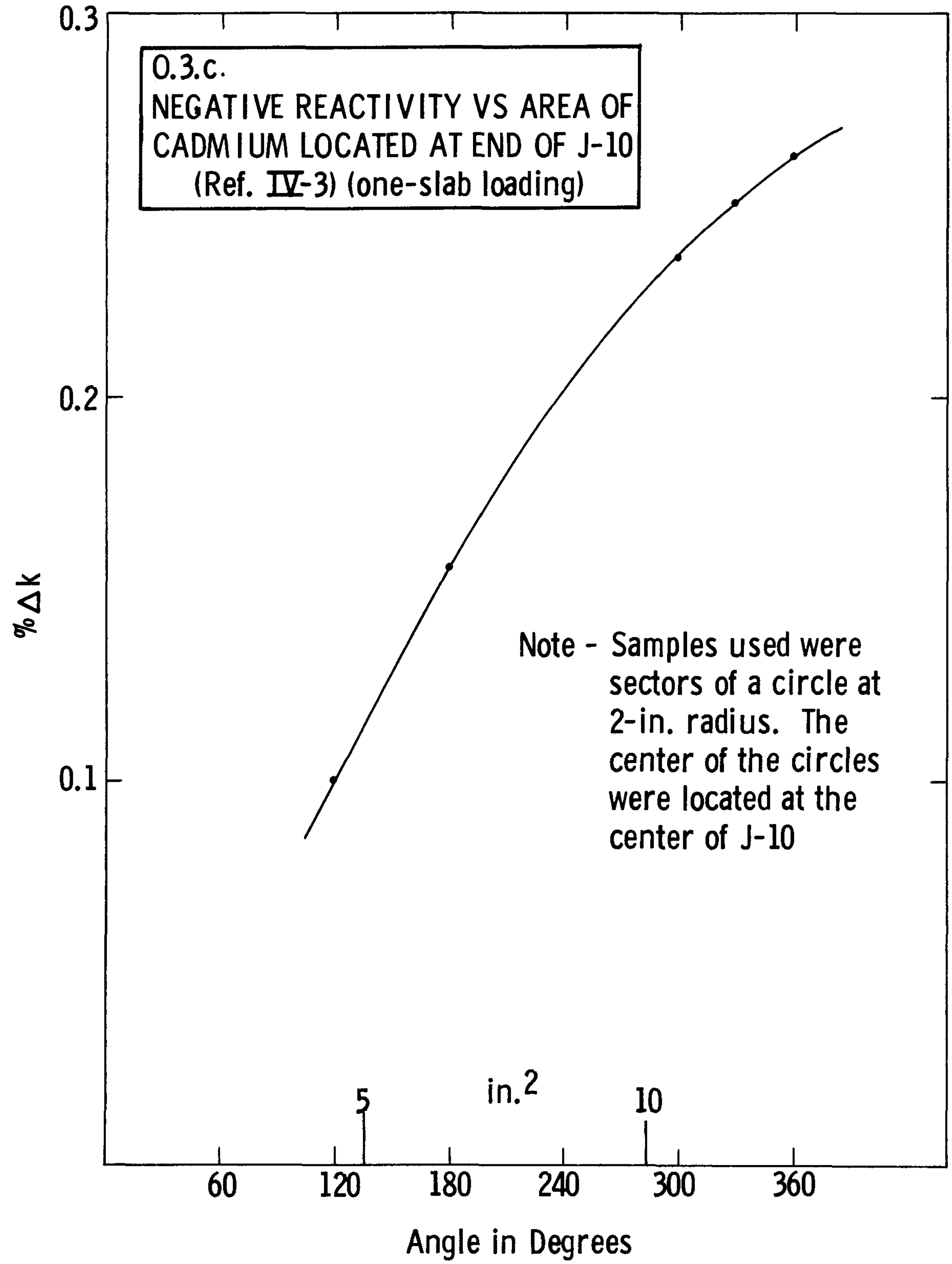
0.3.c.
NEGATIVE REACTIVITY VS AREA OF
CADMIUM LOCATED AT END OF J-10
(Ref. IV-3) (one-slab loading)
0.3
0.2
0.1
%Δk
Note - Samples used were sectors of a circle at 2-in. radius. The center of the circles were located at the center of J-10
5
in.2
10
60
120
180
240
300
360
Angle in Degrees

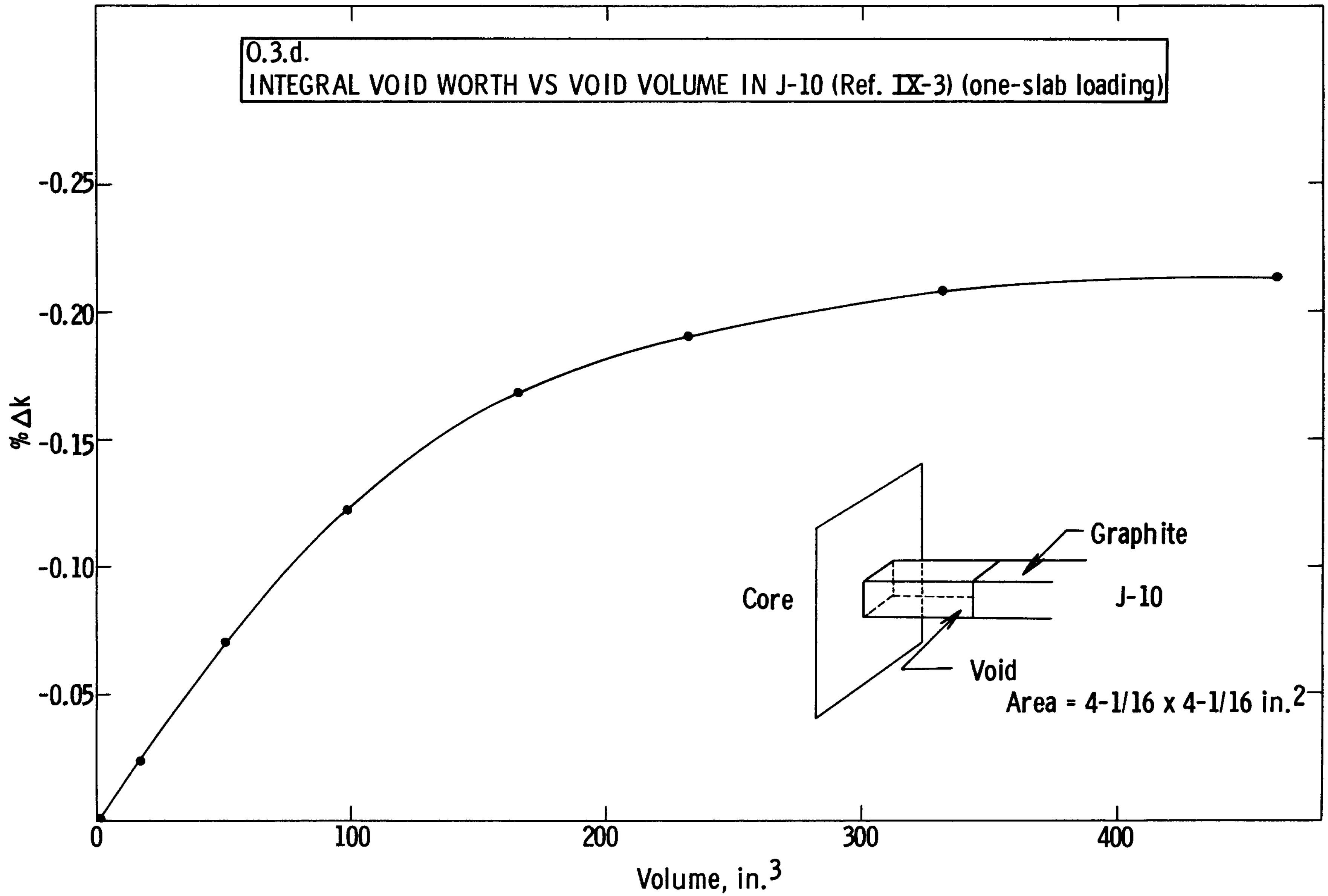

0.3.d.
INTEGRAL VOID WORTH VS VOID VOLUME IN J-10 (Ref. IX-3) (one-slab loading)

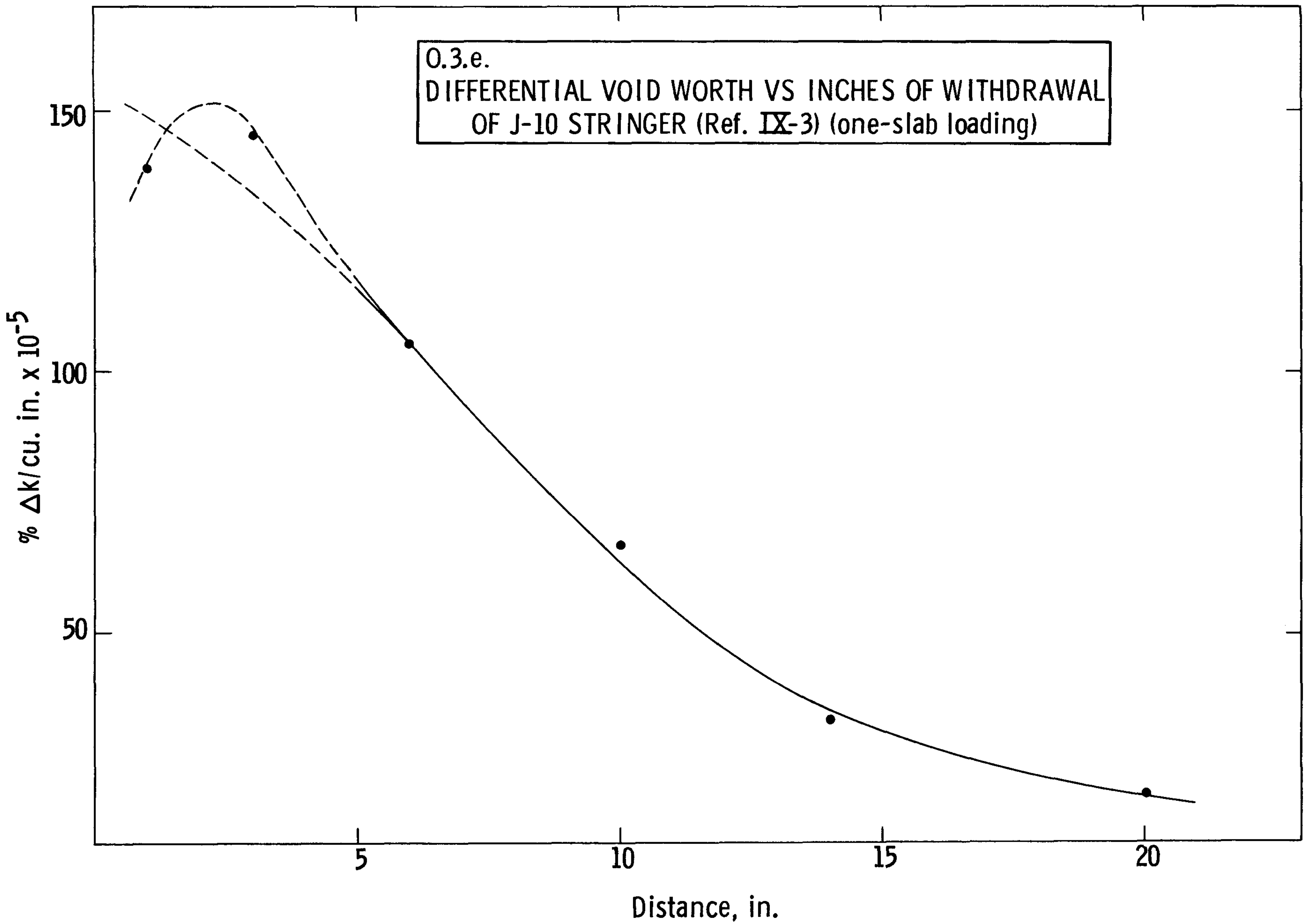
0.3.e.
DIFFERENTIAL VOID WORTH VS INCHES OF WITHDRAWAL OF J-10 STRINGER (Ref. IX-3) (one-slab loading)
150
100
50
5
10
15
20
% Δk/cu. in. x 10^-5
Distance, in.

O.4. Absorbers in Central Thimble (Two-slab Loading) (Ref. IV-8)

Experimental Reactivity Values for Various Absorbers

Absorber	Length, cm	Width, cm	Thickness, mils	Geometric Area, cm^2	Weight, gm	Location	$\Delta k/k$, %
1 Cadmium (sheet)	31	2.5	20	77.5	36.85	Central thimble, 4 in. above mid-plane, & wrapped around graphite cylinder	0 236
	31	1.3	20	40.1	19.07		0.146
	31	0.61	20	18.9	9.00		0.086
	31	0.29	20	8.9	4.22		0.046
	15.5	5.0	20	77.5	36.85		0 222
2 Cadmium (wire)	256		30	61.2		Wire wound around central thimble with 1-cm pitch	0.141
	256		30	61.2		Wire wound around central thimble with 3-cm pitch	0.125
	128.5		30	30 8			0.080
	381		30	91.2			0.191
3. B_4C	30.5	5.1		155.6	3.06	Powder sprinkled on #471 tape. Reactivity of tape not included in $\Delta k/k$ value	0.207
	30.5	5.1		155 6	0.70		0 083
4. U^{235} in Al	28.6	6.7	20-2.5	191.6	3.38	Central thimble, 4 in. above mid-plane	0 0041
5. #480 Tape	2.54						0.0013×10^{-2}
6 #33 Black tape	2.54						0.020×10^{-2}

The effective area for the wire: geometric area/4

The effective area for the sheet: geometric area/2, or total surface area (2A)/4

O.5. Reactivity Worth of Nitrogen Injection (One-slab Loading) (Ref. Private Communication - L. Lawyer, R. Springer)

Nitrogen injection reactivity worth as a function of nitrogen pressure, and also as a function of time. The reactivity vs pressure data is the average of the values at 40 and 50 sec after start of injection.

Core Condition	Mass U^{235}, gm	Water Temp, °F	Nitrogen Pressure, psi	% Δk
Clean	1878.59		11	-0.115
Clean	1878.59		11	-0.165
Clean	1896.08	93	12	-0.056
Modified Fuel Box #16	1900.19	89	14	-0.214
Clean	1896.08	93	16	-0.410
Clean	1896.08	93	16	-0.430
Modified Fuel Box #16	1900.19	89	20	-0.503

Reactivity in % Δk (all changes negative)

Time after start of injection	Time, sec					
	0	10	20	30	40	50
16 psig - run 1	0	0.36	0.40	0.43	0.43	0.44
16 psig - run 2	0	0.32	0.35	0.39	0.41	0.42
12 psig	0	0.043	0.047	0.050	0.055	0.058

O.6. Summary of Miscellaneous Reactivity Changes for a Two-slab Core (Ref. I-1)

Configuration: Two groups of six clusters each, symmetrically arranged.

Critical mass:	3.748 kg U^{235}
Void introduced into fuel cluster:	-0.25% k/% void
Replace graphite with water at edge of fuel cluster:	-4.4×10^{-4} %k/cc water
Bubbles from gas injection system introduced into one fuel cluster:	-0.09% k
7 x 7-in. cadmium sheet centered on fuel midplane next to reactor tank:	-3.1% k
24 x 3-in. cadmium sheet:	
next to tank:	-3.7% k
1.5 in. away from tank:	-2.7% k
3 in. away from tank:	-1.9% k
Removal of stringer from internal reflector:	-0.22% k
Insertion of U^{235} at center of internal reflector:	+0.026% k/gm
1 x 1-in. cadmium sheet at center of internal reflector:	-0.11% k
Insertion of U^{235} next to outer tank:	+0.022% k/gm
Fuel box displaced vertically 1 ft:	-3.2% k
4 x 6-in. void next to outer tank, 36 in. high:	-2.2% k
Rise in temperature:	-1.065×10^{-4} k/C

O.7. Summary of Miscellaneous Reactivity Changes for a 6 x 2 Loading (Ref. II-1)

Uniform addition of fuel to core regions	$0.41906 \times 10^{-4} \Delta\Sigma^{f}_{th}(cm^2)$
Addition of fuel to internal thermal column	$1.105 \times 10^{-4} \Delta\Sigma^{f}_{th}(cm^2)$
Void at center of internal thermal column	$-0.702 \times 10^{-7}/cc$
Void in middle of annular graphite	$-2.862 \times 10^{-7}/cc$
Void in graphite at edge of fuel box	$-20.24991 \times 10^{-7}/cc$
Water replaces graphite at center of internal thermal column	$-1.62 \times 10^{-6}/cc$
Water replaces graphite at middle of annular graphite	$-1.373 \times 10^{-6}/cc$
Water replaces graphite at edge of fuel box	$-0.232 \times 10^{-6}/cc$
Uniform temperature change	$-1.065 \times 10^{-4}/^{\circ}C$

O.8. Sensitivity for Various Absorbers at Center of One-slab Core (Ref. IV-17)

Sample	Weight, gm	Area, cm^2	Reactivity Change, $	Reactivity Change Due to Holder, $	Reactivity Change Due to Sample, $	Sensitivity $/$cm^2$
Cd sphere	1.468	$\pi r^2 = 0.353$	0.0329	-	0.0316	0.0895
Al holder	5.2	22.6	-	0.0013		
Cd tube	0.368	$\frac{\pi dl}{4} = 0.314$	0.0251	-	0.0238	0.0758
Al holder	5.2	22.6	-	0.0013		
Cd strip	0.1850	$\frac{hlw}{4} = 0.299$	0.0247	-	0.0234	0.0746
Al holder	5.2	22.6	-	0.0013		
Cd plate	11.0686	$\frac{lw}{2} = 12.7$	-	-	0.555	0.044
Cd plate	3.400	$\frac{lw}{2} = 3.94$	0.2198	-	0.2185	0.055
Al holder	5.2	22.6	-	0.0013		
Cu	35.994	25.0	-	-	0.0735	0.058
Zn	27.607	25.0	-	-	0.01750	0.065
Brass	35.455	25.0	-	-	0.04795	
Mn	1.336	20.5	0.0265	-	0.0188	0.093
Al	10.5	22.6	-	0.0077		0.051
Mg	28.693	25.0	-	-	0.0055	0.123
Al *2 & 7	20.435	22.6	0.00536	-		0.051

Section P

CRITICAL MASS AND CORE LOADING

The amount of fuel required to sustain a nuclear chain reaction is a function of numerous considerations, one of which is core geometry. The Argonaut is designed to have a flexible core geometry in that the fuel box location and fuel plate spacing are readily variable.

In this section, data of the critical mass for various core geometries and plate spacings are presented. Most of this data was obtained by extrapolation from the multiplication experiments, and the rest from critical reactor work. The results of the two sources are essentially identical.

P.1. Critical Mass (kg) as a Function of Core Geometry (Ref. I-1)

Data from multiplication experiments

	(Kg)
Two groups of six boxes each:	3.748
Four symmetrical groups of three boxes each:	5.2
Three symmetrical groups of four boxes each:	4.6
Slab loading on one side (8 boxes):	2.2
Homogeneous loading with 3-in. annulus on a 2-in. I.D.	4.3

Typical experimental reactor data

One-slab loading of six boxes	1.90
Two-slab loading of six boxes in each slab.	3.8
Annular loading	4.2

P.2. Critical Mass (kg) as a Function of Plate Spacing. (Ref. I-1)

Experimental data taken on one-slab loading.

Plate spacing (in.):

1/8	3.4
2/8	2.2
3/8	2.7

Section Q

RADIATION SURVEYS

The radiation level about an operating reactor is a very important aspect of the design. About a research and training reactor it is of special importance that the radiation level be low because of the number of people who are often in the reactor vicinity. Within the Argonaut reactor building the gamma activity is continuously monitored whether or not the reactor is operating, and eight-hour air filter samples are taken every working day.

The radiation level has been checked many times at various points about the reactor over the years of its operation (Bibliography entries VIII 1 and 4), but few complete surveys have been made. In this section the results of these surveys are presented. More work in this category is being planned.

Q.1.
TOTAL GAMMA-RAY ISODOSE LINES ALONG MIDLINE N - S PLANE OF ARGONAUT
(Ref. VIII-2) (one-slab loading)

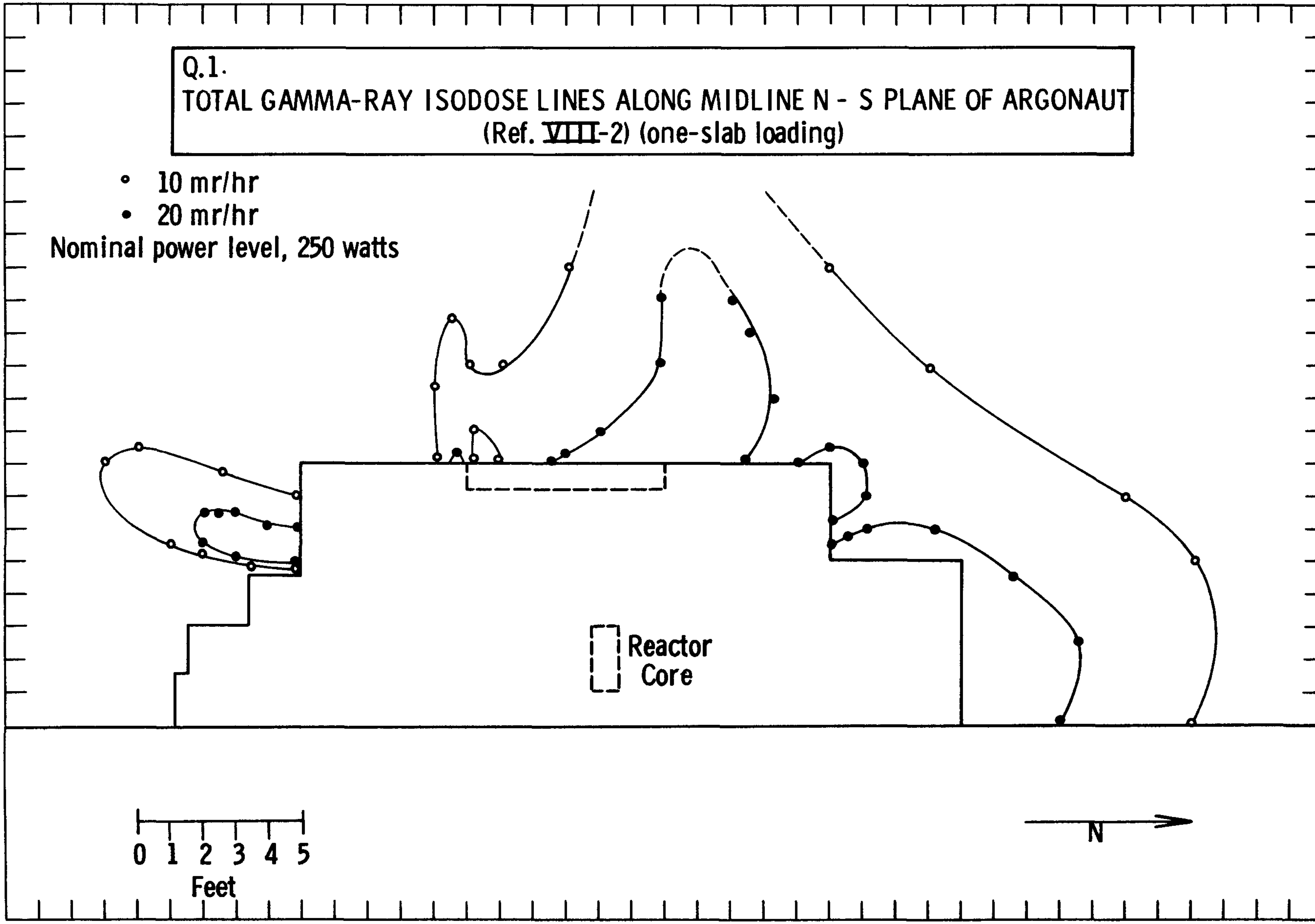

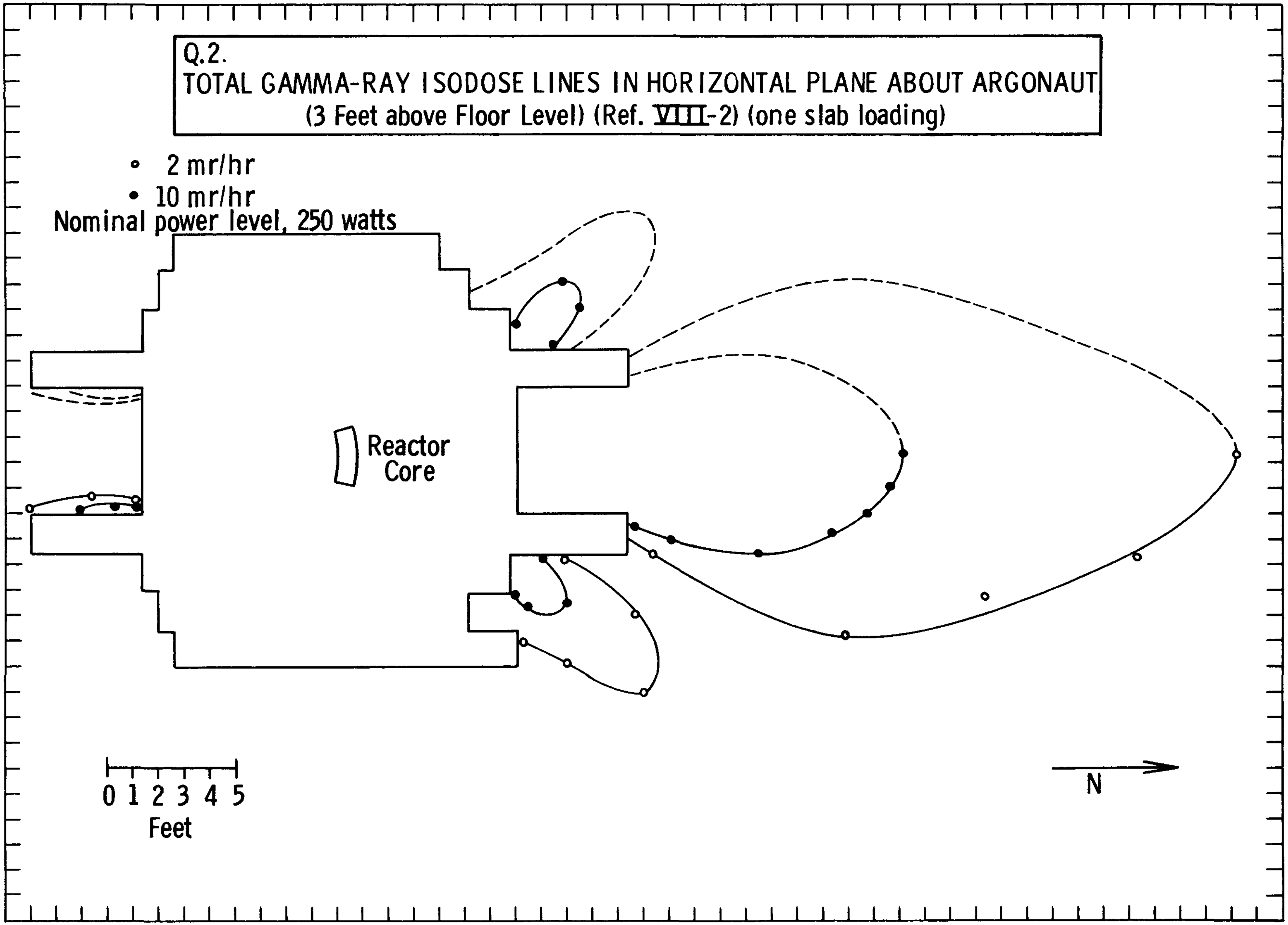
Q.2.
TOTAL GAMMA-RAY ISODOSE LINES IN HORIZONTAL PLANE ABOUT ARGONAUT
(3 Feet above Floor Level) (Ref. VIII-2) (one slab loading)
2 mr/hr
10 mr/hr
Nominal power level, 250 watts
Reactor Core
0 1 2 3 4 5
Feet
N

Q.3.
GAMMA ISODOSE CURVES AT EXTERNAL THERMAL COLUMN (Ref. VIII-3)

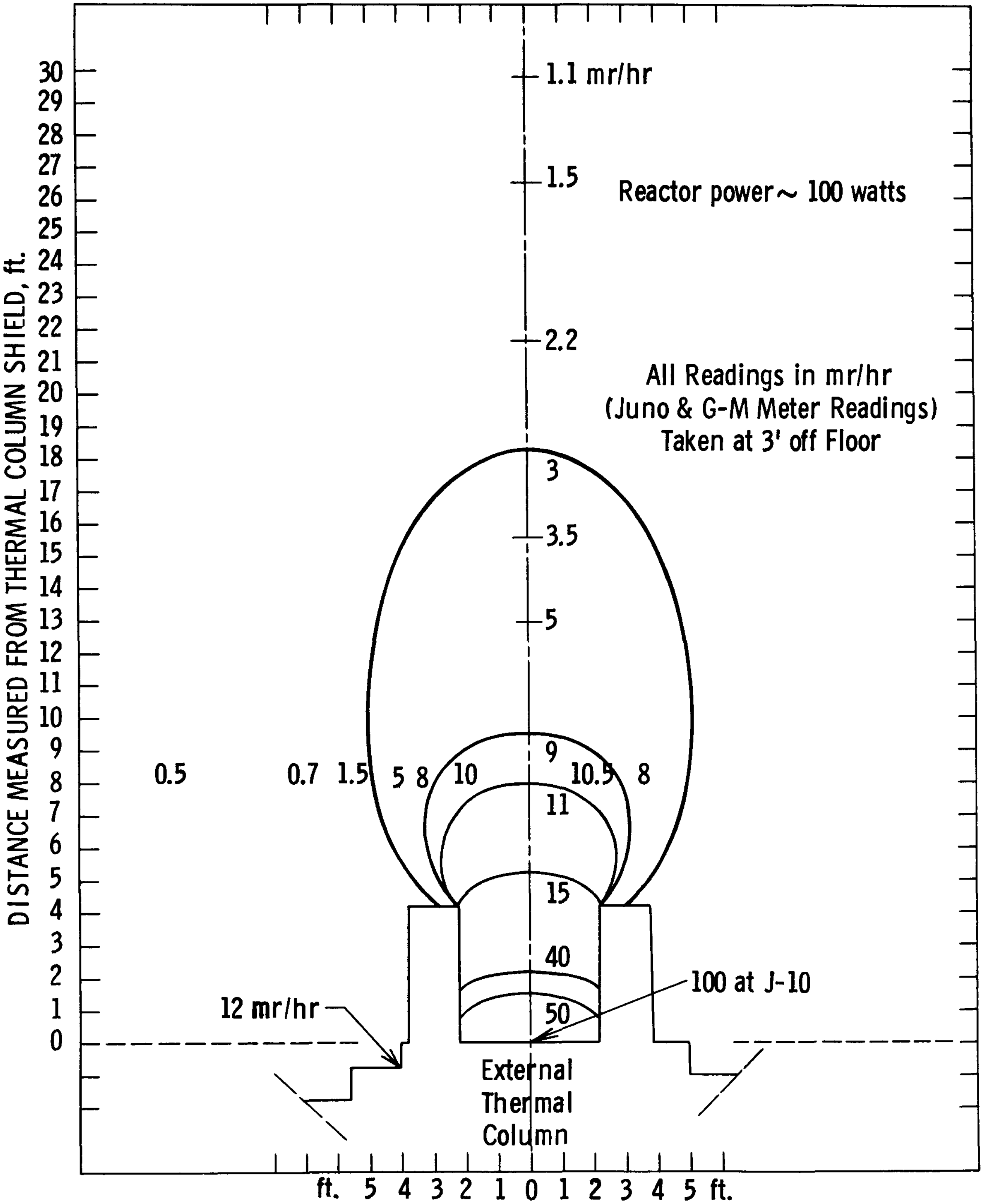

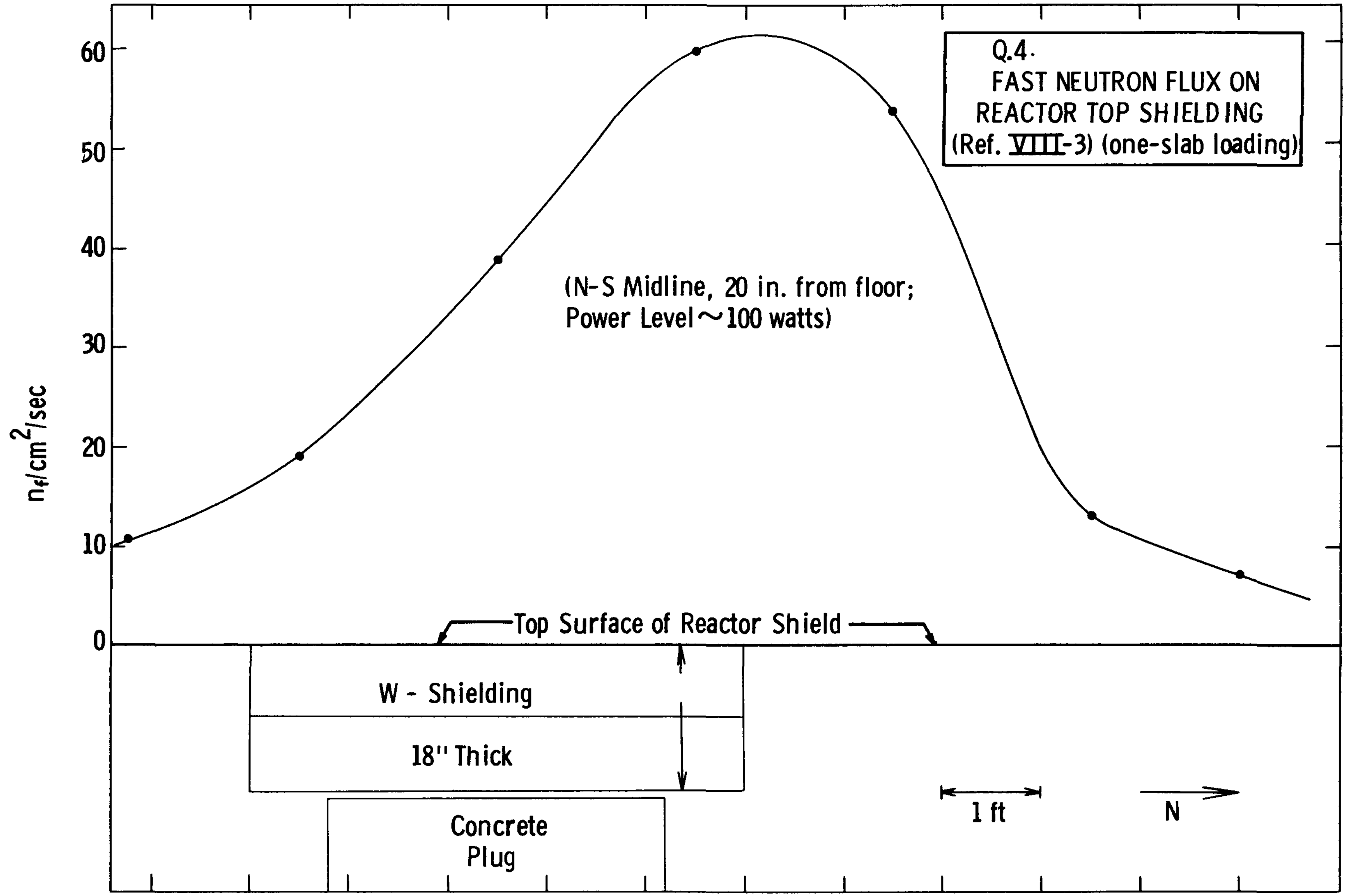
Q.4.
FAST NEUTRON FLUX ON
REACTOR TOP SHIELDING
(Ref. VIII-3) (one-slab loading)
(N-S Midline, 20 in. from floor;
Power Level ~100 watts)
$n_f/cm^2/sec$
60
50
40
30
20
10
0
Top Surface of Reactor Shield
W - Shielding
18" Thick
Concrete
Plug
1 ft
N

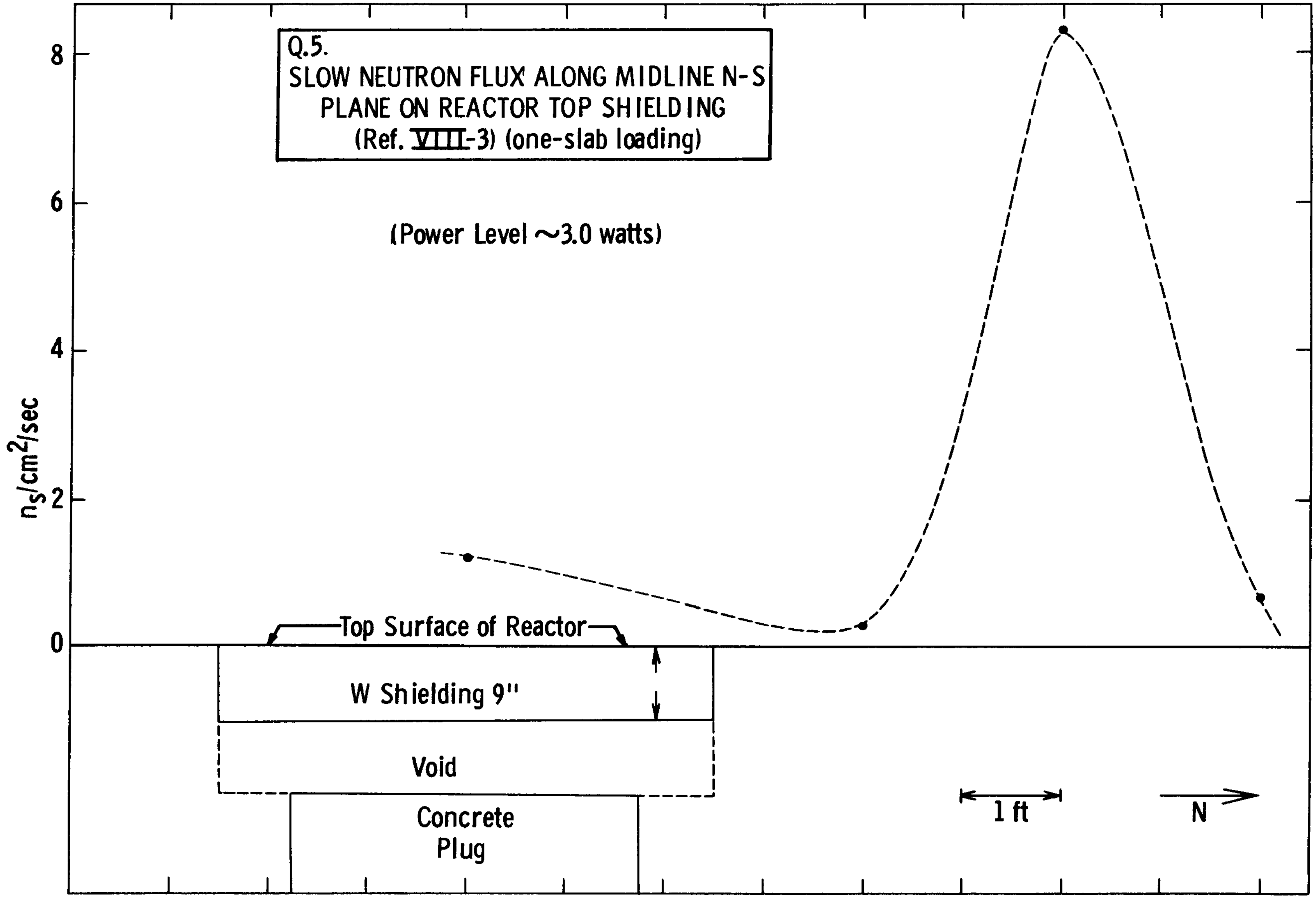

Q.5.
SLOW NEUTRON FLUX ALONG MIDLINE N-S PLANE ON REACTOR TOP SHIELDING (Ref. VIII-3) (one-slab loading)

Section R

WORLD LIST OF ARGONAUT REACTORS

Throughout the world there are about twenty-five reactors of the general Argonaut type, either in operation or in some stage of the planning and construction. This is a relatively large number of reactors to have basically similar designs, probably thus forming one of the largest common design reactor groupings in the world.

This section was compiled in the interest of promoting informal sharing of information by listing the various reactor locations and some reactor data and the name of a representative for each research group. When this section was compiled, all of the desired reactor information was not available and numerous omissions are obvious. Yet, the information is complete enough so that contacts can be made.

R.1. List of Argonaut Reactors

	REACTOR LOCATION	REACTOR NAME	PERSON WHO WILL ANSWER INQUIRIES
1.	Argonne National Laboratory Argonne, Illinois USA	Argonaut 10 kw - (Oper) Annular Core	Dr. William J. Sturm Reactor Supervisor
2.	Argonne National Laboratory Argonne, Illinois USA	Juggernaut 250 kw - (Oper) Annular Core	Mr. John Beidelman Reactor Supervisor
3.	University of Florida Gainesville, Florida USA	10 kw - (Oper) Annular Core	Dr. Uhrig
4.	Iowa State University Ames, Iowa USA	UTR-10 10 kw - (Oper) Two-slab Core	Dr. Glen Murphy, Head Nuclear Eng. Dept.
5.	Kansas State College Manhattan, Kansas USA		Dr. W. R. Kimel, Head Nuclear Eng. Dept.
6.	Virginia Polytechnic Inst. Blacksburg, Virginia USA	UTR-10 10 kw - (Oper) Two-slab Core	Mr. Andrew Robeson Department of Physics
7.	University of Washington Seattle 5, Washington USA		
8.	University of California Los Angeles 24, California USA	Engineering Nuclear Reactor 10 kw - (Oper) Two-slab Core	Mr. Thomas E. Hicks Department of Engineering
9.	Comision Nacional de Secuijia Atomica Avenida Liberatador Qeveral San Martin 8350 Buenos Aires, Argentina	RA-1 - (Oper)	Ing. Otto Gamba Head, Nuclear Reactors Dept.
10.	Atomic Energy Establishment, Winfrith Dorset Dorchester, England	Nestor - (Oper)	
11.	Hawker Siddeley Nuclear Power Co. LTD Sutton Lane Langley Nr. Slough Bucks England	Jason 10 kw - (Oper) Annular Core	

12. AEG - Versuchsanlage Grosswelzheim/Unterfranken Seligenstadter Strasse Western Germany	AEG - Preufreaktor - (UC)	Mr. Gerhard Riesch
13. Siemens Reaktor Station Garching Garching bei Munchen, Western Germany	Siemens Argonaut Reaktor 10 kw - (Oper) Annular Core	
14. Kernreaktor Bau-und Betriebsgesellschaft Karlsruhe, Western Germany	Siemens 10 kw - (UC) Annular Core	Mr. Risse
15. Reactor Centrum Nederland Petten, Netherlands	Low Flux Reactor 10 kw - (Oper) Annular Core	Ir. J. H. B. Madsen
16. Eng. School of Barcelona Barcelona, Spain (constructed by) Junta de Energia Nuclear Serrano 121 Madrid, Spain	Argos - (UC)	
17. Eng. School of Bilbao Bilbao, Spain (constructed by) Junta de Energia Nuclear Serrano 121 Madrid, Spain	Arbi - (UC)	
18. Australian Atomic Energy Commission Lucas Heights New South Wales, Australia	UTR-10 Moata 10 kw - (UC) Two-slab Core	
19. Kinki University Osaki, Japan	UTR-B 10 watts - (UC) Two-slab Core	
20. Rio de Janeiro University Rio de Janeiro Est. da Guanabbara Brazil	Argonaut 10 kw - (UC) Annular Core	
21. Queen Mary College University of London London, England	Jason Special Source Reactor 10 kw - (planned) Annular Core	

22.	Universities of Manchester and Liverpool UKAEA Site Risely, Lancashire England	Jason 10 kw - (planned) Annular Core	
23.	Institut National des Sciences et Technique Nucleaires Saclay France (A total of three are proposed)	ULYSSE 100 kw - (UC)	Prof. Debiesse
24.	USA - AEC Traveling Exhibit	UTR-B 10 watts - (Oper) Two-slab Core	

SYMBOLS

UC - under construction
Oper - operational
Planned - proposed and being planned
Annular Core - core built in the annulus
Two-slab Core - core built in two slabs

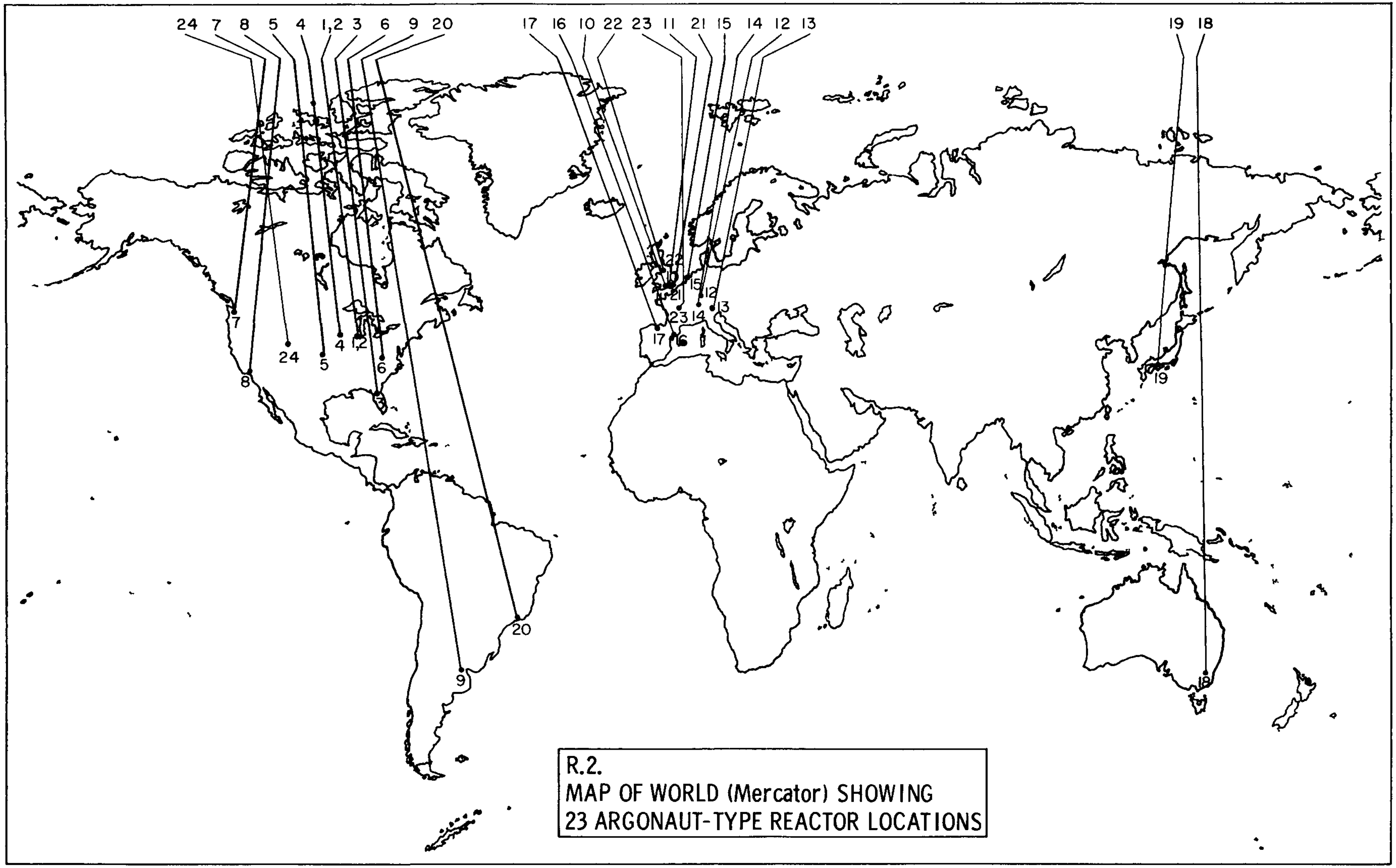

R.2.
MAP OF WORLD (Mercator) SHOWING
23 ARGONAUT-TYPE REACTOR LOCATIONS

Section S

BIBLIOGRAPHY OF ARGONAUT WORK

This is a list of published reports and unpublished work directly related to the Argonaut Reactor. Published reports are available through the usual channels.

The reports have been separated into thirteen classifications according to subject, and each classification is numbered separately. Some of the reports listed contain detailed sections on each of several of the thirteen classifications. These sections are listed as separate entries in their proper classifications, and are marked with an asterisk. A reference is given to the main bibliographical entry.

To emphasize the international character of the efforts, the name of the sponsoring country as well as the school session during which he worked is included after the name of each author. Students from the USA are similarly identified, and work done by Argonne National Laboratory personnel is identified as "ANL Staff." The following coding is used in this identification:

*1 - First Session, ISNSE, March 14, 1955-October 14, 1955.
2 - Second Session, ISNSE, November 1, 1955-June 1, 1956.
3 - Third Session, ISNSE, September 10, 1956-January 11, 1957.
4 - Fourth Session, ISNSE, January 28, 1957-May 24, 1957.
5 - Fifth Session, ISNSE, July 8, 1957-November 8, 1957.
6 - Sixth Session, ISNSE, February 4, 1958-May 29, 1958.
7 - Seventh Session, ISNSE, June 16, 1958-October 31, 1958.
8 - Eighth Session, ISNSE, February 4, 1959-May 29, 1959.
9 - Ninth Session, ISNSE, August 17, 1959-December 11, 1959.
10 - Argonaut Institute, Summer, 1957.
11 - Reactor Instrumentation and Control Institute, Summer, 1958.
12 - Specialized Nuclear Studies Institute, Summer, 1959.
13 - International Industrial Associate.
14 - Special Scientific Employee.
15 - Resident Research Associate.
*16 - Spring Term, IINSE, February 3, 1960-May 27, 1960.
17 - Summer Term, IINSE, June 8, 1960-September 30, 1960.

---

*The International School of Nuclear Science and Engineering (ISNSE) was established at Argonne National Laboratory in March 1955. It became the International Institute of Nuclear Science and Engineering (IINSE) in February 1960.

BIBLIOGRAPHY

I. General Construction and Operation of Reactor

1. Summary Report on the Hazards of the Argonaut Reactor; D. H. Lennox & C. N. Kelber (ANL Staff); ANL-5647, December, 1956.
2. Interim Report on Argonaut - A Generalized Reactor Facility for Nuclear Technology Training & Research; D. H. Lennox & B. I. Spinrad (ANL Staff); ANL-5552, March, 1956.
3. Argonaut-Engineering Construction and Costs; R. H. Armstrong, et al; (ANL Staff); ANL-5704, March, 1957.
4. Argonaut - CP-11; not listed; 1958; Argonne brochure.
5. Argonaut - Argonne's Reactor for University Training; R. H. Armstrong & C. N. Kelber (ANL Staff); Nucleonics reprint, March, 1957.
6. Reactor Data of Argonaut; September, 1958; ASME Reactor Data, Vol. 2, Research Reactors.
7. Operating Manual for the Argonaut Reactor, ANL-6036, May, 1959.
8. Some Characteristics of the Argonaut Reactor; G. W. Gersten (Germany-4) & H. H. Windsor (USA-4); May, 1957.
9. Proceedings of the Conference on Engineering Education and Nuclear Energy; W. W. Grigorieff, Editor; TID-7527, September, 1956.
10. A study of the reactor multiplication interlock; C. Buchler (ANL Staff); August, 1958.
11. An investigation of the value and validity of the reactor multiplication meter; L. Lawyer (ANL Staff); June, 1960.

II. Theoretical Calculations

1. The Theoretical Physics of the Argonaut Reactor; C. N. Kelber (ANL Staff); ANL-5710, May, 1957.
2. Calculations of the annular loading; K. Min (USA-12); August, 1959.
3. A study of cylindrical multiplying regions in an infinite reflector with application to two core configurations; S. Corno (Italy-4) & Y. Yeivin (Israel-4); May, 1957.

4. A calculation of some theoretical two-group constants for the homogenized one-slab loading; D. P. Moon (ANL Staff); August, 1959.

5. Two-Dimensional Two Group Calculations of the Argonaut One-slab Loading; D. P. Moon (ANL Staff); ANL-6154, August, 1959.

6. Some Argonaut parameters obtained in conjunction with the Juggernaut physics analysis; D. P. Moon (ANL Staff); January, 1960.

III. Automatic Control and Transfer Function

1. Design and operational testing of a reactor automatic control system using a reactor simulator; A. Gerba (ANL Staff); June, 1958.

2. Some performance measurements of the reactor automatic control system; A. Gerba & G. S. Pawlicki (ANL Staff); June, 1958.

3. A determination of the transfer functions of the reactor and controller separately with an evaluation of the control system; J. B. Van Erp (Netherlands-7); November, 1958.

4. A measurement of the transfer function of the reactor; G. S. Pawlicki (ANL Staff); April, 1958.

5. Argonne National Laboratory Reactor Control Institute; W. K. Foell, Ed.; September 5, 1958-Data Book, September 20, 1958-Class Notes; (11).

6. Some reactor transfer function and lifetime experiments; Y. Chelet (France-6) & R. Vidal (France-6); May, 1958.

* 7. A measurement of the neutron lifetime of the reactor; (see SVI.1 and SVI.2.)

8. Argonaut Automatic Flux Controller Design Report; A. Gerba, Jr. (ANL Staff); ANL-6110, January, 1960.

IV. Danger Coefficient and Other Absorber and Fuel Reactivity Effects

1. Danger coefficient measurements on the reactor and calibration of the reactor sensitivity; T. Stribel (Germany-13); November, 1958.

2. An evaluation of the reactivity worth of fuel; W. Carey (USA-15); March 1958.

3. A study of the effect of substituting graphite for aluminum and water in the core; W. E. Carey (USA-15) & G. S. Klaiber (USA-15); February, 1958.

4. A study of the spatial reactivity worth of a large graphite wedge; L. Lawyer & R. Springer (ANL Staff); February, 1959.

5. An evaluation of the reactivity worth of cadmium inserted in the external thermal column; W. E.Carey (USA-15) & G. S. Klaiber (USA-15); April, 1958.

6. Determination of the critical mass and worth of various features of the reactor using the multiplication facility; J. C. Denton (USA-3); January, 1957.

7. A study of reactor moderator and reflector worth; N. Chrysochoides (Greece-5) & A. Freire (Ecuador-5); October, 1957.

8. Some danger coefficient measurements in the internal thermal column; A. L. Babb (USA-10), G. Leppert (USA-10), P. Dimotakis (Greece-10), F. Pauls (USA-10) & J. E. Stubbs (USA-10); August, 1957.

9. A neutron temperature measurement using the danger coefficient method; A. L. Babb, F. Pauls, C. Perry, & E. Foster (USA-10); September, 1957.

10. The reactivity effect of plexiglass foil holders in the core; A. Cilesiz (Turkey-5); March, 1958.

11. A measurement of the reactivity effect of plexiglass holders and indium foils inside aluminum cans; A. Cilesiz (Turkey-5); February, 1958.

*12. An estimation of the reactivity value of the upper reflector; (see XIII.4).

*13. The worth of the cadmium used in the Argonaut regulator; (see III.5).

14. A study of some reactivity effects in the J-10 stringer and water tank; W. J. Sturm, L. Lawyer & R. Springer (ANL Staff); September 1959.

15. A measurement of fuel worth in the internal thermal column; L. Lawyer & W. J. Sturm (ANL Staff); November, 1959.

16. An approach to critical and a determination of the critical mass for a modified one-slab core; B. Emerson (Gr. Britain-13) & W. J. Sturm (ANL Staff); July, 1959.

17. Danger coefficient measurements, D. Habermann (Netherlands-16) J. Becker (ANL Staff); May, 1960.

18. Additional danger coefficient measurements; D. Habermann (Netherlands-16); June, 1960.

19. Some measurements of fuel worth in the internal thermal column; L. Lawyer, W. J. Sturm (ANL Staff); March, 1960.

V. Flux and Power Measurement

1. A flux distribution and power calibration of the reactor; F. Alsina (Argentina-10); C. Domingo (Argentina-10), M. Geiger (Argentina-10), W. Gilbert (USA-10), E. Ferrand (USA-10), B. Hildebrand (USA-10), E. Foster (USA-10), & C. Perry (USA-10); August, 1957.

2. A mapping of the neutron flux in the reactor; A. Cilesiz (Turkey-5) & R. Springer (ANL Staff); 1958.

3. A determination of the irradiation time correction for reactor startup and shutdown; T. Stribel (Germany-13); September, 1958.

4. A study of foil activation during startup and shutdown; W.Carey (USA-15); September, 1958.

5. Some measurements of flux in the beam holes and stringers; A. L. Babb, F. Pauls, C. Perry, & E. Foster (USA-10); September 1957.

6. Gold foil absolute flux measurement in the core; J. Becker (ANL Staff); July, 1959.

7. Flux distribution in a one-slab core; A. Cilesiz (Turkey-5); March, 1959; Ap3.

8. Some flux plots in the one-slab core; D. Daavettila (ANL Staff); August, 1959.

9. Flux plots in an annular core; J. Dunlap (ANL Staff) & W. Carey (USA-15); December, 1958.

10. Axial flux distribution in the external graphite thermal column; R. Springer (ANL Staff); September, 1959.

11. A measurement of the absolute thermal flux in the external thermal column; R. Springer (ANL Staff); December, 1959.

12. A method of power calibration for the reactor; W. J. Sturm & L. Lawyer (ANL Staff); December, 1959.

13. Gamma ray intensity in the one-slab core during operation; W. J. Sturm & L. Lawyer (ANL Staff); January, 1960.

14. Power calibration of the two-slab core; W. J. Sturm & L. Lawyer (ANL Staff); June, 1960.

VI. General Experiments

1. Experiments on the AGN-201 and the Argonaut Reactor; Y. Togo (Japan-5); October, 1957.

2. Work done on various Argonaut and AGN-201 reactor experiments; Y. K. Kwon (Korea-5); October, 1958.

VII. Neutron Age in Water and Diffusion in Graphite, etc.

1. A measurement of neutron age in water to the energy of the indium resonance; ANL Staff.

2. Measurement of age and diffusion length in the water shield tank; A. L. Babb (USA-10), P. Dimotakis (Greece-10), G. Leppert (USA-10), F. Pauls (USA-10), and J. Stubbs (USA-10); August, 1957.

3. Measurement of diffusion length in the graphite thermal column; C. Domingo (Argentina-10), E. Ferrand (USA-10), E. Foster (USA-10), W. Gilbert (USA-10), B. Hildebrand (USA-10) and C. Perry (USA-10); August, 1957.

4. A measurement of the fast neutron removal cross section of iron in the water tank; A. L. Babb (USA-10), G. Leppert (USA-10), F. Pauls (USA-10), and J. Stubbs (USA-10); August, 1957.

5. An experimental determination of the age and diffusion length of neutrons in water; W. Grant (So. Africa-16); P. Guenther (Austria-16); R. Kiyose (Japan-16); M. Kirshenbaum (USA-16), F. Kockum (Sweden-16); S. Lawande (India-16); D. Nguyen (Vietnam-9); R. Schroder (Germany-16); D. Smith (USA-16), S. Wang (China-16); June, 1960.

VIII. Radiation Safety

1. Data compilation of radiation safety surveys in the reactor building, from December 1956 to October, 1959; H. J. Moe and C. S. McKee (ANL Staff); October, 1957.

2. Measurements of the gamma ray isodose lines outside the reactor; W. J. Sturm and L. Lawyer (ANL Staff); September, 1959.

3. Some data on the Argonaut shielding; J. Dunlap (ANL Staff); April, 1959.

4. Data compilation of radiation surveys in the reactor building from October, 1957 to July, 1960; J. R. Novak (ANL Staff); July, 1960.

IX. Ramp Startup and General Kinetics

1. An experimental study of linear ramp inputs of reactivity to the reactor and to the analog computer; Bro. J. Elliott (USA-12); August, 1959.

2. Analog Computations of Training Reactor Kinetics; D. F. Hang and E. G. Manning (USA-12); August, 1959; ANL brochure.

3. Ramp startup and some measurements of poison worth in the reflector; W. E. Carey (USA-15) and G. S. Pawlicki (ANL Staff); 1958.

4. The kinetics of a reactor composed of two loosely-coupled cores; G. C. Baldwin (USA-14); 1958.

* 5. Ramp startup of the reactor; (see III.5).

6. The effect of nitrogen injection into the core; D. Habermann (Netherlands-16); June, 1960.

7. A study of the effect of reactivity changes while the reactor is on a positive period; D. Habermann (Netherlands-16); June, 1960.

8. Determination of the Time Behavior of Neutron Density and of Reactivity on the Argonaut Reactor; W. R. Kimel (USA-15), W. E. Carey (USA-15), F. G. Prohammer (ANL Staff), and G. C. Baldwin (USA-14); "Nuclear Science and Engineering," Vol. 6, No. 3, pp. 233-237, September, 1959.

X. Rod Calibrations

1. A calibration of the fine control rod; A. Rivera (Puerto Rico-12); August, 1959.

2. A summary of the control rod calibration experiment; W. E. Carey (USA-15); April, 1958.

3. Measurements of safety and control rod worths with an annular loading; W. E. Carey (USA-15); January, 1959.

4. Control rod calibration by means of the inhour equation; A. Babb, G. Leppert, F. Pauls, J. Stubbs (USA-10) and P. Kimotakis (Greece-10); July, 1957.

5. A determination of the critical position of the control rods; A. Babb, G. Leppert, and F. Pauls (USA-10); June, 1957.

6. An investigation of the discrepancy in period and rod drop methods of determining reactivity worth; L. Lawyer (ANL Staff); August, 1959.

7. Some measurements of control rod worths; L. Lawyer (ANL Staff); August, 1959.

8. A composite control rod calibration; G. C. Baldwin (USA-14); March, 1958.

* 9. Measurements of the worth of control rods; (see XIII.4, III.5, and VI.2).

*10. Control rod drop experiments; (see XII.3).

XI. <u>Temperature Coefficient of Reactivity</u>

1. Description of the equipment used in the temperature coefficient experiment; J. Dunlap (ANL Staff); 1958.

2. A measurement of the temperature coefficient of reactivity with an annular loading; W. E. Carey (USA-15) & J. Dunlap (ANL Staff); January, 1959.

3. A measurement of the temperature coefficient of reactivity with a two-slab loading; C. Domingo (Argentina-10), E. Ferrand, E. Foster, W. Gilbert & B. Hildebrand (USA-10); August, 1957.

4. A measurement of the temperature coefficient of reactivity with a one-slab loading; P. Guenther (Austria-16), R. Jain (India-16), M. Kirshenbaum (USA-16), P. Larsen (Denmark-16), D. Nguyen, (Vietnam-9), D. Smith (USA-16), S. Wang (China-16); April, 1960.

XII. <u>Void Coefficient of Reactivity</u>

1. A measurement of the effect of fuel plate spacing on the void coefficient of reactivity; W. F. Gilbert (USA-12); August, 1959.

2. Summary of the ramp startup experiment with additional measurements of void and poison worth in the reflector; W. E. Carey (USA-15); July, 1958.

3. A compilation of results of the void coefficient experiments; A. Cilesiz (Turkey-5); September, 1958.

4. The measurement of the void coefficient using styrofoam strips; C. Domingo (Argentina-10), E. Ferrand, E. Foster, W. Gilbert, B. Hildebrand (USA-10); July, 1957.

* 5. Integral and differential reactivity worth of void in the external thermal column; (see III.5).

6. A measurement of the effect of fuel plate spacing on the void coefficient of reactivity; P. Ameglio (Italy-15), W. Grant (So. Africa-16), P. Guenther (Austria-16), R. Jain (India-16), M. Kirshenbaum (USA-16), D. Nguyen (Vietnam-9), D. Smith (USA-16), S. Wang (China-16); April, 1960.

XIII. Special Experiments

1. A description of an isotope irradiation, scintillation spectrometer experiment; W. E. Carey (USA-15); November, 1958.

2. A measurement of pile noise; C. E. Cohn (ANL Staff); February, 1958; RED-EPM 13 memo, April 3.

3. A study of the radioactive decay of fuel boxes; J. Dunlap (ANL Staff) and W. E. Carey (USA-15); December, 1958.

4. General experiments on the reactor; A. Cilesiz (Turkey-5); October, 1957.

5. A mapping of the neutron beam from the external thermal column; D. Habermann (Netherlands-17) & J. Spalek (ANL Staff); July, 1960.

6. Cross section measurements with the neutron beam from the external thermal column; D..Habermann (Netherlands-17)& J. Spalek (ANL Staff); July, 1960.

7. Preliminary work done in the development of the pulsed neutron technique for educational purposes; M. Copic (Yugoslavia-15); March, 1960.